UNIVERSITÉ CATHOLIQUE DE LOUVAIN

SECTEUR DES SCIENCES DE LA SANTÉ

INSTITUT DE RECHERCHE CLINIQUE ET EXPÉRIMENTALE (IREC)

PÔLE PNEUMOLOGIE, ORL ET DERMATOLOGIE

EXPLORING THE PLASTICITY OF THE AIRWAY EPITHELIUM IN CHRONIC OBSTRUCTIVE PULMONARY DISEASE

François CARLIER, MD

Promoteur : Charles PILETTE, MD PhD

Thèse présentée en vue de l'obtention du grade de Docteur en Sciences Médicales

Décembre 2021

Members of the jury

Promotor

Professor Charles Pilette
Université catholique de Louvain (UCL)
Institute of Experimental & Clinical Research
Pole of Pneumology, ENT and Dermatology (PNEU)
Avenue Hippocrate 54, B1.54.04
B-1200 Brussels, BELGIUM

Department of Pneumology
Cliniques universitaires Saint-Luc
Avenue Hippocrate 10
B-1200 Brussels, BELGIUM

President

Professor Alain Poncelet
Université catholique de Louvain (UCL)
Institute of Experimental & Clinical Research
Pole of Cardiology (CARD)
Avenue Hippocrate 55, B1.55.05
B-1200 Brussels, BELGIUM

Department of Cardiovascular and Thoracic surgery
Cliniques universitaires Saint-Luc
Avenue Hippocrate 10
B-1200 Brussels, BELGIUM

Members

Professor Jean-Luc Balligand
Université catholique de Louvain (UCL)
Institute of Experimental & Clinical Research
Pole of Pharmacology and Therapeutics (FATH)
Avenue Hippocrate 53, B1.53.09
B-1200 Brussels, BELGIUM

Department of Cardiology
Cliniques universitaires Saint-Luc
Avenue Hippocrate 10
B-1200 Brussels, BELGIUM

Professor Frédéric Lemaigre
Université catholique de Louvain (UCL)
de Duve Institute
Liver and pancreas differentiation Unit (LPAD)
Avenue Hippocrate 75, B1.75.02
B-1200 Brussels, BELGIUM

Professor Christophe Pierreux
Université catholique de Louvain (UCL)
de Duve Institute
Cell Biology Unit (CELL)
Avenue Hippocrate 75, B1.75.02
B-1200 Brussels, BELGIUM

Invited members

Professor Arnaud Bourdin
CHU de Montpellier - Hôpital Arnaud de Villeneuve
Department of Pulmonology and Addictology
Avenue du Doyen Gaston Giraud, 371
F-34295 Montpellier CEDEX 5, France

Professor Bart Vanaudenaerde
Katholieke Universiteit Leuven (KUL)
Laboratory of Respiratory Diseases and Thoracic Surgery
Herestraat 49 - box 706
B-3000 Leuven, BELGIUM

“The important thing is not to stop questioning. Curiosity has its own reason for existing. One cannot help but be in awe when one contemplates the mysteries of eternity, of life, of the marvellous structure of reality. It is enough if one tries to comprehend only a little of this mystery every day.”

Albert Einstein

REMERCIEMENTS

Au cours des cinq années de travail dont ce manuscrit synthétise les principaux résultats, j'ai eu la chance immense de pouvoir bénéficier du soutien, de l'aide et des conseils d'innombrables personnes, sans lesquelles le chemin parcouru aurait certainement été plus tortueux, plus ardu, et surtout moins enrichissant.

J'adresse mes premiers remerciements à mon promoteur, le Professeur Charles Pilette, qui m'a accompagné et conseillé tout au long de mon parcours, avec un calme et un optimisme infaillibles, ainsi qu'une patience, une expertise et une disponibilité à toute épreuve. Sa vision globale du projet, et les constants ajustements qu'il a pu y apporter à petites touches, nous ont permis d'aboutir à la publication d'articles scientifiques originaux et de revues de littérature. Je le remercie particulièrement pour la souplesse et l'attention bienveillante dont il a fait preuve lors des aléas familiaux et personnels qui ont émaillé ces dernières années. J'espère sincèrement que cette thèse constitue le point de départ d'une future collaboration scientifique riche. Je remercie également le Professeur Yves Sibille, initialement co-promoteur de ce travail, qui aura su attendre le moment adéquat pour réveiller ma fibre scientifique, et m'offrir l'opportunité d'entamer une carrière académique. En dépit d'une collaboration écourtée, il aura été un acteur décisif dans mon orientation professionnelle vers la recherche et vers la pneumologie.

J'adresse ensuite ma reconnaissance à l'ensemble des membres de mon comité d'encadrement : les Professeurs Jean-Luc Balligand, Frédéric Lemaigre, Christophe Pierreux, et Alain Poncelet (Président du jury) pour l'intérêt qu'ils ont porté à ce travail, ainsi que pour leur disponibilité et leurs conseils avisés lors des réunions de comité. Je remercie également chaleureusement les Professeurs Arnaud Bourdin et Bart Vanaudenaerde, qui m'ont fait l'honneur d'apporter leur regard extérieur sur ce travail.

Je tiens tout particulièrement à remercier l'ensemble des membres du laboratoire de l'IREC/PNEU, qui m'ont tour à tour enseigné, encadré, épaulé, conseillé, rassuré,

questionné au cours des années passées au sein de l'équipe. En tant que véritable plaque tournante et mémoire vivante de l'unité, je remercie tout d'abord Marylène Lecocq, dont l'enthousiasme, le dynamisme et l'implication sans faille font la vie du laboratoire. Je remercie également Bruno Detry pour m'avoir appris la patience et l'humilité lorsqu'il s'agit de cultiver des cellules bronchiques, le Dr Frank Aboubakar pour avoir éclairé mes premiers tâtonnements de chercheur, pour son enseignement des marquages « tyramide signal amplification », et pour m'avoir torturé les tympans à coup d'Arno, Amandine Collin pour son aide en culture, ses danses incongrues et ses fous-rires communicatifs, Diana Santos Ribeiro pour son expertise en biologie moléculaire et pour m'avoir obligé à perfectionner mon anglais, Charlotte Moulin pour avoir essayé de m'éduquer à l'immunologie pulmonaire et aux chants de Noël, le Dr Ludovic Gérard pour sa zénitude et pour m'avoir rappelé l'intérêt de la clinique, le Pr Sophie Gohy pour m'avoir transmis sa rigueur de relectrice hors-pair et pour notre collaboration lors des publications, et le Pr Antoine Froidure pour avoir ouvert mes horizons pneumologique, cinématographique, musical et zythologique. Au sein du laboratoire, la rencontre du Dr Thomas Planté-Bordeneuve aura été particulièrement enrichissante, tant sur le plan scientifique et professionnel, que sur le plan personnel. Avec cette assurance feinte qui le caractérise, Thomas aura su m'amener à remettre mes conclusions en question, à améliorer ma connaissance de la littérature scientifique, et à ouvrir mon esprit à des techniques nouvelles. Plus qu'un collaborateur aux connaissances parfois intimidantes, j'ai surtout rencontré un futur collègue, rapidement devenu un ami.

Ce travail est également le fruit de nombreuses collaborations. Je tiens à témoigner ma gratitude à Jérôme Ambroise et Bertrand Bearzatto (IREC/CTMA) pour leur aide précieuse dans l'analyse bio-informatique des données générées lors du séquençage d'ARN ainsi que pour les analyses « single-cell RNA » de bases de données, à Chantal Fregimilicka et Michèle De Beukelaer (IREC/2IP) pour leur efficacité à me fournir des lames de tissus, à Aurélie Daumerie, Caroline Bouzin (IREC/2IP) et Nicolas Van Baren (Institut de Duve, GECE) pour leurs conseils et formations à

l’utilisation des scanners et à l’analyse d’images, et à Sandra Ormenese (GIGA, Université de Liège) pour sa disponibilité à m’initier à la microdissection laser. J’adresse par ailleurs mes chaleureux remerciements au Pr Jacques Van Snick (Institut de Duve, MEXP) pour son aide dans la mesure de l’IL-6, ainsi que Stijn Verleden (KULeuven, UZ Antwerpen) pour son aide précieuse dans l’achalandage de tissus pulmonaires et pour son dynamisme dans la collaboration renforcée entre nos laboratoires au cours de cette thèse.

Le paysage de la recherche scientifique fondamentale est tel qu’un soutien financier est primordial pour mener un projet de recherche à bien. Je remercie chaleureusement la Fondation Mont-Godinne pour son soutien inconditionnel, ainsi que le Fonds National de Recherche Scientifique pour m’avoir octroyé un mandat de doctorant-clinicien candidat spécialiste durant mes quatre années de laboratoire.

Je remercie infiniment mes parents pour l’éducation qu’ils m’ont offerte et pour m’avoir toujours poussé à me poser des questions. Je leur dois ma curiosité et mon besoin continuel de comprendre, moteurs précieux lors de mon parcours. Avec mes sœurs et mes frères, ils ont également constitué un soutien familial indéfectible. Ils ont su être à l’écoute de mes questionnements et de mes doutes.

Enfin, mes derniers remerciements sont pour mon épouse Xave. Elle a été d’une aide inestimable tout au long de ces années. Elle a su s’intéresser à un domaine qui n’est pas le sien en montrant une curiosité et une acuité de jugement surprenantes, et a fait preuve d’une flexibilité et d’un soutien constants en dépit des exigences qui ont pu s’imposer, en particulier lors des congrès à l’étranger ou de mon année parisienne entre 2019 et 2020. Avec nos filles, Célestine et Albane, elles constituent un socle sur lequel je m’appuie à tous moments, et elles sont les racines de l’équilibre sur lequel je construis ma vie.

TABLE OF CONTENTS

LIST OF ABBREVIATIONS

Ab	Antibody
AE	Airway epithelium
ALI	Air/Liquid interface
α-SMA	α-Smooth muscle actin
ASL	Airway surface liquid
AU	Arbitrary Unit
BAL	Bronchoalveolar lavage
BEBM	Bronchial epithelial basal medium
BEGM	Bronchial epithelial growth medium
BSA	Bovine serum albumin
CAT	COPD assessment test
CLAD	Chronic lung allograft dysfunction
COPD	Chronic obstructive pulmonary disease
CSE	Cigarette smoke extract
d-Ig	Dimeric immunoglobulin
DL_{CO}	Diffusing capacity of the lung for carbon monoxide
DMEM	Dulbecco's modified Eagle's medium
DMSO	Dimethyl sulfoxide
EGF	Epidermal growth factor
EGFR	Epidermal growth factor receptor
ELISA	Enzyme-linked immunosorbent assay
EMT	Epithelial-to-mesenchymal transition
FEV1	Forced expiratory volume in one second
FGF	Fibroblast growth factor
FOX	Forkhead box
FVC	Forced vital capacity

GAPDH	Glyceraldehyde 3-phosphate dehydrogenase
GM-CSF	Granulocyte-macrophage colony-stimulating factor
GOLD	Global initiative for chronic obstructive lung disease
HAT	Histone acetyltransferase
HBEC	Human broncho-epithelial cells
HDAC	Histone deacetylase
HRP	Horseradish peroxidase
ICS	Inhaled corticosteroids
IFN	Interferon
Ig	Immunoglobulin
IHC	Immunohistochemistry
IL	Interleukin
KO	Knockout
LABA	Long-acting beta-adrenergic agonist
LAMA	Long-acting muscarinic antagonist
LTx	Lung transplantation
MCIDAS	Multiciliate differentiation and DNA synthesis associated cell cycle protein
mMRC	Modified medical research council dyspnoea scale
mRNA	Messenger Ribonucleic acid
MUC	Mucin
MYB	Myb proto-oncogene
p63	Tumour protein 3
PBS	Phosphate buffer saline
pIgR	Polymeric immunoglobulin receptor
RBM	Reticular basement membrane
RFX	Regulatory factor X
RNA-seq	Ribonucleic acid sequencing

RPM	Revolutions per minute
RPMI	Roswell Park Memorial Institute
RPS	Ribosomal protein S
RPMI	Roswell Park Memorial Institute medium
RT	Room temperature
RT-qPCR	Reverse transcription quantitative polymerase chain reaction
SABA	Short-acting beta-adrenergic agonist
SAMA	Short-acting muscarinic antagonist
scRNA-seq	Single cell RNA-Seq
SC	Secretory component
SD	Standard deviation
SEM	Standard error of the mean
S-Ig	Secretory immunoglobulin
SHH	Sonic Hedgehog
SPDEF	SAM-pointed domain containing ETS transcription factor
TBS	Tris-buffered saline
TBS-T	Tris-buffered saline with Triton
TEER	Transepithelial electric resistance
TGF-β	Transforming growth factor-beta
TLR	Toll-like receptor
TNF-α	Tumour necrosis factor-alpha
TSLP	Thymic stromal lymphopoietin
VC	Vital capacity
WNT	Wingless/integrated
ZO-1	Zonula Occludens-1

LIST OF THE FIGURES

LIST OF THE TABLES

SECTION 1.
INTRODUCTION AND GOALS OF THE THESIS

1. Introduction

1.1.COPD

1.1.1. Definition

Chronic obstructive pulmonary disease (COPD) is a major health burden and is currently the third leading cause of death worldwide, according to World Health Organization estimations (1, 2). It is a frequent, preventable and poorly treatable disease characterized by a slowly progressive and mostly irreversible airflow obstruction that is due to a combination of small airway disease (e.g. small airways disappearance, obstructive bronchiolitis, with mucus plugs and peribronchial fibrosis) and destruction of the alveolar walls (emphysema), ultimately leading to respiratory failure (2, 3). Its major cause is cigarette smoking, although genetic predisposition and other toxic exposures (air pollution, occupational, biomass) may also play a role (4).

1.1.2. Diagnosis and assessment

The diagnosis of COPD is evoked based on the combination of suggestive clinical symptoms (such as dyspnoea, chronic cough as defined in (5), or sputum production), and the presence of risk factors, including tobacco smoking, indoor/outdoor pollution, or occupational exposition. The diagnosis of COPD is confirmed by spirometry, in the presence of a post-bronchodilator forced expiratory volume in one second (FEV1)/Forced vital capacity (FVC) ratio below 0.70, confirming persistent airflow limitation(2).

The assessment of COPD severity is crucial to adapt therapy. It aims at determining the level of airflow limitation, the impact of the disease on the patient's health status,

and the risk of future events (such as exacerbations, hospital admissions or death) (2). Until 2011, the severity of COPD based only on the degree of airflow limitation, witnessed by the FEV1 decrease (6, 7), as summarized in table 1. This classification was used in our studies to separate study populations according to objective measurements.

Gold Stage	Severity	FEV1 (% predicted)
Gold 1	Mild	≥ 80
Gold 2	Moderate	50% ≤ FEV1 < 80%
Gold 3	Severe	30% ≤ FEV1 < 50%
Gold 4	Very severe	<30%

Table 1 | COPD classification
COPD classification according to Global Initiative for Chronic Obstructive Lung Disease (GOLD) classification of severity of airflow limitation in COPD (based on post-bronchodilator FEV1) (2001, reviewed in 2003).

In 2013, this classification was modified in order to include clinical features, including exacerbations history and dyspnoea (8). Exacerbations are defined as acute worsening of the respiratory symptoms, resulting in additional therapy, and are particularly important to consider as they negatively affect health status, rates of hospitalization and disease progression (9, 10). Symptoms are evaluated by the COPD assessment test (CAT) or the modified Medical Research Council dyspnoea scale (mMRC) and the number of exacerbations is integrated to further classify the disease into groups A or B (low risk) and groups C or D (high risk). The 2013 classification was finally modified in 2017 (2) to associate functional status (FEV1, grades 1-4) and clinical findings (dyspnoea and exacerbations, groups A-D), as shown in Figure 1. Different treatment regimens are proposed according to this classification, as described hereunder.

Given that COPD also has significant systemic effects, and that patients with COPD often have concomitant chronic illnesses that are identified as bad prognostic factors

(11), it is recommended to look for and treat comorbidities such as cardiovascular diseases (12), sarcopenia, metabolic syndrome, osteoporosis, depression, anxiety and lung cancer (13).

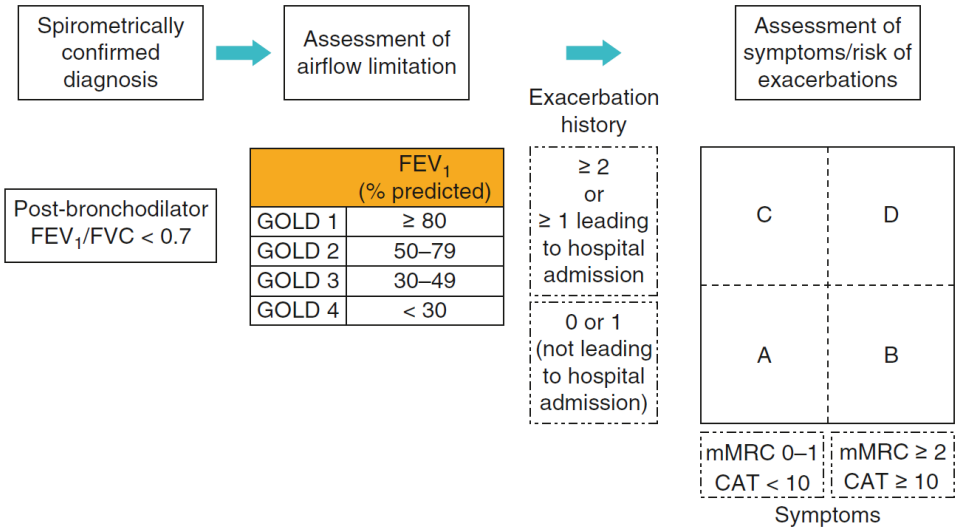

Figure 1 | COPD ABCD assessment tool
The refined ABCD assessment tool, as proposed by the GOLD in 2017 (2). CAT = COPD Assessment Test; COPD = chronic obstructive pulmonary disease; FEV_1, forced expiratory volume in 1 second; FVC, forced vital capacity; GOLD = Global Initiative for Chronic Obstructive Lung Disease; mMRC= modified British Medical Research Council questionnaire.

1.1.3. Treatment

1.1.3.1. Non-pharmacological management of stable COPD

Smoking cessation constitutes the most important therapeutic option, as it carries the greatest capacity to influence the natural history of COPD. Nicotine replacement therapy (nicotine gum, inhaler, nasal spray, lozenge, etc) (14, 15) and physician-delivered counselling (16) increase long-term smoking abstinence rates, while pharmacological products (such as bupropion and nortryptiline), although effective, should be used only as components of a supportive intervention program. Combining

pharmacotherapy and behavioural support increases long-term smoking cessation rates up to 30% (17). When applicable, elimination or reduction of occupational exposure and of indoor/outdoor pollution is advised.

Influenza and pneumococcal vaccination are recommended for COPD patients, as they decrease the incidence of lower respiratory tract infections, of exacerbations, and probably of death (18-21).

Pulmonary rehabilitation is defined as "[…] patient-tailored therapies that include […] exercise training, education, self-management intervention aiming at behaviour change, designed to improve the physical and psychological condition of people with chronic respiratory disease […]" (22). Six to 8 weeks programs (at least twice a week) improve shortness of breath and reduce anxiety and depression, and pulmonary rehabilitation has been shown to be the most (cost)-effective therapeutic strategy to improve dyspnoea, health status and exercise tolerance (23-25). It is appropriate to all COPD patients, although higher benefits are expected in patients with moderate to severe disease.

1.1.3.2. Pharmacological therapy for stable COPD

Pharmacological therapy for COPD is currently used to reduce symptoms, improve exercise tolerance and health status, and reduce the frequency and severity of exacerbations. To date, there is little conclusive clinical trial evidence that any existing medications for COPD modify the long-term decline in lung function (26-30). Evidence of such an effect has nevertheless been observed after treatment with tiotropium (during 2 and 4 years) and salmeterol/fluticasone propionate (3 years) (31-33), matching the reduced exacerbation rate observed in patients treated with bronchodilators (see below), but this still needs to be confirmed in larger cohorts. The treatment regimen needs to be individualized according to patients' symptoms, pulmonary functional tests, and severity of exacerbations.

Commonly used medications in stable COPD mainly include bronchodilators and anti-inflammatory agents, while antibiotics, and mucolytic/antioxidant agents have not been shown to be effective and will not be further discussed in this manuscript.

1.1.3.2.1. Bronchodilators

Bronchodilators improve pulmonary functional tests (notably FEV_1 and dynamic hyperinflation) by altering airway smooth muscle tone and thus widening the airways. They are most often given on a regular basis to prevent or reduce symptoms and include three main therapeutic classes: β_2-agonists, antimuscarinic drugs and méthylxanthines. The two first constitute the cornerstone of the treatment of stable COPD, as summarized in Figures 2 and 3.

Short- and long-acting β-adrenergic agonists (SABA and LABA) relax airway smooth muscle by stimulating β_2-adrenergic receptors. For single-dose, as-needed therapy, LABA (> 12 hours effect) do not provide additional benefit to SABA (4-6 hours effect) (34). However, regular use of LABAs (once or twice daily depending on the molecule) improves FEV_1 and lung volumes, dyspnoea, health status, exacerbation rate and number of hospitalizations (35-39).

Antimuscarinic drugs (short- and long-acting muscarinic antagonists, SAMA and LAMA) antagonize the bronchoconstricor effect of acetylcholine by blocking M3 muscarinic receptors of airway smooth muscle cells. LAMA treatments (especially tiotropium) improve symptoms and health status (40, 41), and reduce exacerbations rate, probably more efficiently than LABAs (42, 43). Their effect on pulmonary function tests remains debated, although recent data show increased FEV_1 in early-stage COPD patients treated with tiotropium (27, 33).

Xanthines derivatives' (i.e., theophylline) use in the treatment of stable COPD remains controversial, and data regarding their mechanism of action and pharmacokinetics are lacking. Moreover, its use is intricate. First, the metabolism of theophylline depends on cytochrome P450, and is therefore modified by numerous other drugs. Second, its therapeutic range is narrow, and its dose-related toxicity

potentially dangerous (44). In COPD, theophylline has nevertheless been shown to improve FEV_1 on top of salmeterol (45, 46). Its efficacy on the exacerbation rate is more debated but recent studies designed to unravel such effect on exacerbations (through improved steroid sensitivity) failed (47, 48).

1.1.3.2.2. Anti-inflammatory drugs

Anti-inflammatory drugs, and more particularly inhaled corticosteroids (ICS), have been widely used in the treatment of stable COPD in the past decades. However, recent studies have shown that ICS might increase the risk of pneumonia, especially in severe and very severe COPD patients (49, 50), therefore they are now only recommended in the prevention of exacerbations (Figures 2-3).

Inhaled corticosteroids. Systematic meta-analyses of the evidence currently show that regular treatment of COPD patients with inhaled corticosteroids ICS alone does not improve the FEV_1 or the mortality (51), in line with *in vitro* data showing that COPD-related inflammation is mostly cortico-resistant (52, 53). However, combining ICS and LABA is more effective than either component alone in moderate to very severe COPD patients in improving lung function, health status and reducing exacerbations (54, 55), while no effect was observed regarding mortality (56, 57). Interestingly, most studies that found an additional effect of ICS (on top of LABA) recruited patients with a recent exacerbation history (55).

Recently, studies have shown that blood eosinophil counts correlated with the magnitude of the effect of ICS (combined with bronchodilators) in preventing future exacerbations (58-62), and thresholds of < 100 eosinophils/µl and > 300 eosinophils/µl, are now recommended, identifying populations in which ICS are expected to have minimal and maximal benefit, respectively (63).

Globally, ICS are recommended in patients with exacerbations history, high blood eosinophils count, or concomitant asthma, as summarized in Figures 2 and 3.

Oral glucocorticoids. Because they have numerous systemic side effects, including steroid myopathy which can induce muscle weakness and worsen respiratory status, oral glucocorticoids have no role in the treatment of stable COPD. However, they are part of the treatment of exacerbations, that are not covered in this manuscript.

Phosphodiesterase-4 (PDE4) inhibitors reduce inflammation by inhibiting the breakdown of intracellular cyclic AMP (64). Roflumilast shows beneficial effects on exacerbations in (very) severe COPD patients, and improved lung function on top of LABA, LAMA and/or ICS treatment (65, 66). Its adverse events are however more frequent than inhaled treatments, and its use therefore is limited to severe COPD patients whose symptoms are poorly controlled under LAMA, LABA and ICS (triple inhaled therapy) (Figure 3).

Other treatments with anti-inflammatory properties have been tested in the past years, targeting cytokines (TNF-α, IL-1, IL-6, IL-8, etc), epithelial-to-mesenchymal (EMT) mediators, matrix metalloproteinases, or components of the inflammasome, as recapitulated in (52). So far, these treatments have brought disappointing results. Recent studies targeting eosinophils (using anti-IL5 and anti-IL5 receptor) showed a non-significant reduction of severe exacerbations rate in very severe patients with eosinophilic inflammation (67, 68), and these results need to be confirmed in larger studies.

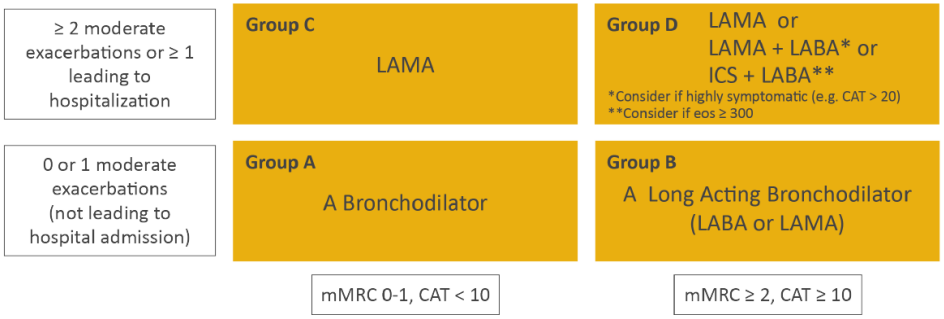

Figure 2 | Initial COPD treatment
Initial pharmacological treatment for stable COPD, as recommended by GOLD **(63)**.

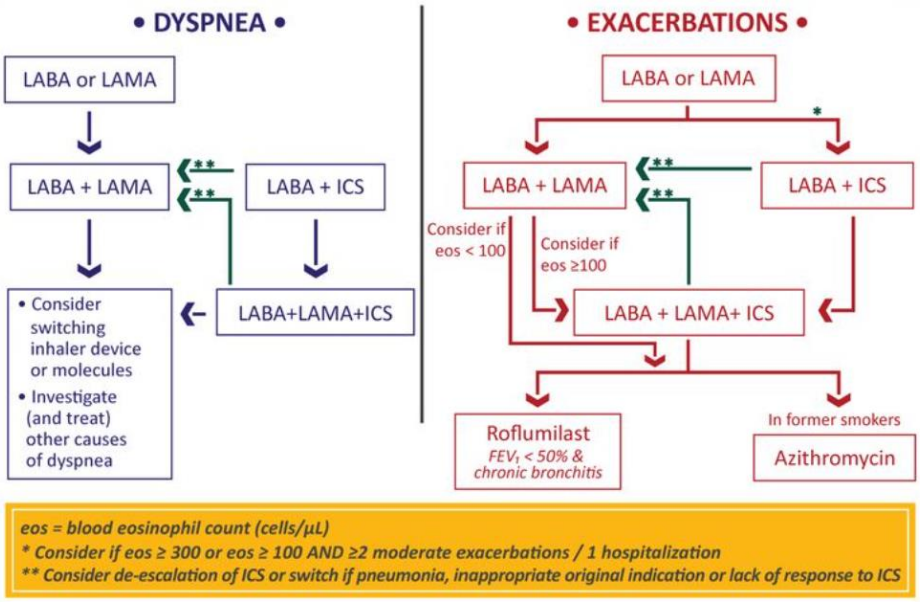

Figure 3 | Follow-up COPD treatment
Follow-up pharmacological treatment for COPD patients that experience dyspnoea or exacerbations after initiation treatment, as recommended by GOLD (63).

1.1.3.2.3. Oxygen

Oxygen administration (> 15 hours per day) has been shown to increase survival in COPD patients with chronic resting arterial hypoxemia, while no benefit was demonstrated in other groups (69).

1.1.3.3. Interventional therapies in COPD

Surgical interventions and lung transplant. Lung volume reduction surgery (LVRS), bullectomy and lung transplantation (LTx) are three surgical treatments that can be proposed to well-selected patients, usually following a pulmonary rehabilitation. LVRS consists in partial lung resection to reduce hyperinflation (70) and improve muscular efficiency and is therefore limited to carefully selected patients with emphysema (71), in which it seems to reduce the frequency of

exacerbations and to improve survival as compared with medical treatment (72). It has been shown to be more effective in heterogeneous upper lobes-predominant emphysema (73). Bullectomy consists in the removal of a large bulla that is responsible for complications, therefore decompressing adjacent lung parenchyma. In selected patients, it ameliorates symptom, lung function and exercise tolerance (74). Finally, LTx improves health status and functional capacity (but not survival) of appropriately selected patients with very severe COPD, with bilateral LTx providing longer survival than single LTx (74-76).

Endoscopic interventions. A variety of different bronchoscopic procedures has been developed as a less invasive approach than LVRS. Their common objective is to decrease thoracic volume and improve muscle mechanics (77). In selected patients with severe emphysema, endobronchial valve placement, lung coils or vapour ablation showed improved exercise tolerance, health status and lung function at 6-12 month following treatment (78-82).

1.2.The airway epithelium (AE)

The airway respiratory epithelium lines the surface of the respiratory tract from nasal cavities to respiratory bronchioles. As this manuscript focusses on the bronchial epithelium, we will not elaborate on the alveolar epithelium, which largely differs from the trachea-bronchial epithelium, both histologically and functionally.

1.2.1. Histology

The human airways are classically separated into upper and lower airways, including nasal cavities, sinuses, pharynx and larynx on upper side, and trachea, bronchi, bronchioles and respiratory bronchioles on the lower side.

The trachea and large bronchi (diameter > 2 mm) are supported by a cartilaginous semi-rigid scaffold, that provides stability, and are characterized by the presence of submucosal glands containing goblet, duct, and serous cells that contribute to mucus production and fluid. Small airways (diameter < 2 mm) display none of these

structures and end with respiratory bronchioles. Most of the bronchial, pseudostratified AE consists of ciliated and goblet cells that together constitute the mucociliary elevator that serves to clear particulates and other irritants out of the airspaces. Besides these cell types, the AE is also composed by basal, club and neuroendocrine cells, and finally ionocytes (83).

Ciliated cells are prominent and represent more than 50% of all airway epithelial cells. They possess around 300 cilia whose synchronized beating pushes the mucus layer towards the trachea and the larynx (84). **Goblet cells**, accounting for 5 to 15% of airway epithelial cells, produce mucus and are not present in small airways (84). **Basal cells** are multipotent stem cells that both anchor the epithelium to the underlying lamina propria and drive epithelial homeostasis and orderly regeneration after injury (85, 86). They represent 5 to 30% of epithelial cells, their proportion decreasing from the trachea down to the respiratory bronchioles (87). **Club cells** are dome-shaped cells involved in host defence, and represent 20% of epithelial cells in small airways, where they also behave as progenitor cells (88, 89). **Neuroendocrine cells** are rare, innervated cells (< 1% of airway epithelial cells) (90) that are thought to be involved in oxygen sensing, smooth muscle tonus and immune responses (91, 92). Finally, recently discovered **ionocytes** seem to control the airway surface liquid and mucus viscosity (93).

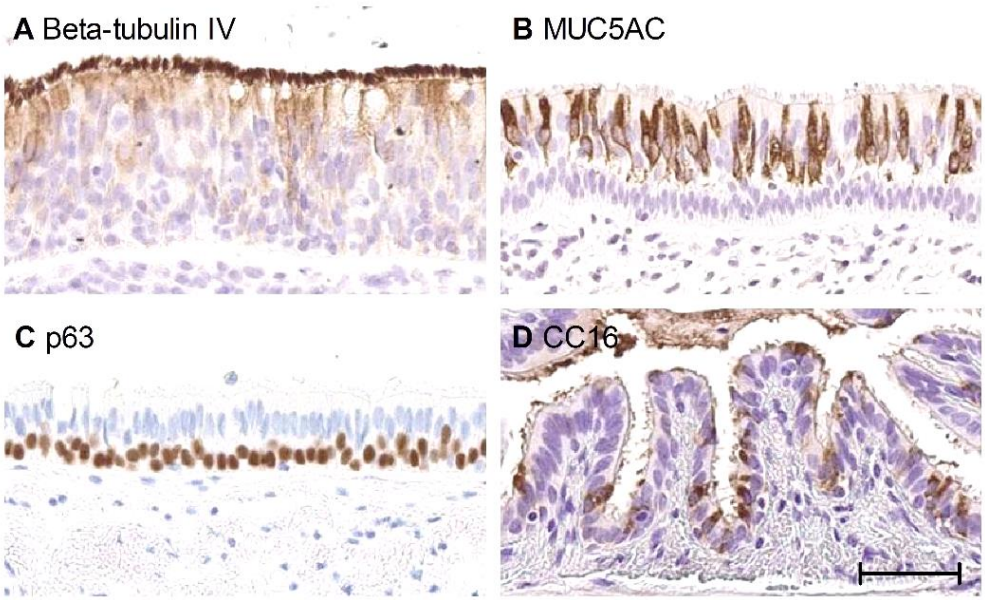

Figure 4 | Main airway epithelium cell types
Identification of airway epithelium cell types in large (A, B, C) and small airways (D) (courtesy of Pr. S. Gohy) **A.** Ciliated cells stained for β-tubulin IV. **B.** Goblet cells stained for MUC5AC. **C.** p63 immunostaining in a large airway portion showing basal cells. **D.** Club cells stained for SCGB1A1. Scale bar, 50 µm.

1.2.2. Functions

1.2.2.1. Physical barrier

The epithelial surface is constantly exposed to inhaled particles, and its physical barrier constitutes the first line of defence against airborne pathogens. Epithelial apical junctional complexes (AJCs) promote cell-cell adhesion and barrier integrity and regulate the paracellular passage of ions and macromolecules. AJCs include both tight junctions and adherens junctions, while desmosomes and gap junctions provide localized cell-cell adhesion sites but are not part of AJCs.

Tight junctions contribute to the highest resistance of the epithelium. They separate the apical and basolateral poles of epithelial cells, and are thereby critical determinants of epithelial polarity (94). Three types of transmembrane proteins compose tight junctions: (a) members of the claudin family, (b) MARVEL family members such as occludin, and (c) Ig-like proteins such as junctional adhesion molecules (JAMs) (95-97). E-cadherin and nectin family members represent the major transmembrane proteins of **adherens junctions** (98, 99). E-cadherin associates with both α- and β-catenin (see paragraph 1.4. for further information about β-catenin signalling pathway) and retains epidermal growth factor receptor (EGFR) ligands in adherens junctions, preventing their interaction with the receptor (100). Adhesive components of the AJCs are stabilized by links to intracellular proteins including zonula occludin (ZO) proteins, catenin-family proteins, and actin perijunctional belt binding proteins (101). A schematic view of AJCs is provided in Figure 5.

Besides AJC structures, **desmosomes** (also known as *macula* adherens) are localized, spot-like adhesions that allow anchoring to the intermediate filaments of the cytoskeleton (through desmoglein, desmocollin, plakoglobin, plakophilin and plakin) (102), while **gap junctions** are specialized in intercellular communications (103).

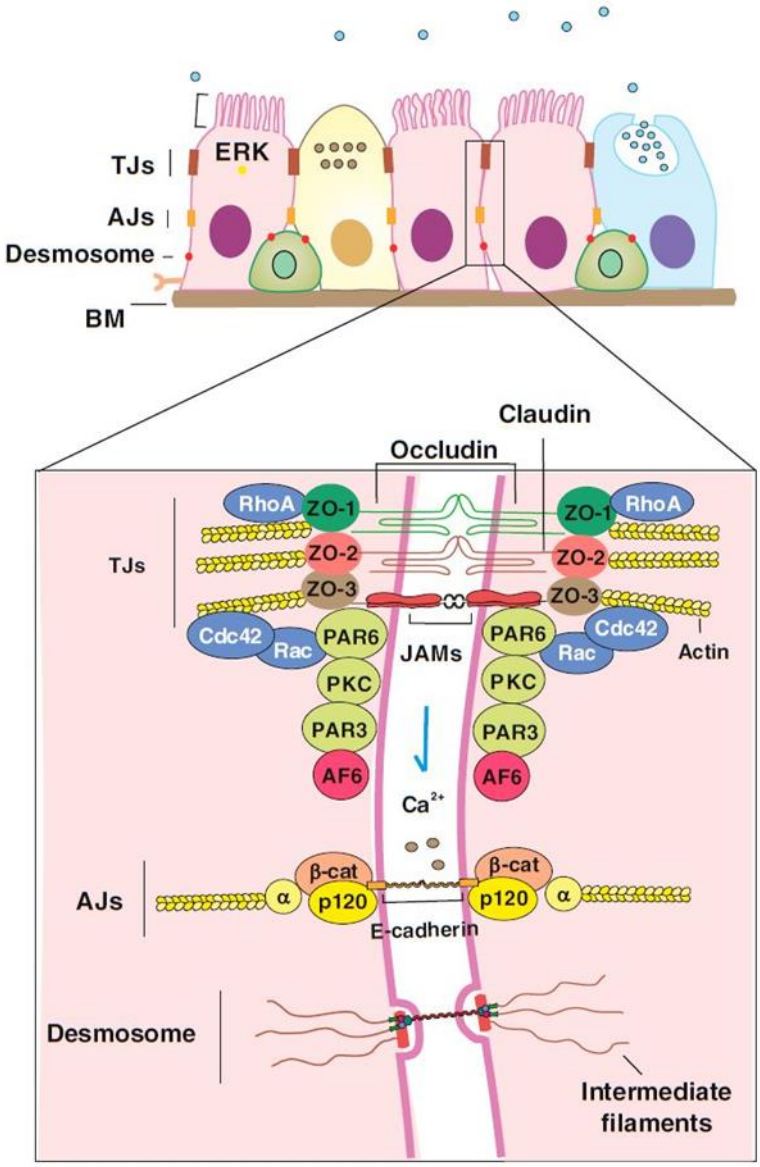

Figure 5 | Apical junctional complexes
Schematic view of AJCs, composed of luminal tight junctions (TJs) and adherens junctions (AJs) (image from (104)).

1.2.2.2. Homeostasis and repair

Homeostasis and regeneration of the AE are crucial functions that are fulfilled by multipotent stem cells (basal cells) (85). In steady state, most of basal cells are quiescent and express p63 and keratin (KRT)-5 (105). The AE renewal is slow, with 30-50 days (106) or even 100 days (107, 108) as turnover periods. The current paradigm from *in vivo* lineage tracing experiments is that basal cells (and probably club cells in small airways, from murine studies) self-renew a pool of progenitors that give rise to luminal, differentiated cells during homeostasis and after injury (86). *In vivo* and *in vitro* studies have shown that during normal epithelial repair, a subtype of basal cells expressing keratin-14 (KRT14) proliferates before differentiating into ciliated and goblet cells, to reconstitute a functional respiratory epithelium (109-111). The signalling network that regulates the restoration and redifferentiation of airway epithelial cells is complex and incompletely understood, and involves Notch (112-115), WNT (116-118), Sonic Hedgehog (SHH) (119), TGF-β (120, 121), EGF (122) and FGF pathways (123).

In chronic respiratory diseases, and more particularly in COPD, repair processes are impaired and result in abnormal epithelial differentiation that promotes tissue remodelling and fibrosis as well as tumorigenesis (124, 125) (see paragraph 1.3.3 on epithelial-to-mesenchymal transition)

1.2.2.3. Mucociliary clearance

Mucociliary clearance results from the coordinated interaction between submucosal glands, goblet cells and ciliated cells, and therefore requires proper ciliary function and appropriate mucus viscosity, quantity and composition. The mucus layer is composed by two distinct layers: (a) a low viscosity periciliary layer that lubricates the epithelial surface and facilitates ciliary beating; and (b) a luminal layer, enriched in mucins (see paragraph 1.2.2.4), that entraps inhaled particles and pathogens (126, 127). The rheological properties of mucus are determined by its composition, with normal mucus being composed of ∼1% mucins, ∼1% salt, ∼1% other proteins, and

~97% water. The mucus hydration is regulated by Cl^- and Ca^{2+} efflux, and Na^+ influx, respectively depending on cystic fibrosis transmembrane conductance regulator (CFTR), Ca^{2+}-activated chloride channels (CaCC) and epithelial Na^+ channel (ENaC) (128). In chronic respiratory diseases, both ciliary beating and mucus quality may be altered, leading to insufficient pathogen eviction, increased infectious risks and chronic inflammation.

1.2.2.4. Innate immunity

Besides its physical barrier and mechanical removal of inhaled pathogens by mucociliary clearance, the AE has developed other functions to limit microbial invasion and trigger adapted immune responses, including the recognition of micro-organisms, the secretion of chemo/cytokines or the active production of anti-microbial substances (129, 130).

Recognition of micro-organisms. Pathogen-associated molecular patterns (PAMPs) are pathogen-specific, invariant molecular structures that can be bound by pattern recognition receptors (PRRs), therefore contributing to the microbial detection by airway epithelial cells, then to the initiation of immune response. PRRs are divided in four families, including Toll-like receptors (TLRs) that are expressed by most airway epithelial cells. After binding PAMPs, PRRs initiate downstream signalling (for instance through MyD88 and TRIF in the case of TLRs), ultimately leading to immune response (131).

Mucins. Mucins are large glycoproteins produced by secretory cells (goblet cells, club cells, and serous and mucous cells of the submucosal glands) (132), and are encoded by 21 MUC genes, coding either for secreted mucins (e.g. MUC2, MUC5AC and MUC5B), or cell-tethered mucins (e.g. MUC1, MUC3A&B or MUC4)(133). MUC5AC, MUC5B and MUC2 predominate in the airway mucus, and MUC5B has been recently reported to play an important role in host defence (134).

Host defence peptides. Host defence peptides of the airways (also known as antimicrobial peptides) include β-defensins, cathelicidins, lysozyme, lactoferrin, secretory leukocyte protease inhibitor (SLPI) and elafin, all of them targeting bacteria, viruses, parasites and/or fungi by diverse mechanisms.

β-defensins are small cationic peptides that interact with microbial lipids and cover gram-positive and -negative bacteria as well as enveloped viruses and fungi (135). Amongst their numerous other roles (136), β-defensins seem also able to attract immune cells and to activate dendritic cells (137).

Cathelicidins regroup a family of three highly cationic peptides (the most studied is LL-37) that interact with negatively charged bacterial membranes, and have antimicrobial effects against fungi, parasites and viruses, mediated by varied mechanisms. They are constitutively secreted in low concentrations by epithelial cells, but higher local concentrations may be reached by neutrophils degranulation (138).

Lysozyme is one of the most abundant protein in the human airway secretions and is secreted by submucosal glands, neutrophils and macrophages. It is a 14kDa protein that has dual activities as lytic enzyme and cationic protein, targeting peptidoglycans from bacterial walls and disrupting their membranes. Similarly to β-defensins and cathelicidins, lysozyme is thought to have immunomodulatory functions that are not yet fully elucidated (139).

Lactoferrin is an iron-binding glycoprotein, mainly produced by neutrophils, that damages the outer membrane of gram-negative bacteria, and that can bind and sequestrate lipopolysaccharide, neutralizing its toxic effects (140).

SLPI and elafin are low-molecular weight antiproteinases that are produced by goblet cells, club cells, and macrophages, while neutrophils contain SLPI. They display distinct spectra, as SLPI inhibits neutrophil elastase, cathepsin G, trypsin, chymotrypsin, and chymase, while elafin inhibits neutrophil elastase and proteinase-3 (141). They both prevent the inappropriate activity of extracellular proteases during inflammation and have antimicrobial (142) and immunoregulatory activities (143, 144).

Finally, *club cell secretory protein* (CCSP), also known as secretoglobulin family 1A member 1 (SCGB1A1), CC16, CC10 or uteroglobin, is the main protein secreted by club cells. It maintains AE homeostasis, contributes to the harmonious composition of epithelial lining fluid (145), and displays anti-inflammatory effects upon CS, allergen and virus challenges (89, 146-148).

Airway epithelial chemokines and cytokines. Epithelial cells are able to shape immune and inflammatory responses by secreting cytokines, chemokines and alarmins that regulate the adaptive immune system. Pro-Th2 cytokines such as thymic stromal lymphopoietin (TSLP), IL-25, and granulocyte-macrophage colony-stimulating factor (GM-CSF) are produced in response to allergen stimulation (149-151), and recent evidence suggests that a type 2-biased response of epithelial cells to allergens probably contributes to the inception of several allergic disorders, including asthma (152). The AE can also produce IL-8, a strong neutrophil chemo-attractant (153), the pro-inflammatory cytokine IL-6 (154), and anti-inflammatory/regulatory molecules such as TGF-β (155, 156). Finally, damaged epithelial cells may also release alarmins such as HMGB1, S100 family proteins, IL-33 and IL-1α that initiate specific immune response through PRRs (157).

1.2.2.5. IgA-mediated lung immunity

Immunoglobulin A (IgA) is the predominant Ig in mucosal secretions (158), and contributes to the frontline immune defence to inhaled antigens. Although IgA also lies in the serum, where it is mainly found as monomers, IgA main functions relates to its mucosal localization, encompassing immune exclusion, blockade of microbial adherence, and regulation of leucocytes. In the airways lumen, IgA is mostly found as secretory (S-)IgA, consisting of two 160 kDa IgA monomers, covalently linked to a 15 kDa joining polypeptide (J-chain) (Figure 6) (159).

To be able to exert its functions at the mucosal surface, dimeric (d-)IgA, once secreted by subepithelial plasma cells, binds to the polymeric immunoglobulin receptor (pIgR), a 100 kDa protein expressed at the basolateral pole of airway epithelial cells (Figure 7). pIgR is then endocytosed in clathrin-coated vesicles that are transported across the epithelial layer towards the apical pole, where a proteolytic cleavage releases dimeric IgA bound to most of the extracellular domain of the pIgR, called secretory component (SC), therefore forming S-IgA (Figure 8). Transcytosis of unbound pIgR also occurs, releasing free SC that can be found in most exocrine secretions (160).

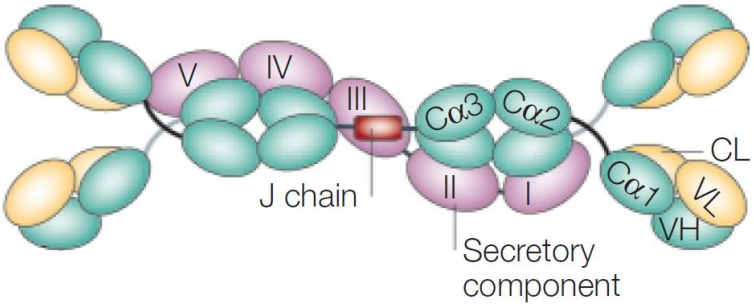

Figure 6 | S-IgA structure
Schematic structure of S-IgA (modified from (161)), composed by dimeric IgA (two IgA monomers linked with a J chain) and SC.

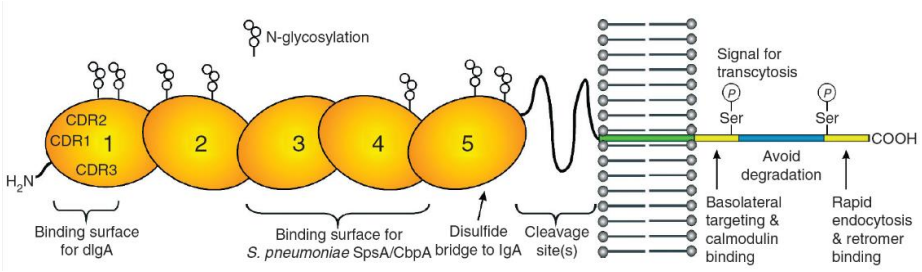

Figure 7 | Human polymeric immunoglobulin receptor structure.
Schematic structure of the human polymeric immunoglobulin receptor (pIgR) (from **(162)**). The pIgR is a transmembrane receptor, composed by (a) an extracellular part comprising five domains that constitutes the secretory component, and (b) a membrano-cytoplasmic domain that regulates transcytosis.

Immune exclusion. At mucosal surfaces, IgA acts as innate immunoprotein by scavenging noxious antigens and preventing adherence of microorganisms to the epithelial surface, achieving the so-called 'immune exclusion' (163). Immune exclusion comprises successive events: (a) agglutination, where S-IgA mediates cross-linking via polyvalent surface antigens (164), (b) entrapment in mucus, that is enhanced by the presence of the secretory component (SC, see below) as it associates with mucus through its oligosaccharide side chains (165, 166), and (c) clearance via the mucociliary escalator.

Blockade of microbial adherence and selection of microbiota. On top of immune exclusion, S-IgA also prevents adhesion of toxins (e.g., cholera toxin) and pathogens to the epithelial surface (167-169), notably by direct recognition of receptor-binding domains. Recently, S-IgA has also been described to control the composition of the gut microbiome (170) with $pIgR^{-/-}$ mice also displaying modified lung microbiome, paving the way for future research in the field (171).

Regulation of leucocytes. IgA is able to interact with neutrophils, eosinophils, monocytes, macrophages and dendritic cells, as these cell types express the Fcα receptor (FcαRI, also known as CD89) (172). The ligation of CD89 could promote protective pathways involved in the clearance of trespassing microorganisms and in the induction of T-cell suppressive mechanisms (173, 174). Moreover, the binding of S-IgA to the DC-SIGN/SIGNR1 receptor on dendritic cells favours the development of tolerogenic dendritic cells (175).

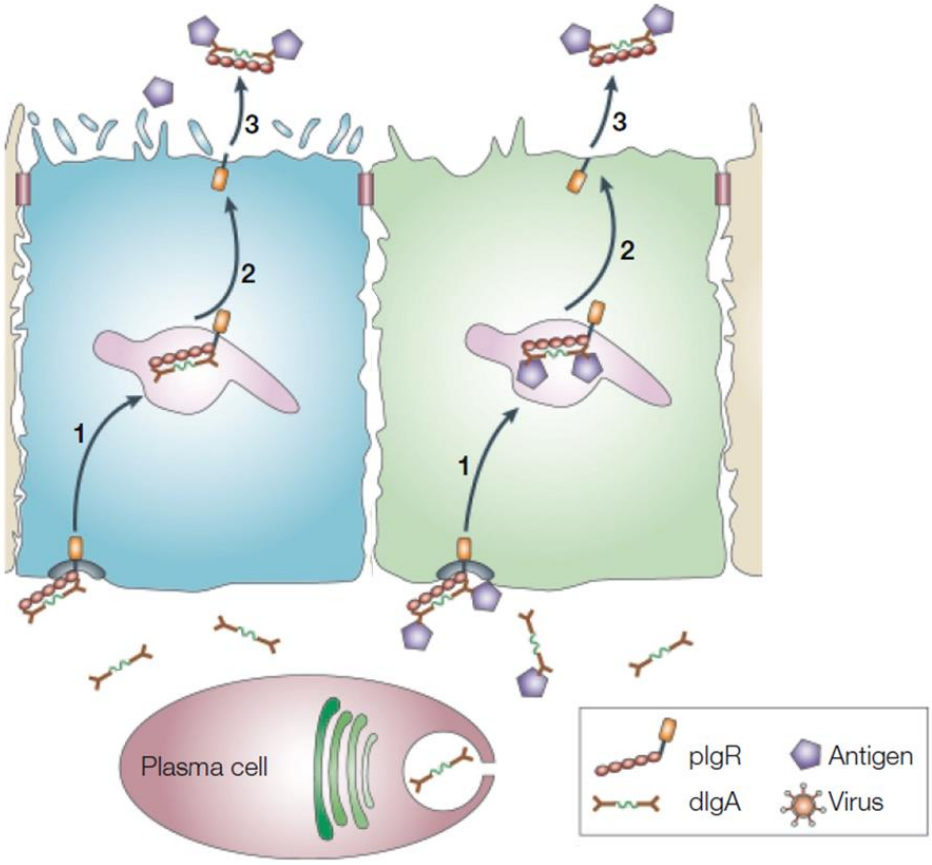

Figure 8 | pIgR-mediated S-IgA transcytosis
The role of pIgR at mucosal surfaces (modified from (161)). Left: formation of S-IgA. d-IgA is secreted by plasma cells and binds to the pIgR at the basolateral pole of the epithelium. The d-IgA-pIgR complex is transported through endosomal compartments (arrow 1) to the apical pole of the epithelium (arrow 2), where a proteinase cleaves the extracellular domain of the pIgR, called secretory component (SC). This process leads to the release of SC bound to d-IgA (arrow 3) and to the formation of S-IgA. Right: immune exclusion of trespassing antigens is allowed by their binding to pIgR–d-IgA, their internalization (arrow 1), their transport across the cell (arrow 2) and their release at the apical pole (arrow 3), where they are cleared.

1.3.The airway epithelium in COPD

The bronchial epithelium, as first line barrier against inhaled particles and antigens, is constantly exposed to airborne pollutants. As cigarette smoke contains more than 7000 chemicals, including oxidative gases, heavy metals and carcinogenic substances, the load of toxic particles is especially high in smokers (176), amongst which approximately 25% will develop COPD. In COPD, the AE structure and biology are profoundly altered by the chronic exposure to cigarette smoke, and the AE displays important changes in terms of barrier function, cell differentiation and epithelial-to-mesenchymal transition (EMT), inflammation and IgA-mediated mucosal immunity.

1.3.1. Barrier dysfunction

Cigarette smoking exposure alone has been shown to impair barrier function (177) and to decrease the expression of tight junction proteins (OCLN1, ZO1) (178), but the AE from COPD patients seems even more prone to develop barrier dysfunction. Indeed, most of the known apical junction genes whose expression is impaired in smokers, are further downregulated in COPD patients (179), while zonula-occludens 1 (ZO1) and occludin protein levels are lower in COPD samples than in those issuing from smokers, both *in* situ in the native AE and *in vitro* in derived air/liquid interface (ALI)-cultured epithelium (180). In addition, COPD human bronchial epithelial cells (HBEC) exposed to cigarette smoke extract showed decreased E-cadherin and ZO-1 expression as compared with HBECs from smokers, possibly due to reactive oxygen species (ROS)-dependent decrease in cAMP (181). Globally, COPD AE displays increased epithelial permeability, probably favouring microbial invasion and COPD exacerbations, which account for a significant part of COPD morbidity (104, 182, 183).

1.3.2. Lineage abnormalities

In COPD, the cell composition of the pseudostratified respiratory epithelium is deeply modified. First, basal cells hyperplasia has historically been considered one

of the earliest change associated with cigarette smoking (184), and recent studies show that in COPD, basal cells exhibit impaired stemness (185, 186) and altered transcriptional program (187, 188). Second, and similarly to asthmatic patients, COPD patients display hyperplastic goblet cells (or mucous metaplasia) (189, 190), a feature that is driven by the transcription factors SPDEF and FOXA3 (191, 192), and that is possibly more related to smoking rather to COPD *per se* (193). Third, decreased numbers of ciliated cells are observed in the COPD AE (190, 194), with remaining cells exhibiting dysfunctional primary cilia (195), reduced cilia beating frequency (196, 197), and cilia shortening (198, 199). Finally, club cells numbers are decreased in the COPD AE, as is their production of secretoglobulin family 1A member 1 (SCGB1A1) also known as CCSP, CC10 or CC16 (200, 201). Interestingly, part of the altered lineage differentiation of the AE may be recapitulated *in vitro*, in the AE reconstituted by culture in ALI of HBEC from COPD patients (190).

1.3.3. Epithelial-to-mesenchymal transition

Epithelial-to-mesenchymal transition (EMT) is a physiological and dynamic process during which epithelial cells lose their polarity, adhesiveness and anchorage to the basal membrane, and acquire mesenchymal features, such as migratory abilities through the reorganization of their cytoskeleton (94, 202) (Figure 9). Thus, epithelial cells ongoing EMT express vimentin, N-cadherin, α-smooth muscle actin (α-SMA), S100A4, and fibronectin.

EMT programming is crucial to embryogenesis (type I EMT), tissue repair (type II), and cancer metastasis (type III), and is regulated by an intricate network of pathways, including WNT and TGF-β (94). In the last decade, several studies showed CS leads to TGF-β-induced EMT that is further enhanced in COPD patients, both in small (181) and large airways (203-205) therefore promoting airway fibrosis, impaired epithelial repair, as well as carcinogenesis and metastasis potential (206-208). As for lineage abnormalities, ALI cultures from COPD patients spontaneously reproduce

mesenchymal features, while cigarette smoke may induce EMT in control HBEC, possibly as a result of TGF-β signalling (209).

1.3.4. Inflammation

Inflammation is a paramount feature in COPD, that is thought to represent a major player in the disease pathophysiology (210), as schematized in Figure 10. Indeed, numerous pro-inflammatory cytokines and inflammatory cells numbers are increased in most compartments of the lung in COPD (211).

Cytokines. In COPD, epithelial cells are activated by cigarette smoke and/or other inhaled irritants, to produce inflammatory mediators such as TNF-α, IL-1β, IL-6, IL-8, or GM-CSF (212). In addition, TNF- α, IL-8 are produced by activated alveolar macrophages, and various other chemokines (including IL-8) are produced by neutrophils. Accordingly, TNF-α, IL-1β, IL-6 and IL-8 increased levels were observed in BAL from smokers (213), and in sputum from smokers and stable COPD patients (214). IL-6 and IL-8 levels were further increased in sputum from exacerbating COPD patients (215). In addition, several other cyto/chemokines are increased in COPD such as GROα, MCP-1, IL-5 and IL-13.

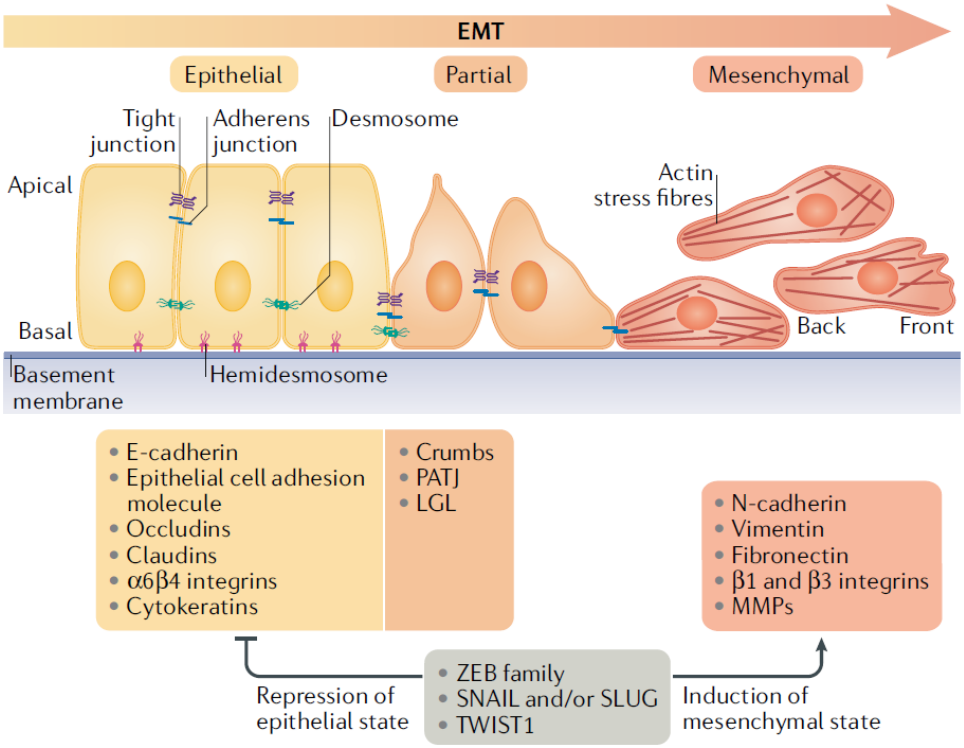

Figure 9 | Epithelial-to-mesenchymal transition process
Schematic representation of EMT process, recapitulating classic epithelial and mesenchymal markers, and main transcription factors promoting EMT (modified from (216)).

Inflammatory cells.

Neutrophils. COPD is generally considered a "neutrophilic disease", as neutrophils have been shown to be increased in the serum (217), bronchoalveolar lavage (218, 219), and sputum (214, 220, 221) from COPD patients, probably as a result of enhanced IL-8 release from activated epithelial cells and alveolar macrophages. Whether neutrophils are increased in the airway wall in COPD remains uncertain, as unchanged (219, 222-225) and increased (226, 227) neutrophil counts have been reported in both small and large airway walls from COPD patients.

Macrophages. The total number of macrophages in the airway lumen (213, 228) and in the BAL (218, 219, 229) is increased in smokers and COPD patients, and they probably play a role in emphysema by releasing elastolytic enzymes such as MMP-9, elastases and cathepsins (230). As for neutrophils, the quantification of the airway subepithelial macrophage population in COPD does not bring conclusive results, with increased (222, 231, 232) or unchanged counts (224, 233) as compared with controls.

Other cell types. Besides neutrophils and macrophages, numerous leucocytes have been studied in COPD, including $CD4^+$ and $CD8^+$ T cells, B cells, eosinophils, mast cells and dendritic cells. Although these studies provide scattered results, the global picture shows increased leucocyte populations in COPD, underlining the inflammatory background of the disease (210).

1.3.5. Transcytosis of IgA

As described in other chronic lung diseases such as asthma (234, 235), and lung cancer (236), the COPD AE displays impaired pIgR expression and SC production, this defect correlating to airway obstruction and inflammation (237-240). Accordingly, decreased S-IgA concentrations are found in BAL from smokers and COPD patients (241). pIgR/SC system dysfunction, in terms of altered pIgR expression and d-IgA transcytosis, is recapitulated in 28-days ALI cultures of airway epithelial cells from COPD patients (237). In addition, $pIgR^{-/-}$ mice are more susceptible to develop airway fibrosis and emphysema (171), probably through inflammatory pathways triggered by increased microbial load.

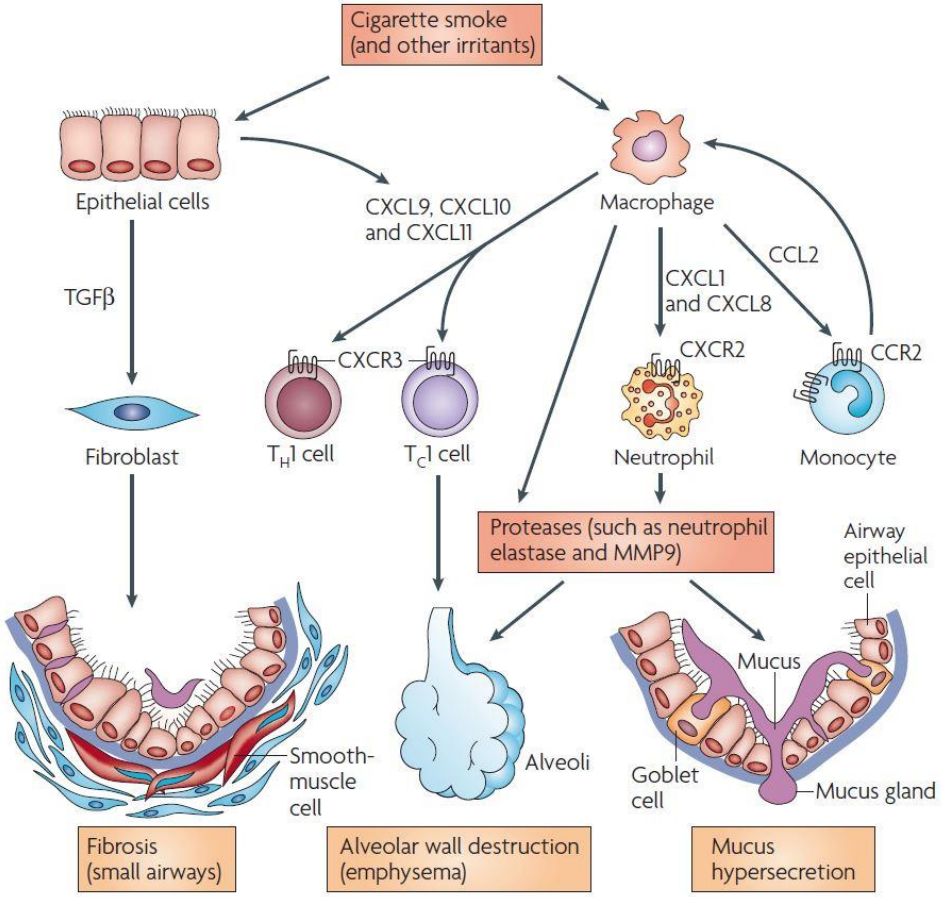

Figure 10 | Inflammation in COPD
The central role of inflammation in the pathogenesis of COPD, both at the bronchial and parenchymal levels (from (242)).

1.4.WNT signalling pathways

Discovered in the early 1980s (243), the Wingless/Integrase-1 (WNT) signalling pathways play a central role in developmental processes along with Notch, SHH, and bone morphogenetic (BMP) pathways, and are crucial to lung morphogenesis (244). In addition, WNT signalling is involved in adulthood in the daily processes of tissue homeostasis and repair in numerous tissues. Given its vast array of functions, the WNT signalling pathways require tight regulation mechanisms, and aberrant

WNT signalling has been associated with various cancers (245), organ fibrosis (246-248), neurodegenerative diseases (249) and metabolic diseases (250).

Nineteen WNT ligands (WNTs) are known in humans. They are secreted, cysteine-rich glycoproteins acting in a short range to couple various receptors, thereby activating different downstream pathways (251), which are classically dichotomized into canonical and noncanonical signalling pathways. Thus, the canonical WNT signalling pathway relies on the activation of β-catenin, a multifunctional protein that acts as transcriptional co-factor, while noncanonical signalling is β-catenin-independent and results in the activation of intracellular signalling molecules involved in planar cell polarity (PCP pathway), calcium/calmodulin-dependent protein kinase II signalling (Ca^{2+}/CAMKII) and other less well defined molecular cascades (252).

1.4.1. Canonical WNT/β-catenin pathway

In the absence of canonical WNT stimulation (e.g. WNT-3a and -8), a multiprotein complex called "β-catenin destruction complex" regulates the pool of intracellular β-catenin by phosphorylation (via subunits casein kinase 1 and glycogen synthase kinase 3β) and ubiquitination (via β-Transducin Repeat Containing E3 Ubiquitin Protein Ligase), ultimately addressing β-catenin to proteasomal degradation (253). This mechanism prevents β-catenin migration to the nucleus, where expression of WNT target genes is constitutively repressed by a complex composed by T-cell factor/lymphoid enhancer-binding factor (TCF/LEF) and transducing-like enhancer of split protein (TLE/Groucho). The binding of a specific WNT ligand to one of the Frizzled receptors (FZD_{1-10}) and lipoprotein receptor-related protein (LRP_{5-6}) co-receptor indirectly leads to the inactivation of the destruction complex and to the accumulation of intracytoplasmic, unphosphorylated β-catenin, whose migration to the nucleus and binding to TCF/LEF will transactivate its target genes (254), including epithelial-to-mesenchymal (EMT)-promoting transcription factors (255). Figure 11 schematizes the canonical WNT signalling.

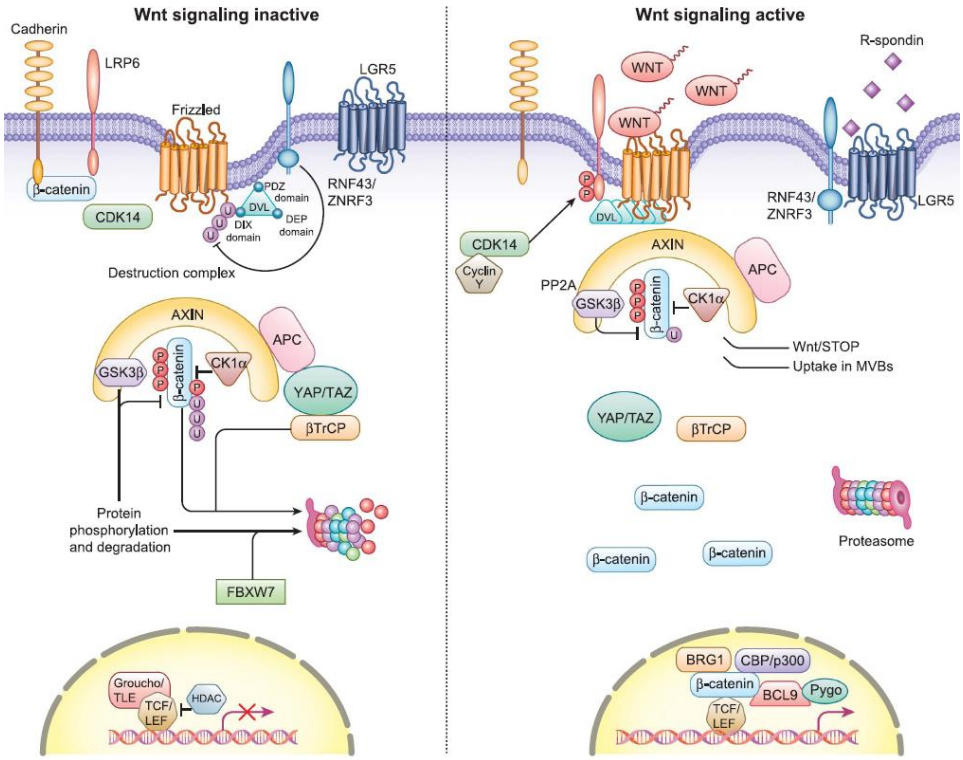

Figure 11 | Canonical WNT pathway
Schematic overview of the canonical WNT pathway. Left panel: in the absence of canonical WNT ligand, the β-catenin destruction complex addresses β-catenin to proteasomal degradation. Right panel: the binding of a canonical WNT ligand leads to the inactivation of the destruction complex, allowing the cytoplasmi**c** (and then nuclear) accumulation of unphosphorylated (active) β-catenin (modified image from (256)).

1.4.2. Noncanonical WNT pathways

Activation of the noncanonical WNT pathways depends on the binding of a noncanonical WNT ligand (such as WNT-4 and WNT-5a) to a FZD receptor. Unlike canonical signalling, noncanonical WNT pathways do not require the recruitment of LRP_{5-6} co-receptors. On the one hand, WNT/PCP signalling is initiated by the binding of a WNT to the ROR-FZV receptor complex, to recruit and activate

Dishevelled (DVL). DVL then activates the ROC kinase and JNK pathways, ultimately driving rearrangements of the cytoskeleton and (116, 257). On the other hand, WNT/Ca^{2+} signalling is initiated by G-protein-triggered phospholipase C activity, leading to intracellular calcium fluxes and downstream Ca^{2+}-dependent cytoskeletal modifications and transcriptional responses (258, 259). Noncanonical WNT pathways are schematized in Figure 12.

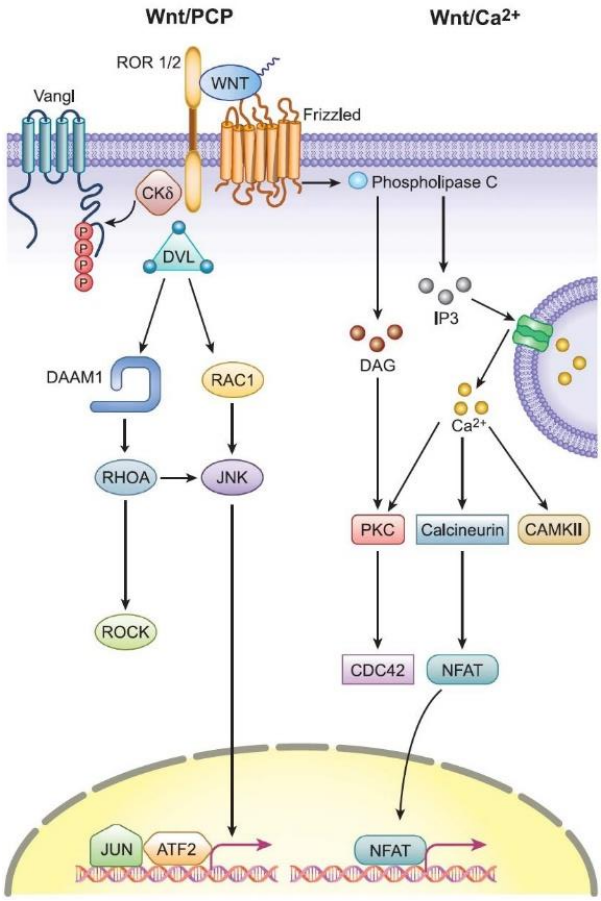

Figure 12 | Noncanonical WNT pathways
Main noncanonical WNT signalling pathways, namely WNT/PCP and WNT Ca^{2+} pathways (modified image from (256)).

1.4.3. WNT pathways in chronic respiratory diseases

As key players in organ development, tissue homeostasis and repair, WNT pathways have been widely studied in various diseases, including chronic respiratory diseases.

Pulmonary fibrosis. Impairment of WNT pathways in chronic lung diseases was first identified in idiopathic pulmonary fibrosis (IPF), a devastating disease characterized by fibroblast activation and extracellular matrix deposition, leading to distorted lung architecture and loss of function (260). Gene expression profiling of experimental models of lung fibrosis provided "WNT signature" in the IPF lung, where canonical WNT signalling is active as witnessed by increased mRNA abundance of many of its components, including *WNT-1, -7B* and *-10*, *CTNNB1*, as well as *FZD2* and *FZD3* (261-263). WNT-inducible signalling protein-1 (WISP1), a downstream target of both canonical WNT signalling and other profibrotic pathways including TGF-β), is also increased in IPF and is thought to be a promising therapeutic target.

Asthma. Asthma is an immune-mediated disease that includes airway hyperreactivity, with a prevalence ranging from 1 to 22% of the population according to the countries (264). It is most frequently associated with a type 2 (T2) immuno-inflammatory phenotype (265) that includes increased eosinophils, while different subsets can be distinguished according to age of onset, allergic background and comorbidities (obesity, nasal disease, aspirin sensitivity). A "non-T2" phenotype, often with increased neutrophils and Th17 cells, also exists but remains poorly understood.

Global evidence reveals that aberrant canonical WNT signalling during embryonic lung development could contribute to later asthmatic remodelling. For instance, *WISP1* and WNT-inhibitory factor-1 (*WIF-1*) genes have been associated with impaired lung functions in children, while a single nucleotide polymorphisms in *WISP1* has been linked with decreased FEV_1 (266, 267). In parallel data obtained from maternal smoking (268) and childhood wheezers (269-271) suggest an

association between differential expression of canonical WNT components and asthmatic airway remodelling. More recently, Hachim and colleagues demonstrated an imbalance between WNT enhancers and inhibitors in the bronchial epithelium of severe asthma patients (272), with T2 phenotype being associated with upregulated WNT inhibitors, while neutrophilic asthma displays enhanced canonical WNT signalling. Finally, in human asthmatic airways, multiple WNT ligands mRNA abundance is associated with a T2 inflammation, such as *WNT-3A*, *WNT-5A*, *WNT-6* and *WNT-10A*, while WNT receptor *FZD5* is upregulated in patients with T2-high asthma (273).

COPD. In COPD, persistent reactivation of developmental signalling cascades has emerged as a new paradigm (274). Upregulated noncanonical WNT signalling, through increased WNT-5a and -5b, has been demonstrated in COPD (275, 276), contributing notably to emphysema (characterized by the disruption of alveolar walls) by negatively regulating alveolar repair, while decreased FZD4 in COPD leads to reduced canonical signalling and impaired alveolar repair capacity (277). On the other hand, extrinsic activation of the canonical pathway (by LiCl or CHIR99021) in elastase-induced murine emphysema (278) and *ex-vivo* three-dimensional murine lung tissue cultures (279) attenuated emphysema. Moreover, the FAM13A gene, associated with COPD in genome-wide association studies (280), is suspected to promote β-catenin degradation, increasing disease susceptibility in murine elastase-induced emphysema (281). Taken together, these results suggest a shift from canonical to noncanonical WNT signalling in the COPD alveolar epithelium that underlies emphysema.

In contrast, data regarding WNT dysregulation at the *airway* epithelium (AE) level remain controversial. Thus, the noncanonical ligand WNT-4 was upregulated in COPD bronchial biopsies (282), and potentiated cigarette smoke-induced inflammation in 16HBE cells (283). The expression of noncanonical ligands WNT-4 and -5b was increased in COPD-derived primary human bronchial epithelial cells (HBECs) redifferentiated upon air/liquid interface (ALI), compared with controls

(283, 284). Nicotine-exposed HBECs showed increased canonical WNT-3a expression that further induced EMT (285), and the canonical FZD8 receptor was found to promote epithelial inflammation in cigarette smoke-exposed mice (286). The activation of the WNT/β-catenin pathway by CHIR99021 in ALI-HBEC also inhibited the commitment towards ciliated cells (117). Conversely it was however shown that several canonical components, including β-catenin, were downregulated in the small AE from COPD patients, either from endobronchial biopsies and brushings (287) or surgical lung tissue (288). Globally, these results consistently show an activation of the noncanonical WNT pathways in the proximal AE in COPD, while divergent results are seen concerning the WNT/β-catenin pathway.

1.5. Air/liquid interface cultures

Most of the data and results reported in this manuscript were obtained by using ALI-reconstituted airway epithelial layers. This model allows the reconstitution of a pseudostratified airway epithelium from surgical or endoscopic bronchial samples and is widely used in respiratory research to assess epithelial biology in health and disease.

1.5.1. Technical aspects

After lung surgery (either lobectomy or lung transplant), a large piece of cartilaginous bronchus is selected, and submitted to pronase digestion overnight at 4°C, allowing the detachment of bronchoepithelial cells. After removal of the surgical piece, HBEC in suspension are pelleted by centrifugation, then re-suspended at a pre-defined concentration. Next, cells are seeded into flasks in retinoic acid-supplemented Bronchial Epithelial Cell Growth Basal Medium (BEBM, Lonza, Verviers, Belgium). A small proportion (~10%) of seeded cells will attach to the plate and grow until ~80% confluence is reached, after 5 to 14 days depending on the number of seeded cells and the replication rates. Culture medium is emptied and renewed every other day.

Once near-confluence is reached (3-6 x 10^6 cells in 75 cm^2 flasks), cells are detached using trypsin 0,25% (Reagent Pack CC-5034, Lonza, Verviers, Belgium), assessed for viability (~80-90%) and seeded at a density of 80,000 cells/well on 24-well polyester filter-type inserts (0.4-µm pore size; Corning, Corning, NY) coated with 0.2 mg/ml collagen IV (Sigma-Aldrich, Saint-Louis, MO). Most alive cells will attach to the membrane and grow in submerged conditions in retinoic acid-supplemented Bronchial Epithelial Cell Growth Basal Medium (BEBM, Lonza, Verviers, Belgium) until a confluent monolayer of mesenchymal cells is obtained, after 7-10 days submerged cultures. Culture medium is emptied and renewed every other day.

Afterwards, the apical liquid is removed, and HBEC are cultured in BEBM:Dulbecco's Modified Eagles Medium (DMEM) (1:1) medium supplemented with penicillin (100U/ml), streptomycin (100µg/ml) (Lonza, Verviers, Belgium), bovine serum albumin (BSA) (1.5 µg/ml), retinoic acid (30ng/ml) (Sigma, Saint-Louis, MO), and BEGM SingleQuotsTM Supplements and Growth Factors (Lonza), including bovine pituitary extract (52µg/ml), insulin (5µg/ml), hydrocortisone (0.5g/ml), transferrin (10µg/ml), epinephrine (0.5µg/ml), epidermal growth factor (0.5ng/ml) and triiodothyronine (3.25ng/ml). The exposure to air (ALI) allows undifferentiated cells to grow and differentiate into a pseudostratified, respiratory epithelium, whose full differentiation and steady-state is reached after 4 weeks culture.

Although the ALI-cultures model has been used for years by many respiratory research teams, the number of cell divisions occurring at each culture phase has not been reported yet.

1.5.2. Advantages and limitations of the model

Apart from replicating the originating phenotype of COPD patients (see below), the ALI model offers some other advantages. First, ALI-cultures, although costly and time-consuming, offer the unique opportunity to focus on the sole airway epithelium,

allowing to get rid of direct effects/contributions of the mesenchymal compartment (e.g. for bulk RNA-sequencing), to avoid unwanted extraepithelial signals (e.g. chemo- and cytokines from surrounding leukocytes and fibroblasts), and to assess the physical properties of the epithelial layer. Second, precise modulation may be applied by supplementing the culture medium with pathway inhibitors or activators, cytokines, hormones, growth factors or other components, whose effect on the epithelial biology can be carefully addressed. Similarly, IgA-transcytosis may be assessed by adding d-IgA at the basolateral pole, while apical stimulation by pathogens, particulate matter, or cigarette smoke is possible. Third, cell-cell interaction may be studied by developing co-cultures models, by growing another cell population (e.g., fibroblasts, endothelial cells) at the basolateral pole of the semi-permeable membrane.

Of course, the model also has limitations, the first of them being that isolating epithelial cells from their native environment could lead to somewhat artificial cell development and biology. Second, culture media do not represent truthfully *in vivo* interstitial fluids and may modify the fate of airway progenitors. As an example, supplementing the medium with EGF is known to "proximalize" the reconstituted epithelium issued from distal sampling (289). Finally, the absence of airflow may also impact on cell differentiation and function.

In the present work, a dedicated analysis of cell proliferation at culture initiation and of cell numbers at steady-state is lacking, and should be performed in the future to strengthen the conclusions proposed in this thesis.

1.5.3. ALI cultures in COPD

In COPD, ALI cultures constitute a powerful tool to explore the biology and structure of the airway epithelium, as ALI-cultures issued from COPD patients recapitulate several features of the COPD epithelial phenotype. Indeed, COPD HBEC exposed to CS display decreased E-cadherin and ZO-1 expression when compared with HBEC from non-COPD smokers (181), replicating COPD-related

AJC disruption. In addition, ALI-cultures from COPD samples display decreased pIgR protein expression and impaired d-IgA transcytosis (237). Such reconstituted epithelium also exhibits enhanced EMT features (209) and altered cell differentiation, with decreased ciliated cells number and goblet cell hyperplasia (190). Most of these anomalies, however, have been observed at 4 weeks ALI-culture, and it remains unclear whether (and to what extent) these structural changes are persistent in COPD on the long-term, matching the irreversible nature of the disease.

2. Hypothesis and objectives of the thesis

COPD currently constitutes the third cause of death worldwide, accounting for approximately 3.2 million of deaths in 2019 (2). In spite of a continuous increase in knowledge of the disease physiopathology, current therapies fail at substantially improving its outcomes. Although the COPD AE phenotype is currently well defined, its cellular roots and the nature (and depth) of its imprinting remain poorly understood.

The working hypothesis is that the phenotype exhibited by the AE in COPD is imprinted – at least partly – at the epithelial level, permanently and independently of external insults (such as cigarette smoke) and pro-inflammatory surrounding cells (e.g. neutrophils and activated fibroblasts).

The current project addressing this hypothesis is divided in two main parts, whose objectives are:

(i) to determine the level to which the COPD epithelial phenotype is imprinted (or reversible) *ex vivo*, using long-term *in vitro* cultures of ALI-reconstituted AE and assessing the evolution of multiple parameters of the epithelial integrity in samples issued from non-smokers, non-COPD smokers, and COPD patients;

(ii) to explore the activation of the canonical, β-catenin dependent WNT signalling pathway in the COPD AE as compared with (non)-smoker

controls and explore the role of extrinsic activation/inhibition of the pathway on the expression of the COPD-related epithelial phenotype.

3. References

1. World Health Organization. Global Health Estimates 2016: Estimated deaths by age, sex, and cause. 2016 [Available from: https://www.who.int/healthinfo/global_burden_disease/estimates/en/.
2. Vogelmeier CF, Criner GJ, Martinez FJ, Anzueto A, Barnes PJ, Bourbeau J, et al. Global Strategy for the Diagnosis, Management, and Prevention of Chronic Obstructive Lung Disease 2017 Report. GOLD Executive Summary. Am J Respir Crit Care Med. 2017;195(5):557-82.
3. McDonough JE, Yuan R, Suzuki M, Seyednejad N, Elliott WM, Sanchez PG, et al. Small-airway obstruction and emphysema in chronic obstructive pulmonary disease. N Engl J Med. 2011;365(17):1567-75.
4. Salvi SS, Barnes PJ. Chronic obstructive pulmonary disease in non-smokers. Lancet. 2009;374(9691):733-43.
5. Definition and classification of chronic bronchitis for clinical and epidemiological purposes. A report to the Medical Research Council by their Committee on the Aetiology of Chronic Bronchitis. Lancet. 1965;1(7389):775-9.
6. Fabbri LM, Hurd SS, Committee GS. Global Strategy for the Diagnosis, Management and Prevention of COPD: 2003 update. Eur Respir J. 2003;22(1):1-2.
7. Pauwels RA, Buist AS, Calverley PM, Jenkins CR, Hurd SS, Committee GS. Global strategy for the diagnosis, management, and prevention of chronic obstructive pulmonary disease. NHLBI/WHO Global Initiative for Chronic Obstructive Lung Disease (GOLD) Workshop summary. Am J Respir Crit Care Med. 2001;163(5):1256-76.
8. Vestbo J, Hurd SS, Agusti AG, Jones PW, Vogelmeier C, Anzueto A, et al. Global strategy for the diagnosis, management, and prevention of chronic obstructive pulmonary disease: GOLD executive summary. Am J Respir Crit Care Med. 2013;187(4):347-65.
9. Vijayasaratha K, Stockley RA. Reported and unreported exacerbations of COPD: analysis by diary cards. Chest. 2008;133(1):34-41.
10. Wilkinson TM, Donaldson GC, Hurst JR, Seemungal TA, Wedzicha JA. Early therapy improves outcomes of exacerbations of chronic obstructive pulmonary disease. Am J Respir Crit Care Med. 2004;169(12):1298-303.
11. Soriano JB, Visick GT, Muellerova H, Payvandi N, Hansell AL. Patterns of comorbidities in newly diagnosed COPD and asthma in primary care. Chest. 2005;128(4):2099-107.
12. Chen W, Thomas J, Sadatsafavi M, FitzGerald JM. Risk of cardiovascular comorbidity in patients with chronic obstructive pulmonary disease: a systematic review and meta-analysis. Lancet Respir Med. 2015;3(8):631-9.
13. Fry JS, Hamling JS, Lee PN. Systematic review with meta-analysis of the epidemiological evidence relating FEV1 decline to lung cancer risk. BMC Cancer. 2012;12:498.

14. Clinical Practice Guideline Treating Tobacco U, Dependence Update Panel L, Staff. A clinical practice guideline for treating tobacco use and dependence: 2008 update. A U.S. Public Health Service report. Am J Prev Med. 2008;35(2):158-76.
15. van der Meer RM, Wagena EJ, Ostelo RW, Jacobs JE, van Schayck CP. Smoking cessation for chronic obstructive pulmonary disease. Cochrane Database Syst Rev. 2003(2):CD002999.
16. Stead LF, Buitrago D, Preciado N, Sanchez G, Hartmann-Boyce J, Lancaster T. Physician advice for smoking cessation. Cochrane Database Syst Rev. 2013(5):CD000165.
17. Stead LF, Koilpillai P, Fanshawe TR, Lancaster T. Combined pharmacotherapy and behavioural interventions for smoking cessation. Cochrane Database Syst Rev. 2016;3:CD008286.
18. Alfageme I, Vazquez R, Reyes N, Munoz J, Fernandez A, Hernandez M, et al. Clinical efficacy of anti-pneumococcal vaccination in patients with COPD. Thorax. 2006;61(3):189-95.
19. Kopsaftis Z, Wood-Baker R, Poole P. Influenza vaccine for chronic obstructive pulmonary disease (COPD). Cochrane Database Syst Rev. 2018;6:CD002733.
20. Wongsurakiat P, Maranetra KN, Wasi C, Kositanont U, Dejsomritrutai W, Charoenratanakul S. Acute respiratory illness in patients with COPD and the effectiveness of influenza vaccination: a randomized controlled study. Chest. 2004;125(6):2011-20.
21. Walters JA, Tang JN, Poole P, Wood-Baker R. Pneumococcal vaccines for preventing pneumonia in chronic obstructive pulmonary disease. Cochrane Database Syst Rev. 2017;1:CD001390.
22. Spruit MA, Singh SJ, Garvey C, ZuWallack R, Nici L, Rochester C, et al. An official American Thoracic Society/European Respiratory Society statement: key concepts and advances in pulmonary rehabilitation. Am J Respir Crit Care Med. 2013;188(8):e13-64.
23. McCarthy B, Casey D, Devane D, Murphy K, Murphy E, Lacasse Y. Pulmonary rehabilitation for chronic obstructive pulmonary disease. Cochrane Database Syst Rev. 2015(2):CD003793.
24. Alison JA, McKeough ZJ, Johnston K, McNamara RJ, Spencer LM, Jenkins SC, et al. Australian and New Zealand Pulmonary Rehabilitation Guidelines. Respirology. 2017;22(4):800-19.
25. Vogiatzis I, Rochester CL, Spruit MA, Troosters T, Clini EM, American Thoracic Society/European Respiratory Society Task Force on Policy in Pulmonary R. Increasing implementation and delivery of pulmonary rehabilitation: key messages from the new ATS/ERS policy statement. Eur Respir J. 2016;47(5):1336-41.
26. Vestbo J, Sorensen T, Lange P, Brix A, Torre P, Viskum K. Long-term effect of inhaled budesonide in mild and moderate chronic obstructive pulmonary disease: a randomised controlled trial. Lancet. 1999;353(9167):1819-23.

27. Tashkin DP, Celli B, Senn S, Burkhart D, Kesten S, Menjoge S, et al. A 4-year trial of tiotropium in chronic obstructive pulmonary disease. N Engl J Med. 2008;359(15):1543-54.
28. Pauwels RA, Lofdahl CG, Laitinen LA, Schouten JP, Postma DS, Pride NB, et al. Long-term treatment with inhaled budesonide in persons with mild chronic obstructive pulmonary disease who continue smoking. European Respiratory Society Study on Chronic Obstructive Pulmonary Disease. N Engl J Med. 1999;340(25):1948-53.
29. Anthonisen NR, Connett JE, Kiley JP, Altose MD, Bailey WC, Buist AS, et al. Effects of smoking intervention and the use of an inhaled anticholinergic bronchodilator on the rate of decline of FEV1. The Lung Health Study. JAMA. 1994;272(19):1497-505.
30. Burge PS, Calverley PM, Jones PW, Spencer S, Anderson JA, Maslen TK. Randomised, double blind, placebo controlled study of fluticasone propionate in patients with moderate to severe chronic obstructive pulmonary disease: the ISOLDE trial. BMJ. 2000;320(7245):1297-303.
31. Celli BR, Thomas NE, Anderson JA, Ferguson GT, Jenkins CR, Jones PW, et al. Effect of pharmacotherapy on rate of decline of lung function in chronic obstructive pulmonary disease: results from the TORCH study. Am J Respir Crit Care Med. 2008;178(4):332-8.
32. Decramer M, Celli B, Kesten S, Lystig T, Mehra S, Tashkin DP, et al. Effect of tiotropium on outcomes in patients with moderate chronic obstructive pulmonary disease (UPLIFT): a prespecified subgroup analysis of a randomised controlled trial. Lancet. 2009;374(9696):1171-8.
33. Zhou Y, Zhong NS, Li X, Chen S, Zheng J, Zhao D, et al. Tiotropium in Early-Stage Chronic Obstructive Pulmonary Disease. N Engl J Med. 2017;377(10):923-35.
34. Cazzola M, Rogliani P, Ruggeri P, Segreti A, Proietto A, Picciolo S, et al. Chronic treatment with indacaterol and airway response to salbutamol in stable COPD. Respir Med. 2013;107(6):848-53.
35. Kempsford R, Norris V, Siederer S. Vilanterol trifenatate, a novel inhaled long-acting beta2 adrenoceptor agonist, is well tolerated in healthy subjects and demonstrates prolonged bronchodilation in subjects with asthma and COPD. Pulm Pharmacol Ther. 2013;26(2):256-64.
36. Koch A, Pizzichini E, Hamilton A, Hart L, Korducki L, De Salvo MC, et al. Lung function efficacy and symptomatic benefit of olodaterol once daily delivered via Respimat(R) versus placebo and formoterol twice daily in patients with GOLD 2-4 COPD: results from two replicate 48-week studies. Int J Chron Obstruct Pulmon Dis. 2014;9:697-714.
37. Han J, Dai L, Zhong N. Indacaterol on dyspnea in chronic obstructive pulmonary disease: a systematic review and meta-analysis of randomized placebo-controlled trials. BMC Pulm Med. 2013;13:26.
38. Geake JB, Dabscheck EJ, Wood-Baker R, Cates CJ. Indacaterol, a once-daily beta2-agonist, versus twice-daily beta(2)-agonists or placebo for chronic obstructive pulmonary disease. Cochrane Database Syst Rev. 2015;1:CD010139.

39. Kew KM, Mavergames C, Walters JA. Long-acting beta2-agonists for chronic obstructive pulmonary disease. Cochrane Database Syst Rev. 2013(10):CD010177.
40. Karner C, Chong J, Poole P. Tiotropium versus placebo for chronic obstructive pulmonary disease. Cochrane Database Syst Rev. 2014(7):CD009285.
41. Melani AS. Long-acting muscarinic antagonists. Expert Rev Clin Pharmacol. 2015;8(4):479-501.
42. Decramer ML, Chapman KR, Dahl R, Frith P, Devouassoux G, Fritscher C, et al. Once-daily indacaterol versus tiotropium for patients with severe chronic obstructive pulmonary disease (INVIGORATE): a randomised, blinded, parallel-group study. Lancet Respir Med. 2013;1(7):524-33.
43. Vogelmeier C, Hederer B, Glaab T, Schmidt H, Rutten-van Molken MP, Beeh KM, et al. Tiotropium versus salmeterol for the prevention of exacerbations of COPD. N Engl J Med. 2011;364(12):1093-103.
44. Ram FS, Jones PW, Castro AA, De Brito JA, Atallah AN, Lacasse Y, et al. Oral theophylline for chronic obstructive pulmonary disease. Cochrane Database Syst Rev. 2002(4):CD003902.
45. Zacarias EC, Castro AA, Cendon S. Effect of theophylline associated with short-acting or long-acting inhaled beta2-agonists in patients with stable chronic obstructive pulmonary disease: a systematic review. J Bras Pneumol. 2007;33(2):152-60.
46. ZuWallack RL, Mahler DA, Reilly D, Church N, Emmett A, Rickard K, et al. Salmeterol plus theophylline combination therapy in the treatment of COPD. Chest. 2001;119(6):1661-70.
47. Devereux G, Cotton S, Fielding S, McMeekin N, Barnes PJ, Briggs A, et al. Effect of Theophylline as Adjunct to Inhaled Corticosteroids on Exacerbations in Patients With COPD: A Randomized Clinical Trial. Jama. 2018;320(15):1548-59.
48. Jenkins CR, Wen FQ, Martin A, Barnes PJ, Celli B, Zhong NS, et al. The effect of low-dose corticosteroids and theophylline on the risk of acute exacerbations of COPD: the TASCS randomised controlled trial. Eur Respir J. 2021;57(6):2003338.
49. Suissa S, Patenaude V, Lapi F, Ernst P. Inhaled corticosteroids in COPD and the risk of serious pneumonia. Thorax. 2013;68(11):1029-36.
50. Crim C, Calverley PM, Anderson JA, Celli B, Ferguson GT, Jenkins C, et al. Pneumonia risk in COPD patients receiving inhaled corticosteroids alone or in combination: TORCH study results. Eur Respir J. 2009;34(3):641-7.
51. Yang IA, Clarke MS, Sim EH, Fong KM. Inhaled corticosteroids for stable chronic obstructive pulmonary disease. Cochrane Database Syst Rev. 2012(7):CD002991.
52. Barnes PJ. New anti-inflammatory targets for chronic obstructive pulmonary disease. Nat Rev Drug Discov. 2013;12(7):543-59.
53. Boardman C, Chachi L, Gavrila A, Keenan CR, Perry MM, Xia YC, et al. Mechanisms of glucocorticoid action and insensitivity in airways disease. Pulm Pharmacol Ther. 2014;29(2):129-43.

54. Nannini LJ, Poole P, Milan SJ, Kesterton A. Combined corticosteroid and long-acting beta(2)-agonist in one inhaler versus inhaled corticosteroids alone for chronic obstructive pulmonary disease. Cochrane Database Syst Rev. 2013(8):CD006826.
55. Nannini LJ, Lasserson TJ, Poole P. Combined corticosteroid and long-acting beta(2)-agonist in one inhaler versus long-acting beta(2)-agonists for chronic obstructive pulmonary disease. Cochrane Database Syst Rev. 2012(9):CD006829.
56. Calverley PM, Anderson JA, Celli B, Ferguson GT, Jenkins C, Jones PW, et al. Salmeterol and fluticasone propionate and survival in chronic obstructive pulmonary disease. N Engl J Med. 2007;356(8):775-89.
57. Vestbo J, Anderson JA, Brook RD, Calverley PM, Celli BR, Crim C, et al. Fluticasone furoate and vilanterol and survival in chronic obstructive pulmonary disease with heightened cardiovascular risk (SUMMIT): a double-blind randomised controlled trial. Lancet. 2016;387(10030):1817-26.
58. Bafadhel M, McKenna S, Terry S, Mistry V, Reid C, Haldar P, et al. Acute exacerbations of chronic obstructive pulmonary disease: identification of biologic clusters and their biomarkers. Am J Respir Crit Care Med. 2011;184(6):662-71.
59. Papi A, Vestbo J, Fabbri L, Corradi M, Prunier H, Cohuet G, et al. Extrafine inhaled triple therapy versus dual bronchodilator therapy in chronic obstructive pulmonary disease (TRIBUTE): a double-blind, parallel group, randomised controlled trial. Lancet. 2018;391(10125):1076-84.
60. Siddiqui SH, Guasconi A, Vestbo J, Jones P, Agusti A, Paggiaro P, et al. Blood Eosinophils: A Biomarker of Response to Extrafine Beclomethasone/Formoterol in Chronic Obstructive Pulmonary Disease. Am J Respir Crit Care Med. 2015;192(4):523-5.
61. Vestbo J, Papi A, Corradi M, Blazhko V, Montagna I, Francisco C, et al. Single inhaler extrafine triple therapy versus long-acting muscarinic antagonist therapy for chronic obstructive pulmonary disease (TRINITY): a double-blind, parallel group, randomised controlled trial. Lancet. 2017;389(10082):1919-29.
62. Pascoe S, Locantore N, Dransfield MT, Barnes NC, Pavord ID. Blood eosinophil counts, exacerbations, and response to the addition of inhaled fluticasone furoate to vilanterol in patients with chronic obstructive pulmonary disease: a secondary analysis of data from two parallel randomised controlled trials. Lancet Respir Med. 2015;3(6):435-42.
63. Disease GIfCOL. Global Strategy for the Diagnosis, Management, and Prevention of Chronic Obstructive Pulmonary Disease (2020 Report) 2020 [Available from: https://goldcopd.org/wp-content/uploads/2019/12/GOLD-2020-FINAL-ver1.2-03Dec19_WMV.pdf.
64. Rabe KF. Update on roflumilast, a phosphodiesterase 4 inhibitor for the treatment of chronic obstructive pulmonary disease. Br J Pharmacol. 2011;163(1):53-67.
65. Fabbri LM, Calverley PM, Izquierdo-Alonso JL, Bundschuh DS, Brose M, Martinez FJ, et al. Roflumilast in moderate-to-severe chronic obstructive pulmonary disease treated with longacting bronchodilators: two randomised clinical trials. Lancet. 2009;374(9691):695-703.

66. Calverley PM, Rabe KF, Goehring UM, Kristiansen S, Fabbri LM, Martinez FJ, et al. Roflumilast in symptomatic chronic obstructive pulmonary disease: two randomised clinical trials. Lancet. 2009;374(9691):685-94.
67. Criner GJ, Celli BR, Brightling CE, Agusti A, Papi A, Singh D, et al. Benralizumab for the Prevention of COPD Exacerbations. N Engl J Med. 2019;381(11):1023-34.
68. Pavord ID, Chanez P, Criner GJ, Kerstjens HAM, Korn S, Lugogo N, et al. Mepolizumab for Eosinophilic Chronic Obstructive Pulmonary Disease. N Engl J Med. 2017;377(17):1613-29.
69. Cranston JM, Crockett AJ, Moss JR, Alpers JH. Domiciliary oxygen for chronic obstructive pulmonary disease. Cochrane Database Syst Rev. 2005(4):CD001744.
70. Cooper JD, Trulock EP, Triantafillou AN, Patterson GA, Pohl MS, Deloney PA, et al. Bilateral pneumectomy (volume reduction) for chronic obstructive pulmonary disease. J Thorac Cardiovasc Surg. 1995;109(1):106-16; discussion 16-9.
71. National Emphysema Treatment Trial Research G, Fishman A, Fessler H, Martinez F, McKenna RJ, Jr., Naunheim K, et al. Patients at high risk of death after lung-volume-reduction surgery. N Engl J Med. 2001;345(15):1075-83.
72. Fishman A, Martinez F, Naunheim K, Piantadosi S, Wise R, Ries A, et al. A randomized trial comparing lung-volume-reduction surgery with medical therapy for severe emphysema. N Engl J Med. 2003;348(21):2059-73.
73. van Agteren JE, Carson KV, Tiong LU, Smith BJ. Lung volume reduction surgery for diffuse emphysema. Cochrane Database Syst Rev. 2016;10:CD001001.
74. Marchetti N, Criner GJ. Surgical Approaches to Treating Emphysema: Lung Volume Reduction Surgery, Bullectomy, and Lung Transplantation. Semin Respir Crit Care Med. 2015;36(4):592-608.
75. Chambers DC, Cherikh WS, Harhay MO, Hayes D, Jr., Hsich E, Khush KK, et al. The International Thoracic Organ Transplant Registry of the International Society for Heart and Lung Transplantation: Thirty-sixth adult lung and heart-lung transplantation Report-2019; Focus theme: Donor and recipient size match. J Heart Lung Transplant. 2019;38(10):1042-55.
76. Stavem K, Bjortuft O, Borgan O, Geiran O, Boe J. Lung transplantation in patients with chronic obstructive pulmonary disease in a national cohort is without obvious survival benefit. J Heart Lung Transplant. 2006;25(1):75-84.
77. Criner GJ, Cordova F, Sternberg AL, Martinez FJ. The National Emphysema Treatment Trial (NETT) Part II: Lessons learned about lung volume reduction surgery. Am J Respir Crit Care Med. 2011;184(8):881-93.
78. Sciurba FC, Criner GJ, Strange C, Shah PL, Michaud G, Connolly TA, et al. Effect of Endobronchial Coils vs Usual Care on Exercise Tolerance in Patients With Severe Emphysema: The RENEW Randomized Clinical Trial. JAMA. 2016;315(20):2178-89.
79. Shah PL, Gompelmann D, Valipour A, McNulty WH, Eberhardt R, Grah C, et al. Thermal vapour ablation to reduce segmental volume in patients with severe emphysema: STEP-UP 12 month results. Lancet Respir Med. 2016;4(9):e44-e5.

80. Herth FJ, Valipour A, Shah PL, Eberhardt R, Grah C, Egan J, et al. Segmental volume reduction using thermal vapour ablation in patients with severe emphysema: 6-month results of the multicentre, parallel-group, open-label, randomised controlled STEP-UP trial. Lancet Respir Med. 2016;4(3):185-93.
81. Davey C, Zoumot Z, Jordan S, Carr DH, Polkey MI, Shah PL, et al. Bronchoscopic lung volume reduction with endobronchial valves for patients with heterogeneous emphysema and intact interlobar fissures (the BeLieVeR-HIFi trial): study design and rationale. Thorax. 2015;70(3):288-90.
82. Criner GJ, Sue R, Wright S, Dransfield M, Rivas-Perez H, Wiese T, et al. A Multicenter Randomized Controlled Trial of Zephyr Endobronchial Valve Treatment in Heterogeneous Emphysema (LIBERATE). Am J Respir Crit Care Med. 2018;198(9):1151-64.
83. Travaglini KJ, Nabhan AN, Penland L, Sinha R, Gillich A, Sit RV, et al. A molecular cell atlas of the human lung from single-cell RNA sequencing. Nature. 2020.
84. Knight DA, Holgate ST. The airway epithelium: structural and functional properties in health and disease. Respirology. 2003;8(4):432-46.
85. Rock JR, Randell SH, Hogan BL. Airway basal stem cells: a perspective on their roles in epithelial homeostasis and remodeling. Dis Model Mech. 2010;3(9-10):545-56.
86. Hogan BL, Barkauskas CE, Chapman HA, Epstein JA, Jain R, Hsia CC, et al. Repair and regeneration of the respiratory system: complexity, plasticity, and mechanisms of lung stem cell function. Cell Stem Cell. 2014;15(2):123-38.
87. Boers JE, Ambergen AW, Thunnissen FB. Number and proliferation of basal and parabasal cells in normal human airway epithelium. Am J Respir Crit Care Med. 1998;157(6 Pt 1):2000-6.
88. Zuo WL, Shenoy SA, Li S, O'Beirne SL, Strulovici-Barel Y, Leopold PL, et al. Ontogeny and Biology of Human Small Airway Epithelial Club Cells. Am J Respir Crit Care Med. 2018.
89. Hiemstra PS, Bourdin A. Club cells, CC10 and self-control at the epithelial surface. Eur Respir J. 2014;44(4):831-2.
90. Boers JE, den Brok JL, Koudstaal J, Arends JW, Thunnissen FB. Number and proliferation of neuroendocrine cells in normal human airway epithelium. Am J Respir Crit Care Med. 1996;154(3 Pt 1):758-63.
91. Linnoila RI. Functional facets of the pulmonary neuroendocrine system. Lab Invest. 2006;86(5):425-44.
92. Branchfield K, Nantie L, Verheyden JM, Sui P, Wienhold MD, Sun X. Pulmonary neuroendocrine cells function as airway sensors to control lung immune response. Science. 2016;351(6274):707-10.
93. Montoro DT, Haber AL, Biton M, Vinarsky V, Lin B, Birket SE, et al. A revised airway epithelial hierarchy includes CFTR-expressing ionocytes. Nature. 2018;560(7718):319-24.
94. Lamouille S, Xu J, Derynck R. Molecular mechanisms of epithelial-mesenchymal transition. Nat Rev Mol Cell Biol. 2014;15(3):178-96.

95. Hartsock A, Nelson WJ. Adherens and tight junctions: structure, function and connections to the actin cytoskeleton. Biochim Biophys Acta. 2008;1778(3):660-9.
96. Niessen CM. Tight junctions/adherens junctions: basic structure and function. J Invest Dermatol. 2007;127(11):2525-32.
97. Schulzke JD, Fromm M. Tight junctions: molecular structure meets function. Ann N Y Acad Sci. 2009;1165:1-6.
98. Indra I, Hong S, Troyanovsky R, Kormos B, Troyanovsky S. The adherens junction: a mosaic of cadherin and nectin clusters bundled by actin filaments. J Invest Dermatol. 2013;133(11):2546-54.
99. Meng W, Takeichi M. Adherens junction: molecular architecture and regulation. Cold Spring Harb Perspect Biol. 2009;1(6):a002899.
100. Qian X, Karpova T, Sheppard AM, McNally J, Lowy DR. E-cadherin-mediated adhesion inhibits ligand-dependent activation of diverse receptor tyrosine kinases. The EMBO journal. 2004;23(8):1739-48.
101. Ivanov AI, Parkos CA, Nusrat A. Cytoskeletal regulation of epithelial barrier function during inflammation. Am J Pathol. 2010;177(2):512-24.
102. Garrod D. Desmosomes in vivo. Dermatology research and practice. 2010;2010:212439.
103. Brooke MA, Nitoiu D, Kelsell DP. Cell-cell connectivity: desmosomes and disease. J Pathol. 2012;226(2):158-71.
104. Aghapour M, Raee P, Moghaddam SJ, Hiemstra PS, Heijink IH. Airway Epithelial Barrier Dysfunction in Chronic Obstructive Pulmonary Disease: Role of Cigarette Smoke Exposure. Am J Respir Cell Mol Biol. 2018;58(2):157-69.
105. Smirnova NF, Schamberger AC, Nayakanti S, Hatz R, Behr J, Eickelberg O. Detection and quantification of epithelial progenitor cell populations in human healthy and IPF lungs. Respir Res. 2016;17(1):83.
106. Bowden DH. Cell turnover in the lung. Am Rev Respir Dis. 1983;128(2 Pt 2):S46-8.
107. Evans MJ, Johnson LV, Stephens RJ, Freeman G. Renewal of the terminal bronchiolar epithelium in the rat following exposure to NO2 or O3. Lab Invest. 1976;35(3):246-57.
108. Breuer R, Zajicek G, Christensen TG, Lucey EC, Snider GL. Cell kinetics of normal adult hamster bronchial epithelium in the steady state. Am J Respir Cell Mol Biol. 1990;2(1):51-8.
109. Rawlins EL, Hogan BL. Epithelial stem cells of the lung: privileged few or opportunities for many? Development. 2006;133(13):2455-65.
110. Rock JR, Onaitis MW, Rawlins EL, Lu Y, Clark CP, Xue Y, et al. Basal cells as stem cells of the mouse trachea and human airway epithelium. Proc Natl Acad Sci U S A. 2009;106(31):12771-5.
111. Lazard DS, Moore A, Hupertan V, Martin C, Escabasse V, Dreyfus P, et al. Muco-ciliary differentiation of nasal epithelial cells is decreased after wound healing in vitro. Allergy. 2009;64(8):1136-43.

112. Boucherat O, Chakir J, Jeannotte L. The loss of Hoxa5 function promotes Notch-dependent goblet cell metaplasia in lung airways. Biol Open. 2012;1(7):677-91.
113. Li S, Hu X, Wang Z, Wu M, Zhang J. Different profiles of notch signaling in cigarette smoke-induced pulmonary emphysema and bleomycin-induced pulmonary fibrosis. Inflamm Res. 2015;64(5):363-71.
114. Tilley AE, Harvey BG, Heguy A, Hackett NR, Wang R, O'Connor TP, et al. Down-regulation of the notch pathway in human airway epithelium in association with smoking and chronic obstructive pulmonary disease. Am J Respir Crit Care Med. 2009;179(6):457-66.
115. Whitsett JA, Kalinichenko VV. Notch and basal cells take center stage during airway epithelial regeneration. Cell Stem Cell. 2011;8(6):597-8.
116. Clevers H. Wnt/beta-catenin signaling in development and disease. Cell. 2006;127(3):469-80.
117. Malleske DT, Hayes D, Jr., Lallier SW, Hill CL, Reynolds SD. Regulation of human airway epithelial tissue stem cell differentiation by beta-catenin, P300, and CBP. Stem Cells. 2018.
118. Carlier FM, Dupasquier S, Ambroise J, Detry B, Lecocq M, Bietry-Claudet C, et al. Canonical WNT pathway is activated in the airway epithelium in chronic obstructive pulmonary disease. EBioMedicine. 2020;61:103034.
119. Kugler MC, Joyner AL, Loomis CA, Munger JS. Sonic hedgehog signaling in the lung. From development to disease. Am J Respir Cell Mol Biol. 2015;52(1):1-13.
120. Saito A, Horie M, Nagase T. TGF-beta Signaling in Lung Health and Disease. Int J Mol Sci. 2018;19(8).
121. Ojiaku CA, Yoo EJ, Panettieri RA, Jr. Transforming Growth Factor beta1 Function in Airway Remodeling and Hyperresponsiveness. The Missing Link? Am J Respir Cell Mol Biol. 2017;56(4):432-42.
122. Zuo WL, Yang J, Gomi K, Chao I, Crystal RG, Shaykhiev R. EGF-Amphiregulin Interplay in Airway Stem/Progenitor Cells Links the Pathogenesis of Smoking-induced Lesions in the Human Airway Epithelium. Stem Cells. 2016.
123. Yuan T, Volckaert T, Chanda D, Thannickal VJ, De Langhe SP. Fgf10 Signaling in Lung Development, Homeostasis, Disease, and Repair After Injury. Front Genet. 2018;9:418.
124. Ganesan S, Sajjan US. Repair and Remodeling of airway epithelium after injury in Chronic Obstructive Pulmonary Disease. Curr Respir Care Rep. 2013;2(3).
125. Puchelle E, Zahm JM, Tournier JM, Coraux C. Airway epithelial repair, regeneration, and remodeling after injury in chronic obstructive pulmonary disease. Proc Am Thorac Soc. 2006;3(8):726-33.
126. Knowles MR, Boucher RC. Mucus clearance as a primary innate defense mechanism for mammalian airways. J Clin Invest. 2002;109(5):571-7.
127. Wanner A, Salathe M, O'Riordan TG. Mucociliary clearance in the airways. Am J Respir Crit Care Med. 1996;154(6 Pt 1):1868-902.

128. Tarran R, Button B, Picher M, Paradiso AM, Ribeiro CM, Lazarowski ER, et al. Normal and cystic fibrosis airway surface liquid homeostasis. The effects of phasic shear stress and viral infections. J Biol Chem. 2005;280(42):35751-9.
129. Hiemstra PS, McCray PB, Jr., Bals R. The innate immune function of airway epithelial cells in inflammatory lung disease. Eur Respir J. 2015;45(4):1150-62.
130. Parker D, Prince A. Innate immunity in the respiratory epithelium. Am J Respir Cell Mol Biol. 2011;45(2):189-201.
131. Leiva-Juarez MM, Kolls JK, Evans SE. Lung epithelial cells: therapeutically inducible effectors of antimicrobial defense. Mucosal Immunol. 2018;11(1):21-34.
132. Fahy JV, Dickey BF. Airway mucus function and dysfunction. N Engl J Med. 2010;363(23):2233-47.
133. Thornton DJ, Rousseau K, McGuckin MA. Structure and function of the polymeric mucins in airways mucus. Annu Rev Physiol. 2008;70:459-86.
134. Roy MG, Livraghi-Butrico A, Fletcher AA, McElwee MM, Evans SE, Boerner RM, et al. Muc5b is required for airway defence. Nature. 2014;505(7483):412-6.
135. Sorensen OE, Borregaard N, Cole AM. Antimicrobial peptides in innate immune responses. Contrib Microbiol. 2008;15:61-77.
136. Meade KG, O'Farrelly C. beta-Defensins: Farming the Microbiome for Homeostasis and Health. Front Immunol. 2018;9:3072.
137. Yang D, Chertov O, Bykovskaia SN, Chen Q, Buffo MJ, Shogan J, et al. Beta-defensins: linking innate and adaptive immunity through dendritic and T cell CCR6. Science. 1999;286(5439):525-8.
138. van Harten RM, van Woudenbergh E, van Dijk A, Haagsman HP. Cathelicidins: Immunomodulatory Antimicrobials. Vaccines (Basel). 2018;6(3).
139. Ragland SA, Criss AK. From bacterial killing to immune modulation: Recent insights into the functions of lysozyme. PLoS Pathog. 2017;13(9):e1006512.
140. Caccavo D, Pellegrino NM, Altamura M, Rigon A, Amati L, Amoroso A, et al. Antimicrobial and immunoregulatory functions of lactoferrin and its potential therapeutic application. J Endotoxin Res. 2002;8(6):403-17.
141. Doumas S, Kolokotronis A, Stefanopoulos P. Anti-inflammatory and antimicrobial roles of secretory leukocyte protease inhibitor. Infect Immun. 2005;73(3):1271-4.
142. Hiemstra PS, Maassen RJ, Stolk J, Heinzel-Wieland R, Steffens GJ, Dijkman JH. Antibacterial activity of antileukoprotease. Infection and immunity. 1996;64(11):4520-4.
143. Xu W, He B, Chiu A, Chadburn A, Shan M, Buldys M, et al. Epithelial cells trigger frontline immunoglobulin class switching through a pathway regulated by the inhibitor SLPI. Nature immunology. 2007;8(3):294-303.
144. Samsom JN, van der Marel AP, van Berkel LA, van Helvoort JM, Simons-Oosterhuis Y, Jansen W, et al. Secretory leukoprotease inhibitor in mucosal lymph node dendritic cells regulates the threshold for mucosal tolerance. Journal of immunology. 2007;179(10):6588-95.
145. Stripp BR, Reynolds SD, Boe IM, Lund J, Power JH, Coppens JT, et al. Clara cell secretory protein deficiency alters clara cell secretory apparatus and the

protein composition of airway lining fluid. Am J Respir Cell Mol Biol. 2002;27(2):170-8.
146. Wang SZ, Rosenberger CL, Bao YX, Stark JM, Harrod KS. Clara cell secretory protein modulates lung inflammatory and immune responses to respiratory syncytial virus infection. J Immunol. 2003;171(2):1051-60.
147. Chen LC, Zhang Z, Myers AC, Huang SK. Cutting edge: altered pulmonary eosinophilic inflammation in mice deficient for Clara cell secretory 10-kDa protein. J Immunol. 2001;167(6):3025-8.
148. Laucho-Contreras ME, Polverino F, Gupta K, Taylor KL, Kelly E, Pinto-Plata V, et al. Protective role for club cell secretory protein-16 (CC16) in the development of COPD. Eur Respir J. 2015;45(6):1544-56.
149. Angkasekwinai P, Park H, Wang YH, Wang YH, Chang SH, Corry DB, et al. Interleukin 25 promotes the initiation of proallergic type 2 responses. J Exp Med. 2007;204(7):1509-17.
150. Zhou B, Comeau MR, De Smedt T, Liggitt HD, Dahl ME, Lewis DB, et al. Thymic stromal lymphopoietin as a key initiator of allergic airway inflammation in mice. Nat Immunol. 2005;6(10):1047-53.
151. Chustz RT, Nagarkar DR, Poposki JA, Favoreto S, Jr., Avila PC, Schleimer RP, et al. Regulation and function of the IL-1 family cytokine IL-1F9 in human bronchial epithelial cells. American journal of respiratory cell and molecular biology. 2011;45(1):145-53.
152. Hammad H, Lambrecht BN. Barrier Epithelial Cells and the Control of Type 2 Immunity. Immunity. 2015;43(1):29-40.
153. Standiford TJ, Kunkel SL, Basha MA, Chensue SW, Lynch JP, 3rd, Toews GB, et al. Interleukin-8 gene expression by a pulmonary epithelial cell line. A model for cytokine networks in the lung. The Journal of clinical investigation. 1990;86(6):1945-53.
154. Crestani B, Cornillet P, Dehoux M, Rolland C, Guenounou M, Aubier M. Alveolar type II epithelial cells produce interleukin-6 in vitro and in vivo. Regulation by alveolar macrophage secretory products. The Journal of clinical investigation. 1994;94(2):731-40.
155. Takizawa H, Tanaka M, Takami K, Ohtoshi T, Ito K, Satoh M, et al. Increased expression of transforming growth factor-beta1 in small airway epithelium from tobacco smokers and patients with chronic obstructive pulmonary disease (COPD). American journal of respiratory and critical care medicine. 2001;163(6):1476-83.
156. Gohy ST, Detry BR, Lecocq M, Bouzin C, Weynand BA, Amatngalim GD, et al. Polymeric Immunoglobulin Receptor Downregulation in COPD: Persistence in the Cultured Epithelium and Role of Transforming Growth Factor-beta. American journal of respiratory and critical care medicine. 2014.
157. Carlier FM, Sibille Y, Pilette C. The epithelial barrier and immunoglobulin A system in allergy. Clin Exp Allergy. 2016;46(11):1372-88.
158. Mestecky J, McGhee JR. Immunoglobulin A (IgA): molecular and cellular interactions involved in IgA biosynthesis and immune response. Adv Immunol. 1987;40:153-245.

159. Brandtzaeg P. Presence of J chain in human immunocytes containing various immunoglobulin classes. Nature. 1974;252(5482):418-20.
160. Brandtzaeg P, Kiyono H, Pabst R, Russell MW. Terminology: nomenclature of mucosa-associated lymphoid tissue. Mucosal Immunol. 2008;1(1):31-7.
161. Rojas R, Apodaca G. Immunoglobulin transport across polarized epithelial cells. Nat Rev Mol Cell Biol. 2002;3(12):944-55.
162. Kaetzel CS. The polymeric immunoglobulin receptor: bridging innate and adaptive immune responses at mucosal surfaces. Immunol Rev. 2005;206:83-99.
163. Pilette C, Durham SR, Vaerman JP, Sibille Y. Mucosal immunity in asthma and chronic obstructive pulmonary disease: a role for immunoglobulin A? Proc Am Thorac Soc. 2004;1(2):125-35.
164. Williams RC, Gibbons RJ. Inhibition of bacterial adherence by secretory immunoglobulin A: a mechanism of antigen disposal. Science. 1972;177(4050):697-9.
165. Brandtzaeg P. Mucosal and glandular distribution of immunoglobulin components: differential localization of free and bound SC in secretory epithelial cells. J Immunol. 1974;112(4):1553-9.
166. Phalipon A, Cardona A, Kraehenbuhl JP, Edelman L, Sansonetti PJ, Corthesy B. Secretory component: a new role in secretory IgA-mediated immune exclusion in vivo. Immunity. 2002;17(1):107-15.
167. Apter FM, Lencer WI, Finkelstein RA, Mekalanos JJ, Neutra MR. Monoclonal immunoglobulin A antibodies directed against cholera toxin prevent the toxin-induced chloride secretory response and block toxin binding to intestinal epithelial cells in vitro. Infect Immun. 1993;61(12):5271-8.
168. Hutchings AB, Helander A, Silvey KJ, Chandran K, Lucas WT, Nibert ML, et al. Secretory immunoglobulin A antibodies against the sigma1 outer capsid protein of reovirus type 1 Lang prevent infection of mouse Peyer's patches. J Virol. 2004;78(2):947-57.
169. Stubbe H, Berdoz J, Kraehenbuhl JP, Corthesy B. Polymeric IgA is superior to monomeric IgA and IgG carrying the same variable domain in preventing Clostridium difficile toxin A damaging of T84 monolayers. J Immunol. 2000;164(4):1952-60.
170. Fagarasan S. Intestinal IgA synthesis: a primitive form of adaptive immunity that regulates microbial communities in the gut. Curr Top Microbiol Immunol. 2006;308:137-53.
171. Richmond BW, Brucker RM, Han W, Du RH, Zhang Y, Cheng DS, et al. Airway bacteria drive a progressive COPD-like phenotype in mice with polymeric immunoglobulin receptor deficiency. Nat Commun. 2016;7:11240.
172. Mkaddem SB, Christou I, Rossato E, Berthelot L, Lehuen A, Monteiro RC. IgA, IgA receptors, and their anti-inflammatory properties. Curr Top Microbiol Immunol. 2014;382:221-35.
173. Hooper LV, Littman DR, Macpherson AJ. Interactions between the microbiota and the immune system. Science. 2012;336(6086):1268-73.

174. Shen C, Detry B, Lecocq M, Pilette C. A novel IgA/Delta-like 4/Notch axis induces immunosuppressive activity in human dendritic cells. Clin Immunol. 2016;168:37-46.
175. Diana J, Moura IC, Vaugier C, Gestin A, Tissandie E, Beaudoin L, et al. Secretory IgA induces tolerogenic dendritic cells through SIGNR1 dampening autoimmunity in mice. J Immunol. 2013;191(5):2335-43.
176. The Health Consequences of Smoking-50 Years of Progress: A Report of the Surgeon General. Reports of the Surgeon General. Atlanta (GA)2014.
177. Heijink IH, Brandenburg SM, Postma DS, van Oosterhout AJ. Cigarette smoke impairs airway epithelial barrier function and cell-cell contact recovery. Eur Respir J. 2012;39(2):419-28.
178. Schamberger AC, Mise N, Jia J, Genoyer E, Yildirim AO, Meiners S, et al. Cigarette smoke-induced disruption of bronchial epithelial tight junctions is prevented by transforming growth factor-beta. Am J Respir Cell Mol Biol. 2014;50(6):1040-52.
179. Shaykhiev R, Otaki F, Bonsu P, Dang DT, Teater M, Strulovici-Barel Y, et al. Cigarette smoking reprograms apical junctional complex molecular architecture in the human airway epithelium in vivo. Cell Mol Life Sci. 2011;68(5):877-92.
180. Heijink IH, Noordhoek JA, Timens W, van Oosterhout AJ, Postma DS. Abnormalities in airway epithelial junction formation in chronic obstructive pulmonary disease. Am J Respir Crit Care Med. 2014;189(11):1439-42.
181. Milara J, Peiro T, Serrano A, Cortijo J. Epithelial to mesenchymal transition is increased in patients with COPD and induced by cigarette smoke. Thorax. 2013;68(5):410-20.
182. Amatngalim GD, Hiemstra PS. Airway Epithelial Cell Function and Respiratory Host Defense in Chronic Obstructive Pulmonary Disease. Chin Med J (Engl). 2018;131(9):1099-107.
183. Barnes PJ. Cellular and molecular mechanisms of chronic obstructive pulmonary disease. Clin Chest Med. 2014;35(1):71-86.
184. Auerbach O, Stout AP, Hammond EC, Garfinkel L. Changes in bronchial epithelium in relation to cigarette smoking and in relation to lung cancer. N Engl J Med. 1961;265:253-67.
185. Staudt MR, Buro-Auriemma LJ, Walters MS, Salit J, Vincent T, Shaykhiev R, et al. Airway Basal stem/progenitor cells have diminished capacity to regenerate airway epithelium in chronic obstructive pulmonary disease. Am J Respir Crit Care Med. 2014;190(8):955-8.
186. Ghosh M, Miller YE, Nakachi I, Kwon JB, Baron AE, Brantley AE, et al. Exhaustion of Airway Basal Progenitor Cells in Early and Established Chronic Obstructive Pulmonary Disease. Am J Respir Crit Care Med. 2018;197(7):885-96.
187. Hackett NR, Shaykhiev R, Walters MS, Wang R, Zwick RK, Ferris B, et al. The human airway epithelial basal cell transcriptome. PLoS One. 2011;6(5):e18378.
188. Crystal RG. Airway basal cells. The "smoking gun" of chronic obstructive pulmonary disease. Am J Respir Crit Care Med. 2014;190(12):1355-62.

189. Kim V, Kelemen SE, Abuel-Haija M, Gaughan JP, Sharafkaneh A, Evans CM, et al. Small airway mucous metaplasia and inflammation in chronic obstructive pulmonary disease. Copd. 2008;5(6):329-38.
190. Gohy S, Carlier FM, Fregimilicka C, Detry B, Lecocq M, Ladjemi MZ, et al. Altered generation of ciliated cells in chronic obstructive pulmonary disease. Sci Rep. 2019;9(1):17963.
191. Chen G, Korfhagen TR, Karp CL, Impey S, Xu Y, Randell SH, et al. Foxa3 induces goblet cell metaplasia and inhibits innate antiviral immunity. Am J Respir Crit Care Med. 2014;189(3):301-13.
192. Park KS, Korfhagen TR, Bruno MD, Kitzmiller JA, Wan H, Wert SE, et al. SPDEF regulates goblet cell hyperplasia in the airway epithelium. J Clin Invest. 2007;117(4):978-88.
193. Saetta M, Turato G, Baraldo S, Zanin A, Braccioni F, Mapp CE, et al. Goblet cell hyperplasia and epithelial inflammation in peripheral airways of smokers with both symptoms of chronic bronchitis and chronic airflow limitation. Am J Respir Crit Care Med. 2000;161(3 Pt 1):1016-21.
194. Jeffery PK. Comparison of the structural and inflammatory features of COPD and asthma. Giles F. Filley Lecture. Chest. 2000;117(5 Suppl 1):251s-60s.
195. Perotin JM, Coraux C, Lagonotte E, Birembaut P, Delepine G, Polette M, et al. Alteration of primary cilia in COPD. Eur Respir J. 2018;52(1).
196. Yaghi A, Dolovich MB. Airway Epithelial Cell Cilia and Obstructive Lung Disease. Cells. 2016;5(4).
197. Yaghi A, Zaman A, Cox G, Dolovich MB. Ciliary beating is depressed in nasal cilia from chronic obstructive pulmonary disease subjects. Respir Med. 2012;106(8):1139-47.
198. Leopold PL, O'Mahony MJ, Lian XJ, Tilley AE, Harvey BG, Crystal RG. Smoking is associated with shortened airway cilia. PLoS One. 2009;4(12):e8157.
199. Ballenger JJ. Experimental effect of cigarette smoke on human respiratory cilia. N Engl J Med. 1960;263:832-5.
200. Pilette C, Godding V, Kiss R, Delos M, Verbeken E, Decaestecker C, et al. Reduced epithelial expression of secretory component in small airways correlates with airflow obstruction in chronic obstructive pulmonary disease. Am J Respir Crit Care Med. 2001;163(1):185-94.
201. Gamez AS, Gras D, Petit A, Knabe L, Molinari N, Vachier I, et al. Supplementing defect in club cell secretory protein attenuates airway inflammation in COPD. Chest. 2015;147(6):1467-76.
202. Kalluri R, Weinberg RA. The basics of epithelial-mesenchymal transition. J Clin Invest. 2009;119(6):1420-8.
203. Sohal SS, Reid D, Soltani A, Ward C, Weston S, Muller HK, et al. Reticular basement membrane fragmentation and potential epithelial mesenchymal transition is exaggerated in the airways of smokers with chronic obstructive pulmonary disease. Respirology. 2010;15(6):930-8.
204. Sohal SS, Reid D, Soltani A, Ward C, Weston S, Muller HK, et al. Evaluation of epithelial mesenchymal transition in patients with chronic obstructive pulmonary disease. Respir Res. 2011;12:130.

205. Mahmood MQ, Sohal SS, Shukla SD, Ward C, Hardikar A, Noor WD, et al. Epithelial mesenchymal transition in smokers: large versus small airways and relation to airflow obstruction. Int J Chron Obstruct Pulmon Dis. 2015;10:1515-24.
206. Bartis D, Mise N, Mahida RY, Eickelberg O, Thickett DR. Epithelial-mesenchymal transition in lung development and disease: does it exist and is it important? Thorax. 2014;69(8):760-5.
207. Jolly MK, Ward C, Eapen MS, Myers S, Hallgren O, Levine H, et al. Epithelial-mesenchymal transition, a spectrum of states: Role in lung development, homeostasis, and disease. Dev Dyn. 2018;247(3):346-58.
208. Sohal SS. Chronic Obstructive Pulmonary Disease (COPD) and Lung Cancer: Epithelial Mesenchymal Transition (EMT), the Missing Link? EBioMedicine. 2015;2(11):1578-9.
209. Gohy ST, Hupin C, Fregimilicka C, Detry BR, Bouzin C, Gaide Chevronay H, et al. Imprinting of the COPD airway epithelium for dedifferentiation and mesenchymal transition. Eur Respir J. 2015;45(5):1258-72.
210. Barnes PJ. Inflammatory mechanisms in patients with chronic obstructive pulmonary disease. J Allergy Clin Immunol. 2016;138(1):16-27.
211. Eapen MS, Myers S, Walters EH, Sohal SS. Airway inflammation in chronic obstructive pulmonary disease (COPD): a true paradox. Expert Rev Respir Med. 2017;11(10):827-39.
212. Gao W, Li L, Wang Y, Zhang S, Adcock IM, Barnes PJ, et al. Bronchial epithelial cells: The key effector cells in the pathogenesis of chronic obstructive pulmonary disease? Respirology. 2015;20(5):722-9.
213. Kuschner WG, D'Alessandro A, Wong H, Blanc PD. Dose-dependent cigarette smoking-related inflammatory responses in healthy adults. Eur Respir J. 1996;9(10):1989-94.
214. Keatings VM, Collins PD, Scott DM, Barnes PJ. Differences in interleukin-8 and tumor necrosis factor-alpha in induced sputum from patients with chronic obstructive pulmonary disease or asthma. Am J Respir Crit Care Med. 1996;153(2):530-4.
215. Wedzicha JA, Seemungal TA, MacCallum PK, Paul EA, Donaldson GC, Bhowmik A, et al. Acute exacerbations of chronic obstructive pulmonary disease are accompanied by elevations of plasma fibrinogen and serum IL-6 levels. Thromb Haemost. 2000;84(2):210-5.
216. Dongre A, Weinberg RA. New insights into the mechanisms of epithelial-mesenchymal transition and implications for cancer. Nat Rev Mol Cell Biol. 2018.
217. Gunay E, Sarinc Ulasli S, Akar O, Ahsen A, Gunay S, Koyuncu T, et al. Neutrophil-to-lymphocyte ratio in chronic obstructive pulmonary disease: a retrospective study. Inflammation. 2014;37(2):374-80.
218. Traves SL, Culpitt SV, Russell RE, Barnes PJ, Donnelly LE. Increased levels of the chemokines GROalpha and MCP-1 in sputum samples from patients with COPD. Thorax. 2002;57(7):590-5.
219. Lacoste JY, Bousquet J, Chanez P, Van Vyve T, Simony-Lafontaine J, Lequeu N, et al. Eosinophilic and neutrophilic inflammation in asthma, chronic

bronchitis, and chronic obstructive pulmonary disease. J Allergy Clin Immunol. 1993;92(4):537-48.
220. Leckie MJ, Jenkins GR, Khan J, Smith SJ, Walker C, Barnes PJ, et al. Sputum T lymphocytes in asthma, COPD and healthy subjects have the phenotype of activated intraepithelial T cells (CD69+ CD103+). Thorax. 2003;58(1):23-9.
221. Pesci A, Majori M, Cuomo A, Borciani N, Bertacco S, Cacciani G, et al. Neutrophils infiltrating bronchial epithelium in chronic obstructive pulmonary disease. Respir Med. 1998;92(6):863-70.
222. Saetta M, Di Stefano A, Maestrelli P, Ferraresso A, Drigo R, Potena A, et al. Activated T-lymphocytes and macrophages in bronchial mucosa of subjects with chronic bronchitis. Am Rev Respir Dis. 1993;147(2):301-6.
223. O'Shaughnessy TC, Ansari TW, Barnes NC, Jeffery PK. Inflammation in bronchial biopsies of subjects with chronic bronchitis: inverse relationship of CD8+ T lymphocytes with FEV1. Am J Respir Crit Care Med. 1997;155(3):852-7.
224. Lams BE, Sousa AR, Rees PJ, Lee TH. Immunopathology of the small-airway submucosa in smokers with and without chronic obstructive pulmonary disease. Am J Respir Crit Care Med. 1998;158(5 Pt 1):1518-23.
225. Eapen MS, McAlinden K, Tan D, Weston S, Ward C, Muller HK, et al. Profiling cellular and inflammatory changes in the airway wall of mild to moderate COPD. Respirology. 2017;22(6):1125-32.
226. Di Stefano A, Capelli A, Lusuardi M, Balbo P, Vecchio C, Maestrelli P, et al. Severity of airflow limitation is associated with severity of airway inflammation in smokers. Am J Respir Crit Care Med. 1998;158(4):1277-85.
227. Hogg JC, Chu F, Utokaparch S, Woods R, Elliott WM, Buzatu L, et al. The nature of small-airway obstruction in chronic obstructive pulmonary disease. N Engl J Med. 2004;350(26):2645-53.
228. Kaku Y, Imaoka H, Morimatsu Y, Komohara Y, Ohnishi K, Oda H, et al. Overexpression of CD163, CD204 and CD206 on alveolar macrophages in the lungs of patients with severe chronic obstructive pulmonary disease. PLoS One. 2014;9(1):e87400.
229. Profita M, Sala A, Bonanno A, Riccobono L, Ferraro M, La Grutta S, et al. Chronic obstructive pulmonary disease and neutrophil infiltration: role of cigarette smoke and cyclooxygenase products. Am J Physiol Lung Cell Mol Physiol. 2010;298(2):L261-9.
230. Russell RE, Thorley A, Culpitt SV, Dodd S, Donnelly LE, Demattos C, et al. Alveolar macrophage-mediated elastolysis: roles of matrix metalloproteinases, cysteine, and serine proteases. Am J Physiol Lung Cell Mol Physiol. 2002;283(4):L867-73.
231. Rutgers SR, Postma DS, ten Hacken NH, Kauffman HF, van Der Mark TW, Koeter GH, et al. Ongoing airway inflammation in patients with COPD who do not currently smoke. Thorax. 2000;55(1):12-8.
232. Utokaparch S, Sze MA, Gosselink JV, McDonough JE, Elliott WM, Hogg JC, et al. Respiratory viral detection and small airway inflammation in lung tissue of patients with stable, mild COPD. COPD. 2014;11(2):197-203.

233. Lams BE, Sousa AR, Rees PJ, Lee TH. Subepithelial immunopathology of the large airways in smokers with and without chronic obstructive pulmonary disease. Eur Respir J. 2000;15(3):512-6.
234. Ladjemi MZ, Gras D, Dupasquier S, Detry B, Lecocq M, Garulli C, et al. Bronchial Epithelial IgA Secretion Is Impaired in Asthma. Role of IL-4/IL-13. Am J Respir Crit Care Med. 2018;197(11):1396-409.
235. Van Vyve T, Chanez P, Bernard A, Bousquet J, Godard P, Lauwerijs R, et al. Protein content in bronchoalveolar lavage fluid of patients with asthma and control subjects. J Allergy Clin Immunol. 1995;95(1 Pt 1):60-8.
236. Ocak S, Pedchenko TV, Chen H, Harris FT, Qian J, Polosukhin V, et al. Loss of polymeric immunoglobulin receptor expression is associated with lung tumourigenesis. Eur Respir J. 2012;39(5):1171-80.
237. Gohy ST, Detry BR, Lecocq M, Bouzin C, Weynand BA, Amatngalim GD, et al. Polymeric immunoglobulin receptor down-regulation in chronic obstructive pulmonary disease. Persistence in the cultured epithelium and role of transforming growth factor-beta. Am J Respir Crit Care Med. 2014;190(5):509-21.
238. Polosukhin VV, Cates JM, Lawson WE, Zaynagetdinov R, Milstone AP, Massion PP, et al. Bronchial secretory immunoglobulin a deficiency correlates with airway inflammation and progression of chronic obstructive pulmonary disease. Am J Respir Crit Care Med. 2011;184(3):317-27.
239. Polosukhin VV, Richmond BW, Du RH, Cates JM, Wu P, Nian H, et al. Secretory IgA Deficiency in Individual Small Airways Is Associated with Persistent Inflammation and Remodeling. Am J Respir Crit Care Med. 2017;195(8):1010-21.
240. Du RH, Richmond BW, Blackwell TS, Jr., Cates JM, Massion PP, Ware LB, et al. Secretory IgA from submucosal glands does not compensate for its airway surface deficiency in chronic obstructive pulmonary disease. Virchows Arch. 2015;467(6):657-65.
241. Atis S, Tutluoglu B, Salepci B, Ocal Z. Serum IgA and secretory IgA levels in bronchial lavages from patients with a variety of respiratory diseases. J Investig Allergol Clin Immunol. 2001;11(2):112-7.
242. Barnes PJ. Immunology of asthma and chronic obstructive pulmonary disease. Nat Rev Immunol. 2008;8(3):183-92.
243. Nusse R, Varmus HE. Many tumors induced by the mouse mammary tumor virus contain a provirus integrated in the same region of the host genome. Cell. 1982;31(1):99-109.
244. Gavin BJ, McMahon JA, McMahon AP. Expression of multiple novel Wnt-1/int-1-related genes during fetal and adult mouse development. Genes Dev. 1990;4(12B):2319-32.
245. Polakis P. Wnt signaling in cancer. Cold Spring Harb Perspect Biol. 2012;4(5).
246. Tan RJ, Zhou D, Zhou L, Liu Y. Wnt/β-catenin signaling and kidney fibrosis. Kidney International Supplements. 2014;4(1):84-90.
247. Tao H, Yang J-J, Shi K-H, Li J. Wnt signaling pathway in cardiac fibrosis: New insights and directions. Metabolism. 2016;65(2):30-40.

248. Königshoff M, Balsara N, Pfaff EM, Kramer M, Chrobak I, Seeger W, et al. Functional Wnt signaling is increased in idiopathic pulmonary fibrosis. PLoS One. 2008;3(5):e2142.
249. Palomer E, Buechler J, Salinas PC. Wnt Signaling Deregulation in the Aging and Alzheimer's Brain. Frontiers in Cellular Neuroscience. 2019;13(227).
250. Johnson ML, Rajamannan N. Diseases of Wnt signaling. Reviews in endocrine & metabolic disorders. 2006;7(1-2):41-9.
251. Niehrs C. The complex world of WNT receptor signalling. Nature Reviews Molecular Cell Biology. 2012;13:767.
252. Angers S, Moon RT. Proximal events in Wnt signal transduction. Nat Rev Mol Cell Biol. 2009;10(7):468-77.
253. Nusse R, Clevers H. Wnt/beta-Catenin Signaling, Disease, and Emerging Therapeutic Modalities. Cell. 2017;169(6):985-99.
254. Metcalfe C, Mendoza-Topaz C, Mieszczanek J, Bienz M. Stability elements in the LRP6 cytoplasmic tail confer efficient signalling upon DIX-dependent polymerization. J Cell Sci. 2010;123(Pt 9):1588-99.
255. Eapen MS, Sharma P, Gaikwad AV, Lu W, Myers S, Hansbro PM, et al. Epithelial-mesenchymal transition is driven by transcriptional and post transcriptional modulations in COPD: implications for disease progression and new therapeutics. Int J Chron Obstruct Pulmon Dis. 2019;14:1603-10.
256. Zhan T, Rindtorff N, Boutros M. Wnt signaling in cancer. Oncogene. 2017;36(11):1461-73.
257. Tree DR, Shulman JM, Rousset R, Scott MP, Gubb D, Axelrod JD. Prickle mediates feedback amplification to generate asymmetric planar cell polarity signaling. Cell. 2002;109(3):371-81.
258. Sheldahl LC, Slusarski DC, Pandur P, Miller JR, Kuhl M, Moon RT. Dishevelled activates Ca2+ flux, PKC, and CamKII in vertebrate embryos. J Cell Biol. 2003;161(4):769-77.
259. Gao C, Chen YG. Dishevelled: The hub of Wnt signaling. Cell Signal. 2010;22(5):717-27.
260. Gross TJ, Hunninghake GW. Idiopathic pulmonary fibrosis. N Engl J Med. 2001;345(7):517-25.
261. Konigshoff M, Balsara N, Pfaff EM, Kramer M, Chrobak I, Seeger W, et al. Functional Wnt signaling is increased in idiopathic pulmonary fibrosis. PLoS One. 2008;3(5):e2142.
262. Konigshoff M, Kramer M, Balsara N, Wilhelm J, Amarie OV, Jahn A, et al. WNT1-inducible signaling protein-1 mediates pulmonary fibrosis in mice and is upregulated in humans with idiopathic pulmonary fibrosis. J Clin Invest. 2009;119(4):772-87.
263. Selman M, Pardo A, Kaminski N. Idiopathic pulmonary fibrosis: aberrant recapitulation of developmental programs? PLoS Med. 2008;5(3):e62.
264. Masoli M, Fabian D, Holt S, Beasley R. The global burden of asthma: executive summary of the GINA Dissemination Committee report. Allergy. 2004;59(5):469-78.

265. Wenzel SE. Asthma phenotypes: the evolution from clinical to molecular approaches. Nat Med. 2012;18(5):716-25.
266. Wang SH, Xu F, Dang HX, Yang L. Genetic variations in the Wnt signaling pathway affect lung function in asthma patients. Genetics and molecular research : GMR. 2013;12(2):1829-33.
267. Sharma S, Tantisira K, Carey V, Murphy AJ, Lasky-Su J, Celedon JC, et al. A role for Wnt signaling genes in the pathogenesis of impaired lung function in asthma. Am J Respir Crit Care Med. 2010;181(4):328-36.
268. Blacquiere MJ, Timens W, van den Berg A, Geerlings M, Postma DS, Hylkema MN. Maternal smoking during pregnancy decreases Wnt signalling in neonatal mice. Thorax. 2010;65(6):553-4.
269. Saglani S, Payne DN, Zhu J, Wang Z, Nicholson AG, Bush A, et al. Early detection of airway wall remodeling and eosinophilic inflammation in preschool wheezers. Am J Respir Crit Care Med. 2007;176(9):858-64.
270. Regamey N, Ochs M, Hilliard TN, Muhlfeld C, Cornish N, Fleming L, et al. Increased airway smooth muscle mass in children with asthma, cystic fibrosis, and non-cystic fibrosis bronchiectasis. Am J Respir Crit Care Med. 2008;177(8):837-43.
271. Helms PJ. Early environmental influences in the development of asthma and atopic disease. Monaldi Arch Chest Dis. 2001;56(3):265-9.
272. Hachim MY, Elemam NM, Ramakrishnan RK, Bajbouj K, Olivenstein R, Hachim IY, et al. Wnt Signaling Is Deranged in Asthmatic Bronchial Epithelium and Fibroblasts. Front Cell Dev Biol. 2021;9(297):641404.
273. Choy DF, Modrek B, Abbas AR, Kummerfeld S, Clark HF, Wu LC, et al. Gene expression patterns of Th2 inflammation and intercellular communication in asthmatic airways. J Immunol. 2011;186(3):1861-9.
274. Boucherat O, Morissette MC, Provencher S, Bonnet S, Maltais F. Bridging Lung Development with Chronic Obstructive Pulmonary Disease. Relevance of Developmental Pathways in Chronic Obstructive Pulmonary Disease Pathogenesis. Am J Respir Crit Care Med. 2016;193(4):362-75.
275. Baarsma HA, Skronska-Wasek W, Mutze K, Ciolek F, Wagner DE, John-Schuster G, et al. Noncanonical WNT-5A signaling impairs endogenous lung repair in COPD. J Exp Med. 2017;214(1):143-63.
276. Wu X, van Dijk EM, Ng-Blichfeldt JP, Bos IST, Ciminieri C, Konigshoff M, et al. Mesenchymal WNT-5A/5B Signaling Represses Lung Alveolar Epithelial Progenitors. Cells. 2019;8(10).
277. Skronska-Wasek W, Mutze K, Baarsma HA, Bracke KR, Alsafadi HN, Lehmann M, et al. Reduced Frizzled Receptor 4 Expression Prevents WNT/beta-Catenin-driven Alveolar Lung Repair in Chronic Obstructive Pulmonary Disease. Am J Respir Crit Care Med. 2017;196(2):172-85.
278. Kneidinger N, Yildirim AO, Callegari J, Takenaka S, Stein MM, Dumitrascu R, et al. Activation of the WNT/beta-catenin pathway attenuates experimental emphysema. Am J Respir Crit Care Med. 2011;183(6):723-33.
279. Uhl FE, Vierkotten S, Wagner DE, Burgstaller G, Costa R, Koch I, et al. Preclinical validation and imaging of Wnt-induced repair in human 3D lung tissue cultures. Eur Respir J. 2015;46(4):1150-66.

280. Cho MH, McDonald ML, Zhou X, Mattheisen M, Castaldi PJ, Hersh CP, et al. Risk loci for chronic obstructive pulmonary disease: a genome-wide association study and meta-analysis. Lancet Respir Med. 2014;2(3):214-25.
281. Jiang Z, Lao T, Qiu W, Polverino F, Gupta K, Guo F, et al. A Chronic Obstructive Pulmonary Disease Susceptibility Gene, FAM13A, Regulates Protein Stability of beta-Catenin. Am J Respir Crit Care Med. 2016;194(2):185-97.
282. Durham AL, McLaren A, Hayes BP, Caramori G, Clayton CL, Barnes PJ, et al. Regulation of Wnt4 in chronic obstructive pulmonary disease. FASEB J. 2013;27(6):2367-81.
283. Heijink IH, de Bruin HG, van den Berge M, Bennink LJ, Brandenburg SM, Gosens R, et al. Role of aberrant WNT signalling in the airway epithelial response to cigarette smoke in chronic obstructive pulmonary disease. Thorax. 2013;68(8):709-16.
284. Heijink IH, de Bruin HG, Dennebos R, Jonker MR, Noordhoek JA, Brandsma CA, et al. Cigarette smoke-induced epithelial expression of WNT-5B: implications for COPD. Eur Respir J. 2016;48(2):504-15.
285. Zou W, Zou Y, Zhao Z, Li B, Ran P. Nicotine-induced epithelial-mesenchymal transition via Wnt/beta-catenin signaling in human airway epithelial cells. Am J Physiol Lung Cell Mol Physiol. 2013;304(4):L199-209.
286. Spanjer AI, Menzen MH, Dijkstra AE, van den Berge M, Boezen HM, Nickle DC, et al. A pro-inflammatory role for the Frizzled-8 receptor in chronic bronchitis. Thorax. 2016;71(4):312-22.
287. Wang R, Ahmed J, Wang G, Hassan I, Strulovici-Barel Y, Hackett NR, et al. Down-regulation of the canonical Wnt beta-catenin pathway in the airway epithelium of healthy smokers and smokers with COPD. PLoS One. 2011;6(4):e14793.
288. Guo L, Wang T, Wu Y, Yuan Z, Dong J, Li X, et al. WNT/beta-catenin signaling regulates cigarette smoke-induced airway inflammation via the PPARdelta/p38 pathway. Lab Invest. 2015.
289. Yang J, Zuo WL, Fukui T, Chao I, Gomi K, Lee B, et al. Smoking-Dependent Distal-to-Proximal Repatterning of the Adult Human Small Airway Epithelium. Am J Respir Crit Care Med. 2017;196(3):340-52.

SECTION 2.

THE MEMORY OF AIRWAY EPITHELIUM DAMAGE IN SMOKERS AND COPD PATIENTS

Submitted to the European Respiratory Journal. Preprint available on BioRxiv (doi: https://doi.org/10.1101/2021.04.21.439437)

François M. Carlier, Bruno Detry, Marylène Lecocq, Amandine M. Collin, Thomas Planté-Bordeneuve, Stijn E. Verleden, Claudia M. Stanciu-Pop, Benoît Rondelet, Wim Janssens, Jérôme Ambroise, Bart M. Vanaudenaerde, Sophie T. Gohy, and Charles Pilette.

1. Abstract

Background. Chronic obstructive pulmonary disease (COPD) is a devastating lung disease, representing the third cause of mortality worldwide. In COPD, the bronchial epithelium displays several structural and functional abnormalities affecting barrier integrity, cell polarity, and differentiation, as well as epithelial-to-mesenchymal transition (EMT) and inflammation. Although COPD is currently considered an irreversible disease, the (ir)reversible nature of epithelium changes *ex vivo* remains poorly known.

Methods. The persistence of COPD epithelial abnormalities was addressed in very long-term (10 weeks) primary cultures of air/liquid interface (ALI)-reconstituted airway epithelium from non-smoker controls, smoker controls, and COPD patients. The role of inflammation was also explored by stimulating ALI cultures with a cytokine mix consisting of TNF-α, IL-6 and IL-1β. Finally, the cellular niche holding epithelial memory was studied by exploiting a single cell RNA-sequencing database.

Results. Almost all epithelial defects (barrier dysfunction, impaired polarity, lineage abnormalities) observed in smokers and COPD patients persisted *in vitro* up to week 10, except IL-8/CXCL-8 release and EMT which declined over time. Cytokine

treatment induced COPD-like changes and reactivated EMT in COPD cells. Progenitor cells of large and small airways, namely basal and club cells, exhibited EMT-related signatures reminiscent of features observed *in situ*.

Conclusions. The airway epithelium from smokers and COPD patients displays a memory of its native state and previous injuries by cigarette smoking, which is multidimensional and sustained for years. This memory probably resides in progenitor cells of the airway epithelium.

2. Introduction

Chronic obstructive pulmonary disease (COPD) currently represents the third leading cause of death worldwide (1). The key factors underlying this pathology are the exposure to noxious airborne stimuli, most importantly cigarette smoke (CS), and genetic predisposition (2). COPD is characterized by a progressive and mostly irreversible airway obstruction related to the narrowing and disappearance of small conducting airways (3) and the destruction of the alveolar walls, referred to as emphysema (4). The irreversible nature of the disease also refers to the relatively modest effects of currently available therapies (5) including inhaled corticosteroids and bronchodilators, none of which targeting the underlying pathways leading to structural remodeling of the lungs.

The airway epithelium (AE) acts as a first line barrier against inhaled particles and antigens and is as such constantly exposed to airborne pollutants. This AE fulfills multiple functions to maintain pulmonary homeostasis, ensuring adequate barrier function, cell differentiation and polarization, and maintaining a tight control on inflammatory mechanisms.

In COPD, AE structure and biology are profoundly altered, impacting those core epithelial functions. Indeed, the functionality and composition of the COPD bronchial epithelium is modified, notably with altered physical barrier function (6, 7) underpinned by decreased bronchial expression of tight and adherens junction (TJ and AJ) proteins such as zonula occludens-1 (ZO-1) and E-cadherin (8), and

abnormal differentiation with decreased function and numbers of ciliated cells (9, 10), diminished club cells numbers and club cell secretory protein (SCGB1A1) production (11, 12) and hyperplastic goblet cells, the latter being possibly more related to CS exposure than to the disease *per se* (13). In parallel with these anomalies, the COPD AE also displays aberrant epithelial-to-mesenchymal transition (EMT), that is triggered by CS in a TGF-β-dependent manner (14) and further enhanced in COPD, both in large and small airways (15), contributing to subepithelial fibrosis and cancer susceptibility in COPD patients (16)

The AE also expresses the polymeric immunoglobulin receptor (pIgR), which is considered a marker of epithelial polarization (17, 18) and constitutes a key component in local immune mechanisms (19-21). The pIgR ensures the transcytosis and release of subepithelial polymeric immunoglobulins (Ig) into mucosal secretions through epithelial transcytosis, a process finalized by the cleavage of pIgR at the apical side of the epithelium. This results in the secretion in the airway lumen of its extracellular part, the secretory component (SC), either free or bound to polymeric Ig thereby generating secretory (S-)Ig (19). The pIgR/SC system is defective in the COPD AE with decreased epithelial pIgR expression (17) and local S-IgA deficiency in small airways being associated with epithelial inflammation and remodeling (22, 23).

Finally, epithelial inflammation is a paramount feature in COPD and is thought to represent a major player in the disease pathophysiology (24). In line with the increased presence of intraepithelial neutrophils (25), increased levels in tumor necrosis factor (TNF)-α, interleukin-8/C-X-C Motif Chemokine Ligand 8 (IL-8/CXCL-8) and neutrophils have been observed in sputum from COPD patients (26, 27) and correlate with disease severity (28).

The air/liquid interface (ALI) culture model of primary human bronchial epithelial cells (HBEC) allows the reconstitution of the AE *in vitro* and has been shown to recapitulate several of the observed alterations in the native tissue. Indeed, CS extract-exposed COPD human bronchial epithelial cells (HBEC) show decreased E-

cadherin and ZO-1 expression when compared with HBEC from smokers (14) and the *ex vivo* reconstituted epithelium issued from COPD patients displays features of altered lineage differentiation, decreased pIgR expression and EMT, up to 4 weeks after reconstitution (8, 10, 17). Although these data point towards the persistence of AE abnormalities in this primary cell culture model, it remains unclear whether (and to what extent) these structural changes are persistent in COPD on the long-term, matching the irreversible nature of the disease. Heterogeneous data exist regarding this matter as, on the one hand, clinical studies show that COPD patients who quit smoking for more than 3.5 years display less goblet cell hyperplasia and squamous metaplasia (29), and that smoking cessation may slightly improve pulmonary function tests (30) and reduce mortality (31). On the other hand, smoking cessation does not influence COPD-related epidermal growth factor receptor (EGFR) activation (29) and protease activity (32). In COPD, the inflammatory pattern that is shared with 'healthy' smokers is amplified and persists even after smoking cessation (33), although data are conflicting between studies (30, 33, 34). The present study aimed to elucidate whether AE changes are imprinted in a persistent manner, or whether some changes could be reversible, i.e. questioning the memory (31) retained in epithelial cells from COPD patients.

To address this question, the AE was reconstituted in the ALI culture model with primary HBEC from non-smokers, non-COPD smokers (referred to as "control smokers") and COPD patients, and cultured *in vitro* for up to 10 weeks, and the spontaneous evolution of abnormalities was assayed for multiple readouts, namely barrier function, cell differentiation, EMT, pIgR/SC-related polarity and production of inflammatory cytokines. In addition, it was assessed whether exogenous inflammation may trigger COPD-related changes in this model. Existing single-cell RNA sequencing (scRNAseq) databases were finally exploited to identify cell populations that may retain signatures underlying the memory of epithelial damage in COPD.

3. Materials and methods

3.1.Study population and lung tissue samples

A series of lung surgical specimens containing large airways was obtained from four different patients' groups (non-smokers, smoker controls, mild and moderate COPD and severe to very severe COPD). COPD patients were sorted on basis of their pulmonary function tests, according to the GOLD 2001 classification (35). Surgical tissue from lobectomies was used for controls and mild or moderate COPD patients undergoing lung surgery for a solitary tumor, while explants were obtained to analyze lung tissue from patients with (very) severe COPD. Patients with any other lung disease than COPD (e.g., asthma, lung fibrosis) were excluded from the study. All patients received information and signed a written consent to the study protocol, which was approved by the local clinical Ethical committee (reference 2007/19MARS/58 for UCLouvain, S52174 and S55877 for KULeuven). A primary proximal bronchial epithelium was reconstituted *in vitro* from all subjects, and was subjected to mid-term (5 weeks, n_1=51) or long-term (10 weeks, n_2=26) culture. Patients' characteristics are shown in Tables 2, 3 and 4.

	Non-smoker controls (n=10)	Smoker controls (n=15)	COPD 1-2 (n=13)	COPD 3-4 (n=13)	
N (Male/Female)	10 (4/6)	15 (11/4)	13 (6/7)	13 (5/8)	ns
Age (y)	68.7 ± 13.2	64.2 ± 9.0	64.4 ± 9.5	59.8 ± 4.6	ns
Smoking history (never/former/ current n)	10/0/0	0/10/5	0/4/9	0/13/0	p=0.001
Pack-years	0.0 ± 0	32.5 ± 20.7*	43.1 ± 19.6*	43.2 ± 23.1*	p<0.0001
If applicable, duration since smoking cessation (mo)	NA	154.0 ± 154.1	50.0 ± 55.5	90.6 ± 87.0	ns
FEV1 (% of PV)	104.8 ± 15.5	95.5 ± 14.7	74.1 ± 9.7*#	23.6 ± 6.1*#¶	p<0.0001
FEV1/VC ratio (%)	79.4 ± 6.9	78.5 ± 6.8	59.9 ± 9.3*#	33.2 ± 6.6*#¶	p<0.0001
DLCO (% of PV)	77.7 ± 13.0	69.9 ± 14.1	59.2 ± 19.1*	35.6 ± 8.0*#¶	p<0.0001
BMI (kg.m^{-2})	27.8 ± 5.7	26.7 ± 5.2	25.4 ± 5.8	23.8 ± 4.0	ns
Inhaled corticosteroids (n/total N)	0/10	1/15	1/13	12/13	p<0.0001

Table 2 | Patient cohort for ALI-cultures.

Data are presented as mean ± SD, unless otherwise stated. Demographic data, lung function tests, smoking history and inhaled corticotherapy are stated for the patient groups, classified according to smoking history and the presence and severity of airflow limitation. ALI, air/liquid interface; BMI, body mass index; COPD, chronic obstructive pulmonary disease; DLCO, diffusing capacity of the lung for CO; FEV1, forced expiratory volume in 1 s; mo, months; PV, predicted values; SD, standard deviation; VC, vital capacity; y, years.

* = p<0.05 compared to non-smoker controls. # = p<0.05 compared to smoker controls. ¶ = p<0.05 compared to COPD stage 1-2 patients. ns, not significant.

	Non-smoker controls (n=5)	Smoker controls (n=7)	COPD 1-2 (n=7)	COPD 3-4 (n=7)	
N (Male/Female)	5 (2/3)	7 (6/1)	7 (4/3)	7 (2/5)	ns
Age	67.9 ± 13.8	66.1 ± 11.1	66.42 ± 12.3	58.18 ± 5.7	ns
Smoking history (never/former/current n)	5/0/0	0/5/2	0/1/6	0/7/0	p<0.01
Pack-years	0.0 ± 0	28.6 ± 14.4*	43.5 ± 15.6*	34.4 ± 10.8*	p<0.0001
If applicable, duration since smoking cessation (mo)	NA	73.1 ± 98.4	14.5 ± 23.9	75.6 ± 57.0	ns
FEV1 (% of PV)	100.0 ± 12.7	91.3 ± 18.9	77.3 ± 10.4*#	22.0 ± 2.3*#¶	p<0.0001
FEV1/VC ratio (%PV)	81.8 ± 4.7	83.4 ± 6.5	54.6 ± 7.0*#	31.6 ± 5.9*#¶	p<0.0001
DLCO (% of PV)	72.8 ± 13.8	63.5 ± 15.1	54.9 ± 22.1	35.0 ± 10.0*#	p<0.01
BMI ($kg.m^{-2}$)	28.9 ± 3.5	26.6 ± 5.5	23.7 ± 5.1	22.47 ± 3.7	ns
Inhaled corticosteroids (n/total N)	0/5	1/7	0/7	7/7	p<0.001

Table 3 | Patient cohort for long-term (10 weeks) ALI culture.

Data are presented as mean ± SD, unless otherwise stated. Demographic data, lung function tests, smoking history and inhaled corticotherapy are stated for the patient groups, classified according to smoking history and the presence and severity of airflow limitation. ALI, air/liquid interface; BMI, body mass index; COPD, chronic obstructive pulmonary disease; DLCO, diffusing capacity of the lung for CO; FEV1, forced expiratory volume in 1 s; FVC, forced vital capacity; NA, not applicable; PV, predicted values.

* = p<0.05 compared to non-smoker controls. # = p<0.05 compared to smoker controls. ¶ = p<0.05 compared to COPD 1-2 patients. ns, not significant.

	Non-smoker controls (n=5)	Smoker controls (n=8)	COPD 1-2 (n=6)	COPD 3-4 (n=6)	
N (Male/Female)	5 (2/3)	8 (5/3)	6 (2/4)	6 (3/3)	ns
Age	69.4 ± 14.1	62.4 ± 7.1	62.0 ± 4.6	61.7 ± 2.2	ns
Smoking history (never/former/current)	5/0/0	0/5/3	0/3/3	0/6/0	ns
Pack-years	0.0 ± 0	37.0 ± 27.1	42.7 ± 24.6	53.3 ± 30.3	p<0.05
If applicable, duration since smoking cessation (mo)	NA	275.4 ± 149.7	85.6 ± 56.9	108.1 ± 116.5	ns
FEV1 (% of PV)	110.8 ± 18.5	99.1 ± 9.6	70.3 ± 8.00*#	26.7 ± 7.8*#¶	p<0.0001
FEV1/VC ratio (%)	76.5 ± 8.7	74.3 ± 3.3	66.0 ± 7.9	35.2 ± 7.5*#	p<0.01
DLCO (% of PV)	83.8 ± 10.3	75.4 ± 11.3	64.2 ± 15.3	36.5 ± 8.2*#¶	P<0.001
BMI ($kg.m^{-2}$)	26.7 ± 7.6	26.7 ± 5.3	27.5 ± 6.3	25.4 ± 4.2	ns
Inhaled corticosteroids (n/total N)	0/5	0/8	1/6	5/6	p<0.01

Table 4 | Patient cohort for midterm (5 weeks) ALI culture.

Data are presented as mean ± SD, unless otherwise stated. Demographic data, lung function tests, smoking history and inhaled corticotherapy are stated for the patient groups, classified according to smoking history and the presence and severity of airflow limitation. Patients with other lung diseases were excluded from the study. N is specified when data are missing. ALI, air/liquid interface; BMI, body mass index; COPD, chronic obstructive pulmonary disease; DLCO, diffusing capacity of the lung for CO; FEV1, forced expiratory volume in 1 s; FVC, forced vital capacity; NA, not applicable; PV, predicted values.

* = p<0.05 compared to non-smoker controls. # = p<0.05 compared to smoker controls. ¶ = p<0.05 compared to COPD 1-2 patients. ns, not significant.

3.2.*In vitro* reconstitution of primary human bronchial epithelium on ALI culture

A large piece of cartilaginous bronchus was selected from lobectomies or explants, located as far as possible from the tumor site (in the case of lobectomies) and submitted to pronase digestion overnight at 4°C, in order to derive HBEC. HBEC were cultured in flasks in retinoic acid-supplemented Bronchial Epithelial Cell Growth Basal Medium (BEBM, Lonza, Verviers, Belgium) until confluence. Cells were then detached and seeded at a density of 80,000 cells/well on 24-well polyester filter-type inserts (0.4-µm pore size; Corning, Corning, NY) coated with 0.2 mg/ml collagen IV (Sigma-Aldrich, Saint-Louis, MO) until a confluent monolayer was obtained. The culture was then carried out in ALI for 5 (for 25 subjects) or 10 weeks (for 26 subjects). Once in ALI, HBEC were cultured in BEBM:Dulbecco's Modified Eagles Medium (DMEM) (1:1) medium supplemented with penicillin (100U/ml), streptomycin (100µg/ml) (Lonza, Verviers, Belgium), bovine serum albumin (BSA) (1.5 µg/ml), retinoic acid (30ng/ml) (Sigma, Saint-Louis, MO), and BEGM SingleQuotsTM Supplements and Growth Factors (Lonza), including bovine pituitary extract (52µg/ml), insulin (5µg/ml), hydrocortisone (0.5g/ml), transferrin (10µg/ml), epinephrine (0.5µg/ml), epidermal growth factor (0.5ng/ml) and triiodothyronine (3.25ng/ml). Every week during ALI culture, basolateral media were collected, and the apical pole of HBEC was washed with 300µl sterile phosphate-buffered saline (PBS) before centrifugation for 5 minutes at 10,000g. Transwell inserts were fixed by direct immersion in 4% buffered formaldehyde, before incubation in PBS (pH 7.4) and embedding in paraffin blocks. ALI-HBEC were also processed for mRNA abundance or Western blot analyses (see below).

The 25 samples that underwent 5 weeks ALI culture were exposed or not (control condition) to a pro-inflammatory cytokine cocktail including IL-1β, IL-6, TNF-α, each at 5 ng/ml (Miltenyi Biotec, Germany) in the basolateral compartment following a preliminary titration experiment (10, 5, and 2,5 ng/ml) where no

cytotoxicity (release of lactate dehydrogenase < 5%) was shown at 5 ng/ml (data not shown).

3.3.Measurement of the transepithelial electric resistance

Every week and for each sample, the transepithelial electric resistance (TEER) of the reconstituted epithelium was assessed, using the EMD Millipore™ Millicell-ERS Volt-Ohm Meter (Fisher Scientific, Hampton, NH, USA) after transiently filling the apical pole of the cells with sterile PBS. TEER was measured in duplicates and the mean of the measurements was used, after values were corrected for the resistance of the transwell membrane.

3.4.Reverse transcriptase quantitative polymerase chain reaction (RT-qPCR)

RNA extraction, reverse transcription, and RT-qPCR were performed as previously described (36). Total RNA was extracted from reconstituted ALI cultured epithelia using TRIzol reagent (Thermo Fisher Scientific). 500ng of RNA was reverse-transcribed with RevertAid H minus Reverse transcriptase kit with 0.3 µg of random hexamer, 20U of RNase inhibitor and 1mM of each dNTP (Thermo Fisher Scientific, Waltham, MA) following the manufacturer's protocol in a thermocycler (Applied Biosystems, Foster City, CA). The expression levels were quantified by real-time quantitative PCR with the CFX96 PCR (Bio-Rad, Hercules, CA). The reaction mix contained 2.5 µl of complementary desoxyribonucleic acid diluted 10-fold, 200nM of each primer (primers properties are detailed in Table 5) and 2x iTaq UniverSybr Green® Supermix (Bio-Rad) in a final volume of 20 µl. The cycling conditions were 95°C for 3 minutes followed by 40 cycles of 95°C for 5 seconds and 60°C for 30 seconds. To control the specificity of the amplification products, a melting curve analysis was performed. The copy number was calculated from the standard curve. Data analysis was performed using Bio-Rad CFX software (Bio-Rad). Expression levels of target genes were normalized to the geometric mean of the values of 3 housekeeping genes (RPL27, RPS13, RPS18).

Gene	Fw primer (5'-3')	Rv primer (3'-5')	AS	HT
Housekeeping genes				
RPL27	TGG TAG GGC CGG GTG GTT GC	ACT TTG CGG GGG TAG CGG TC	185	60
RPS13	TCG GCT TTA CCC TAT CGA CGC AG	ACG TAC TTG TGC AAC ACC ATG TGA	153	60
RPS18	TGT GGG CCG AAG ATA TGC T	TGA TCA CAC GTT CCA CCT CAT	101	60
Target genes				
CDH1	GCT GGA CCG AGA GAG TTT CC	CGA CGT TAG CCT CGT TCT CA	179	60
IL8	CTC TGT GTG AAG GTG CAG TTT TG	AAC TTC TCC ACA ACC CTC TGC	223	60
DNAI1	GAG TTG ACC GAT GCG GAG TT	GGT TCC CAA CCT GGG TGT AG	163	60
DNAI2	GCG ATT CAT ACA TCT GGG AC	CAG CAG GCT ATC TGT CCA T	145	60
FOXA3	TGC TGG GCT CAG TGA AGA TG	GTC ATG TAG GAG TTG AGG GGG	124	60
FOXJ1	CCT GGC AGA ATT CAA TCC G	GCG TAC TGG GGG TCA AT	115	60
IL6	AGT TCC TGC AGA AAA AGG CAA AG	TGA GGT GCC CAT GCT ACA TTT	198	60
MCIDAS	GAC GCG CTT GTT GAG AAT AA	CAC GTT CCG CTC CTT GAG	84	60
MYB	TAC TGC CTG GAC GAA CTG ATA A	CTG GCT GGC TGG CTT TTG AA	111	60
PIGR	CTC TCT GGA GGA CCA CCG T	CAG CCG TGA CAT TCC CTG	78	60

SPDEF	TGA CCT TGG AGG AGC ACT CG	CAT GGG ATC TGC GGT GAT GTT	110	60
TJP1	GTG GTT CTT CGA GAA GCT GGA	TGC AGG CGA ATA ATG CCA GA	170	60
VIM	CGG GAG AAA TTG CAG GAG GA	AAG GTC AAG ACG TGC CAG AG	105	60

Table 5 | List of the primers used for RT-qPCR.
Fw, Forward; Rv, reverse; AS, Amplicon size (base pair); HT, hybridization temperature (°C).

3.5.Western blot assays

HBEC lysates were analysed by Western blot as previously described (37) except for band revelation (see below). Cells were lyzed with 150µl of Laemmli's sample buffer containing 0.7M 2-mercaptoethanol (Sigma-Aldrich) and lysates were stored at -20°C. After thawing, samples were heated at 100°C for 5 minutes, loaded in a SDS-PAGE gel before migration at 100V for 15 minutes and then at 180V for 50 minutes. Cell proteins were transferred onto a nitrocellulose membrane (Thermo Fisher Scientific) at 0.3A for 2 hours 10 minutes at RT. The membranes were blocked with 5% w/v BSA (Sigma-Aldrich) in Tris-buffered saline with 0.1% Tween 20 (Sigma-Aldrich) for 1 hour at RT, then washed and incubated overnight at 4°C with a primary antibody according to the target protein (see Table 6 listing used primary and secondary antibodies). Membranes were then incubated for 1 hour at room temperature (RT) with horseradish peroxidase (HRP)-conjugated secondary anti-rabbit (Cell Signalling, Danvers, MA) or anti-mouse (Sigma) IgG. Immunoreactive bands were revealed by chemiluminescence (GE Healthcare, Pittsburgh, PA), detected by Chemidoc XRS apparatus (Bio-Rad) and quantified using the Quantity One software (Bio-Rad).

Target	Species	Brand and reference
Primary antibodies		
E-cadherin	Mouse monoclonal antibody	Dako M3612
GAPDH	Rabbit polyclonal antibody	Sigma G9545
pIgR	Rabbit polyclonal antibody	Home made
Occludin	Rabbit polyclonal antibody	Merck-Millipore ABT146
Vimentin	Mouse monoclonal antibody	Dako M0725
Secondary antibodies		
Anti-Rabbit HRP-conjugated	Goat polyclonal antibody	Cell signalling 7074S
Anti-mouse HRP-conjugated	Sheep polyclonal antibody	Sigma A6782

Table 6 | List of the primary and secondary antibodies used for western blot

3.6.Sandwich ELISA for SC, IL-8 and IL-6

SC concentration was determined in apical washes by sandwich ELISA, as previously described (11, 37). Basolateral IL-8 and IL-6 release were assessed by sandwich ELISA, following manufacturer's instructions (Biotechne, Minneapolis, MN). Briefly, 96-well plates were coated overnight, at 4°C, with anti-IL-8, -IL-6, and -SC antibodies diluted in bicarbonate buffer (pH 9,6). Then, after blocking with 1% w/v BSA in phosphate-buffered saline for 90 min at 37°C, HBEC apical washes (for SC) or basolateral supernatants (for IL-8 and IL-6) were incubated for 60 min at 37°C, along with standard samples. Detection was performed with a first incubation with the corresponding biotinylated antibody (anti-fibronectin, -SC, -IL-8 or -IL-6), followed by a second incubation with HRP-linked anti-mouse IgG, for 1 h each. Revelation was performed with 3,3',5,5'-tetramethylbenzidine (TMB, Fisher) and stopped with H_2SO_4 1.8 M.

3.7.Direct ELISA for fibronectin

Fibronectin basolateral release was assessed by direct ELISA as previously described (8, 38). HBEC basolateral washes and fibronectin standard were coated in plates with bicarbonate buffer overnight (pH 9,6), at 4°C. After blocking with 1% w/v BSA in phosphate-buffered saline for 90 min at 37°C, detection was performed with a first incubation with mouse anti-fibronectin, followed by a second incubation with HRP-linked anti-mouse IgG, for 1 h each. Revelation was performed with TMB and stopped with H_2SO_4 1.8 M.

3.8.Single-cell RNA sequencing database analysis

Data from a recent single-cell RNA sequencing study were downloaded. In that study, COPD pathogenesis was analysed in COPD patients, non-COPD smokers and never-smokers in order to investigate the disease progression at single-cell resolution (39). Data from this study were imported and analysed into R using the R software package Seurat v.3.1.5 and the source code made available by the author on Github (https://github.com/JunNakayama/scRNAseq-COPD). In that respect, normalization, scaling, clustering of cells and identifying cluster marker genes, were performed with the same parameter than in the corresponding study (39). Progenitor cells of the airways (namely basal and club cells) were then selected, and EMT-related genes (VIM, FN1, SNAI1, SNAI2, S100A2, S100A4) were specifically assessed for a more comprehensive analysis.

3.9.Statistical analysis

Results were analysed with JMP® Pro, Version 14 (SAS Institute Inc., Cary, NC, USA) and GraphPad Prism version 8.0.2 for Windows (GraphPad Software, La Jolla, CA, USA), and were expressed as medians and interquartile ranges unless otherwise stated. p-values < 0.05 were considered statistically significant.

4. Results

Readouts were assessed (for each sample, according to availability) at different timepoints of redifferentiation, which are referred to as early (1 week ALI), short-term (2-3 weeks ALI), mid-term (4-7 weeks ALI) and long-term (8-10 weeks ALI) cultures.

4.1.Barrier and junctional properties in the COPD vs control AE

As physical barrier constitutes a first-line defense provided by the AE, this function was first assessed for impairment in COPD by measuring the transepithelial electric resistance (TEER) of ALI-reconstituted primary AE cultured for 5 weeks (n_1=51 patients) or up to 10 weeks (n_2=26 patients). According to their smoking status and lung function (GOLD 2001 classification (35)), the study population was divided into 4 groups: non-smoker controls (NS; n_1=10 for 5 weeks and n_2=5 for 10 weeks), smoker controls (Smo; n_1=15 and n_2=7), mild and moderate COPD (COPD GOLD 1-2; n_1=13 and n_2=7) and severe to very severe COPD (COPD GOLD 3-4; n_1=13 and n_2=7). The characteristics of the complete study population are summarized in Table 1, and detailed analysis of separate populations is provided in Tables 3 and 4.

The reconstituted AE from COPD patients displayed substantially decreased TEER as compared with that of non-smoker controls, and to a lesser extent with that of smoker controls (Figure 13). In addition, smoker controls AE also showed decreased TEER compared with that of non-smoker controls. This defect appeared in early ALI cultures and was progressively more prominent over time (Figure 13 A-D), persisting in long-term cultures (Figure 13 F). In short-term up to long-term ALI-AE, TEER inversely correlated modestly but significantly with the disease severity witnessed by the forced expiratory volume in one second (FEV1) (as represented at mid-term in Figure 13 E).

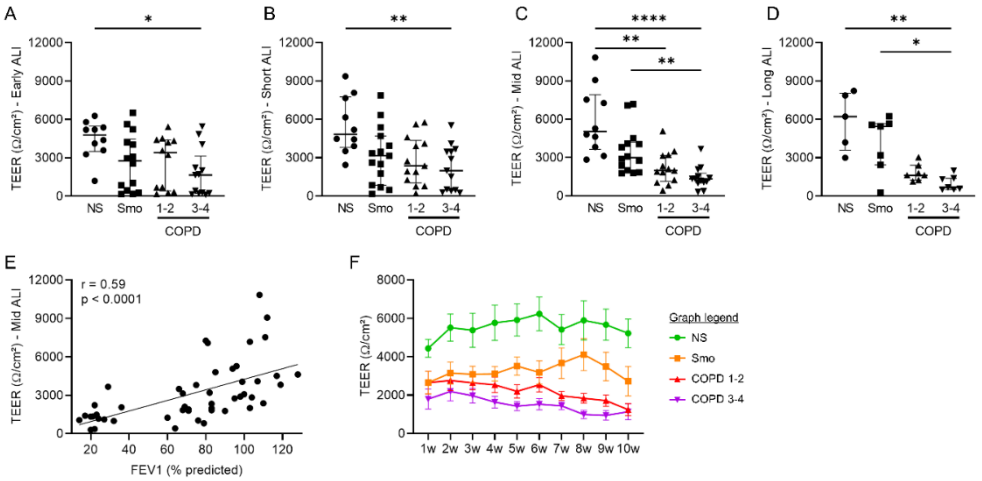

Figure 13 | TEER in ALI-AE from COPD and controls

COPD and smokers AE displays persistent decreased TEER compared with non-smokers AE.

A-D. TEER in the ALI-AE from non-smokers and smoker controls and COPD patients (GOLD classification from 1 to 4 according to the spirometric severity of the disease). Severe and very severe COPD AE show a sharp decrease in TEER as compared with (non)-smokers at all time periods, that is also observed to a lesser extent in mild and moderate COPD.

E. The barrier dysfunction observed in COPD, witnessed by the TEER decrease, significantly correlates with the disease severity assessed by the FEV1. This is observed from short-term up to long-term cultures.

F. Longitudinal analysis of the evolution of the TEER in the ALI-AE from non-smokers, smoker controls, mild-to-moderate COPD and (very) severe COPD patients, showing a smoking-related persistent barrier dysfunction that is further enhanced in COPD. °, $^{\#}$, §, $^{£}$ < 0.0001, $^{\$}$, ¶ < 0.001, mixed model analysis.

*, **, ***, **** indicate p-values of less than 0.05, 0.01, 0.001, and 0.0001, respectively (analysed using the Kruskal-Wallis test followed by Dunn's post-hoc test, except for H). Bars indicate median ± interquartile range, except for H, mean ± SEM. °: CT NS *versus* Smo; $^{\#}$: CT NS *versus* COPD 1-2, §: CT NS *versus* COPD 3-4, $^{\$}$: CT S *versus* COPD 1-2, $^{£}$: CT S *versus* COPD 3-4, ¶: COPD 1-2 *versus* COPD 3-4

AE, airway epithelium; ALI, air-liquid interface; COPD, chronic obstructive pulmonary disease; FEV1, forced expired volume in 1 second; GAPDH, glyceralderhyde-3-phosphate dehydrogenase; NS, non-smokers; SEM, standard error of the mean; Smo, smokers; TEER, transepithelial electric resistance; w, weeks.

To elucidate the molecular substratum of this long-lasting barrier disruption, mRNA abundance and protein expression of major components of the tight and adherens junctions were assayed, namely claudin-1 (*CLDN1*), E-cadherin (*CDH1*), occludin (*OCLN*) and ZO-1/tight junction protein 1 (*TJP1*). Although no difference was observed between groups regarding mRNA abundance (Figure 14), protein expression of E-cadherin was reduced in COPD as compared with non-smoker controls in early and short-term ALI cultures, but not at mid-term and long-term (Figure 15 A-D), while that of occludin was decreased in short-, mid- and long-term ALI-AE from smokers and COPD patients (Figure 15 E-G), and inversely correlated with the disease severity, assessed by the FEV1 (as represented at mid-term in Figure 15 H). Figure 15 I and 15 J show representative blots for E-cadherin (early and short-term) and occludin (mid- and long-term) in reconstituted AE from non-smokers and severe COPD. These data globally depict a defect in the barrier function of the AE that is engaged in smokers, further worsens in COPD following disease severity, and which is persistent in prolonged *in vitro* culture.

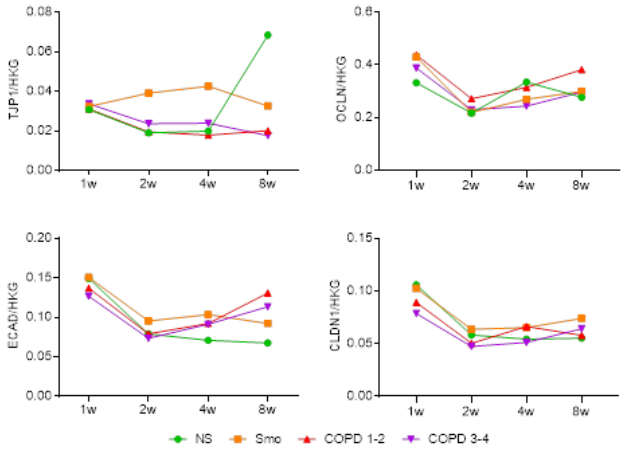

Figure 14 | mRNA abundance of tight and adherens junctions key components
No difference was seen over time regarding the mRNA abundance of *TJP1*, *OCLN*, *ECAD* and *CLDN1* in the AE of non-smokers, smoker controls, mild-to-moderate COPD and (very) severe COPD patients.
Graphs plot means. AE, airway epithelium; COPD, chronic obstructive pulmonary disease; NS, non-smokers; Smo, smokers; PV, predicted values.

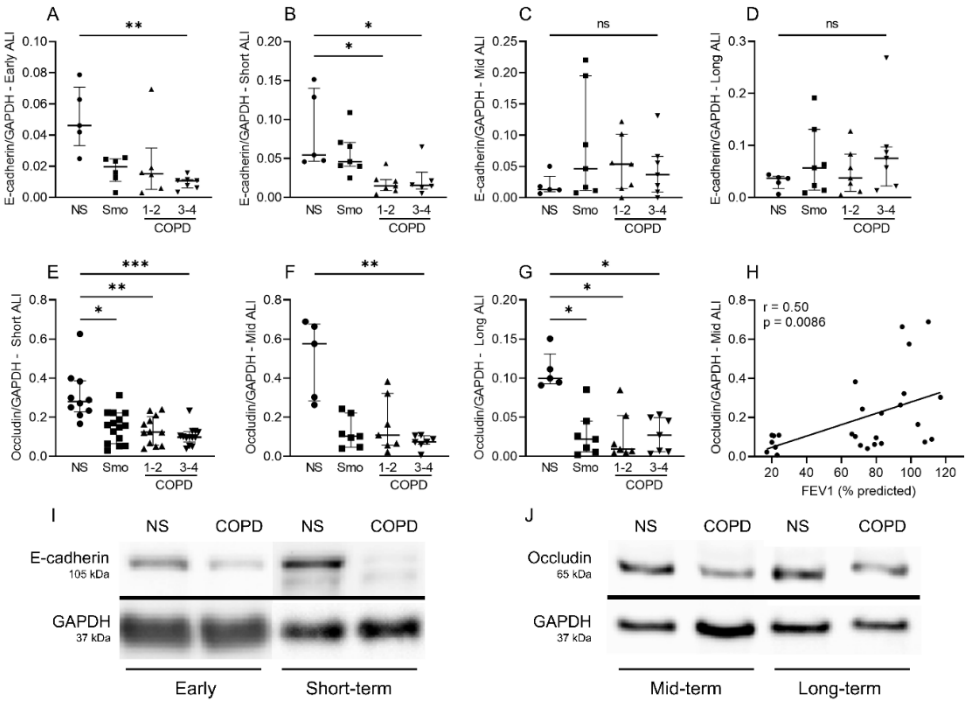

Figure 15 | E-cadherin and occludin expression in ALI-AE

COPD and smokers AE displays decreased E-cadherin and occludin protein expression compared with non-smokers AE.

A-D. Decreased E-cadherin protein levels in early and short-term ALI-AE, but no more at mid-term and long-term, in smoker controls and COPD ALI-AE as compared with that of non-smokers.

E-G. Decreased occludin protein levels, observable from short-term up to long-term cultures, in smoker controls and COPD ALI-AE as compared with that of non-smokers.

H. Occludin decrease in COPD AE significantly correlates with disease severity witnessed by the FEV1.

I. Representative blots for E-cadherin in non-smokers and very severe COPD AE, in early and short-term ALI-AE, showing decreased expression of E-cadherin at these time periods in COPD.

J. Representative blots for occludin in non-smokers and very severe COPD AE, in mid-term and long-term ALI-AE, showing decreased expression of occludin at these time periods in COPD.

*, **, *** indicate p-values of less than 0.05, 0.01, and 0.001, respectively (analysed using the Kruskal-Wallis test followed by Dunn's post-hoc test). Bars indicate median ± interquartile range.

AE, airway epithelium; ALI, air-liquid interface; COPD, chronic obstructive pulmonary disease; FEV1, forced expired volume in 1 second; NS, non-smokers; ns, not significant; SEM, standard error of the mean; Smo, smokers.

4.2.Epithelial differentiation of the COPD vs control AE

In order to assess the persistence of the abnormal programming of epithelial differentiation in COPD, specific markers and transcription factors of early differentiation, intermediate, goblet, club and ciliated cells were assayed in long-term ALI cultures.

4.2.1. Epithelial pre-differentiation

mRNA abundance of MYB Proto-Oncogene (*MYB*), a recently described marker of early differentiation of basal cells (37), was significantly decreased up to long-term in smokers- and COPD-derived AE as compared with non-smokers (Figures 16 A and 17 A). In addition, *MYB* mRNA levels in early up to long-term cultures correlated with disease severity in terms of FEV1 (Figures 16 D & 17 A).

4.2.2. Differentiation towards ciliated cells

It was next assessed whether the defect in ciliated cell numbers classically observed in COPD persisted in long-term ALI cultures by measuring the mRNA abundance of Forkhead Box J1 (*FOXJ1*), a transcription factor involved in the commitment towards ciliated cells, and of the dynein axonemal intermediate chain 1 (*DNAI1*), a marker of terminal differentiation of ciliated cells. Smokers- and COPD-derived cultures displayed a marked and persisting mRNA level decrease of both targets as compared with non-smoker controls (Figures 16 B-C and 17 B-C). This decrease significantly correlated with disease severity (assessed by FEV1) in early, short-term, and long-term ALI culture (Figures 16 D and 17 B-C).

4.2.3. Differentiation towards goblet cells

We next assessed the mRNA abundance of SAM Pointed Domain Containing ETS Transcription Factor (*SPDEF*) and Forkhead Box A3 (*FOXA3*), two transcription

factors inducing the differentiation towards goblet cells (40-42). On one hand, *SPDEF* expression was increased in smoker controls' AE (and in COPD AE, although to a lesser, non-significant extent), as compared with that of non-smokers (Figures 16 E and 17 D). This was also observed by a longitudinal analysis comparing smoker controls and non-smokers, with this upregulation persisting in long-term cultures (Figure 16 E). When assessing the potential effect of (active) smoking on the expression pattern, *SPDEF* expression was decreased in smokers who quit smoking for more than 4 years as compared with active smokers and ex-smokers with a smoking cessation of less than 4 years, in early, short-term, mid-term and to long-term cultures (Figure 16 F and 17 E). Similarly, longitudinal analysis showed that *FOXA3* was also upregulated in smoker controls as compared with non-smokers and mild and moderate COPD (Figure 17 F), and that it was decreased in smokers who quit smoking for more than 4 years (Figure 16 G and 17 G). These data show that goblet cell hyperplasia relates to smoking and demonstrate that this feature persists over time *in vitro*.

4.3.Epithelial-to-mesenchymal transition of the COPD AE

The expression of EMT protein markers (vimentin, fibronectin) was assessed in long-term ALI cultures. Increased vimentin content was observed in early, short-term and mid-term cultures, but no more in long-term cultures of (very) severe COPD AE as compared with non-smoker controls (Figure 18 A-B), as well as in smokers and mild/moderate COPD AE in early ALI-AE. Accordingly, mild/moderate and (very) severe COPD AE displayed increased fibronectin release in the basolateral medium up to mid-term cultures, as compared with non-smokers, while it was significantly increased only in early ALI-AE from control smokers (Figure 18 C). No difference was seen anymore in long-term cultures. No striking difference was seen regarding vimentin mRNA abundance (*VIM*, Figure 19). These data show EMT features are slowly but progressively vanishing in COPD, and even more rapidly in smokers, as summarized in Figure 18 D.

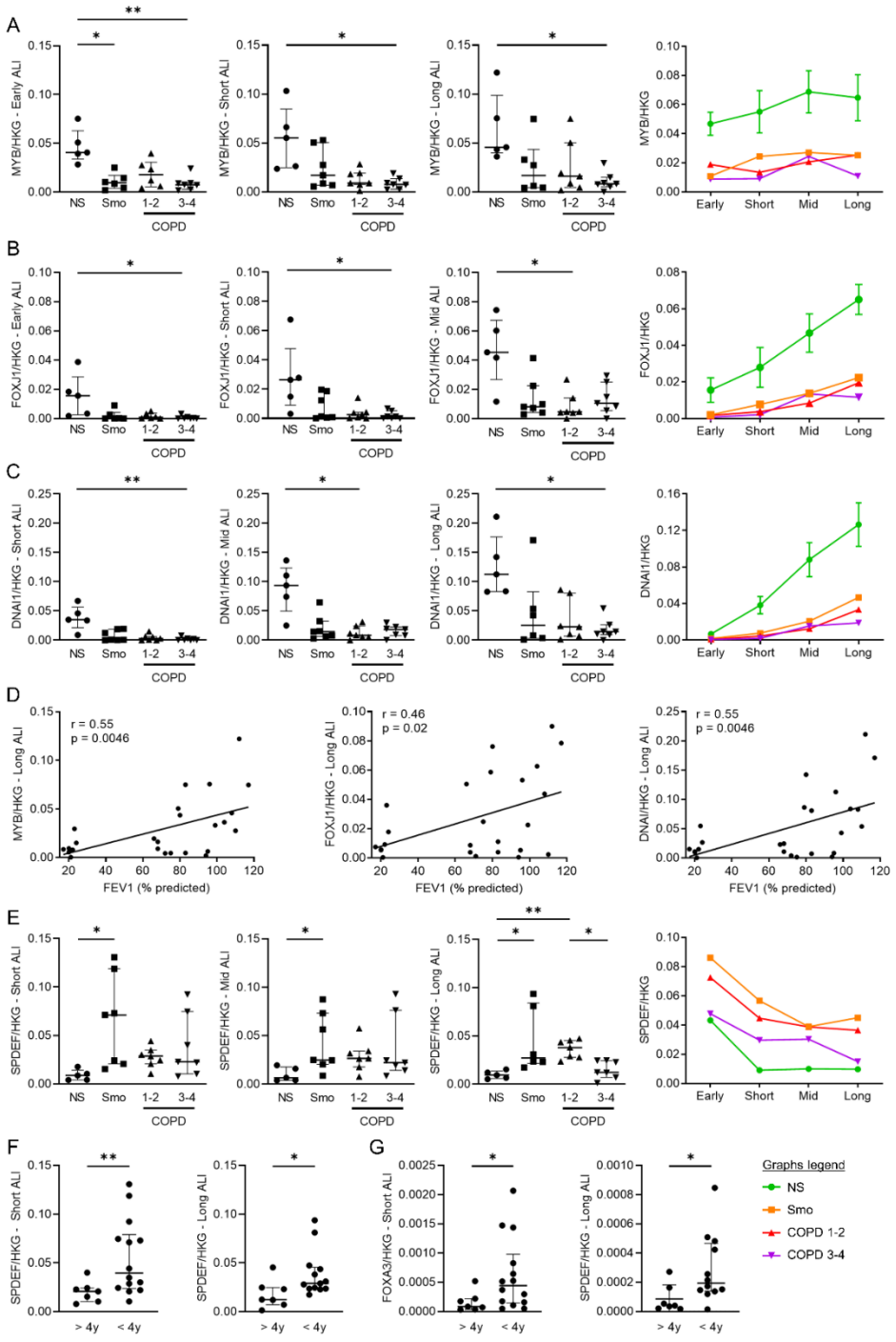

Figure 16 | Altered differentiation programming in smokers and COPD

A. Decreased *MYB* expression in smokers and COPD AE, in early, short-term, and long-term ALI culture. Longitudinal analysis shows a strong, persistent down expression as compared with non-smokers. Right graph: $^{\#}$, $^{\S} < 0.0001$, $^{\circ} < 0.001$, $^{£} = 0.07$, mixed model analysis.
B. Decreased *FOXJ1* expression in smokers and COPD AE, in early, short-term, and mid-term ALI culture. Longitudinal analysis shows a strong, persistent down expression as compared with non-smokers. Right graph: $^{\#}$, $^{\S} < 0.0001$, $^{\circ} < 0.001$, mixed model analysis.
C. Decreased *DNAI1* expression in smokers and COPD AE, in short-term, mid-term and long-term ALI culture. Longitudinal analysis shows a strong, persistent down expression as compared with non-smokers. Right graph: $^{\#}$, §, $^{\circ} < 0.0001$, mixed model analysis.
D. *MYB*, *FOXJ1*, and *DNAI1* downregulation in COPD patients correlates moderately with the disease severity, assessed by the FEV1.
E. Increased *SPDEF* expression in smokers AE as compared with non-smokers in short-term, mid-term and long-term ALI culture. Moreover, complementary longitudinal analysis shows increased expression in smokers as compared with COPD. Right graph: $^{\#}$, $^{\S} < 0.01$, $^{£} < 0.05$, mixed model analysis.
F. *SPDEF* expression is decreased in smokers who quit smoking for more than 4 years.
G. *FOXA3* expression is decreased in smokers who quit smoking for more than 4 years.
*, **, ***, **** indicate p-values of less than 0.05, 0.01, 0.001, and 0.0001, respectively (analysed using the Kruskal-Wallis test followed by Dunn's post-hoc test, except for longitudinal data, mixed model). Bars indicate median ± interquartile range, except for longitudinal analysis, mean ± SEM. °: CT NS *versus* Smo; $^{\#}$: CT NS *versus* COPD 1-2, §: CT NS *versus* COPD 3-4, $^{£}$: CT S *versus* COPD 3-4.
AE, airway epithelium; ALI, air-liquid interface; COPD, chronic obstructive pulmonary disease; CT, control; FEV1, forced expired volume in 1 second; HKG, housekeeping genes; NS, non-smokers; SEM, standard error of the mean; Smo, smokers; y, years.

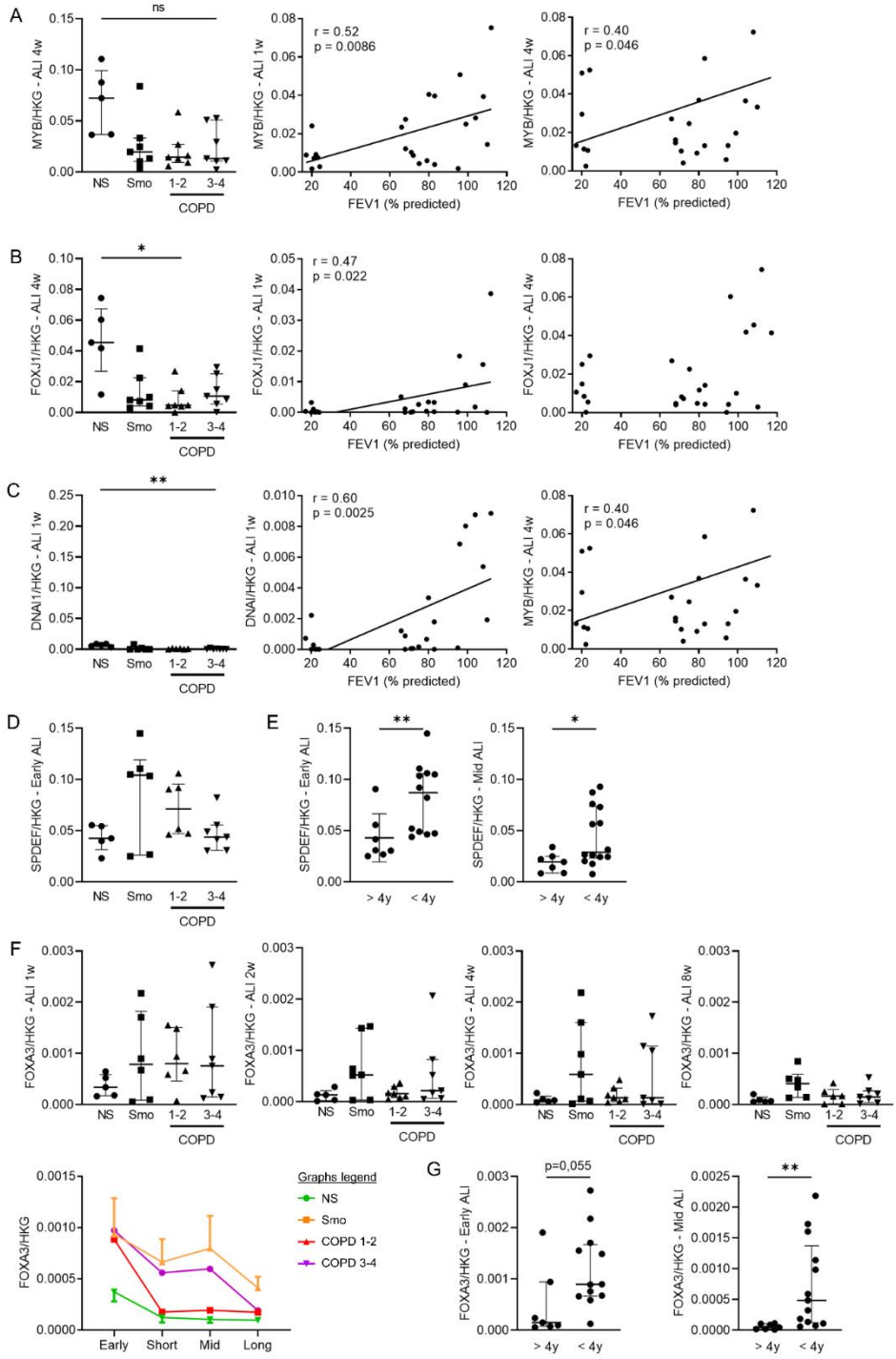

Figure 17 | Altered differentiation of the COPD AE (complementary data)

A. Decreased *MYB* expression in mid-term ALI culture in smokers and COPD AE, as compared with non-smokers. This downregulation correlated weakly but significantly with the COPD severity, witnessed by the FEV1 (represented in early and mid-term cultures).
B. Decreased *FOXJ1* expression in mid-term ALI culture in smokers and COPD AE, as compared with non-smokers. At 1 week, this downregulation correlated with the COPD severity, witnessed by the FEV1 (represented in early and mid-term cultures).
C. Decreased *DNAI1* expression in early cultures from smokers and COPD patients, as compared with non-smokers. This downregulation moderately correlated with the COPD severity, witnessed by the FEV1 (represented in early and mid-term cultures).
D. Increased *SPDEF* expression in early ALI culture in smokers.
E. Decreased *SPDEF* expression in early and mid-term cultures issued from smokers who quit smoking for more than 4 years.
F. *FOXA3* expression in smokers AE is non-significantly increased at all time periods, as compared with non-smokers. Longitudinal analysis confirms this upward trend and depicts significantly increased *FOXA3* expression in smokers AE as compared with non-smokers and COPD.
G. *FOXA3* expression is decreased in smokers who quit smoking for more than 4 years.
*, ** indicate p-values of less than 0.05 and 0.01, respectively (analyzed using the Kruskal-Wallis test followed by Dunn's post-hoc test). Bars indicate median ± interquartile range. AE, airway epithelium; ALI, air-liquid interface; COPD, chronic obstructive pulmonary disease; FEV1, forced expired volume in 1 second; NS, non-smokers; ns, not significant; Smo, smokers; PV, predicted values; y, years.

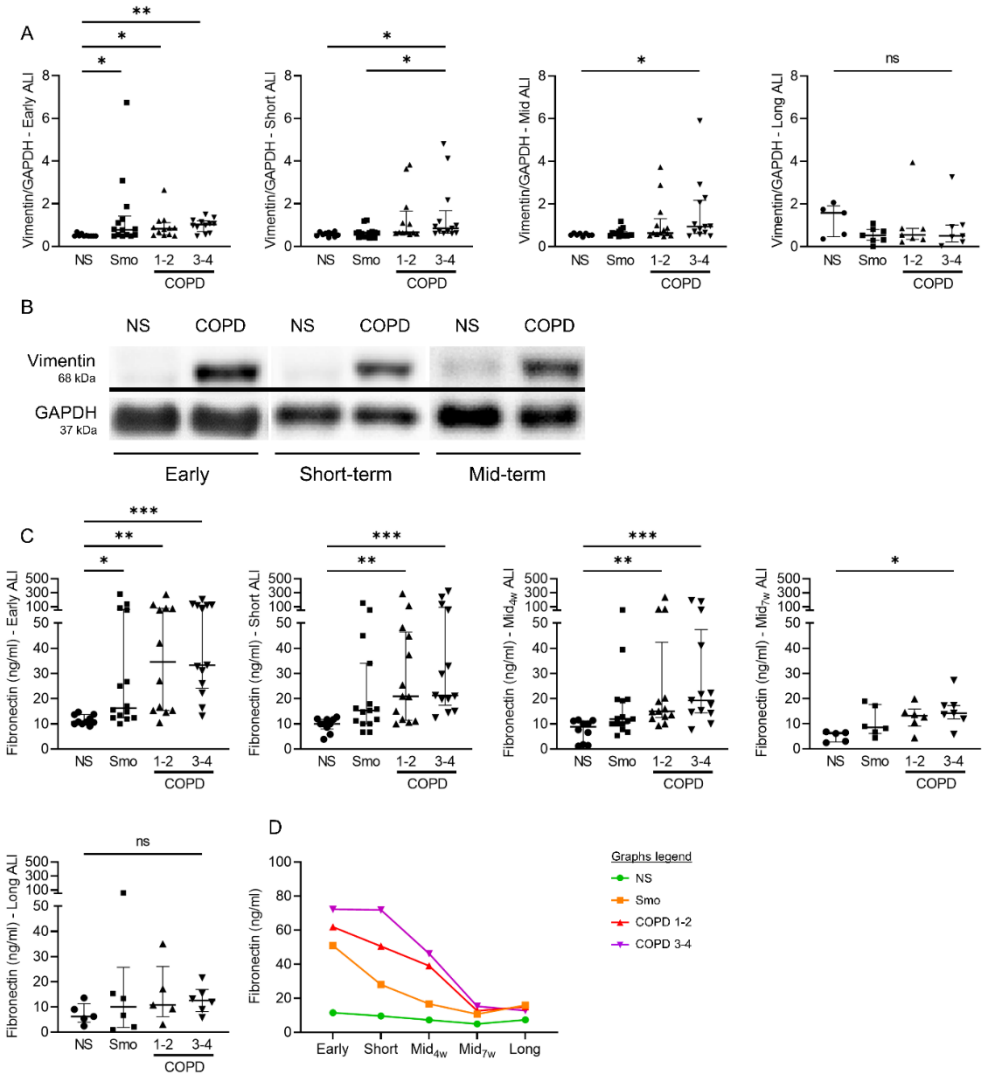

Figure 18 | EMT features expression in ALI-AE

COPD-related EMT features fade away after 7 to 10 weeks ALI culture.

A. Increased vimentin expression disappears early in smokers' ALI AE but persists up to mid-term cultures in (very) severe COPD AE.

B. Illustrative gels from non-smokers and very severe COPD-derived AE in early, short-term and mid-term ALI cultures, illustrating the vimentin increased content in COPD.

C. Increased fibronectin release disappears in early ALI culture from smokers, in mid-term (4 weeks) cultures from mild-to-moderate COPD patients, while it persists up to later mid-term cultures (7 weeks) in (very) severe COPD AE.

D. Longitudinal analysis of the fibronectin release over time. °, $^{\#}$ < 0.05; § < 0.01, mixed model analysis.
*, **, *** indicate p-values of less than 0.05, 0.01, and 0.001, respectively (analysed using the Kruskal-Wallis test followed by Dunn's post-hoc test, except for D, mixed model). Bars indicate median ± interquartile range, except for D, mean ± SEM. °: CT NS *versus* Smo; $^{\#}$: CT NS *versus* COPD 1-2, §: CT NS *versus* COPD 3-4.
AE, airway epithelium; ALI, air-liquid interface; COPD, chronic obstructive pulmonary disease; GAPDH, glyceraldehyde-3-phosphate dehydrogenase; NS, non-smokers; ns, not significant; SEM, standard error of the mean; Smo, smokers; w, weeks.

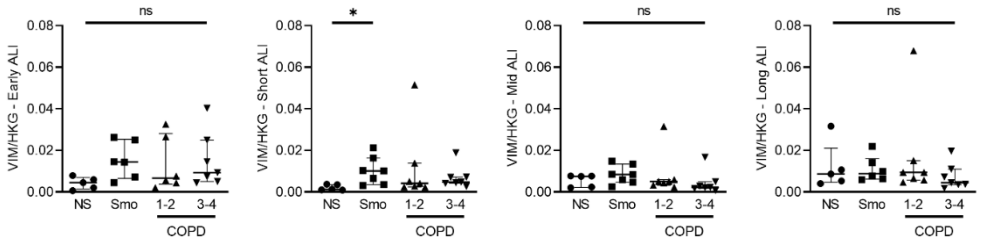

Figure 19 | Vimentin mRNA abundance in ALI-reconstituted AE.
Vimentin mRNA abundance does not vary across groups, as o difference was observed regarding *VIM* expression in smokers and COPD-derived AE, as compared with that of non-smokers, at all time periods, except for an increased expression in smokers in short-term ALI cultures.
* indicates a p-value of less than 0.05 (analyzed using the Kruskal-Wallis test followed by Dunn's post-hoc test). Bars indicate median ± interquartile range. AE, airway epithelium; ALI, air-liquid interface; COPD, chronic obstructive pulmonary disease; NS, non-smokers; ns, not significant; Smo, smokers.

4.4.Polarity and pIgR/SC expression in the COPD vs control AE

Smokers- and COPD-derived AE released less apical SC than non-smokers, from short-term up to long-term ALI cultures (Figure 20 A), a decrease that correlates with disease severity (Figure 20 B and 21 A). When analyzed longitudinally over 10 weeks, this decrease was more pronounced in (very) severe COPD as compared with smoker controls and mild/moderate COPD (Figure 20 C). Similarly, the (very) severe COPD AE displayed decreased *PIGR* mRNA abundance throughout the long-term cultures as compared with the other groups. Although this was not significant on isolated time points (Figure 20 D and 21 B), longitudinal data analysis demonstrated decreased *PIGR* mRNA abundance in (very) severe COPD AE as compared with non-smokers, smoker controls, and mild/moderate COPD AE (Figure 20 D). In addition, considering that epithelial differentiation is completed at 5 weeks, we show that the acquisition of optimal pIgR protein levels was delayed in COPD AEs compared with controls, as depicted in Figure 20 E, where representative blots of pIgR expression kinetics (1-5 weeks) in non-smoker (upper gel) and very severe COPD (lower gel) ALI-AE are represented.

These data show that airway epithelial polarity, witnessed by the pIgR/SC expression, is deeply impaired in COPD in a persistent manner.

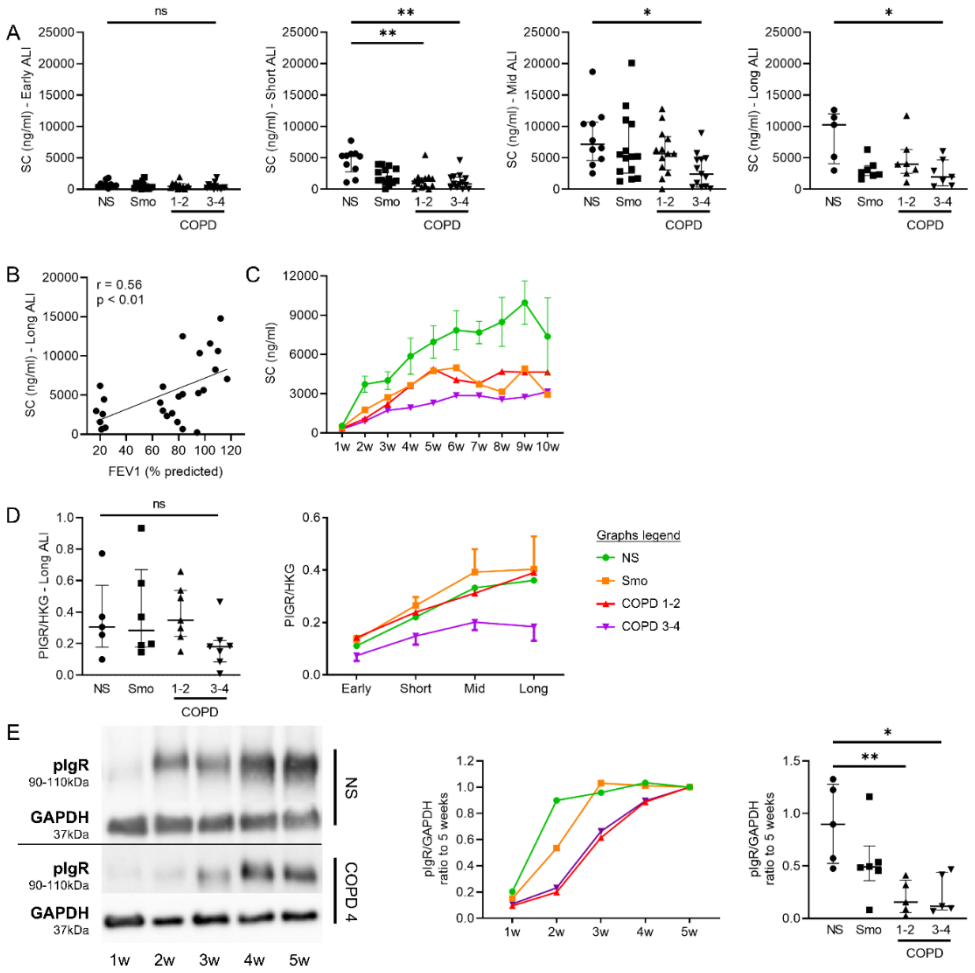

Figure 20 | Impaired polarized transcytosis in COPD ALI-AE

Impaired polarity witnessed by a disruption and a delayed acquisition of the PIGR/SC system, is imprinted in the COPD AE.

A. SC apical release in ALI-AE from smokers and COPD patients is decreased as compared with non-smokers, from short-term ALI-AE up to long-term ALI-AE.

B. SC decreased release in the COPD AE moderately correlates with the disease severity, witnessed by the FEV1.

C. Longitudinal analysis of SC apical release demonstrates a decreased release in smokers and mild-to-moderate COPD, as compared with non-smokers. This impaired SC production is enhanced in (very) severe COPD AE. °, #, § < 0.0001; £, ¶ < 0.001, mixed model analysis.

D. *PIGR* mRNA abundance is not significantly decreased in (very) severe COPD ALI-AE at separate time-points, as depicted here in long-term ALI cultures (see also Figure S4B), but longitudinal analysis shows a significant decrease in *PIGR* expression in (very) severe COPD AE as compared with non-smokers, smokers and mild-to-moderate COPD. $^{£}$, ¶ < 0.001, § < 0.01, mixed model analysis.

E. pIgR acquisition is delayed during the differentiation of the AE in COPD as compared with non-smokers, as represented at 2 weeks ALI culture, and catches it up only after 4 weeks.

*, **, ***, **** indicate p-values of less than 0.05, 0.01, 0.001, and 0.0001, respectively (analyzed using the Kruskal-Wallis test followed by Dunn's post-hoc test, except for longitudinal analysis in B and C, mixed model). Bars indicate median ± interquartile range, except for longitudinal analysis in B and C, mean ± SEM.

°: CT NS *versus* Smo; $^{#}$: CT NS *versus* COPD 1-2, §: CT NS *versus* COPD 3-4, $^{£}$: CT S *versus* COPD 3-4, ¶: COPD 1-2 *versus* COPD 3-4.

AE, airway epithelium; ALI, air-liquid interface; COPD, chronic obstructive pulmonary disease; FEV1, forced expired volume in 1 second; GAPDH, glyceraldehyde-3-phosphate dehydrogenase; HKG, housekeeping genes; NS, non-smokers; ns, not significant; pIgR, polymeric immunoglobulin receptor; PV, predicted values; SC, secretory component; SEM, standard error of the mean; Smo, smokers; w, weeks.

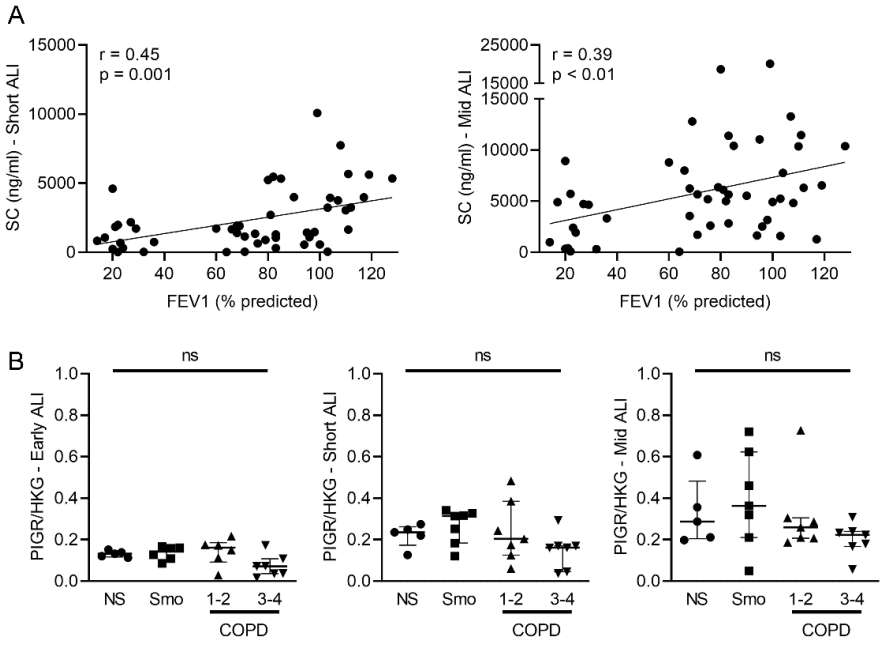

Figure 21 | Impaired polarized transcytosis in COPD AE

A. SC decreased release in COPD-derived AE correlates mildly but significantly with COPD severity, assessed by the FEV1 (represented here in short-term and mid-term ALI-AE).

B. Non-significantly decreased *PIGR* gene expression was observed in (very) severe COPD-derived AE in early and short-term ALI cultures.

Graphs B were analyzed using the Kruskal-Wallis test followed by Dunn's post-hoc test. Bars indicate median ± interquartile range. AE, airway epithelium; ALI, air-liquid interface; COPD, chronic obstructive pulmonary disease; FEV, forced expiratory volume in one second; NS, non-smokers; ns, not significant; Smo, smokers; PV, predicted values.

4.5.Inflammatory cytokine production by the COPD vs control AE

Epithelial production of IL-8/CXCL-8 and IL-6 was next assayed in the reconstituted AE. A trend for increased *CXCL8* mRNA abundance was seen in smokers and COPD groups, that was more marked in early to mid-term ALI culture (Figure 22 A). Accordingly, IL-8/CXCL-8 release was strongly increased in early, short-term and mid-term AE from smokers- and COPD-derived as compared with that of non-smokers, whilst this difference disappeared afterwards (Figure 23 A). Although no difference was observed regarding *IL6* mRNA abundance (Figure 22 B), the IL-6 production in the basolateral medium was increased in smokers and COPD ALI-AE. In contrast to IL-8, IL-6 upregulation persisted over time (up to long-term cultures), both in smokers and COPD (Figures 23 B).

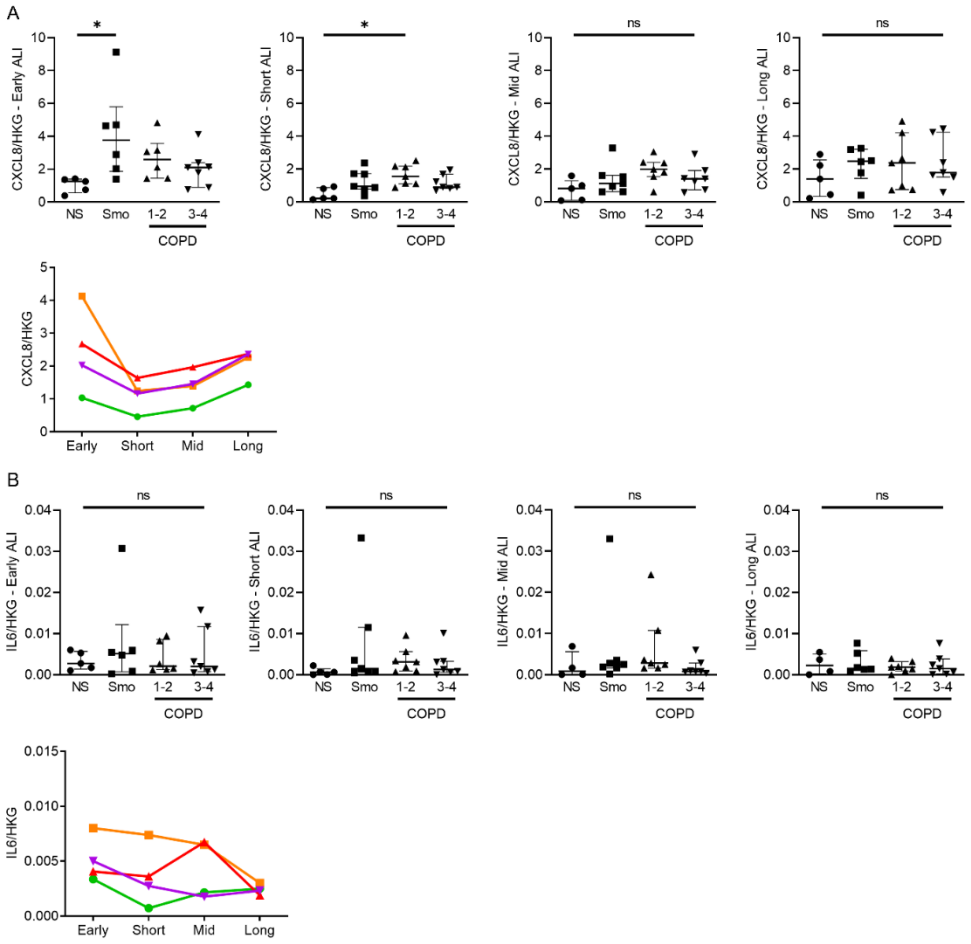

Figure 22 | *IL8* and *IL6* mRNA abundance in ALI/AE

IL8 and *IL6* mRNA abundance is not significantly modified in smokers and COPD AE.

A. *IL8* gene expression was enhanced in smokers and mild-to-moderate COPD in early and short-term ALI cultures, respectively, but no striking difference was observed in later time periods, nor in (very) severe COPD.

B. No difference was observed in *IL6* gene expression in smokers and COPD-derived ALI-AE as compared with non-smokers.

* indicates a p-value of less than 0.05 (analyzed using the Kruskal-Wallis test followed by Dunn's post-hoc test). Bars indicate median ± interquartile range, except for longitudinal analysis, mean. AE, airway epithelium; ALI, air-liquid interface; COPD, chronic obstructive pulmonary disease; NS, non-smokers; ns, not significant; SEM, standard error of the mean; Smo, smokers; transepithelial electric resistance.

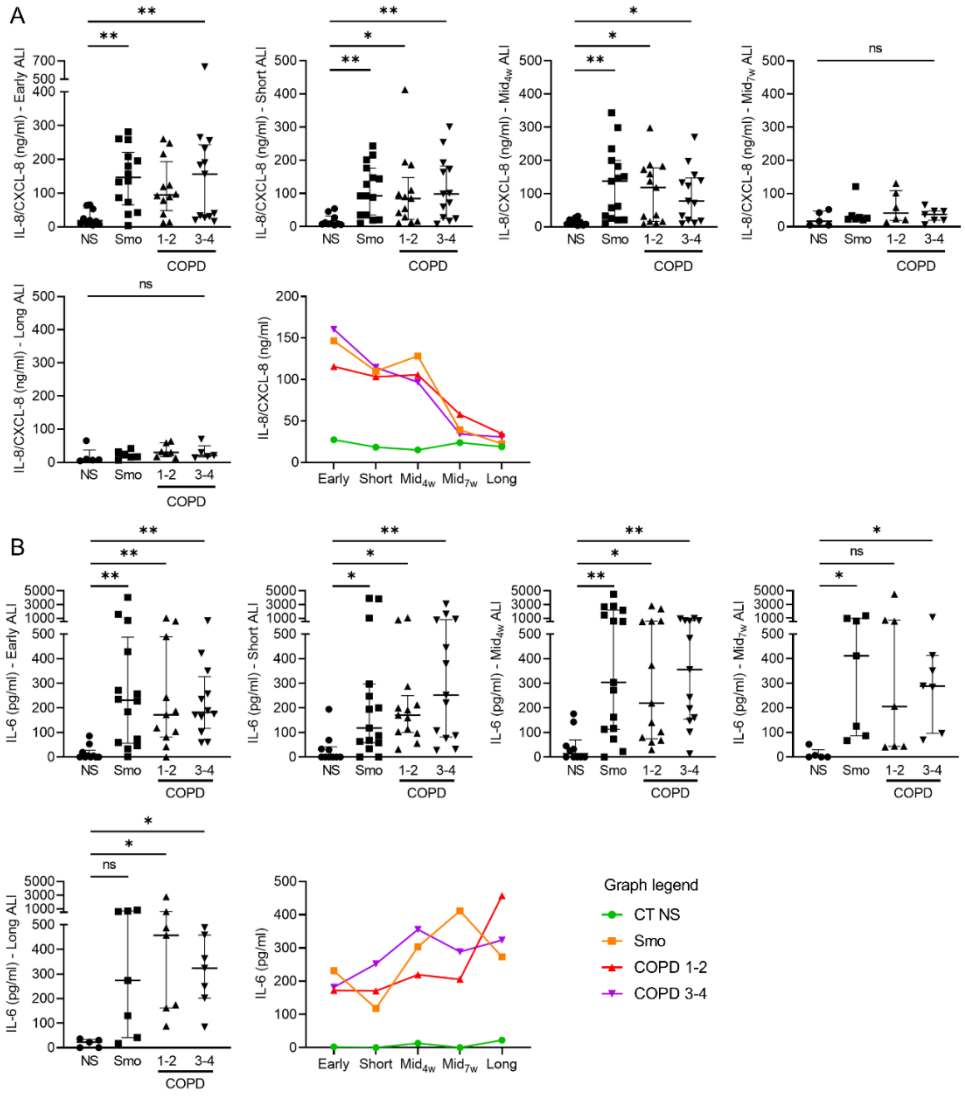

Figure 23 | IL-8 and IL-6 release in ALI AE

Epithelial release of inflammatory cytokines partly persists in COPD AE.

A. IL-8 production by the reconstituted ALI-AE is increased in early, short-term and mid-term ALI-AE from and COPD patients, but disappears afterwards, although a non-significant upward trend persists. °, #, § < 0.0001, mixed model analysis.

B. IL-6 production by the reconstituted ALI-AE is increased in smokers and COPD and persists in long-term cultures.

*, ** indicate p-values of less than 0.05 and 0.01, respectively (analysed using the Kruskal-Wallis test followed by Dunn's post-hoc test, except for longitudinal

analysis, mixed model). Bars indicate median ± interquartile range, except for longitudinal analysis, mean. °, #, § < 0.0001, mixed model analysis.
°: CT NS *versus* Smo; #: CT NS *versus* COPD 1-2, §: CT NS *versus* COPD 3-4.
AE, airway epithelium; ALI, air-liquid interface; COPD, chronic obstructive pulmonary disease; IL, interleukin; NS, non-smokers; ns, not significant; SEM, standard error of the mean; Smo, smokers; w, weeks.

4.6.Exogenous inflammation induces COPD-like features in the AE

Next, we assessed whether exogenous inflammation could promote COPD-like changes in the AE by supplementing the culture medium with IL-6, TNF-α and IL-1β (all at 5ng/ml) for 5 weeks. These cytokines are relevant to human COPD pathogenesis, as besides the abovementioned CXCL-8/IL-8 and IL-6, TNF-α and IL-1β are also increased in COPD (26, 43), even though their concentration did not reach the detection threshold in our culture supernatants (not shown).

First, TEER was dramatically decreased upon exposure to the inflammatory stimuli. This was already observed in early cultures but was more pronounced in the subsequent weeks (Figure 24 A). Cytokine-exposed cultures displayed similar values irrespectively of the original phenotype, with TEER values comprised between 300 and 600 Ω/cm² in early and mid-term cultures, possibly indicating a maximal effect on barrier (dys)function at the used concentrations.

Second, cultures that were exposed to inflammatory cytokines displayed sharper EMT features, with increased fibronectin release in early, short-term and mid-term cultures (Figure 24 B). Interestingly, this induction that was not observed in non-smokers' AE, was strikingly upregulated in COPD as compared to (non-)smoker controls (Figure 24 C). Congruently, similar results could be observed when assessing vimentin expression (Figure 24 D). These results show that the cultured AE from COPD patients, whilst losing its intrinsic EMT features, remains prone to develop EMT upon exposure to inflammatory cytokines. Third, cytokine-induced inflammation altered epithelial polarity assayed through the pIgR/SC system, as SC apical release was decreased in cytokine-exposed AE from non-smoker controls,

smoker controls and mild-to-moderate COPD (Figure 24 E). This was not observed in (very) severe COPD AE, probably because the pIgR/SC system is already severely impaired in this group.

In conclusion, exogenous inflammation was able to induce COPD-like changes such as barrier dysfunction, EMT and altered polarity in the AE from non-smoker and smoker controls. In addition, the COPD-derived AE remained prone to develop EMT features upon inflammatory stimulation.

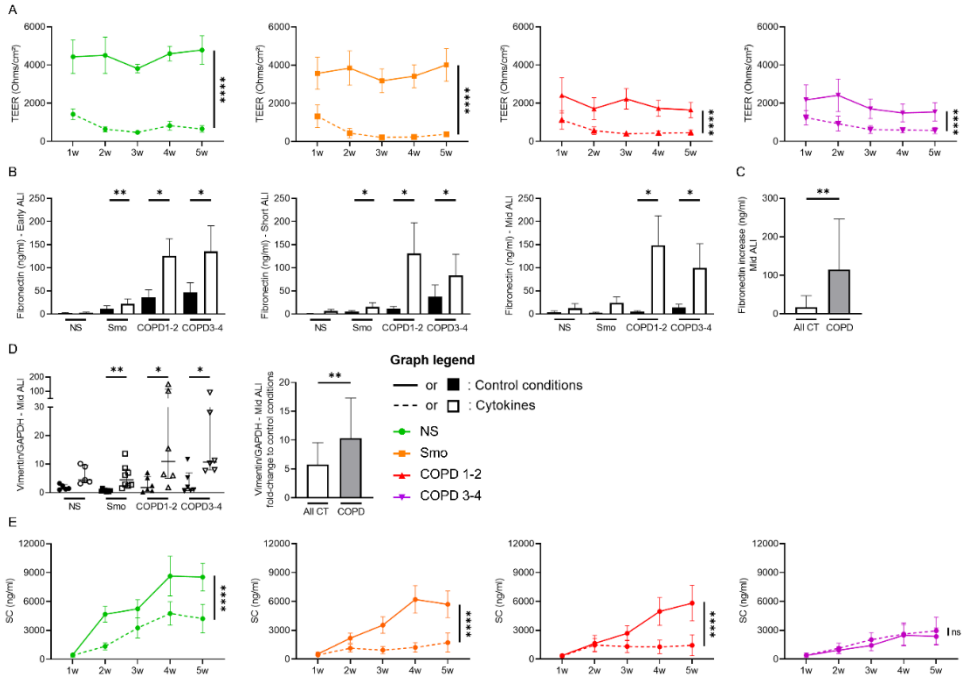

Figure 24 | Effects of inflammation on AE phenotype

Cytokine activation triggers COPD-like epithelial changes.

A. Epithelial inflammation, driven by exogenous TNF-α, IL-1β and IL-6, induces barrier dysfunction, witnessed by a dramatic decrease in TEER that is present in each group (NS, Smo, COPD 1-2, COPD 3-4).

B-D. Cytokine-induced epithelial inflammation induces EMT in smokers and COPD-derived ALI AE, witnessed by increased fibronectin release in early, short-term and mid-term cultures (B) and vimentin expression in mid-term cultures (D). The absolute increase in fibronectin and vimentin was significantly higher in mid-term COPD AE than in controls (pooled smokers and non-smokers) (C, D).

E. Cytokine-induced epithelial inflammation deteriorates the epithelial polarity, witnessed by the SC apical release. No difference was seen in (very) severe COPD, due to low baseline levels.

*, **, ***, **** indicate p-values of less than 0.05, 0.01, 0.001, and 0.0001, respectively (analyzed using the Mann-Whitney test for B, C and D, and a mixed model for A and E). Bars indicate median ± interquartile range for B, C and D, and mean ± SEM for A and E.

AE, airway epithelium; ALI, air-liquid interface; COPD, chronic obstructive pulmonary disease; CT, controls; EMT, epithelial-to-mesenchymal transition; GAPDH, glyceraldehyde-3-phosphate dehydrogenase; IL, interleukin; NS, non-

smokers; ns, not significant; SC, secretory component; SEM, standard error of the mean; Smo, smokers; TEER, transepithelial electric resistance; TNF-α, tumor necrosis factor α; w, weeks.

4.7. Epithelial progenitors as keepers of the memory of epithelial damage in COPD

Basal cells and club cells constitute progenitor cells of the airway epithelium, with the latter being restricted to small airways (44). In COPD, recent data unanimously depict impaired basal cells functionality in terms of differentiation, signalling and transcriptome (18, 45-47), while little is known about club cells progenitor (dys)function in COPD. Using a scRNAseq database assessing distal lung cell populations from non-smokers, non-COPD smokers and COPD patients (courtesy of Pr. Yamamoto, National Cancer Center Research Institute, Tokyo, Japan; preprint available at reference (39)), airway progenitor populations (both basal and club cells, Figure 25 A-B) were selectively explored for the transcription of EMT-related genes in COPD, as compared with non-smokers and non-COPD smokers. We show that *VIM*, *FN1*, *SNAI1*, *SNAI2*, *S100A2*, and *S100A4* mRNA abundance was increased in basal and club cells from COPD patients, as compared with controls (pooled non-smokers and non-COPD smokers), suggesting EMT reprogramming of these cells (Figure 25 C-H). However, this increase does not reach statistical significance, due to two main factors: first, stringent false discovery rate correction has been applied, as more than 10.000 genes have been studied in the original study; second, low basal and club cell counts were observed in those distal (and mostly parenchymal) samples.

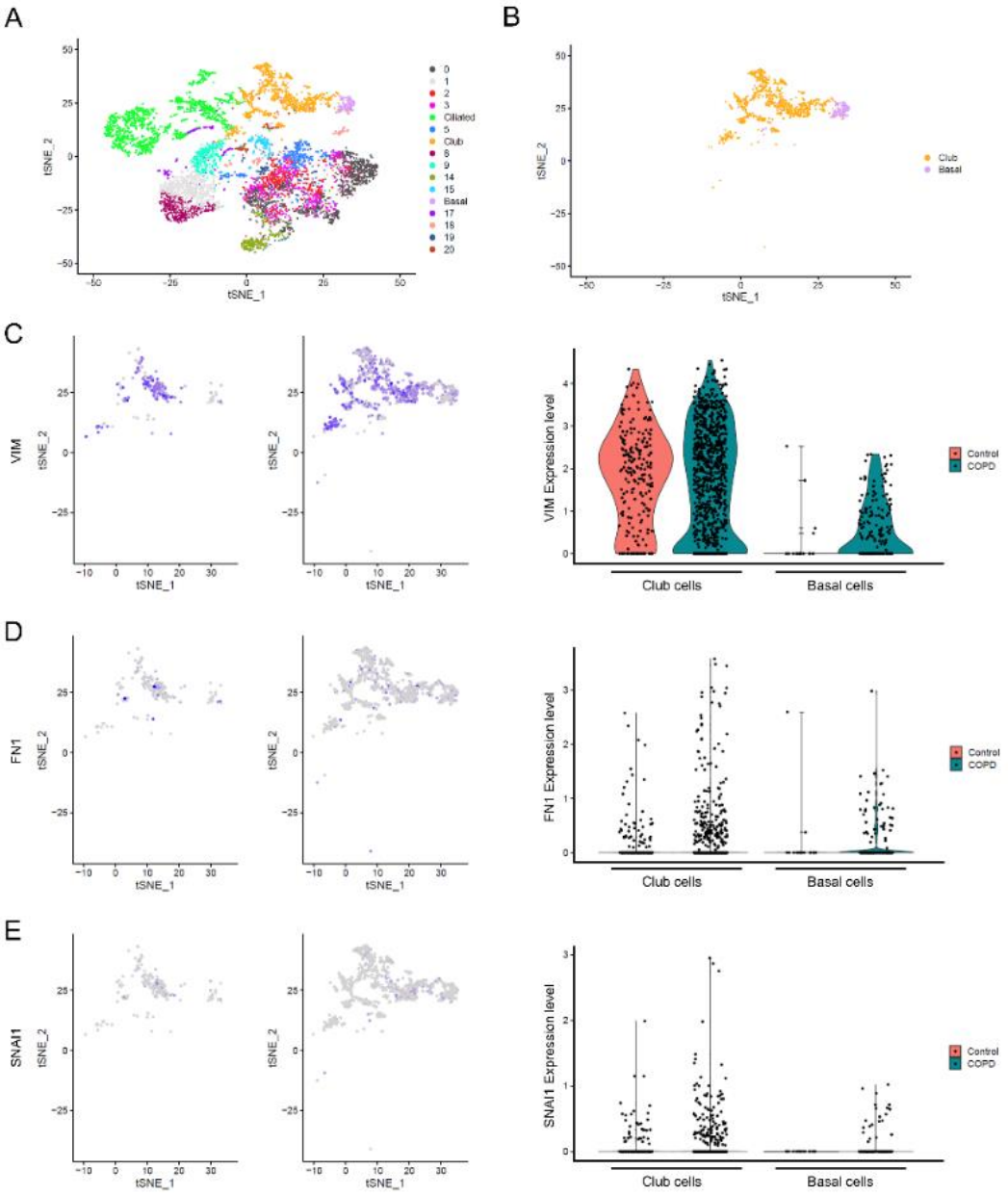
A
B
C
D
E
tSNE_1
tSNE_2
Ciliated
Club
Basal
VIM
FN1
SNAI1
VIM Expression level
FN1 Expression level
SNAI1 Expression level
Control
COPD
Club cells
Basal cells

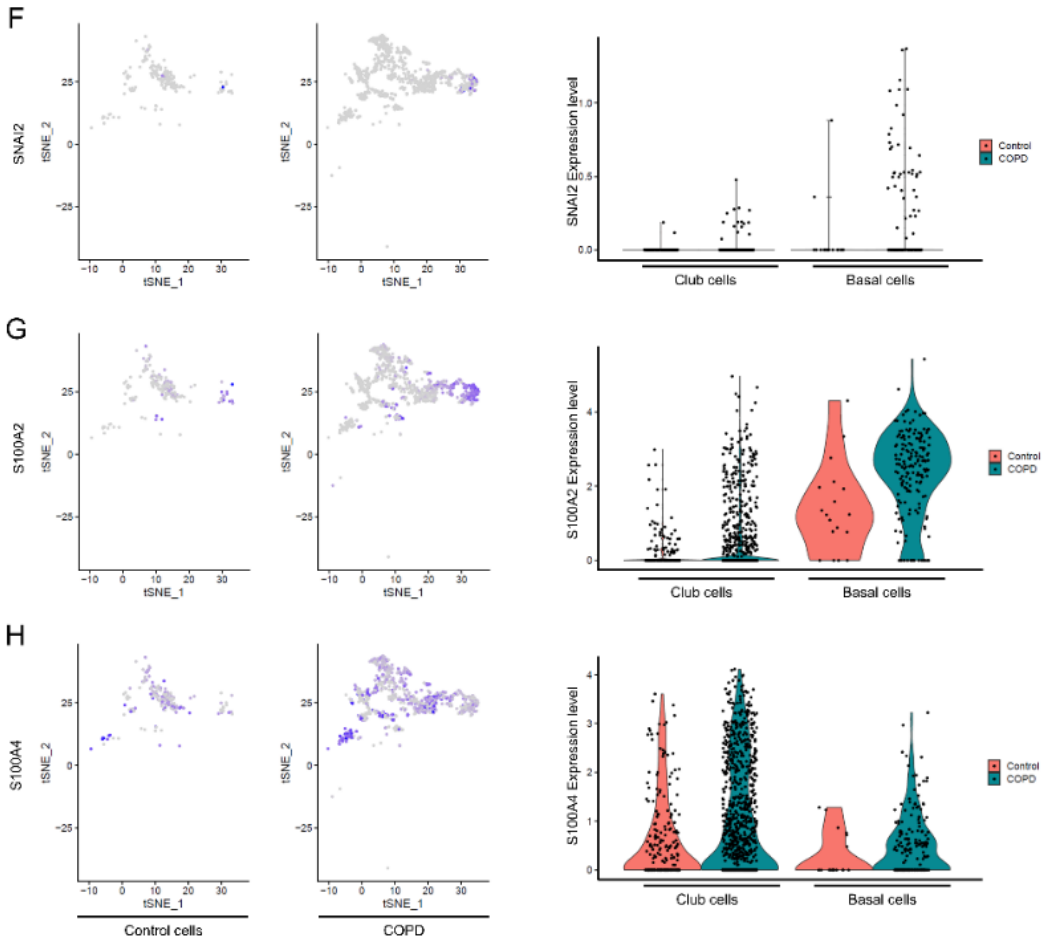

Figure 25 | EMT-related genes in airway progenitor cells.
A. t-SNE plot displaying the major clusters of human distal lung cells. **B.** t-SNE plot isolating clusters of basal and club cells, that were further analysed. **C.** Left graphs: t-SNE showing the expression of *VIM* in basal and club cells of controls and COPD patients. Right graphs: violin plots summarizing transcription levels of *VIM* in club and basal cells from controls (red violins) and COPD patients (blue violins). **D.** Left graphs: t-SNE showing the expression of *FN1* in basal and club cells of controls and COPD patients. Right graphs: violin plots summarizing transcription levels of *FN1* in club and basal cells from controls (red violins) and COPD patients (blue violins). **E.** Left graphs: t-SNE showing the expression of *SNAI1* in basal and club cells of controls and COPD patients. Right graphs: violin plots summarizing transcription levels of *SNAI1* in club and basal cells from controls (red violins) and COPD patients (blue violins). **F.** Left graphs: t-SNE showing the expression of *SNAI2* in basal and

club cells of controls and COPD patients. Right graphs: violin plots summarizing transcription levels of *SNAI2* in club and basal cells from controls (red violins) and COPD patients (blue violins). **G.** Left graphs: t-SNE showing the expression of *S100A42* in basal and club cells of controls and COPD patients. Right graphs: violin plots summarizing transcription levels of *S100A2* in club and basal cells from controls (red violins) and COPD patients (blue violins). **H.** Left graphs: t-SNE showing the expression of *S100A4* in basal and club cells of controls and COPD patients. Right graphs: violin plots summarizing transcription levels of *S100A4* in club and basal cells from controls (red violins) and COPD patients (blue violins).

5. Discussion

This study demonstrates, by exploiting long-term cultures of the ALI-reconstituted human AE from well-characterized COPD and control patients, that the AE retains its native abnormalities for prolonged periods of time (e.g. barrier dysfunction, altered cell differentiation, and impaired polarity) whereas some features (IL-8 upregulation, EMT) disappear. It also demonstrates that inflammation, driven by TNF-α, IL-6 and IL-1β, may induce a COPD-like phenotype and reactivates EMT programming in the diseased (COPD) epithelium. Single-cell RNAseq data suggest that the mechanisms underlying the persistence of COPD-related airway epithelium alterations lay in progenitor cells.

COPD is a chronic and progressive disease that is developed upon repeated injury of the airway epithelial-mesenchymal unit by toxics, leading to activation and remodeling of the AE, and ultimately to irreversible airway obstruction. It has been shown that COPD patients who quit smoking may benefit from decreases in mortality (31), respiratory symptoms and lung function decline as compared with active smokers (30, 48, 49). They also display reduced AE remodeling and goblet cell hyperplasia when smoking cessation exceeds 3.5 years (29), as well as improvements in nasal mucociliary clearance (50). In contrast, no change was observed following smoking cessation regarding axonemal abnormalities in ciliated cells (51), airway mucosal inflammation (33), sputum IL-8/CXCL-8 (52) or sputum neutrophils (32, 52), potentially suggesting permanent alterations in these compartments.

In this study, we assessed whether the irreversible nature of the disease is imprinted in the AE in such a way that aberrant features of the native epithelium persist in long-term cultures, independently of signals provided by repeated insults and/or by mesenchymal cells and surrounding leukocytes. The ALI model was used, as it was previously shown to recapitulate, at least to some extent, the native COPD phenotype

(8, 10, 17, 18, 53). We prolonged the culture up to 10 weeks, an unusually long duration in this model, that had not yet been reported so far in COPD.

A major abnormality that persists in the cultured smokers' and COPD AE is the barrier and junctional defect (7). Thus, the AE from smokers displays a persistent TEER decrease as compared with that from non-smokers, which was associated with decreased protein levels of E-cadherin and occludin, key components of adherens and tight junctions, respectively. This observation is in line with a previous study showing that CS exposure leads to disruption of apical junctional complexes (54). We here show that this alteration further persists in long-term cultures for occludin. In addition, those changes in TEER and E-cadherin/occludin expression were further downregulated according to the presence and severity of COPD. Meanwhile, mRNA abundance for the main apical junctional complexes' components (*TJP1*, *OCLN*, *ECAD*, *CLDN11*, Figure 14) did not differ across the groups, suggesting an effect of post-transcriptional regulation.

In line with the requirement of the integrity of apical junctional complexes to ensure baso-apical epithelial polarity (55), our study shows that AE polarity is persistently impaired in COPD. The pIgR/SC system, that allows baso-apical transcytosis of polymeric immunoglobulins (mostly dimeric IgA) across the epithelium and constitutes a marker of epithelial polarity (19), was previously shown to be defective in COPD, both *in situ* in surgical tissue and *in vitro* in ALI-HBEC evaluated at 2 weeks cultures (17). The present study demonstrates that this impairment persists over time, with decreases in the apical release of SC and in the mRNA abundance of *PIGR*, observed in very severe COPD (Figures 20 and 21). In addition, the dynamics of optimal pIgR protein expression, were delayed in COPD AE (Figure 21 D). Interestingly, those data are contrasting with previous findings in asthma where pIgR downregulation, although being similarly present *in situ*, does not persist in ALI cultures from asthma patients (56), suggesting distinct mechanisms driving epithelial pathology in asthma and COPD.

Aside from these findings, our study demonstrates that ciliated cell hypoplasia – with decreased *FOXJ1* and *DNAI1* mRNA abundance – also persists in long-term ALI cultures from COPD patients. In addition, it shows that goblet cell hyperplasia persists in smokers, as witnessed by *SPDEF* upregulation which remains higher in active smokers and ex-smokers who quit for less than 4 years, as compared with ex-smokers who quit for more than 4 years (Figures 16 F and 17 D). These results corroborate previous findings indicating that this secretory trait relates more directly to smoking rather than to the disease (29).

In contrast with those changes, some abnormalities are observed only in short-term culture, such as EMT. EMT is a dynamic process where cells lose their epithelial features and gain mesenchymal properties, including migratory abilities, which is required for normal embryogenesis (type I EMT), tissue repair (type II), or cancer metastasis (type III). In COPD, airway fibrosis probably follows persistent type II EMT (57). ALI-AE from COPD patients spontaneously exhibit mesenchymal features, and CS may induce EMT in control HBEC (14), possibly as a result of TGF-β signalling (8). Accordingly, our results show EMT features (vimentin expression, fibronectin release) overexpression in the AE from control smokers and COPD patients during the first weeks of culture. However, these features further vanish from mid-term cultures onwards, with complete disappearance occurring earlier in smoker controls than in COPD samples. Moreover, we highlight that, even though EMT markers are vanishing, the COPD AE remains prone to reactivate EMT programming upon inflammatory condition, suggesting the existence of a priming state in the COPD AE, imprinted by previous (*in vivo*) exposures conditioning its responses to further stimulation. As a dedicated analysis of airway progenitor cells transcriptome, issued from a scRNAseq database from distal lung samples (39) shows that EMT-related genes are upregulated *in situ* in basal and club cells from COPD patients, we suggest that this priming state resides in these cell types.

As observed for EMT, upregulation of IL-8/CXCL-8 release by the smokers' and COPD AE is also fading away from mid-term cultures onwards. In contrast, IL-6

overproduction persisted in long term ALI-AE from both control smokers and COPD patients. Finally, *in vitro* exposure to inflammatory cytokines reproduced or aggravated alterations in barrier and polarity features as well as EMT in controls and COPD AE, respectively.

The fundamental mechanisms of these observations question the nature of epithelial memory. Inflammatory memory refers to memories of previous immune events enabling barrier tissues to rapidly recall distinct environmental exposures, which may be stored not only in immune cells but also in epithelial and mesenchymal cells (58, 59). While memory classically refers in the immune system to somatic mutations underlying adaptive antibody responses to recall antigens, "inflammatory memory" is less well defined and may include epigenetic modifications and chromatin changes that may drive persistent changes in damaged tissues. It was proposed that the memory distribution could promote maladaptation in disease, particularly if cellular cooperation is potentiated (i.e. collective memory owing to different cell types) during recall responses. Progenitor basal cells are prime candidates to retain epithelial memory in the airways, as do epithelial progenitors in the skin towards inflammatory or mechanical stress by maintaining accessibility of key stress response genes through chromatin modifications (59) as well as in the gut towards dietary components (60). Interestingly, WNT signalling, which is upregulated in the COPD AE (18), has been shown to be involved in the latter form of epithelial memory abd may regulate stemness and tumorigenicity. In line with the recent hypothesis that basal cells serve as repositories of allergic inflammatory memory in respiratory epithelial cells (58), and based on the differences observed in EMT-related genes in COPD basal cells, one could propose that airway stem cells (basal cells, and club cells in small airways) also store the memory of repeated previous injuries by inhaled toxics such as cigarette smoke.

Our study has several limitations. First, an effect of treatments (especially inhaled corticosteroids in severe patients) on the findings cannot be excluded. However, *in vitro* studies on intestinal cell lines and primary human bronchial and nasal epithelial

cells in ALI culture showed dexamethasone-induced increases in TEER, claudin-2 (61), and E-cadherin (62, 63) expression, while budesonide exposure of ALI-HBEC counter-acted CS-induced barrier dysfunction (64). In addition, dexamethasone and fluticasone propionate improved TGF-β_1-induced EMT in A549 cells and in primary airway nasal cells (65), suggesting that corticosteroids may rather improve barrier function and EMT changes. Second, the imprinting observed in this model of *ex vivo* reconstituted epithelium, which involves (following proliferation and differentiation of basal cells) prolonged culture of slowly-to-non-dividing cells, should be confirmed in other models such as airway organoids and culture following multiple passages.

In conclusion, this study demonstrates that the AE from smokers and COPD stores the memory of its native state and previous insults from cigarette smoking, in addition to additional signals that underlie the development of the disease itself. This memory is multidimensional, including alterations in barrier function, epithelial polarity, and lineage differentiation, as well as IL-6 release and EMT reprogramming. In line with other studies and based on scRNAseq data in basal and club cells, we suggest that the COPD-related memory is imprinted in progenitor cells which contribute to the persistence of disease by serving as repositories for toxic inflammatory memories in the airways.

6. References

1. Organization WH. Chronic respiratory diseases. 2017 [Available from: http://www.who.int/respiratory/copd/burden/en/.
2. Salvi SS, Barnes PJ. Chronic obstructive pulmonary disease in non-smokers. Lancet. 2009;374(9691):733-43.
3. McDonough JE, Yuan R, Suzuki M, Seyednejad N, Elliott WM, Sanchez PG, et al. Small-airway obstruction and emphysema in chronic obstructive pulmonary disease. N Engl J Med. 2011;365(17):1567-75.
4. Vogelmeier CF, Criner GJ, Martinez FJ, Anzueto A, Barnes PJ, Bourbeau J, et al. Global Strategy for the Diagnosis, Management, and Prevention of Chronic Obstructive Lung Disease 2017 Report. GOLD Executive Summary. Am J Respir Crit Care Med. 2017;195(5):557-82.
5. Celli BR, Anderson JA, Cowans NJ, Crim C, Hartley BF, Martinez FJ, et al. Pharmacotherapy and Lung Function Decline in Patients with Chronic Obstructive Pulmonary Disease: A Systematic Review. Am J Respir Crit Care Med. 2020.
6. Aghapour M, Raee P, Moghaddam SJ, Hiemstra PS, Heijink IH. Airway Epithelial Barrier Dysfunction in Chronic Obstructive Pulmonary Disease: Role of Cigarette Smoke Exposure. Am J Respir Cell Mol Biol. 2018;58(2):157-69.
7. Carlier FM, de Fays C, Pilette C. Epithelial Barrier Dysfunction in Chronic Respiratory Diseases. Frontiers in Physiology. 2021;12(861).
8. Gohy ST, Hupin C, Fregimilicka C, Detry BR, Bouzin C, Gaide Chevronay H, et al. Imprinting of the COPD airway epithelium for dedifferentiation and mesenchymal transition. Eur Respir J. 2015;45(5):1258-72.
9. Yaghi A, Dolovich MB. Airway Epithelial Cell Cilia and Obstructive Lung Disease. Cells. 2016;5(4).
10. Gohy S, Carlier FM, Fregimilicka C, Detry B, Lecocq M, Ladjemi MZ, et al. Altered generation of ciliated cells in chronic obstructive pulmonary disease. Sci Rep. 2019;9(1):17963.
11. Pilette C, Godding V, Kiss R, Delos M, Verbeken E, Decaestecker C, et al. Reduced epithelial expression of secretory component in small airways correlates with airflow obstruction in chronic obstructive pulmonary disease. Am J Respir Crit Care Med. 2001;163(1):185-94.
12. Gamez AS, Gras D, Petit A, Knabe L, Molinari N, Vachier I, et al. Supplementing defect in club cell secretory protein attenuates airway inflammation in COPD. Chest. 2015;147(6):1467-76.
13. Saetta M, Turato G, Baraldo S, Zanin A, Braccioni F, Mapp CE, et al. Goblet cell hyperplasia and epithelial inflammation in peripheral airways of smokers with both symptoms of chronic bronchitis and chronic airflow limitation. Am J Respir Crit Care Med. 2000;161(3 Pt 1):1016-21.
14. Milara J, Peiro T, Serrano A, Cortijo J. Epithelial to mesenchymal transition is increased in patients with COPD and induced by cigarette smoke. Thorax. 2013;68(5):410-20.

15. Mahmood MQ, Sohal SS, Shukla SD, Ward C, Hardikar A, Noor WD, et al. Epithelial mesenchymal transition in smokers: large versus small airways and relation to airflow obstruction. Int J Chron Obstruct Pulmon Dis. 2015;10:1515-24.
16. Sohal SS. Chronic Obstructive Pulmonary Disease (COPD) and Lung Cancer: Epithelial Mesenchymal Transition (EMT), the Missing Link? EBioMedicine. 2015;2(11):1578-9.
17. Gohy ST, Detry BR, Lecocq M, Bouzin C, Weynand BA, Amatngalim GD, et al. Polymeric immunoglobulin receptor down-regulation in chronic obstructive pulmonary disease. Persistence in the cultured epithelium and role of transforming growth factor-beta. Am J Respir Crit Care Med. 2014;190(5):509-21.
18. Carlier FM, Dupasquier S, Ambroise J, Detry B, Lecocq M, Bietry-Claudet C, et al. Canonical WNT pathway is activated in the airway epithelium in chronic obstructive pulmonary disease. EBioMedicine. 2020;61:103034.
19. Carlier FM, Sibille Y, Pilette C. The epithelial barrier and immunoglobulin A system in allergy. Clin Exp Allergy. 2016;46(11):1372-88.
20. Pilette C, Ouadrhiri Y, Godding V, Vaerman JP, Sibille Y. Lung mucosal immunity: immunoglobulin-A revisited. Eur Respir J. 2001;18(3):571-88.
21. Pilette C, Durham SR, Vaerman JP, Sibille Y. Mucosal immunity in asthma and chronic obstructive pulmonary disease: a role for immunoglobulin A? Proc Am Thorac Soc. 2004;1(2):125-35.
22. Polosukhin VV, Richmond BW, Du RH, Cates JM, Wu P, Nian H, et al. Secretory IgA Deficiency in Individual Small Airways Is Associated with Persistent Inflammation and Remodeling. Am J Respir Crit Care Med. 2017;195(8):1010-21.
23. Polosukhin VV, Cates JM, Lawson WE, Zaynagetdinov R, Milstone AP, Massion PP, et al. Bronchial secretory immunoglobulin a deficiency correlates with airway inflammation and progression of chronic obstructive pulmonary disease. Am J Respir Crit Care Med. 2011;184(3):317-27.
24. Barnes PJ. Inflammatory mechanisms in patients with chronic obstructive pulmonary disease. J Allergy Clin Immunol. 2016;138(1):16-27.
25. Eapen MS, Myers S, Walters EH, Sohal SS. Airway inflammation in chronic obstructive pulmonary disease (COPD): a true paradox. Expert Rev Respir Med. 2017;11(10):827-39.
26. Keatings VM, Collins PD, Scott DM, Barnes PJ. Differences in interleukin-8 and tumor necrosis factor-alpha in induced sputum from patients with chronic obstructive pulmonary disease or asthma. Am J Respir Crit Care Med. 1996;153(2):530-4.
27. Rutgers SR, Timens W, Kaufmann HF, van der Mark TW, Koeter GH, Postma DS. Comparison of induced sputum with bronchial wash, bronchoalveolar lavage and bronchial biopsies in COPD. Eur Respir J. 2000;15(1):109-15.
28. Di Stefano A, Capelli A, Lusuardi M, Balbo P, Vecchio C, Maestrelli P, et al. Severity of airflow limitation is associated with severity of airway inflammation in smokers. Am J Respir Crit Care Med. 1998;158(4):1277-85.
29. Lapperre TS, Sont JK, van Schadewijk A, Gosman MM, Postma DS, Bajema IM, et al. Smoking cessation and bronchial epithelial remodelling in COPD: a cross-sectional study. Respir Res. 2007;8:85.

30. Willemse BW, Postma DS, Timens W, ten Hacken NH. The impact of smoking cessation on respiratory symptoms, lung function, airway hyperresponsiveness and inflammation. Eur Respir J. 2004;23(3):464-76.
31. Bai JW, Chen XX, Liu S, Yu L, Xu JF. Smoking cessation affects the natural history of COPD. Int J Chron Obstruct Pulmon Dis. 2017;12:3323-8.
32. Louhelainen N, Rytila P, Haahtela T, Kinnula VL, Djukanovic R. Persistence of oxidant and protease burden in the airways after smoking cessation. BMC Pulm Med. 2009;9:25.
33. Gamble E, Grootendorst DC, Hattotuwa K, O'Shaughnessy T, Ram FS, Qiu Y, et al. Airway mucosal inflammation in COPD is similar in smokers and ex-smokers: a pooled analysis. Eur Respir J. 2007;30(3):467-71.
34. Lapperre TS, Postma DS, Gosman MM, Snoeck-Stroband JB, ten Hacken NH, Hiemstra PS, et al. Relation between duration of smoking cessation and bronchial inflammation in COPD. Thorax. 2006;61(2):115-21.
35. Pauwels RA, Buist AS, Ma P, Jenkins CR, Hurd SS, Committee GS. Global strategy for the diagnosis, management, and prevention of chronic obstructive pulmonary disease: National Heart, Lung, and Blood Institute and World Health Organization Global Initiative for Chronic Obstructive Lung Disease (GOLD): executive summary. Respir Care. 2001;46(8):798-825.
36. Bustin SA, Benes V, Garson J, Hellemans J, Huggett J, Kubista M, et al. The need for transparency and good practices in the qPCR literature. Nat Methods. 2013;10(11):1063-7.
37. Pilette C, Ouadrhiri Y, Dimanche F, Vaerman JP, Sibille Y. Secretory component is cleaved by neutrophil serine proteinases but its epithelial production is increased by neutrophils through NF-kappa B- and p38 mitogen-activated protein kinase-dependent mechanisms. Am J Respir Cell Mol Biol. 2003;28(4):485-98.
38. Collin AM, Lecocq M, Noel S, Detry B, Carlier FM, Aboubakar Nana F, et al. Lung immunoglobulin A immunity dysregulation in cystic fibrosis. EBioMedicine. 2020;60:102974.
39. Watanabe N, Nakayama J, Fujita Y, Mori Y, Kadota T, Shimomura I, et al. Single-cell Transcriptome Analysis Reveals an Anomalous Epithelial Variation and Ectopic Inflammatory Response in Chronic Obstructive Pulmonary Disease. medRxiv. 2020:2020.12.03.20242412.
40. Chen G, Korfhagen TR, Karp CL, Impey S, Xu Y, Randell SH, et al. Foxa3 induces goblet cell metaplasia and inhibits innate antiviral immunity. Am J Respir Crit Care Med. 2014;189(3):301-13.
41. Park KS, Korfhagen TR, Bruno MD, Kitzmiller JA, Wan H, Wert SE, et al. SPDEF regulates goblet cell hyperplasia in the airway epithelium. J Clin Invest. 2007;117(4):978-88.
42. Rajavelu P, Chen G, Xu Y, Kitzmiller JA, Korfhagen TR, Whitsett JA. Airway epithelial SPDEF integrates goblet cell differentiation and pulmonary Th2 inflammation. J Clin Invest. 2015;125(5):2021-31.
43. Bafadhel M, McKenna S, Terry S, Mistry V, Reid C, Haldar P, et al. Acute exacerbations of chronic obstructive pulmonary disease: identification of biologic clusters and their biomarkers. Am J Respir Crit Care Med. 2011;184(6):662-71.

44. Rawlins EL, Okubo T, Xue Y, Brass DM, Auten RL, Hasegawa H, et al. The role of Scgb1a1+ Clara cells in the long-term maintenance and repair of lung airway, but not alveolar, epithelium. Cell Stem Cell. 2009;4(6):525-34.
45. Rock JR, Randell SH, Hogan BL. Airway basal stem cells: a perspective on their roles in epithelial homeostasis and remodeling. Dis Model Mech. 2010;3(9-10):545-56.
46. Ryan DM, Vincent TL, Salit J, Walters MS, Agosto-Perez F, Shaykhiev R, et al. Smoking dysregulates the human airway basal cell transcriptome at COPD risk locus 19q13.2. PLoS One. 2014;9(2):e88051.
47. Zuo WL, Yang J, Gomi K, Chao I, Crystal RG, Shaykhiev R. EGF-Amphiregulin Interplay in Airway Stem/Progenitor Cells Links the Pathogenesis of Smoking-induced Lesions in the Human Airway Epithelium. Stem Cells. 2016.
48. Anthonisen NR, Connett JE, Kiley JP, Altose MD, Bailey WC, Buist AS, et al. Effects of smoking intervention and the use of an inhaled anticholinergic bronchodilator on the rate of decline of FEV1. The Lung Health Study. JAMA. 1994;272(19):1497-505.
49. Fletcher C, Peto R. The natural history of chronic airflow obstruction. Br Med J. 1977;1(6077):1645-8.
50. Ramos EM, De Toledo AC, Xavier RF, Fosco LC, Vieira RP, Ramos D, et al. Reversibility of impaired nasal mucociliary clearance in smokers following a smoking cessation programme. Respirology. 2011;16(5):849-55.
51. Verra F, Escudier E, Lebargy F, Bernaudin JF, De Cremoux H, Bignon J. Ciliary abnormalities in bronchial epithelium of smokers, ex-smokers, and nonsmokers. Am J Respir Crit Care Med. 1995;151(3 Pt 1):630-4.
52. Willemse BW, ten Hacken NH, Rutgers B, Lesman-Leegte IG, Postma DS, Timens W. Effect of 1-year smoking cessation on airway inflammation in COPD and asymptomatic smokers. Eur Respir J. 2005;26(5):835-45.
53. Carlier F, Detry B, Sibille Y, Pilette C. COPD epithelial phenotype shows partial reversibility in long-term primary epithelial ALI-cultures. Eur Respir J. 2018;52(suppl 62).
54. Shaykhiev R, Otaki F, Bonsu P, Dang DT, Teater M, Strulovici-Barel Y, et al. Cigarette smoking reprograms apical junctional complex molecular architecture in the human airway epithelium in vivo. Cell Mol Life Sci. 2011;68(5):877-92.
55. Cereijido M, Valdes J, Shoshani L, Contreras RG. Role of tight junctions in establishing and maintaining cell polarity. Annu Rev Physiol. 1998;60:161-77.
56. Ladjemi MZ, Gras D, Dupasquier S, Detry B, Lecocq M, Garulli C, et al. Bronchial Epithelial IgA Secretion Is Impaired in Asthma. Role of IL-4/IL-13. Am J Respir Crit Care Med. 2018;197(11):1396-409.
57. Bartis D, Mise N, Mahida RY, Eickelberg O, Thickett DR. Epithelial-mesenchymal transition in lung development and disease: does it exist and is it important? Thorax. 2014;69(8):760-5.
58. Ordovas-Montanes J, Beyaz S, Rakoff-Nahoum S, Shalek AK. Distribution and storage of inflammatory memory in barrier tissues. Nat Rev Immunol. 2020;20(5):308-20.

59. Naik S, Larsen SB, Gomez NC, Alaverdyan K, Sendoel A, Yuan S, et al. Inflammatory memory sensitizes skin epithelial stem cells to tissue damage. Nature. 2017;550(7677):475-80.
60. Beyaz S, Mana MD, Roper J, Kedrin D, Saadatpour A, Hong SJ, et al. High-fat diet enhances stemness and tumorigenicity of intestinal progenitors. Nature. 2016;531(7592):53-8.
61. Fischer A, Gluth M, Weege F, Pape UF, Wiedenmann B, Baumgart DC, et al. Glucocorticoids regulate barrier function and claudin expression in intestinal epithelial cells via MKP-1. Am J Physiol Gastrointest Liver Physiol. 2014;306(3):G218-28.
62. Carayol N, Vachier I, Campbell A, Crampette L, Bousquet J, Godard P, et al. Regulation of E-cadherin expression by dexamethasone and tumour necrosis factor-alpha in nasal epithelium. Eur Respir J. 2002;20(6):1430-6.
63. Carayol N, Campbell A, Vachier I, Mainprice B, Bousquet J, Godard P, et al. Modulation of cadherin and catenins expression by tumor necrosis factor-alpha and dexamethasone in human bronchial epithelial cells. Am J Respir Cell Mol Biol. 2002;26(3):341-7.
64. Heijink I, van den Berge M, Kliphuis N, ten Hacken N, Postma D, van Oosterhout A. Corticosteroids improve airway epithelial regeneration and restore oxidative stress-induced epithelial barrier dysfunction. Eur Respir J. 2012;40(Suppl 56).
65. Yang HW, Lee SA, Shin JM, Park IH, Lee HM. Glucocorticoids ameliorate TGF-beta1-mediated epithelial-to-mesenchymal transition of airway epithelium through MAPK and Snail/Slug signaling pathways. Sci Rep. 2017;7(1):3486.

SECTION 3.
CANONICAL WNT PATHWAY IS ACTIVATED IN THE AIRWAY EPITHELIUM IN CHRONIC OBSTRUCTIVE PULMONARY DISEASE

Adapted from EBioMedicine, 2020 Nov;61:103034

Carlier FM, Dupasquier S, Ambroise J, Detry B, Lecocq M, Biétry--Claudet C, Boukala Y, Gala JL, Bouzin C, Verleden SE, Hoton D, Gohy S, Bearzatto B, Pilette C.

1. Abstract

Background. Chronic obstructive pulmonary disease (COPD) is a devastating lung disease, mainly due to cigarette smoking, which represents the third cause of mortality worldwide. The mechanisms driving its epithelial salient features remain largely elusive. We aimed to evaluate the activation and the role of the canonical, β-catenin-dependent WNT pathway in the airway epithelium from COPD patients.

Methods. The WNT/β-catenin pathway was first assessed by WNT-targeted RNA sequencing of the air/liquid interface-reconstituted bronchial epithelium from COPD and control patients. Airway expression of total and active β-catenin was assessed in lung sections, as well as WNT components in laser-microdissected airway epithelium. Finally, we evaluated the role of WNT at the bronchial epithelial level by modulating the pathway in the reconstituted COPD epithelium.

Results. We show that the WNT/β-catenin pathway is upregulated in the COPD airway epithelium as compared with that of non-smokers and control smokers, in targeted RNA-sequencing of in vitro reconstituted airway epithelium, and in situ in lung tissue and laser-microdissected epithelium. Extrinsic activation of this pathway in COPD-derived airway epithelium inhibited epithelial differentiation, polarity and

barrier function, and induced TGF-β-related epithelial-to-mesenchymal transition (EMT). Conversely, canonical WNT inhibition increased ciliated cell numbers, epithelial polarity and barrier function, whilst inhibiting EMT, thus reversing COPD features.

Conclusion. The aberrant reactivation of the canonical WNT pathway in the adult airway epithelium recapitulates the diseased phenotype observed in COPD patients, suggesting that this pathway or its downstream effectors could represent a future therapeutic target.

2. Introduction

Chronic obstructive pulmonary disease (COPD) is a major health burden and is currently the third leading cause of death worldwide, according to World Health Organization estimations (1). Its major cause is cigarette smoking, although genetic predisposition and other toxic exposures (air pollution, occupational, biomass) may also play a role (2). COPD is characterized by a slowly progressive and mostly irreversible airway obstruction that is due to a combination of small airway disease (with mucus plugs and peribronchial fibrosis) and emphysema (destruction of the alveolar walls), ultimately leading to respiratory failure (3). Besides alveoli and small airways, large airways are also altered in COPD, with inflammation (4), increased extracellular matrix deposition (5), lineage abnormalities (6) and barrier dysfunction of the epithelium (7). The relevance of large airway disease in COPD relates to its association with increased risk of exacerbations and of lung cancer (8, 9).

Discovered in the early 1980s (10), the Wingless/Integrase-1 (WNT) signalling pathways play a crucial role in lung morphogenesis (11) and have been widely studied in chronic respiratory diseases (12, 13). Canonical WNT signalling involves the activation of the transcriptional coactivator β-catenin, while noncanonical WNT signalling is β-catenin independent and subdivided in planar polarity cell signalling, calcium/calmodulin-dependent protein kinase II signalling, and other less well-

defined cascades (14). In the absence of canonical WNT stimulation (e.g. WNT-3a and WNT-8), the so-called "β-catenin destruction complex" regulates the pool of intracellular β-catenin by phosphorylation and ubiquitination, ultimately addressing β-catenin to proteasomal degradation (15). This prevents its migration to the nucleus, where expression of WNT target genes is constitutively repressed by a complex consisting of T-cell factor/lymphoid enhancer-binding factor (TCF/LEF) and transducing-like enhancer of split protein (TLE/Groucho). The binding of a canonical WNT ligand to one of the Frizzled receptors (FZD_{1-10}) leads to the inactivation of the destruction complex and to the accumulation of intracytoplasmic, unphosphorylated β-catenin, whose migration to the nucleus will transactivate its target genes (16), including epithelial-to-mesenchymal (EMT)-promoting transcription factors (17).

WNT pathways have been studied in COPD where persistent reactivation of developmental pathways – such as WNT, Notch, SHH, as well as TGF-β – emerged as a new paradigm (18). Previous studies showed that upregulated noncanonical WNT signalling, through increased WNT-5a and -5b (19, 20), contributes to emphysema (characterized by the disruption of alveolar walls) by negatively regulating alveolar repair, while decreased FZD4 in COPD leads to reduced canonical signalling and impaired alveolar repair capacity (21). On the other hand, extrinsic activation of the canonical pathway (by LiCl or CHIR99021) in elastase-induced murine emphysema (22) and *ex-vivo* three-dimensional murine lung tissue cultures (23) attenuated those COPD features at the alveolar level. Moreover, the FAM13A gene, associated with COPD in genome-wide association studies (24), is suspected to promote β-catenin degradation, increasing disease susceptibility in murine elastase-induced emphysema (25). Taken together, these results suggest a shift from canonical to noncanonical WNT signalling in the COPD alveolar epithelium that underlies emphysema.

In contrast, data regarding WNT dysregulation at the airway epithelium (AE) level remain controversial. Thus, the noncanonical ligand WNT-4 was upregulated in

COPD bronchial biopsies (26), and potentiated cigarette smoke-induced inflammation in 16HBE cells (27). The expression of noncanonical ligands WNT-4 and -5b was increased in COPD-derived primary human bronchial epithelial cells (HBECs) redifferentiated upon air/liquid interface (ALI), compared with controls (27, 28). Nicotine-exposed HBECs showed increased canonical WNT-3a expression that further induced EMT (29), and the canonical FZD8 receptor was found to promote epithelial inflammation in cigarette smoke-exposed mice (30). The activation of the WNT/β-catenin pathway by CHIR99021 in ALI-HBEC also inhibited the commitment towards ciliated cells (31). Conversely it was however shown that several canonical components, including β-catenin, were downregulated in the small AE from COPD patients, either from endobronchial biopsies and brushings (32), or surgical lung tissue (33). Globally, these results consistently show an activation of the noncanonical WNT pathways in the proximal AE in COPD, while divergent results are seen concerning the WNT/β-catenin pathway.

EMT is a dynamic process where epithelial cells lose their polarity and adhesiveness, and gain migratory abilities and mesenchymal features. EMT programming is crucial to embryogenesis (type I EMT), tissue repair (type II), and cancer metastasis (type III), and is regulated by an intricate network of pathways, including WNT and TGF-β (34). In the last decade, several studies showed that EMT occurs in the COPD AE, both in small (35) and large airways (36, 37), therefore promoting airway fibrosis, impaired epithelial repair, as well as carcinogenesis and metastasis potential (38, 39). It was reported that ALI-cultures from COPD patients spontaneously display mesenchymal features and that cigarette smoke may induce EMT in control HBECs, possibly as a result of TGF-β signalling (40). Moreover, upon TGF-β_1 stimulation, pulmonary fibroblasts from COPD patients seemed more prone to express EMT markers (fibronectin, collagen-1α1, α-smooth muscle actin), in a WNT/β-catenin dependent fashion (41). Although canonical WNT activation has been extensively reported in (idiopathic) pulmonary fibrosis, as recently reviewed (12), little is known about the role of WNT in EMT-related COPD airway fibrosis.

In the present study, we aimed at clarifying whether the WNT/β-catenin pathway is activated in the proximal AE in COPD and at addressing the hypothesis that WNT dysregulation contributes to the aberrant airway epithelial phenotype observed in this disease, including EMT.

3. Materials and methods

3.1.Experimental design, study population and lung tissue samples

A series of lung surgical specimens containing large airways was selected from five different patients groups (non-smokers, smoker controls, mild COPD, moderate COPD and severe to very severe COPD). COPD patients were sorted on basis of their pulmonary function tests, according to the GOLD 2001 classification. Patients with any other lung disease than COPD (e.g. asthma, pulmonary fibrosis) were excluded from the study. All patients received information and signed a written consent to the study protocol, which was approved by the local clinical Ethical committee (reference 2007/19MARS/58 for UCLouvain, S52174 and S55877 for KULeuven). Smoking history was recorded according to patient reporting, a status of former smoker referring to as patients who quit smoking at least 12 months before surgery. A primary proximal bronchial epithelium was reconstituted in vitro from all subjects as described hereunder, and was subjected to WNT-targeted RNA-sequencing (RNA-seq, n=47 subjects), RT-qPCR for validation (n=21), and WNT modulation experiments (n=6). In parallel, the surgical specimens were embedded for immunostaining of the bronchial epithelium (n=56). Patients' characteristics are shown in Tables 7, 8, 9, and 10.

	Non-smoker controls	Smoker controls	COPD stage 1	COPD stage 2	COPD stage 3-4	
Subjects, n (Female/Male)	9 (8/1)	10 (3/7)	9 (2/7)	10 (0/10)	9 (5/4)	p=0.001
Age	63 ± 13	61 ± 8	65 ± 6	70 ± 7	63 ± 4	ns
BMI (kg.m^{-2})	23 ± 3	25 ± 3	30 ± 4*	28 ± 4	22 ± 4$^{¶\$}$	p<0.001
Smoking history (never /former /current)	9/0/0	0/1/9	0/7/2	0/6/4	0/7/2	p<0.01
Pack-year units	0 ± 0	38 ± 23*	49 ± 29*	50 ± 15*	46 ± 23*	p<0.0001
FEV1 pre-BD (% of PV)	101 ± 18	91 ± 12	91 ± 9	66 ± 10*$^{\#¶}$	23 ± 11*$^{\#¶\$}$	p<0.0001
FEV1 post-BD (% of PV) (n)	74 ± 0 (n=1)	91 ± 15 (n=2)	94 ± 12 (n=6)	69 ± 11$^{\#¶}$ (n=7)	25 ± 13$^{\#¶\$}$ (n=9)	p<0.0001
FEV1 absolute increase after BD, ml (n)	190 ± 0	85 ± 35	95 ± 99	96 ± 66	56 ± 54	ns
FVC pre-BD (% of PV)	102 ± 15	95 ± 12	109 ± 13	81 ± 10*¶	57 ± 14*$^{\#¶\$}$	p<0.0001
FVC post-BD (% of PV) (n)	92 ± 0 (n=1)	97 ± 8 (n=2)	112 ± 12 (n=6)	90 ± 10 (n=7)	64 ± 16$^{\#¶\$}$ (n=9)	p<0.0001
FEV1/FVC ratio pre-BD (%)	79 ± 5	75 ± 4	65 ± 4*$^{\#}$	62 ± 9*$^{\#}$	32 ± 9*$^{\#¶\$}$	p<0.0001
FEV1/FVC ratio post-BD (%)	70 ± 0 (n=1)	76 ± 6 (n=2)	65 ± 3 (n=6)	60 ± 9 (n=7)	32 ± 11$^{\#¶\$}$ (n=9)	p<0.0001
DLCO (% of PV)	91 ± 20	73 ± 9	63 ± 4*	61 ± 12*	28 ± 11*$^{\#¶\$}$	p<0.0001
Inhaled corticosteroids, n	0	0	1	1	8	p<0.001
Inhaled corticosteroids mean dosage, µg (BDP equivalent)	NA	NA	400 ± 0	200 ± 0	1438 ± 1131	NA
Inhaled corticosteroids, device (meter dose	NA	NA	0/1	0/1	0/8	NA

inhalers / dry powder inhalers)						
Radiological findings						
Bronchiectasis	1/9	1/10	3/9	0/10	3/9	
Emphysema	0/9	5/10	6/9	5/10	9/9	
- **Mild**		2	4	1	1	
- **Moderate**		2	2	2	1	
- **Severe**		1		2	7	
Surgical indication						
Cancer	8/9	9/10	9/9	10/10	2/9	
- **AC**	5	8	7	4	2	
- **Squamous**	1	1	1	3		
- **NE**	2		1	2		
- **Other**				1		
Non-cancer	1/9	1/10	0/9	0/10	7/9	
- **LTx**					7	
- **Other**	1	1				

Table 7 | Patient series for RNA-seq

Patient cohort for the epithelial WNT-targeted RNA-seq in cultured airway epithelial cells. Data are presented as mean ± SD, unless otherwise stated. Demographic data, lung function tests, smoking history, and inhaled corticotherapy as well as radiological findings and surgery indication are stated for the patient groups, classified according to smoking history and the presence of airflow limitation. Patients with other lung diseases (e.g., asthma) were excluded from the study.

AC, adenocarcinoma; BDP, beclomethasone dipropionate; BD, bronchodilation; BMI, body mass index; COPD, chronic obstructive pulmonary disease; DLCO, diffusing capacity of the lung for CO; FEV1, forced expiratory volume in 1 s; FVC, forced vital capacity; LTx, lung transplantation; NA, not applicable; NE, neuroendocrine; PV, predicted values; RNA-seq, RNA-sequencing.

* = $p<0.05$ compared to non-smoker controls; # = $p<0.05$ compared to smoker controls; ¶ = $p<0.05$ compared to COPD stage 1 patients; $ = $p<0.05$ compared to COPD stage 2 patients; ns, not significant

	Non-smoker controls	Smoker controls	COPD stage 1	COPD stage 2	COPD stage 3-4	
Subjects, n (Female/Male)	7 (3/4)	14 (6/8)	12 (6/6)	12 (4/8)	11 (8/3)	ns
Age	60 ± 8	64 ± 9	65 ± 7	68 ± 10	60 ± 4	ns
BMI (kg.m^{-2})	24 ± 3	27 ± 5	26 ± 6	27 ± 4	23 ± 4	ns
Smoking history (never /former /current /missing)	11/0/0/0	0/4/9/1	0/4/8/0	0/6/6/0	0/11/0/0	p<0.01
Pack-years	0 ± 0	48 ± 17*	57 ± 25*	46 ± 23*	43 ± 14*	p<0.0001
FEV1 pre-BD (% of PV)	108 ± 11	91 ± 16*	88 ± 9*	65 ± 9*$^{\#\P}$	19 ± 5*$^{\#\P\$}$	p<0.0001
FEV1 post-BD (% of PV) (n)	NA (n=0)	70 ± 4 (n=2)	92 ± 10 (n=10)	67 ± 9 (n=11)	21 ± 7$^{\#}$ (n=11)	p<0.0001
FEV1 absolute increase after BD, ml (n)	NA (n=0)	100 ± 0 (n=2)	77 ± 89$^{\#}$ (n=10)	70 ± 76¶ (n=11)	22 ± 32$^{\#\P\$}$ (n=11)	p<0.05
FVC pre-BD (% of PV)	112 ± 21	95 ± 15	105 ± 12	86 ± 13*¶	55 ± 13*$^{\#\P\$}$	p<0.0001
FVC post-BD (% of PV) (n)	NA (n=0)	80 ± 3 (n=2)	110 ± 12 (n=10)	90 ± 15¶ (n=11)	58 ± 15$^{\P\$}$ (n=11)	p<0.0001
FEV1/FVC ratio pre-BD (%)	79 ± 6	78 ± 6	65 ± 4*$^{\#}$	60 ± 8*$^{\#}$	31 ± 7*$^{\#\P\$}$	p<0.0001
FEV1/FVC ratio post-BD (%)	NA (n=0)	83 ± 15 (n=2)	65 ± 3$^{\#}$ (n=10)	59 ± 9$^{\#}$ (n=11)	32 ± 7$^{\#\P\$}$ (n=11)	p<0.0001
DLCO (% of PV)	107 ± 14	75 ± 18*	69 ± 19*	57 ± 20*	28 ± 14*$^{\#\P\$}$	p<0.0001
Inhaled corticosteroids, n	0	0	3	3	11	p<0.0001
Inhaled corticosteroids mean dosage, µg (BDP equivalent)	NA	NA	967 ± 896	967 ± 896	1445 ± 787	NA

Inhaled corticosteroids, device (meter dose inhalers / dry powder inhalers)	NA	NA	0/3	0/3	1/10	ns
Radiological findings						
Bronchiectasis	1/7	0/14	1/12	2/12	1/11	
Emphysema	0/7	5/14	7/12	5/12	11/11	
- **Mild**		4	4	1	1	
- **Moderate**			3	3	2	
- **Severe**		1		1	8	
Surgical indication						
Cancer	7/7	14/14	12/12	12/12	0/11	
- **AC**	4	9	9	8		
- **Squamous**		3	3	2		
- **NE**	2	2		1		
- **Other**	1			1		
Non-cancer	0/7	0/14	0/9	0/12	11/11	
- **LTx**					11	

Table 8 | Patient series for total, unphosphorylated and nuclear β-catenin staining.

Data are presented as mean ± SD, unless otherwise stated. Demographic data, lung function tests, smoking history, and inhaled corticotherapy as well as radiological findings and surgery indication are stated for the patient groups, classified according to smoking history and the presence of airflow limitation. Patients with other lung diseases (e.g., asthma) were excluded from the study. N is specified when data are missing.

AC, adenocarcinoma; BDP, beclomethasone dipropionate; BD, bronchodilation; BMI, body mass index; COPD, chronic obstructive pulmonary disease; DLCO, diffusing capacity of the lung for CO; FEV1, forced expiratory volume in 1 s; FVC, forced vital capacity; LTx, lung transplantation; NA, not applicable; NE, neuroendocrine; PV, predicted values; RNA-seq, RNA-sequencing.

* = $p<0.05$ compared to non-smoker controls, # = $p<0.05$ compared to smoker controls, ¶ = $p<0.05$ compared to COPD stage 1 patients, $ = $p<0.05$ compared to COPD stage 2 patients, ns, not significant.

	Non-smoker controls	COPD stage 4	
Subjects, n (Female/Male)	6 (4/2)	6 (5/1)	ns
Age	59 ± 9	58 ± 4	ns
BMI (kg.m^{-2})	27 ± 6	24 ± 5	ns
Smoking history (never /former /current)	6/0/0	0/6/0	p<0.001
Pack-years	0 ± 0	38 ± 12	p<0.01
FEV1 pre-BD (% of PV)	91 ± 15	22 ± 8	p<0.01
FEV1 post-BD (% of PV)	NA	24 ± 8	NA
FEV1 absolute increase after BD, ml	NA	52 ± 73	NA
FVC pre-BD (% of PV)	97 ± 13	62 ± 11	p<0.01
FVC post-BD (% of PV)	NA	67 ± 10	NA
FEV1/FVC pre-BD ratio (%)	77 ± 6	45 ± 16	p<0.01
FEV1/FVC post-BD ratio (%)	NA	42 ± 15	NA
DLCO (% of PV)	89 ± 24	28 ± 17	p<0.01
Inhaled corticosteroids, n	0	4	p<0,05
Inhaled corticosteroids mean dosage, µg (BDP equivalent)	NA	950 ± 900	NA
Inhaled corticosteroids, device (meter dose inhalers / dry powder inhalers)	NA	0/4	NA
Radiological findings			
Bronchiectasis	0/6	1/6	
Emphysema	0/6	6/6	
- **Mild**			
- **Moderate**		1	
- **Severe**		5	
Surgical indication			
Cancer	6/6	0/6	
- **Adenocarcinoma**	2		
- **Squamous**			
- **Neuroendocrine**	2		
- **Other**	2		
Non-cancer	0/6	6/6	
- **Lung transplant**		6	

Table 9 | Patient series for microdissection.

Data are presented as mean ± SD, unless otherwise stated. Demographic data, lung function tests, smoking history, and inhaled corticotherapy as well as radiological findings and surgery indication are stated for the patient groups, classified according to smoking history and the presence of airflow limitation. Patients with other lung diseases (e.g., asthma) were excluded from the study.

BMI, body mass index; COPD, chronic obstructive pulmonary disease; DLCO, diffusing capacity of the lung for CO; FEV1, forced expiratory volume in 1 s; FVC, forced vital capacity; NA, not applicable; ns, not significant; PV, predicted values.

	Non-smoker controls	Smoker controls	COPD stage 1	COPD stage 2	COPD stage 3-4	
Subjects, n (Female/Male)	13 (112)	17 (4/13)	11 (3/8)	14 (2/12)	13 (8/5)	p<0.001
Age	66 ± 11	63 ± 10	67 ± 7	67 ± 10	60 ± 5	ns
BMI (kg.m^{-2})	23 ± 3¶	25 ± 3	30 ± 4	28 ± 4	22 ± 4$^{¶\$}$	p<0.05
Smoking history (never /former /current)	13/0/0	0/5/12	0/6/5	0/7/7	0/12/1	p<0.05
Pack-year units	0 ± 0	36 ± 16*	45 ± 26*	46 ± 16*	39 ± 21*	p<0.0001
FEV1 pre-BD (% of PV)	102 ± 16	92 ± 15	89 ± 9	66 ± 9*$^{#¶}$	21 ± 7*$^{#¶\$}$	p<0.0001
FEV1 post-BD (% of PV)	74 ± 0 (n=1)	84 ± 15 (n=3)	92 ± 11 (n=8)	69 ± 9¶ (n=11)	22 ± 9$^{#¶\$}$ (n=13)	p<0.0001
FEV1 absolute increase after BD, ml	190 ± 0 (n=1)	123 ± 71 (n=3)	104 ± 85 (n=8)	75 ± 90 (n=11)	42 ± 51 (n=13)	ns
FVC pre-BD (% of PV)	103 ± 13	97 ± 12	113 ± 17$^{#}$	86 ± 12*¶	56 ± 9*$^{#¶\$}$	p<0.0001
FVC post-BD (% of PV)	92 ± 0 (n=1)	92 ± 10 (n=3)	118 ± 17$^{#}$ (n=8)	94 ± 12¶ (n=11)	61 ± 10$^{#¶\$}$ (n=13)	p<0.0001
FEV1/FVC ratio pre-BD (%)	80 ± 5	78 ± 6	62 ± 7*$^{#}$	60 ± 9*$^{#}$	31 ± 8*$^{#¶\$}$	p<0.0001
FEV1/FVC ratio post-BD (%)	70 ± 0 (n=1)	82 ± 11 (n=3)	61 ± 8$^{#}$ (n=8)	58 ± 8$^{#}$ (n=11)	31 ± 9$^{#¶\$}$ (n=13)	p<0.0001
DLCO (% of PV)	83 ± 20	69 ± 12	61 ± 17*	59 ± 13*	30 ± 12*$^{#¶\$}$	p<0.0001
BMI (kg.m^{-2})	25 ± 4	25 ± 4	27 ± 6	27 ± 4	22 ± 3$^{\$}$	p<0.05
Inhaled corticosteroids, n	0	2	1	1	12	p<0.0001
Inhaled corticosteroids mean dosage, µg (BDP equivalent)	NA	600 ± 283	400 ± 0	200 ± 0	1013 ± 538	NA

Inhaled corticosteroids, device (meter dose inhalers / dry powder inhalers)	NA	0/2	0/1	0/1	1/11	NA
Radiological findings						
Bronchiectasis	1/13	3/17	4/11	0/14	3/13	
Emphysema	0/13	9/17	8/11	7/14	13/13	
- **Mild**		5	5	1	1	
- **Moderate**		3	3	4	2	
- **Severe**		1	0	2	10	
Surgical indication						
Cancer	12/13	16/17	11/11	14/14	1/13	
- **AC**	7	10	8	7	1	
- **Squamous**	1	6	2	3		
- **NE**	2		1	2		
- **Other**	2			2		
Non-cancer	1/7	1/17	0/11	0/14	12/13	
- **LTx**					12	
- **Other**	1	1				
History of respiratory allergy	2/13	0/17	1/11	0/14	0/13	

Table 10 | Patient series for PCR validation.

Data are presented as mean ± SD, unless otherwise stated. Demographic data, lung function tests, smoking history, and inhaled corticotherapy as well as comorbid findings (radiologic, surgery indication, history of allergy) are stated for the patient groups, classified according to smoking history and the presence of airflow limitation. Patients with other lung diseases (e.g. asthma) were excluded from the study.

AC, adenocarcinoma; BDP, beclomethasone dipropionate; BD, bronchodilation; BMI, body mass index; COPD, chronic obstructive pulmonary disease; DLCO, diffusing capacity of the lung for CO; FEV1, forced expiratory volume in 1 s; FVC, forced vital capacity; LTx, lung transplantation; NA, not applicable; NE, neuroendocrine; PV, predicted values; RNA-seq, RNA-sequencing.

* = $p<0.05$ compared to non-smoker controls, # = $p<0.05$ compared to smoker controls, ¶ = $p<0.05$ compared to COPD 1 patients, $ = $p<0.05$ compared to COPD patients, ns, not significant.

3.2.*In vitro* reconstitution of primary human AE on ALI culture

A large piece of cartilaginous bronchus was selected from lobectomies or explants, located as far as possible from the tumour site (in the case of lobectomies) and submitted to pronase digestion overnight at 4°C, in order to isolate HBECs. HBECs were cultured in flasks in retinoic acid-supplemented Bronchial Epithelial Cell Growth Basal Medium (Lonza, Verviers, Belgium) until confluence. Cells were then detached and seeded at a density of 80,000 cells/well on 24-well polyester filter-type inserts (0.4-µm pore size; Corning, Corning, NY) coated with 0.2mg/ml collagen IV (Sigma-Aldrich, Saint-Louis, MO) until a confluent monolayer was obtained. The culture was then carried out in air/liquid interface (ALI) for 14 to 21 days, according to the experiment. Once in ALI, HBECs were cultured in BEBM:DMEM (1:1) medium supplemented with penicillin (100U/ml), streptomycin (100µg/ml) (Lonza), bovine serum albumin (BSA) (1.5µg/ml), retinoic acid (30ng/ml) (Sigma-Aldrich), and BEGM SingleQuotsTM Supplements and Growth Factors (Lonza), including bovine pituitary extract (52µg/ml), insulin (5µg/ml), hydrocortisone (0.5g/ml), transferrin (10µg/ml), epinephrine (0.5µg/ml), epidermal growth factor (0.5ng/ml) and triiodothyronine (3.25ng/ml).

At the end of the ALI culture, basolateral media were collected, and the apical pole of HBEC was washed with 300µl sterile PBS, then centrifuged for 5 minutes at 10,000 g. Transwell inserts were fixed by direct immersion in 4% buffered formaldehyde, before incubation in PBS at pH 7.4 and embedding in paraffin blocks. ALI-HBEC were also processed for mRNA abundance or Western blot analyses (see below).

The modulation of the WNT/β-catenin pathway was performed in 6 very severe COPD-derived ALI-HBECs, by adding to the culture medium either the canonical WNT activator CHIR99021 (Sigma-Aldrich; 10µM) or the canonical WNT inhibitor XAV939 (Sigma-Aldrich; 10µM) for 5 days at different predefined time-periods: ALI D6-D10 (referred to as T1), D11-D15 (T2) or D16-D20 (T3). The absence of

significant toxicity at those concentrations was confirmed by using a LDH release assay.

3.3.WNT-targeted RNA-sequencing

RNA isolation and quantification. RNA was isolated from 70, ALI cultures at 2 weeks, in order to establish signature genes in pure cultures of airway epithelial cells at an early differentiation time-point. RiboPure™ RNA Purification kit from Ambion with bromochloropropane (BCP) was used instead of chloroform to avoid DNA contamination. RNA quantity was evaluated for each sample with Qubit™ RNA HS Assay Kit (Thermo Fisher Scientific, Waltham, MA). RNA integrity and quality were assessed with an Agilent Bioanalyzer, using the Agilent RNA 6000 Nano kit. We selected 47 amongst the 70 samples, in order to use RNA with a RIN > 9.2 and a percentage of RNA fragments above 200 nucleotides (DV_{200}) > 90%.

Panel design. mRNA abundance was evaluated using a TruSeq® custom Targeted RNA Expression kit from Illumina. The design was based on a predesigned mRNA abundance profiling solution from Illumina (TruSeq Targeted RNA Expression WNT Panel; Illumina Inc., San Diego, CA). This panel was designed by Illumina to study WNT signalling pathway and included assays targeting 93 genes. Five other WNT-related genes were added, as well as 8 EMT-related genes and 9 potential housekeeping genes, as recapitulated in Table 11. Moreover, 75 Notch-related and 21 epithelium-related genes were added to the panel but dedicated for a separated analysis. Thus, among these 211 genes, 115 genes were investigated and allocated into two separated panels according to their expression level (lowly or highly expressed).

N°	Gene Name	Protein
1	*ABCB1*	ATP Binding Cassette Subfamily B Member 1
2	*AES*	Amino-Terminal Enhancer Of Split
3	*APC*	Adenomatosis Polyposis Coli
4	*AXIN1*	Axin-1
5	*AXIN2*	Axin-2
6	*BCL9*	B Cell CLL/Lymphoma 9
7	*BIRC5*	Baculoviral IAP Repeat Containing 5
8	*BMP4*	Bone Morphogenetic Protein 4
9	*BTRC*	Beta-Transducin Repeat Containing E3 Ubiquitin Protein Ligase
10	*CCND1*	Cyclin D1
11	*CCND2*	Cyclin D2
12	*CD44*	CD44 Molecule
13	*CSNK1A1*	Casein Kinase 1 Alpha 1
14	*CSNK2A1*	Casein Kinase 2 Alpha 1
15	*CSNK2A2*	Casein Kinase 2 Alpha 2
16	*CTBP1*	C-Terminal Binding Protein 1
17	*CTNNB1*	Catenin Beta 1
18	*CTNNBIP1*	Catenin Beta Interacting Protein 1
19	*CXXC4*	CXXC Finger Protein 4
20	*DAAM1*	Dishevelled Associated Activator Of Morphogenesis 1
21	*DKK1*	Dickkopf WNT Signalling Pathway Inhibitor 1
22	*DVL1*	Dishevelled Segment Polarity Protein 1
23	*DVL2*	Dishevelled Segment Polarity Protein 2
24	*EGFR*	Epidermal Growth Factor Receptor
25	*EP300*	E1A Binding Protein P300
26	*FBXW11*	F-Box And WD Repeat Domain Containing 11
27	*FGF20*	Fibroblast Growth Factor 20
28	*FGF4*	Fibroblast Growth Factor 4
29	*FGF9*	Fibroblast Growth Factor 9
30	*FOSL1*	FOS Like 1, AP-1 Transcription Factor Subunit
31	*FOXN1*	Forkhead Box N1
32	*FRZB*	Frizzled Related Protein
33	*FZD1*	Frizzled Class Receptor 1
34	*FZD2*	Frizzled Class Receptor 2
35	*FZD3*	Frizzled Class Receptor 3
36	*FZD4*	Frizzled Class Receptor 4
37	*FZD5*	Frizzled Class Receptor 5

38	*FZD6*	Frizzled Class Receptor 6
39	*FZD7*	Frizzled Class Receptor 7
40	*FZD8*	Frizzled Class Receptor 8
41	*FZD9*	Frizzled Class Receptor 9
42	*GSK3A*	Glycogen Synthase Kinase 3 Alpha
43	*GSK3B*	Glycogen Synthase Kinase 3 Beta
44	*ID2*	Inhibitor Of DNA Binding 2
45	*IL6*	Interleukin 6
46	*JUN*	Jun Proto-Oncogene, AP-1 Transcription Factor Subunit
47	*LEF1*	Lymphoid Enhancer Binding Factor 1
48	*LRP5*	LDL Receptor Related Protein 5
49	*LRP6*	LDL Receptor Related Protein 6
50	*MAPK8*	Mitogen-Activated Protein Kinase 8
51	*MET*	MET Proto-Oncogene, Receptor Tyrosine Kinase
52	*MMP2*	Matrix Metallopeptidase 2
53	*MMP7*	Matrix Metallopeptidase 7
54	*MMP9*	Matrix Metallopeptidase 9
55	*MYC*	MYC Proto-Oncogene, BHLH Transcription Factor
56	*NANOG*	Nanog Homeobox
57	*NFATC1*	Nuclear Factor Of Activated T Cells 1
58	*NKD1*	Naked Cuticle Homolog 1
59	*NLK*	Nemo Like Kinase
60	*PITX2*	Paired Like Homeodomain 2
61	*PLAUR*	Plasminogen Activator, Urokinase Receptor
62	*PORCN*	Porcupine O-Acyltransferase
63	*PPARD*	Peroxisome Proliferator Activated Receptor Delta
64	*PRICKLE1*	Prickle Planar Cell Polarity Protein 1
65	*PYGO1*	Pygopus Family PHD Finger 1
66	*RHOA*	Ras Homolog Family Member A
67	*RUNX2*	Runt Related Transcription Factor 2
68	*RUVBL1*	RuvB Like AAA ATPase 1
69	*SFRP1*	Secreted Frizzled Related Protein 1
70	*SFRP2*	Secreted Frizzled Related Protein 2
71	*SFRP4*	Secreted Frizzled Related Protein 4
72	*SOX17*	SRY-Box 17
73	*SOX2*	SRY-Box 2
74	*SOX4*	SRY-Box 4
75	*SOX9*	SRY-Box 9
76	*TCF7*	Transcription Factor 7

77	*TCF7L1*	Transcription Factor 7 Like 1
78	*TCF7L2*	Transcription Factor 7 Like 2
79	*TLE1*	Transducin Like Enhancer Of Split 1
80	*TWIST1*	Twist Family BHLH Transcription Factor 1
81	*VANGL2*	VANGL Planar Cell Polarity Protein 2
82	*VEGFA*	Vascular Endothelial Growth Factor A
83	*WIF1*	WNT Inhibitory Factor 1
84	*WISP1*	WNT1 Inducible Signalling Pathway Protein 1 Cellular Communication Network Factor 4
85	*WNT1*	WNT Family Member 1
86	*WNT10A*	WNT Family Member 10A
87	*WNT11*	WNT Family Member 11
88	*WNT16*	WNT Family Member 16
89	*WNT2B*	WNT Family Member 2B
90	*WNT3*	WNT Family Member 3
91	*WNT3A*	WNT Family Member 3A
92	*WNT4*	WNT Family Member 4
93	*WNT5A*	WNT Family Member 5A
94	*WNT5B*	WNT Family Member 5B
95	*WNT6*	WNT Family Member 6
96	*WNT7B*	WNT Family Member 7B
97	*WNT8A*	WNT Family Member 8A
98	*WNT9A*	WNT Family Member 9A
EMT-related genes		
99	*FN1*	Fibronectin 1
100	*TGFA*	Transforming Growth Factor Alpha
101	*TGFB1*	Transforming Growth Factor Beta 1
102	*TGFB2*	Transforming Growth Factor Beta 2
103	*TGFB3*	Transforming Growth Factor Beta 3
104	*TGFBR1*	Transforming Growth Factor Beta Receptor 1
105	*TGFBR2*	Transforming Growth Factor Beta Receptor 2
106	*VIM*	Vimentin
Housekeeping genes		
107	*GAPDH*	Glyceraldehyde-3-Phosphate Dehydrogenase
108	*HPRT1*	Hypoxanthine Phosphoribosyltransferase 1
109	*POLR2A*	RNA Polymerase II Subunit A
110	*PPIA*	Peptidylprolyl Isomerase A

111	*RPL13A*	Ribosomal Protein L13a
112	*RPL27*	Ribosomal Protein L27
113	*RPLP0*	Ribosomal Protein Lateral Stalk Subunit P0
114	*RPS13*	Ribosomal Protein S13
115	*RPS18*	Ribosomal Protein S18

Table 11 | WNT-related RNA-seq target genes.

Next generation sequencing (NGS). The library preparation was performed using 50ng total RNA, according to the manufacturer's protocol (#15034665 v01, January 2016). The first cDNA strand synthesis was performed following the CDNASYN1 program for intact total RNA. Targets were amplified using 30 and 32 cycles for the lowly and highly expressed genes panels, respectively. The quality of the final libraries was controlled with an Agilent Bioanalyzer, using the Agilent DNA 1000 kit, and samples were equimolarly pooled (4nM). The pooled libraries were then diluted to 15pM and 10pM (for the lowly and highly expressed genes panels, respectively), and loaded on a MiSeq Reagent Kit v3 (Illumina Inc.). The libraries were sequenced using 51 cycles single read.

Statistical analysis. RNA-seq data analysis was performed separately for each panel (lowly and highly expressed genes), according to the following bioinformatics pipeline. Reads were aligned to the sequences of the targeted transcript retrieved from the human reference genome (UCSC assembly hg19) using BWA (v.0.7.17). Samtools (v.1.9) was used to generate, to sort and to index the BAM files. Read counting for each transcript was performed with the GenomicAlignments (v.1.36.0) Bioconductor package. The geNorm algorithm implemented within the ctrlGene (v.1.0.1). R package was used to identify stably expressed genes among the set of measured housekeeping genes. The selected housekeeping genes were used within the DESeq2 (1.24.0) Bioconductor package in order to compute the size factors associated with each library. The DESeq2 package was then used to estimate fold-changes and p-values for each transcript between group of interest (e.g. COPD1 versus non-smoker controls, COPD2 versus non-smoker controls, …). Multiple

testing correction of the p-value was performed within DESeq2 by the Benjamini-Hochberg procedure (42) in order to control the false discovery rate (FDR) at a level of 0.10. Accordingly, genes associated with an adjusted p-values < 0.10 were considered significant and were therefore expected to include 10% of false positive results. While less conservative than the Bonferroni's correction, this approach and associated threshold is commonly used in transcriptomic studies and selected here to increase the statistical power. All statistical analyses were performed using R.3.6.1.

Both raw and processed RNA-seq data were deposited on the Gene Expression Omnibus (GEO) and made publicly available (GSE155588).

3.4. Reverse transcriptase quantitative polymerase chain reaction (RT-qPCR) assays

RNA extraction, reverse transcription, and RT-qPCR were performed as previously described (43). Total RNA was extracted from reconstituted ALI-cultured epithelia using TRIzol reagent (Thermo Fisher Scientific). 500ng of RNA was reverse-transcribed with RevertAid H Minus Reverse transcriptase kit with 0.3µg of random hexamer, 20U of RNase inhibitor and 1mM of each dNTP (Thermo Fisher Scientific) following the manufacturer's protocol in a thermocycler (Applied Biosystems, Foster City, CA). The expression levels were quantified by real-time quantitative PCR using the CFX96 PCR (Bio-Rad, Hercules, CA). The reaction mix contained 2.5µl of complementary desoxyribonucleic acid diluted 10-fold, 200nM of each primer (primers properties are detailed in Table 12) and 2x iTaq UniverSybr Green® Supermix (Bio-Rad) in a final volume of 20µl. The cycling conditions were 95°C for 3 minutes followed by 40 cycles of 95°C for 5 seconds and 60°C for 30 seconds. To control the specificity of the amplification products, a melting curve analysis was performed. The copy number was calculated from the standard curve. Data analysis was performed using Bio-Rad CFX software (Bio-Rad). Expression levels of target genes were normalized to the geometric mean of the values of the 3 housekeeping genes (RPL27, RPS13, RPS18).

Gene	Fw primer (5'-3')	Rv primer (3'-5')	AS	HT
Housekeeping genes				
RPL27	TGG TAG GGC CGG GTG GTT GC	ACT TTG CGG GGG TAG CGG TC	185	60
RPS13	TCG GCT TTA CCC TAT CGA CGC AG	ACG TAC TTG TGC AAC ACC ATG TGA	153	60
RPS18	TGT GGG CCG AAG ATA TGC T	TGA TCA CAC GTT CCA CCT CAT	101	60
Target genes				
AXIN2	TGT GAG GTC CAC GGA AAC TG	TCC ATC TAC ACT GCT GTC CG	184	60
CDH1	GCT GGA CCG AGA GAG TTT CC	CGA CGT TAG CCT CGT TCT CA	179	60
CTNNB1	GCG CCA TTT TAA GCC TCT CG	AAA TAC CCT CAG GGG AAC AGG	183	60
DNAI1	GAG TTG ACC GAT GCG GAG TT	GGT TCC CAA CCT GGG TGT AG	163	60
DNAI2	GCG ATT CAT ACA TCT GGG AC	CAG CAG GCT ATC TGT CCA T	145	60
FOXJ1	CCT GGC AGA ATT CAA TCC G	GCG TAC TGG GGG TCA AT	115	60
FOXM1	TGG AGC AGC GAC AGG TTA AG	GGC GGA TGG AGT TCT TCC AG	225	60
FZD7	GCG CTC ATG AAC AAG TTC GG	TAG GGC GCG GTA GGG TAG	155	60
MCIDAS	GAC GCG CTT GTT GAG AAT AA	CAC GTT CCG CTC CTT GAG	84	60
MMP2	GAG CTC TAT GGG GCC TCT CC	CGT CAC AGT CCG CCA AAT GA	168	60
MMP7	AAG TGG TCA CCT ACA GGA TCG	TGG CCC ATC AAA TGG GTA GG	197	60
MYB	TAC TGC CTG GAC GAA CTG ATA A	CTG GCT GGC TGG CTT TTG AA	111	60
P63	GGA ACA GCC ATG CCC AGT AT	CAG GAC TTG CCC ATC TCT GG	200	60

PIGR	CTC TCT GGA GGA CCA CCG T	CAG CCG TGA CAT TCC CTG	78	60
SOX4	GCA CTA GGA CGT CTG CCT TT	ACA CGG CAT ATT GCA CAG GA	92	60
SPDEF	TGA CCT TGG AGG AGC ACT CG	CAT GGG ATC TGC GGT GAT GTT	110	60
TCF7L2	TAA CAA AGT GCC AGT GGT GCA G	ACG GGG ATA TAT CTG GAG GGT G	170	60
TJP1	GTG GTT CTT CGA GAA GCT GGA	TGC AGG CGA ATA ATG CCA GA	170	60

Table 12 | List of the primers (validation and WNT modulation RT-qPCR).
AS, amplicon size (base pairs); Fw, forward; HT, hybridization temperature (°C); Rv, reverse.

3.5. Western blot assays

HBEC lysates were analysed by Western blot as previously described (44), except for band revelation (see below). Cells were lyzed with 150µl of Laemmli's sample buffer containing 0.7M 2-mercaptoethanol (Sigma-Aldrich) and lysates were stored at -20°C. After thawing, samples were heated at 100°C for 5 minutes, loaded in a SDS-PAGE gel before migration at 100V for 15 minutes and then at 180V for 50 minutes. Cell proteins were transferred onto a nitrocellulose membrane (Thermo Fisher Scientific) at 0.3A for 2 hours 10 minutes at RT. The membranes were blocked with 5% w/v BSA (Sigma-Aldrich) in TBS with 0.1% Tween 20 (Sigma-Aldrich) for 1.5 hour at RT, then washed and incubated overnight at 4°C with a primary antibody according to the target protein (see Table 13 listing used primary and secondary antibodies). Membranes were then incubated for 1 hour at RT with horseradish peroxidase (HRP)-conjugated secondary anti-rabbit (Cell Signalling, Danvers, MA) or anti-mouse (Sigma) immunoglobulin G (IgG). Immunoreactive bands were revealed by chemiluminescence (GE Healthcare, Pittsburgh, PA), detected by Chemidoc XRS apparatus (Bio-Rad) and quantified using the Quantity One software (Bio-Rad).

Target	Antibody species	Brand and reference
Primary antibodies		
Unphosphorylated β-catenin	Rabbit polyclonal	Cell Signalling 4270S
Total β-catenin	Mouse monoclonal	Millipore 05-613
FOXJ1	Rabbit polyclonal	Sigma HPA005714
MUC5AC	Mouse monoclonal	Acris AM50143PU-N
pIgR	Rabbit polyclonal	Homemade antibody
Occludin	Rabbit polyclonal	Merck-Millipore ABT146
β-tubulin	Mouse monoclonal	Sigma T7941
Mouse IgG_1 Isotype	Mouse monoclonal	eBiosciences 14-4714-82
Rabbit IgG Isotype	Rabbit polyclonal	Homemade antibody
E-cadherin	Mouse monoclonal	Dako M3612
Vimentin	Mouse monoclonal	Dako M0725
α-SMA	Mouse monoclonal	Santa Cruz sc-53142
GAPDH	Rabbit polyclonal	Sigma G9545
Secondary antibodies		
SuperBoost™ Goat anti-Mouse Poly HRP	Goat polyclonal antibody	ThermoFisher Scientific B40961
SuperBoost™ Goat anti-Rabbit Poly HRP	Goat polyclonal antibody	ThermoFisher Scientific B40962
Anti-Rabbit HRP-conjugated	Goat polyclonal antibody	Cell signalling 7074S
Anti-mouse HRP-conjugated	Sheep polyclonal antibody	Sigma A6782

Table 13 | List of used antibodies
List of the antibodies that were used for Western-blot, immunohistochemistry, and TSA immunofluorescence staining.

3.6.Immunohistochemistry, image acquisition and analysis

Samples were processed as previously described (45). Lung samples were fixed in 4% formaldehyde and embedded in paraffin wax. Sections were deparaffinised in toluene and rehydrated through a graded series from methanol to water, then underwent antigen retrieval treatment using cooker pressure treatment at 15 pound-force per square inch (PSI) for 5 minutes. Endogenous peroxidase, biotin and streptavidin sites were inactivated by hydrogen peroxide and Bloxall (Vector Laboratories Inc., Burlingame, CA). Nonspecific protein binding sites were blocked with goat serum (Abcam Inc., Cambridge, MA) for 1 h. Primary antibodies were incubated overnight at 4°C. Mouse IgG_1 or rabbit IgG isotype were used as negative controls, according to the primary antibody species and to their concentration. After washes with TBS 0.1% Tween 20, sections were incubated with goat anti-rabbit or anti-mouse polyHRP-conjugated IgG. Table 13 recapitulates the primary and secondary antibodies that were used. Revelation was performed by using 3,3'-Diaminobenzidine (DAB) (Sigma-Aldrich). Sections were counterstained with Hematoxylin (Sigma-Aldrich) and coverslipped. Images were acquired with Leica SCN400 slide scanner (Leica Biosystems, Newcastle, United Kingdom).

After manual delineation of the AE (10 fields per slide, 20x magnification), quantification was selectively performed on these zones with Leica software (Leica Biosystems). "% of positive area" states for the percentage of the epithelium surface displaying a stronger staining than the determined threshold. "Staining concentration" is defined as the measure of the concentration of the stain within the delineated tissue area. The staining concentration is calculated using the following formula:

$$Concentration = \frac{\sum_{i=0}^{i=31}[h(i)*absorbance\ (i)]}{TotalTissuePixels} * 10000,$$

with $Absorbance = -\ln\frac{(\mathrm{i}*8+4)}{\mathrm{TissueThreshold}}$

where i is an intensity bin number from 0 to 31; h(i) is the number of positive pixels with intensity i, absorbance(i) is the absorbance at intensity i; TotalTissuePixels is the total number of tissue pixels in the delineated analysis area; TissueThreshold is the input tissue threshold intensity.

3.7.Immunofluorescence staining using tyramide signal amplification

Five micron-sections of lung tissue or reconstituted ALI epithelium, fixed in 4% formaldehyde and paraffin-embedded, were deparaffinised in toluene and rehydrated through a graded series from ethanol to water. Antigen retrieval was performed in citrate buffer (pH 6**.**0 containing 0**.**1% of triton) using a pressure cooker at 15 PSI for 5 minutes. Sections were blocked for non-specific antigen binding by incubation in Bloxall (Vector Laboratories Inc.) for 15 min and then in 0**.**3% hydrogen peroxide with 5% goat serum (Bio-Rad) for 30 min. Staining first included a 30 min protein blocking with 5% goat serum, then the primary antibodies diluted in 5% normal goat serum solution were applied, then the appropriate SuperBoost™ goat anti-rabbit or anti-mouse, poly-HRP-conjugated secondary antibody (Thermo Fisher Scientific) was applied for 40 min. HRP-conjugated polymer mediated the focal covalent binding of a fluorophore using tyramide signal amplification. Table 13 recapitulates the antibodies and fluorophores that were used. Finally, sections were counterstained with Hoechst (Thermo Fisher Scientific) diluted at 10µg/ml in TBS-BSA 5% and mounted with Dako fluorescence mounting medium (Dako, Carpinteria, CA). For negative controls, we used rabbit or mouse isotype controls at the same concentration as the corresponding primary antibodies (diluted in 5% normal goat serum).

3.8.Laser capture microdissection of the AE

Optimal Cutting Temperature (OCT)-embedded proximal bronchial tissue from non-smoker controls (n=5) and very severe COPD patients (n=6) was selected. The day before microdissection, 20 µm thick sections were obtained, in RNase-free conditions on a microtome-cryostat (cryochamber temperature, -20°C). Sections

were disposed on polyethylene naphtalate (PEN) Membrane Frame Slides (Thermo Fisher Scientific) and stored at -80°C. Less than an hour before microdissection, sections were dehydrated in graded ethanol solutions, stained with cresyl violet (Ambion) and re-dehydrated with xylene. Epithelial microdissection was performed using the Leica LMD 6000. RNA was extracted from microdissected samples as previously described (43). Detailed information on sample preparation, staining and microdissection is provided elsewhere (46).

3.9.Enzyme-linked immunosorbent assay (ELISA)

Secretory component (SC) concentration was determined in apical washes by sandwich ELISA, as previously described (45). Fibronectin basolateral release was assessed as previously described (40). Total TGF-β_1 concentration in basolateral supernatants was measured according to manufacturer's instructions (Bio-Techne, Minneapolis, MN). Briefly, 96-well plates were first coated overnight, at 4°C, with anti-fibronectin, -TGF-β_1, or -SC antibodies diluted in bicarbonate buffer (pH 9.6). Then, after blocking with phosphate-buffered saline BSA 1% for 90 min at 37°C, HBEC apical washes (for SC) or basolateral supernatants (for fibronectin and total TGF-β_1) were incubated for 60 min at 37°C, along with standard samples. Detection was performed with a first incubation with the corresponding biotinylated antibody (anti-fibronectin, -TGF-β_1, or -SC), followed by a second incubation with HRP-linked anti-mouse IgG, for 1 h each. Revelation was performed with 3,3',5,5'-tetramethylbenzidine and stopped with H2SO4 1.8 M.

3.10. Statistical analysis

Results were analysed with JMP® Pro, Version 14 (SAS Institute Inc., Cary, NC) and GraphPad Prism version 8.0.2 (GraphPad Software, La Jolla, CA), and were expressed as medians and interquartile ranges. p-values < 0.05 were considered statistically significant.

4. Results

4.1. WNT/β-catenin pathway is upregulated in ex vivo reconstituted COPD proximal AE

ALI-HBEC constitute a model in which epithelial cells recapitulate, *in vitro*, several features of the native epithelial phenotype as observed *in situ* (40, 47), therefore allowing to focus on epithelial pathobiology whilst avoiding mesenchymal (including leucocytes) contamination. This approach is particularly relevant to WNT signalling, as surrounding mesenchymal cells strongly express WNT and could) interfere with the resulting bulk data. Whether the canonical WNT pathway is activated in the bronchial epithelium in COPD was thus assessed by targeted RNA-sequencing (RNA-seq) of reconstituted AE (analysed at 2 weeks of ALI-culture, a time window of active differentiation) from 47 samples originating from 5 groups: non-smoker controls (n=9), smoker controls (n=10), mild COPD (n=9), moderate COPD (n=10), and (very) severe COPD (n=9). The characteristics of the study population are summarized in Table 7. A total of 115 genes was studied, including 98 selected WNT-related genes. As WNT signalling has been recently linked with EMT (28, 29, 48), possibly through TGF-β signalling (28), we also selected 8 EMT and TGF-β-related genes. Finally, 9 potential housekeeping genes were assessed. The expression of all 115 genes was measured by using a MiSeq™ Sequencing Platform, and each group was compared to non-smoker controls. A second analysis, comparing pooled COPD patients with non-smoker controls, was performed separately (see below).

The RNA-seq showed a significant dysregulation of 25 genes of the panel, involving several components of the WNT pathway. Increased expression of the WNT receptor *FZD7* was observed as well as of the β-catenin gene (*CTNNB1*), cytoplasmic and nuclear WNT pathway components (*CD44*, *CSNK2A1*, *CSNK2A2*, *FBXW11*, *TCF7L1*, *SOX4*), and WNT downstream targets including components of other pathways (*TGFB2, TGFBR1, TGFBR2, EGFR, IL6, VEGFA*), EMT-related proteins

(*VIM*, *FN1*), matrix metalloproteinases (*MMP2*, *MMP7*), and cell cycle-related proteins (*JUN*, *CCND1*). Conversely, WNT inhibitors *CTNNBIP1*, *RUVBL1* and *SOX2* were consistently downregulated. These changes prevailed in severe COPD, as shown in the heat map recapitulating the most affected genes (Figure 26 A) and in volcano plots allowing the comparison between each group with non-smoker controls (Figure 27). These pictures are consistent with canonical WNT activation in the COPD AE, in particular in patients with severe disease, as schematized in Figure 26 B. The most affected target genes (> 2-fold change) in RNA-seq, namely *MMP2*, *MMP7*, *FZD7*, *SOX4*, as well as *CTNNB1*, the cardinal factor of canonical WNT, were validated by RT-qPCR. As qPCR was expected to be less sensitive than RNA-seq, the initial 47 patients series used for RNA-seq was enriched with 21 additional samples (also from 2 weeks ALI cultures); clinical characteristics of the resulting 68 patients are shown in Table 10. Upregulation of *MMP2* and *MMP7* was confirmed in all COPD groups, while *FZD7* and *SOX4* expression was increased when pooling COPD patients (Figure 26 C). Although *CTNNB1* was not significantly upregulated, these data globally validated RNA-seq data and activation of WNT/β-catenin pathway in the COPD airway epithelium.

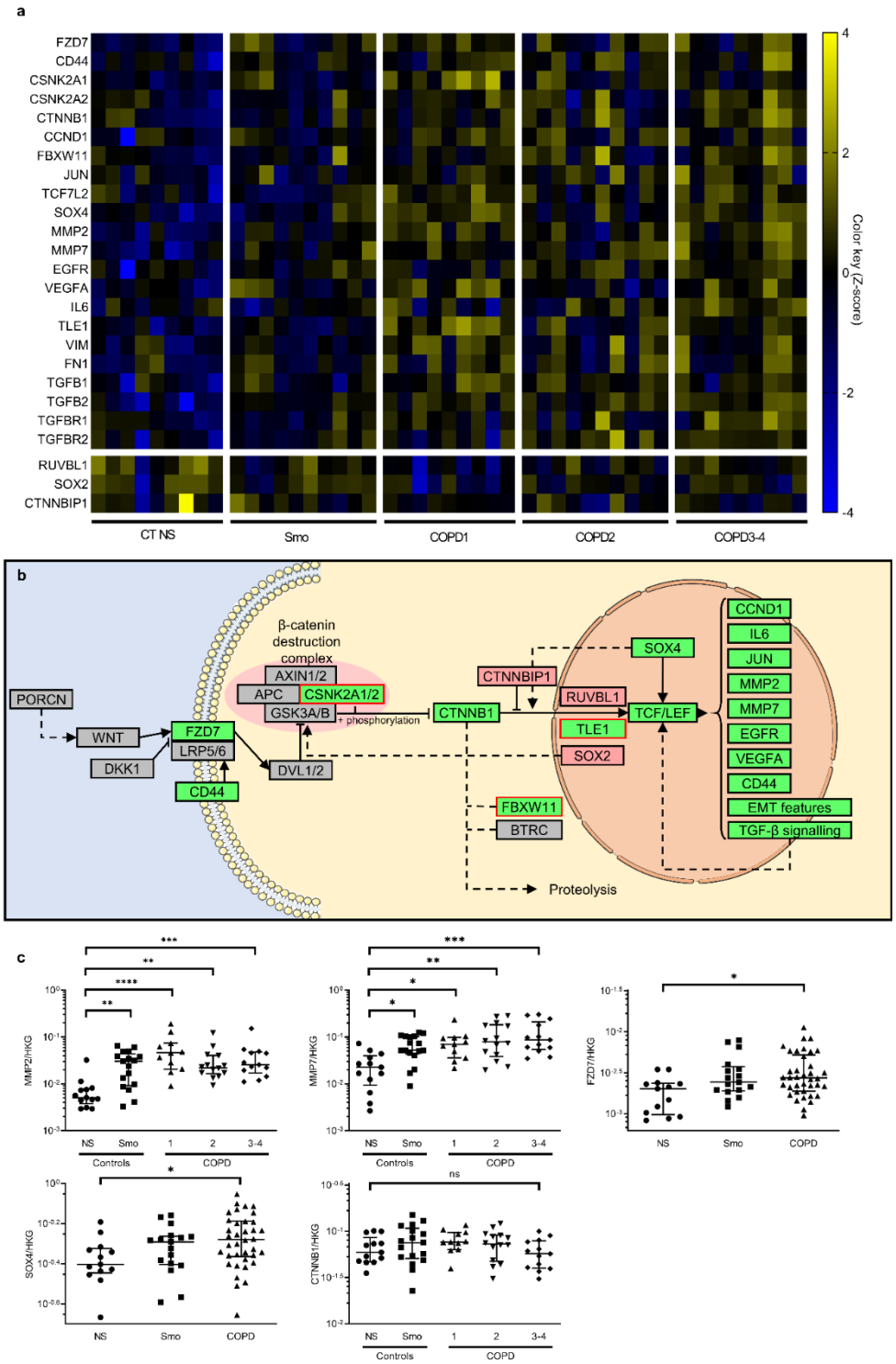
a
FZD7
CD44
CSNK2A1
CSNK2A2
CTNNB1
CCND1
FBXW11
JUN
TCF7L2
SOX4
MMP2
MMP7
EGFR
VEGFA
IL6
TLE1
VIM
FN1
TGFB1
TGFB2
TGFBR1
TGFBR2
RUVBL1
SOX2
CTNNBIP1
CT NS
Smo
COPD1
COPD2
COPD3-4
Color key (Z-score)
4
2
0
-2
-4
b
β-catenin destruction complex
AXIN1/2
APC
CSNK2A1/2
GSK3A/B
+ phosphorylation
PORCN
WNT
DKK1
FZD7
LRP5/6
CD44
DVL1/2
CTNNB1
CTNNBIP1
RUVBL1
TLE1
SOX2
SOX4
TCF/LEF
FBXW11
BTRC
Proteolysis
CCND1
IL6
JUN
MMP2
MMP7
EGFR
VEGFA
CD44
EMT features
TGF-β signalling
c
MMP2/HKG
MMP7/HKG
FZD7/HKG
SOX4/HKG
CTNNB1/HKG
NS
Smo
1
2
3-4
Controls
COPD
ns

Figure 26 | WNT/β-catenin upregulation in COPD AE

Canonical WNT pathway is upregulated in COPD proximal epithelium.

A. Heat map of RNA-seq expression Z-score, computed for all significantly modified genes (fold discovery range < 0.1) in smokers and COPD, as compared with non-smoker controls. These results depict a global WNT activation in COPD, that is more pronounced in very severe disease. The horizontal gap separates upregulated and downregulated targets.

B. Schematized overview of the canonical WNT pathway and its most important components. Green and red-filled rectangles respectively represent significantly up- and downregulated genes in COPD, according to RNA-seq data (dedicated statistical analysis, comparing pooled COPD versus non-smoker controls). Red-framed rectangles (*CSNKA1&2*, *FBXW11*, *TLE1*) point genes whose upregulation does support canonical WNT activation. Interestingly, two of these genes are involved in the phosphorylation and ubiquitination of the β-catenin, and their divergent regulation could be a direct consequence of the increased β-catenin cytosolic pool.

C. The most affected target genes (>2-fold change) in RNA-seq, namely *MMP2*, *MMP7*, *FZD7*, *SOX4*, as well as *CTNNB1*, the cardinal factor of canonical WNT, were validated by RT-qPCR in the initial 47 patients series enriched with 21 additional samples

*, **, ***, **** indicate p-values of less than 0.05, 0.01, 0.001, and 0.0001, respectively (analysed using the Kruskal-Wallis test followed by Dunn's post-hoc test). Bars indicate median ± interquartile range. COPD, chronic obstructive pulmonary disease; EMT, epithelial-to-mesenchymal transition; NS, non-smokers; ns, not significant; Smo, smokers.

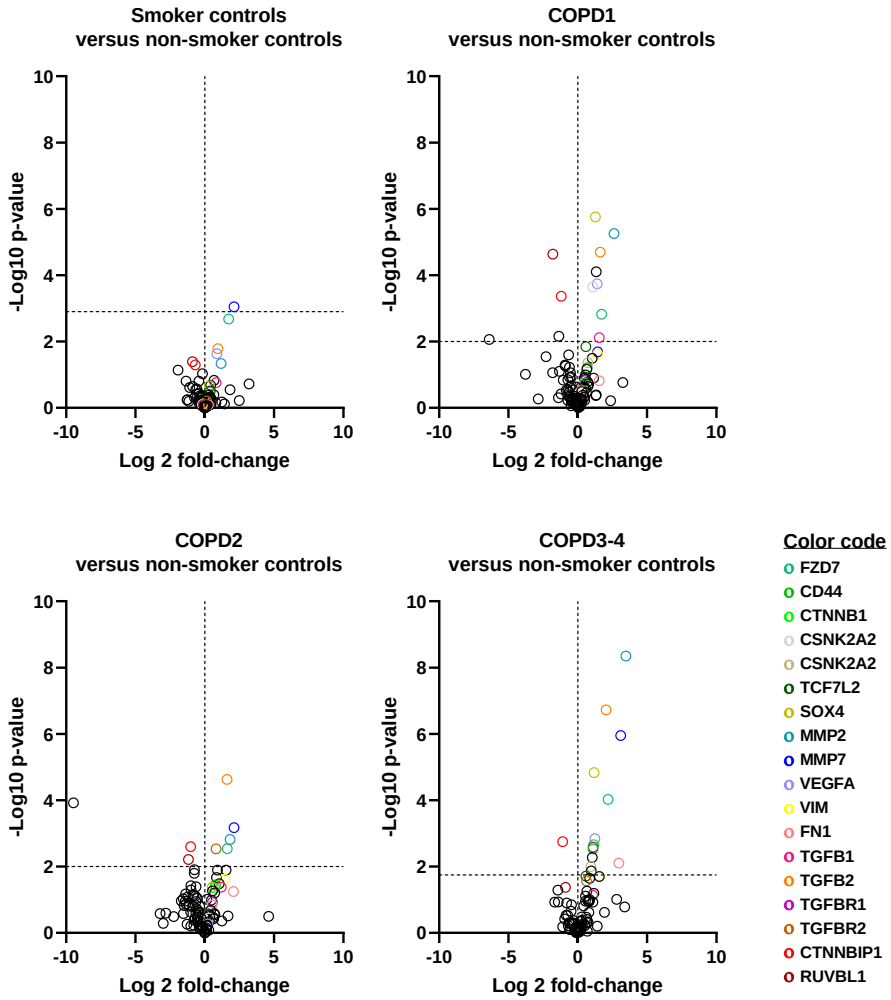

Figure 27 | RNA-seq volcano plots.
Representation of the progressive dysregulation of the canonical WNT pathway in COPD according to disease severity. Graphs plot fold-changes and p-values, obtained by comparing each group (smoker controls, COPD1, COPD2, COPD3-4) with non-smoker controls. Horizontal lines separate significantly dysregulated genes (FDR < 0.1) from the other (unaltered) genes.

4.2.β-catenin expression is increased in the COPD AE

The canonical WNT pathway depends on the nuclear accumulation of the transcriptional co-activator β-catenin. Therefore, for both total and unphosphorylated β-catenin, we stained bronchial sections from 56 patients divided into 5 groups (as for RNA-seq): non-smokers (n=7), smoker controls (n=14), mild COPD (n=12), moderate COPD (n=12), and (very) severe COPD (n=11). The population characteristics are detailed in Table 8.

Firstly, the expression of total β-catenin protein was increased in the proximal AE of patients with very severe COPD, compared with non-smokers and smoker controls, in terms of both percentage of stained area (Figure 28 A) and staining concentration (Figure 29 A). Accordingly, the increase in β-catenin expression correlated with airflow limitation depicted by decreased FEV_1 (Figure 28 B and 29 B). Secondly, the immunostaining for unphosphorylated β-catenin was increased in the large AE of patients with severe COPD compared with non-smokers and smoker controls, in terms of percentage of stained area (Figure 28 D) and staining concentration (Figure 29 C), and also correlated modestly with airflow limitation (Figure 28 E and 29 D). Representative pictures of staining for total and unphosphorylated β-catenin in non-smoker controls and very severe COPD epithelium are shown in Figures 28 C and 29 F.

As unphosphorylated β-catenin includes nuclear and junctional β-catenin, nuclear unphosphorylated β-catenin was quantified separately, demonstrating that severe COPD patients displayed more positive β-catenin nuclei than non-smokers and smoker controls (Figure 28 G), which significantly correlated with disease severity (Figure 28 H). Increased nuclear expression of β-catenin was also observed in the *ex-vivo* ALI-reconstituted epithelium from a series of 22 COPD patients, as compared to 19 controls (Figure 30), further demonstrating the replication of the original phenotype by this model.

In order to confirm WNT/β-catenin activation in the proximal AE in COPD, laser microdissection was used in lung tissue sections from non-smoker controls and

severe COPD patients (n=6 per group) to selectively assess key WNT-related mRNA abundance at the AE level, while avoiding the interference of WNT expression by surrounding, non-epithelial tissues (Figure 31 A). The clinical characteristics of this patient series are summarized in Table 9. *AXIN2*, *CTNNB1*, *SOX4*, *TCF7L2* and *FZD7* genes were upregulated in the COPD epithelium as compared with controls (Figure 31 B), while trends for upregulation were observed for *MMP2* and *MMP7*.

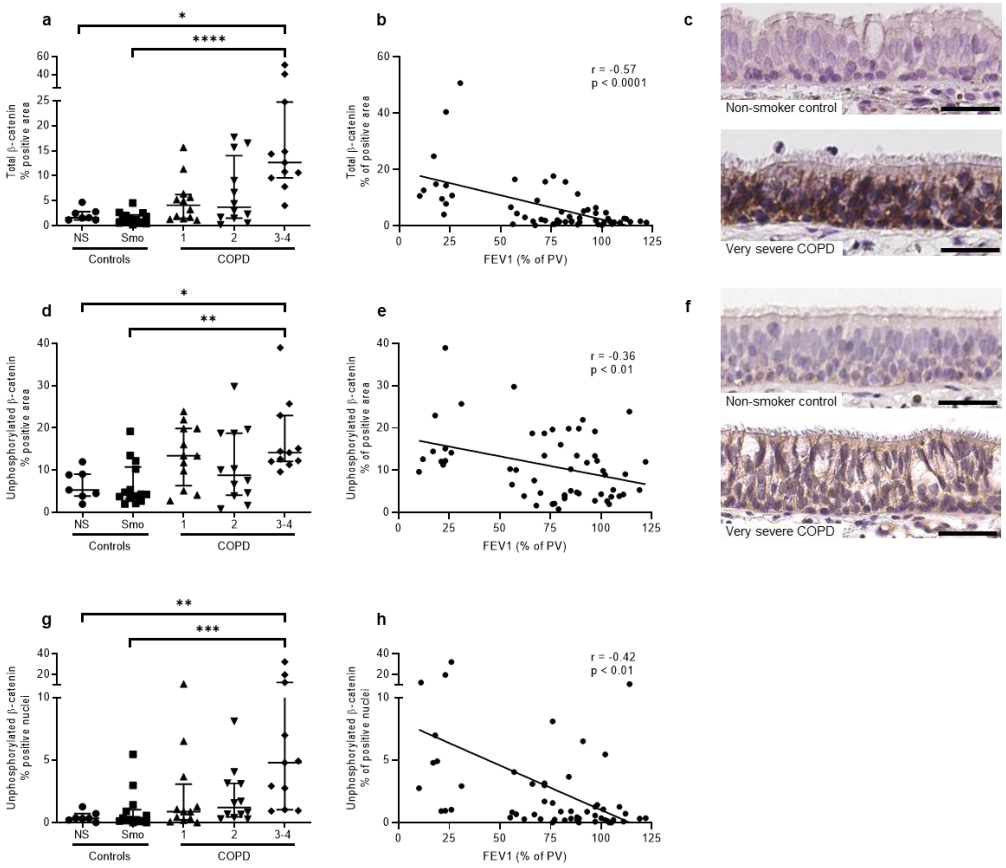

Figure 28 | β-catenin staining in the AE

Total, unphosphorylated and nuclear β-catenin staining is increased in the COPD bronchial epithelium.

A. Total β-catenin staining in the airway epithelium from non-smokers and smoker controls and COPD patients (GOLD classification from 1 to 4 according to the spirometric severity of the disease), in terms of percentage of positive area.

B. Correlation between total β-catenin in terms of percentage of positive area, and disease severity evaluated by the FEV1 (% of predicted values).

C. Representative picture of control and very severe COPD airway epithelium, stained for total β-catenin.

D. Unphosphorylated β-catenin staining was also increased in (very) severe COPD epithelium as compared with non-smokers and control smokers, in terms of percentage of positive area.

E. Correlation between unphosphorylated β-catenin in terms of percentage of positive area, and disease severity evaluated by the FEV1.
F. Representative picture of control and very severe COPD airway epithelium, stained for unphosphorylated β-catenin.
G-H. The percentage of positive unphosphorylated β-catenin nuclei was higher in the epithelium of (very) severe COPD patients as compared with non-smokers and control smokers (g), and correlated with COPD severity witnessed by the FEV1 (h). *, **, ***, **** indicate p-values of less than 0.05, 0.01, 0.001, and 0.0001, respectively (analysed using the Kruskal-Wallis test followed by Dunn's post-hoc test). Bars indicate median ± interquartile range. COPD, chronic obstructive pulmonary disease; FEV1, forced expired volume in 1 second; NS, non-smokers; Smo, smokers; PV, predicted values. Scale bars, 50μm.

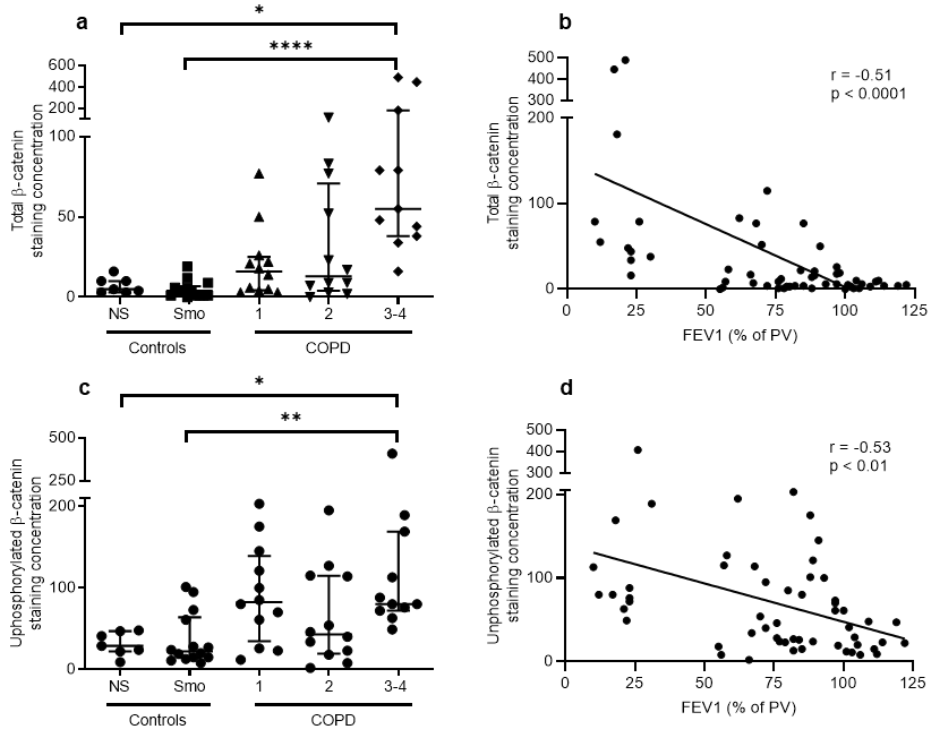

Figure 29 | β-catenin staining in the AE (complementary data)
Total and unphosphorylated β-catenin staining is increased in the COPD bronchial epithelium.
A. Total β-catenin staining in the airway epithelium from non-smokers and smoker controls and COPD patients (GOLD classification from 1 to 4 according to the spirometric severity of the disease), in terms of staining concentration.
B. Correlation between total β-catenin and disease severity evaluated by the FEV1 (% of predicted values).
C. Unphosphorylated β-catenin staining is increased in (very) severe COPD epithelium as compared with non-smokers and control smokers, in terms of staining concentration.
D. Correlation between unphosphorylated β-catenin and disease severity evaluated by the FEV_1.
*, **, ***, **** indicate p-values of less than 0.05, 0.01, 0.001, and 0.0001, respectively (analysed using the Kruskal-Wallis test followed by Dunn's post-hoc test). Bars indicate median ± interquartile range. COPD, chronic obstructive pulmonary disease; FEV1, forced expired volume in 1 second; NS, non-smokers; Smo, smokers; PV, predicted values.

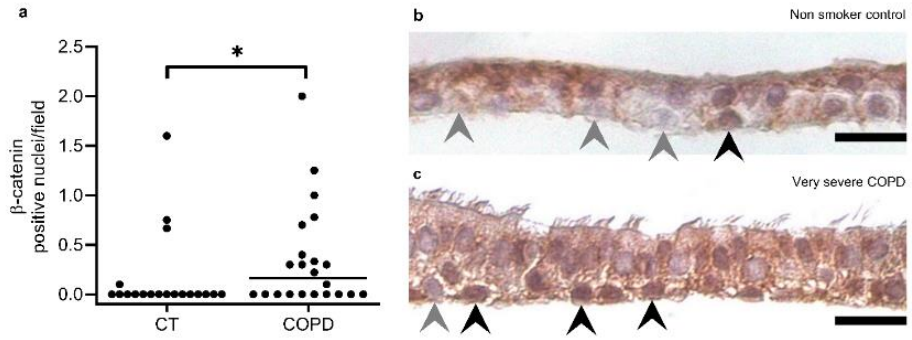

Figure 30 | Nuclear β-catenin staining in ALI-AE

Nuclear unphosphorylated β-catenin staining is increased in COPD ALI-cultured epithelium.

A. The number of positive β-catenin nuclei was increased in 2 weeks ALI cultures from COPD patients, compared with those from controls, recapitulating *in situ* findings.

B-C. Typical pictures of reconstituted epithelium from controls (B) and COPD patients (C), stained for unphosphorylated β-catenin. Grey and black arrowheads point representative negative and positive nuclei, respectively. Scale bar, 20µm. COPD, chronic obstructive pulmonary disease; CT, controls. Scale bars, 50µm

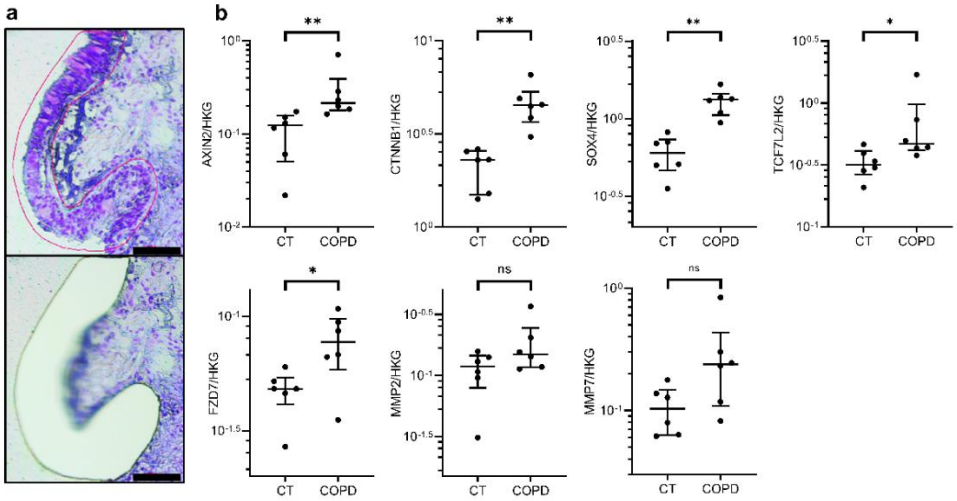

Figure 31 | Expression of WNT-related genes in laser-microdissected AE

Canonical WNT pathway is upregulated *in situ* in laser-microdissected COPD airway epithelium.

A. Illustrative pictures of the microdissection of the airway epithelium. The upper picture shows the manually delineated epithelium (red line), while the lower picture shows the slide after laser microdissection.

B. Expression of key genes of the WNT/β-catenin pathway (*AXIN2*, *CTNNB1*, *TCF7L2*, *SOX4*, *and FZD7*) was increased in laser-microdissected epithelium from very severe COPD patients as compared with that of non-smoker controls. Concordantly, upward trends were found for *MMP2* and *MMP7*.

* indicates p-values of less than 0.05 (analysed using the Mann-Whitney test). Bars indicate median ± interquartile range. COPD, chronic obstructive pulmonary disease; CT, controls; ns, not significant. Scale bar, 100µm.

4.3.β-catenin upregulation in COPD AE correlates with altered differentiation

We next explored whether the increased β-catenin expression observed *in situ*, in the COPD proximal AE, could be linked with differentiation abnormalities such as lineage changes (basal, ciliated and secretory/goblet cell numbers). Data from a previous study from our laboratory (6), where bronchial sections were stained for basal, ciliated and goblet cells markers (p63 – Forkhead Box J1 [FOXJ1] – and MUC5AC, respectively), were extracted for the same 56 patients of this study. In airway tissue from those patients, the COPD proximal AE displayed decreased numbers of ciliated cells and increased numbers of goblet cells, as compared with non-smokers and smoker controls (Figure 32A a and 32D). Both changes correlated modestly but significantly with total and unphosphorylated β-catenin staining (Figure 32 B-C and E-F), suggesting that WNT activation in COPD is linked with differentiation abnormalities. In contrast, no change in basal cell numbers was observed (Figure 32 G). Representative pictures of FOXJ1 and MUC5AC staining in non-smoker controls and very severe COPD AE are shown in Figure 32 H-I.

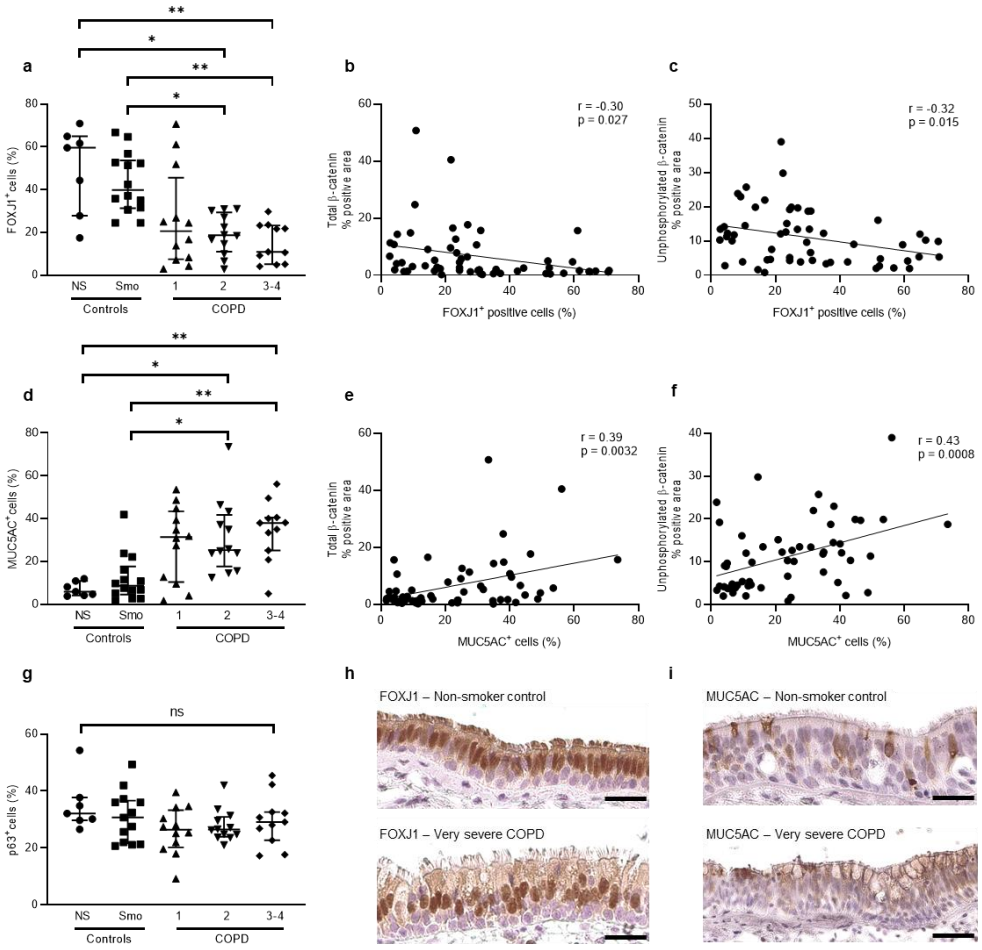

Figure 32 | COPD-related abnormalities in epithelial differentiation.
A. FOXJ1$^+$ cells percentage is decreased in the airway epithelium from COPD2 and COPD3-4 patients, as compared with non-smokers and smoker controls.
B-C. FOXJ1$^+$ cells percentage significantly correlates to both total (b) and unphosphorylated (c) β-catenin staining, in terms of percentage of positive area.
D. MUC5AC$^+$ cells percentage is increased in the airway epithelium from COPD2 and COPD3-4 patients, as compared with non-smokers and smoker controls.
E-F. MUC5AC$^+$ cells percentage significantly correlates to both total (E) and unphosphorylated (F) β-catenin staining, in terms of percentage of positive area.
G. Basal cell populations, assessed by p63$^+$ cells, did not vary in COPD as compared with (non-) smoker controls.
H-I. Representative pictures of FOXJ1 (g) and MUC5AC (h) staining in bronchial sections of non-smoker controls and very severe COPD patients.

*, ** indicate p-values of less than 0.05 and 0.01, respectively (analysed using the Kruskal-Wallis test followed by Dunn's post-hoc test). Bars indicate median ± interquartile range. COPD, chronic obstructive pulmonary disease; NS, non-smokers; Smo, smokers. Scale bars, 50µm

4.4. WNT/β-catenin activation contributes to epithelial pathology in COPD airways

Following the demonstration that WNT/β-catenin is activated in the COPD AE, both *in vitro* and *in situ*, it was next assessed whether the modulation of the WNT/β-catenin pathway during epithelial redifferentiation could influence the expression of COPD-related features such as altered polarization and barrier function, lineage specification, and EMT. To this aim, the ALI-reconstituted epithelium from 6 very severe COPD patients was treated at different time-periods of the redifferentiation (after ALI D1-5, during which modulation completely suppressed epithelial growth, *not shown*) with a specific canonical WNT activator (CHIR99021, 10µM) or inhibitor (XAV939, 10µM) as compared to vehicle control (DMSO). First, it was confirmed that CHIR99021 activates and XAV939 inhibits the canonical WNT pathway; CHIR99021 induced at each time-period a sharp increase in unphosphorylated β-catenin protein level (Figure 33 A-B) and in *AXIN2* mRNA abundance, a good reporter of canonical WNT activation (Figure 33 C), although no effect was observed on the expression of the β-catenin gene (*CTNNB1*, Figure 33 D). Conversely, XAV939 decreased the unphosphorylated β-catenin protein levels and AXIN2 mRNA abundance (Figure 33 A-Dd). CHIR-induced unphosphorylated β-catenin increase was associated with its translocation from the cell membrane to the nucleus (Figure 33 E).

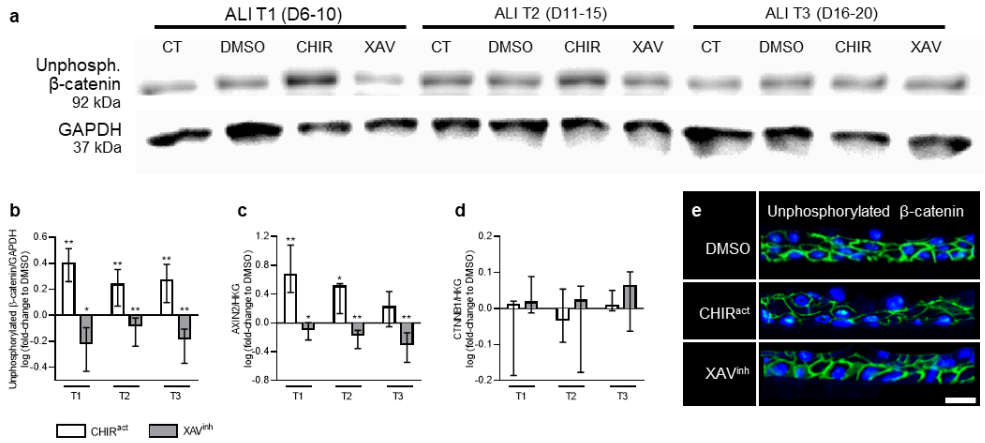

Figure 33 | *In vitro* WNT/β-catenin pathway modulation

Validation of canonical WNT pathway modulation by CHIR99021 and XAV939 on β-catenin protein and AXIN2 mRNA abundance.

A. Representative western blot for unphosphorylated β-catenin in control (CT), vehicle (DMSO), WNT activation (CHIR99021) and WNT inhibition (XAV939) conditions.

B. Unphosphorylated β-catenin protein expression was increased upon WNT activation (CHIR99021) and decreased upon WNT inhibition (XAV939).

C-D. Accordingly, the expression of *AXIN2*, a good marker of canonical WNT pathway activation, was increased by CHIR99021 and decreased by upon XAV939-induced WNT inhibition, while WNT modulation had no effect on the transcription of the β-catenin gene (CTNNB1).

E. Representative picture of ALI-reconstituted epithelium cultured under control condition (DMSO vehicle), WNT activation (CHIR99021) or WNT inhibition regimen (XAV939). WNT activation increased nuclear unphosphorylated β-catenin whilst decreasing its membrane localization, whereas WNT inhibition decreased nuclear unphosphorylated β-catenin and had no clear effect on membrane (adherens junction)-bound β-catenin.

*, ** indicate p-values of less than 0.05 and 0.01, respectively (analysed using the Mann-Whitney test). Columns in the graphs represent medians. ALI, air/liquid interface; ns, not significant; unphosph, unphosphorylated.

4.4.1. WNT activation alters the early differentiation programming of the AE

WNT activation (induced by CHIR99021) strongly suppressed *MYB* expression at all time-periods, a transcription factor involved in early epithelial differentiation. WNT inhibition (induced by XAV939) had no effects on *MYB* expression at T2, but also inhibited its transcription at T1 and T3, although to a lesser extent than WNT activation (Figure 34 A).

4.4.2. WNT modulation regulates AE specification and commitment

Firstly, goblet cell commitment was assessed by measuring the expression of the SAM Pointed Domain Containing ETS Transcription Factor (*SPDEF*). WNT activation completely suppressed *SPDEF* expression at all time-periods, while WNT inhibition resulted in a 1.5 to 2-fold increase of its transcription (Figure 34 B). Secondly, CHIR99021-induced WNT activation resulted in a marked decrease in Multiciliate Differentiation And DNA Synthesis Associated Cell Cycle Protein (*MCIDAS*) expression (Figure 34 C), a transcription regulator involved in the specification of ciliated cells, and almost completely suppressed the transcription of *FOXJ1*, a transcription factor ensuring the commitment towards ciliated cells (Figure 34 D). XAV939-induced WNT inhibition also downregulated *MCIDAS* expression, although to a lesser extent, but upregulated *FOXJ1* at T2 and T3 (Figure 34 C-D). These results indicate that WNT activation inhibits the muco-ciliary programming, and highlight dual effects of WNT inhibition on specification or commitment of ciliated cells, while WNT inhibition favours commitment towards ciliated and goblet cells. In addition, WNT activation also decreased *FOXM1* expression and thus presumably the differentiation towards club cells, which was not significantly affected by WNT inhibition (Figure 34 E). Figure 34 F illustrates CHIR-induced decrease and XAV-induced increase in terminal differentiation proteins of goblet and ciliated cells, respectively MUC5AC and β-tubulin.

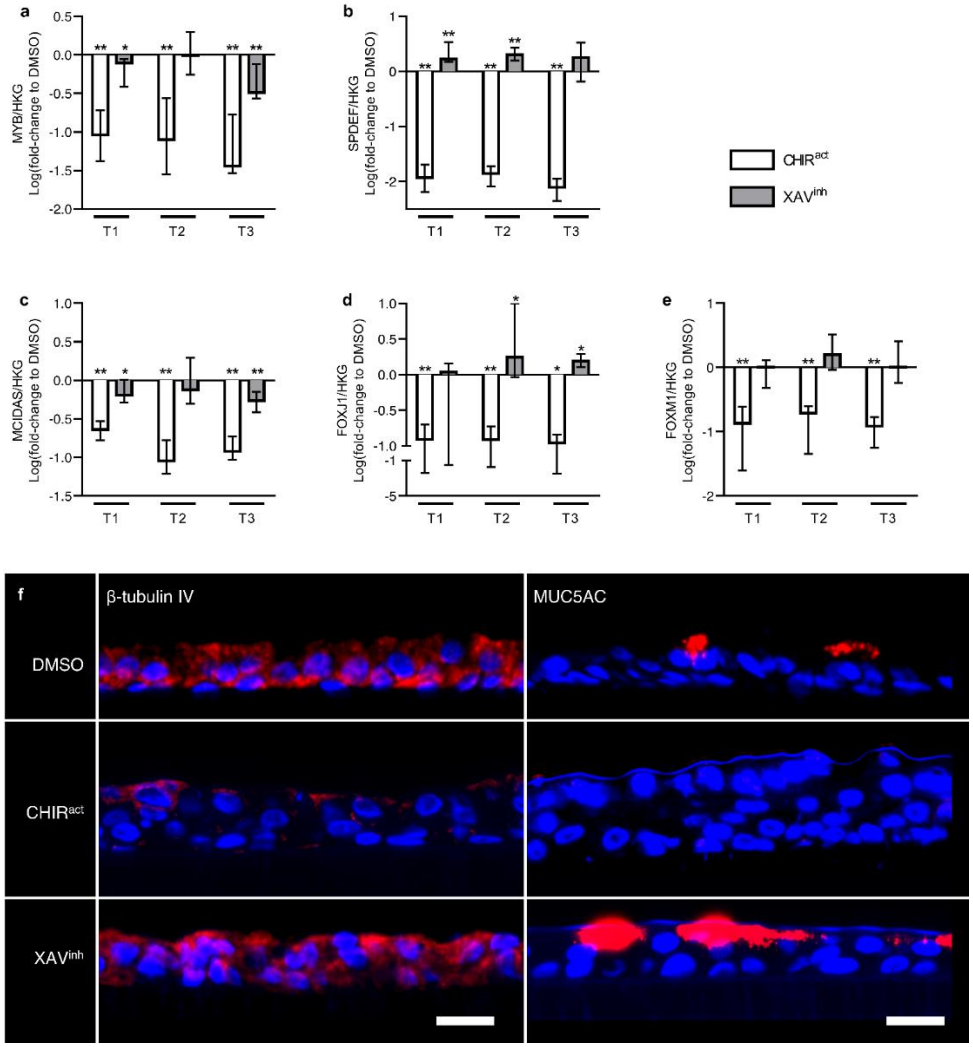

Figure 34 | WNT modulation regulates AE cells differentiation

A. CHIR99021-induced WNT activation strongly downregulated the expression of *MYB*, an early epithelial differentiation marker, at all time periods. XAV939-induced WNT inhibition also downregulated it at T1 and T3, although in a lesser extent.

B. WNT activation inhibited the commitment towards goblet cells, as *SPDEF* expression was completely suppressed by CHIR99021. Conversely, WNT inhibition increased *SPDEF* expression.

C-D. WNT activation repressed the specification and commitment towards ciliated cells, as CHIR99021 decreased the expression of *MCIDAS* (c) and *FOXJ1* (d). WNT inhibition decreased *MCIDAS* (c) expression but increased *FOXJ1* (d), demonstrating an opposite effect on specification/commitment towards ciliated cells.

E. WNT activation by CHIR99021 decreased the expression of *FOXM1*, a transcription factor involved in the commitment towards club cells, while WNT inhibition by XAV939 had no significant effect.
F. Representative pictures of ALI-reconstituted epithelia, cultured under vehicle condition (DMSO), WNT activation (CHIR99021) or WNT inhibition regimen (XAV939). The epithelium were stained for ciliated cells (β-tubulin IV, left panel) and goblet cells (MUC5AC, right panel), showing a sharp decrease of both cell types upon WNT activation. Conversely, WNT inhibition increased MUC5AC expression and tended to increase β-tubulin IV expression.
*, ** indicate p-values of less than 0.05 and 0.01, respectively (analysed using the Mann-Whitney test). Columns and bars in the graphs represent medians ± interquartile range. Scale bars, 20µm. $CHIR^{act}$, CHIR99021-induced WNT activation condition; HKG, housekeeping genes; XAV^{inh}, XAV939-induced inhibition condition.

4.4.3. WNT/β-catenin pathway regulates epithelial polarity and barrier function

WNT activation also alters AE polarization and barrier function. Thus, WNT activation strongly decreases the expression of polymeric immunoglobulin receptor (PIGR, Figure 35 A), a transmembrane protein involved in the basal-to-apical transcytosis of polymeric immunoglobulins at mucosal surfaces and a marker of epithelial polarity. This transcriptional defect was corroborated by a decreased release of the secretory component (SC) in apical washes (Figure 35 B), SC release resulting from the cleavage of the pIgR extracellular part following its baso-apical transcytosis. In addition, CHIR99021 regimen also decreased the expression of tight junction protein 1 (*TJP1*)/Zonula Occludens (ZO)-1 and *CDH1*/E-cadherin 1 (Figure 35 C-F), as key components of epithelial tight and adherens junctions, respectively. Conversely, XAV939-induced WNT inhibition increased *PIGR* (Figure 35 A), *TJP1* (Figure 35C), and E-cadherin expression (Figure 35 D-F), as well as SC release (Figure 35 B). These results were confirmed by immunofluorescence staining for PIGR and occludin, which were respectively decreased or increased upon WNT activation or inhibition (Figure 35 G).

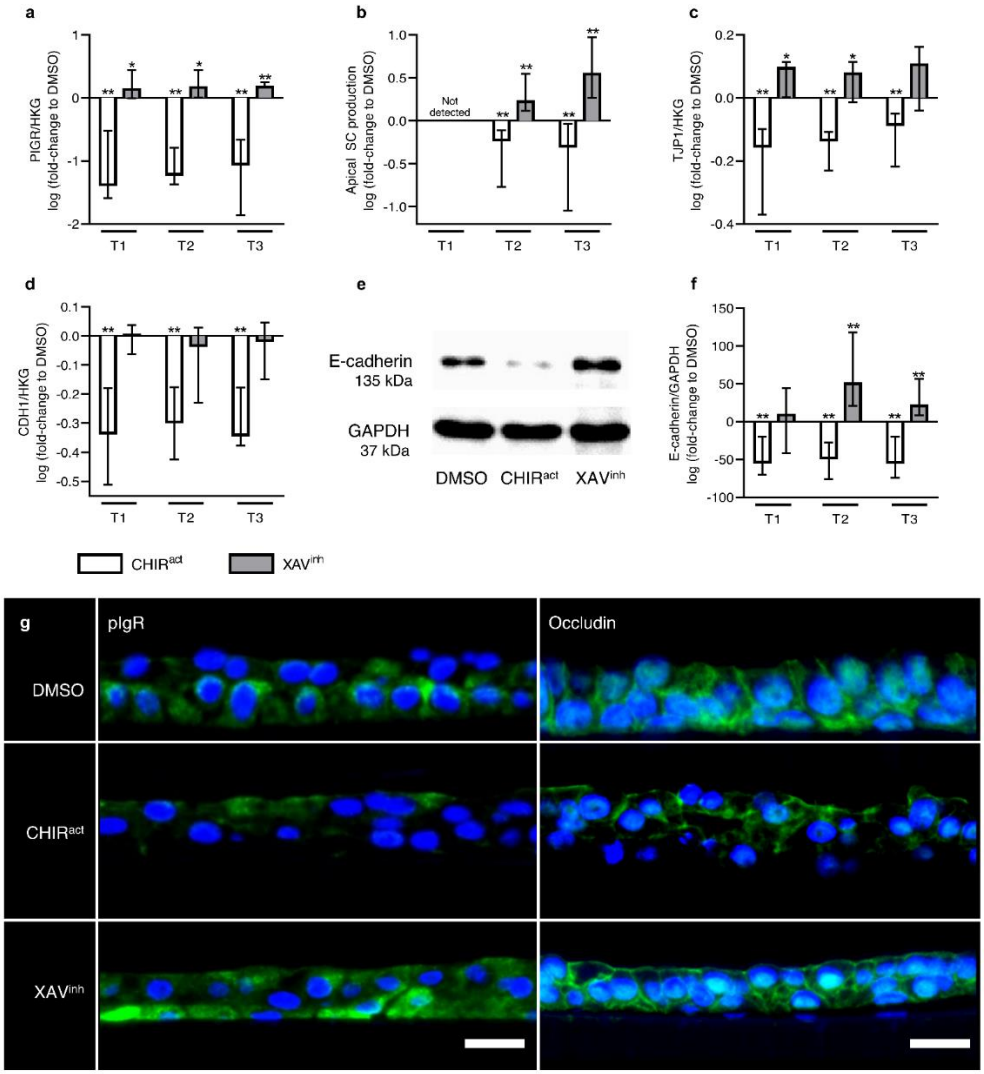

Figure 35 | WNT/β-catenin modulation effects on AE polarity.
Canonical WNT pathway regulates AE polarity and barrier function.
A-B. WNT activation impaired *PIGR* mRNA abundance at all time periods (a) and decreased SC release (b), while WNT inhibition increased *PIGR* expression (a) and SC release (b), used as indices of basal-to-apical polarity as this system allows the transcytosis of polymeric IgA and IgM across the epithelial layer.
C-F. CHIR99021-induced WNT activation also decreased the expression of key components of tight and adherens junctions, namely *TJP1* (c) and *CDH1* (d), and resulted in diminished E-cadherin protein levels (e-f), while WNT inhibition

increased *TJP1* (c) and E-cadherin (e-f), underscoring the importance of WNT in the epithelial barrier function and tightness.
G. Representative pictures of ALI-reconstituted epithelium, cultured under vehicle condition (DMSO), WNT activation (CHIR99021) or WNT inhibition regimen (XAV939), and immunostained for markers of polarity (pIgR, left panel) and tightness/barrier function (occludin, right panel). WNT activation decreased pIgR and occludin, while WNT inhibition increased pIgR. Occludin staining shows both junctional occludin (cell membrane) and off-target nuclear occludin 1B, an alternatively spliced transcript.
*, ** indicate p-values of less than 0.05 and 0.01, respectively (analysed using the Mann-Whitney test). Columns and bars in the graphs represent medians ± interquartile range. Scale bars, 20µm. $CHIR^{act}$, CHIR99021-induced WNT activation condition; HKG, housekeeping genes; XAV^{inh}, XAV939-induced inhibition condition.

4.4.4. WNT modulation regulates the EMT programming

The modulation of the WNT/β-catenin pathway also regulated EMT programming, indicated by vimentin (gene and protein) expression (Figure 36 A-B and 36 D) and fibronectin release (Figure 36 C), which were both increased following WNT activation, while WNT inhibition strongly reduced them (Figure 36 A-D). The awakening of the EMT program in ALI-HBEC probably resulted from the activation of the TGF-β pathway, as phospho-SMAD2 levels paralleled vimentin expression (Figure 36 D-E), and TGF-β_1 basolateral release (but not mRNA transcription) were increased by CHIR99021 (Figure 36 F-G). In contrast, WNT inhibition consistently decreased SMAD2 phosphorylation at T3 (Figure 36 D-E). These results demonstrate an upregulated WNT/TGF-β/EMT axis in the COPD AE and are consistent with aforementioned RNA-seq findings where COPD patients displayed signals of activation of TGF-β signalling pathway and upregulated EMT-related genes (VIM and FN1) (Figure 26).

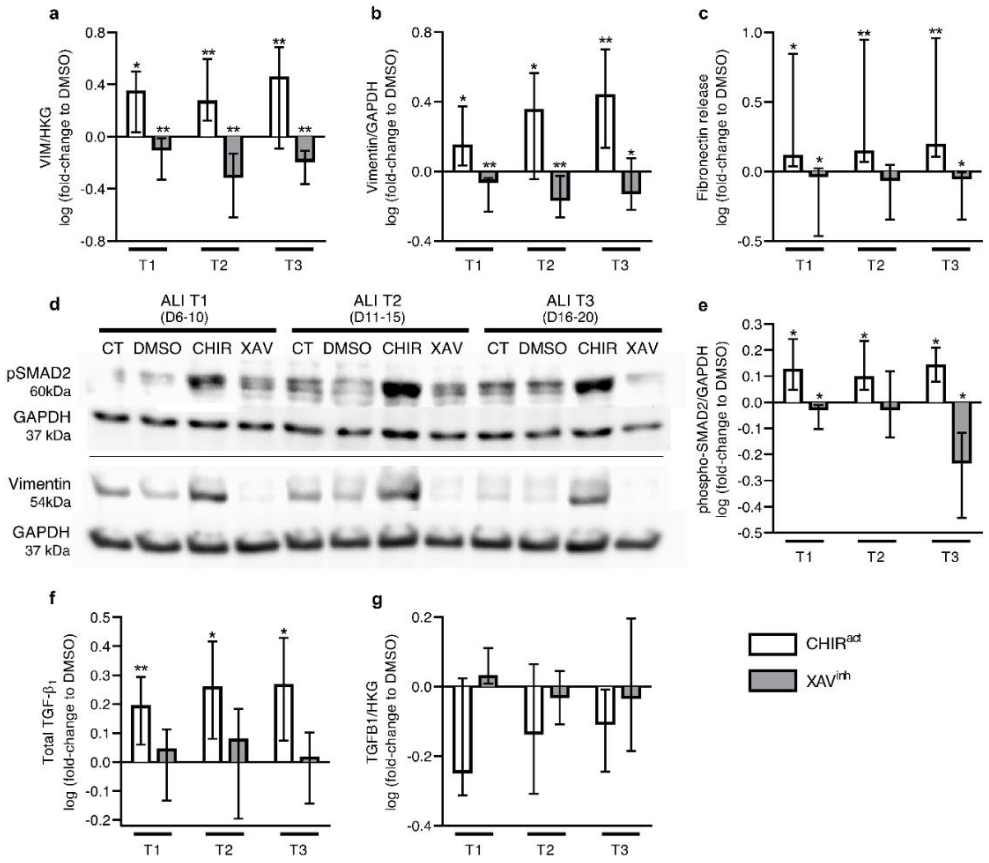

Figure 36 | Canonical WNT activation induces EMT programming.

A-C. WNT activation induced EMT at all time periods, witnessed by the increase in the transcription (A) and protein expression (B) of vimentin, and in the release of fibronectin (C), both being markers of EMT. WNT inhibition, conversely, slightly but significantly decreased them.

D-E. Representative blots for phospho (p)-SMAD2, vimentin, and housekeeping GAPDH proteins (D), and quantitative analysis for phospho (p)-SMAD2, upon control (CT), vehicle (DMSO), WNT activation (CHIR99021), and WNT inhibition (XAV939) conditions (E). In parallel with increased EMT markers, CHIR99021-induced WNT activation increased the phosphorylation of SMAD2, a pivotal component of the canonical TGF-β pathway. In contrast, XAV939 decreased its expression at T1 and T3.

F-G. Concordantly with increased pSMAD2 expression upon CHIR99021-induced WNT activation, TGF-β_1 release in basolateral supernatants was increased in WNT activation conditions (F), whilst no difference was seen upon WNT inhibition. No difference was observed at the transcriptional level (G).

*, ** indicate p-values of less than 0.05 and 0.01, respectively (analysed using the Mann-Whitney test). Columns in graphs represent medians. ALI, air/liquid interface; $CHIR^{act}$, CHIR99021-induced WNT activation condition; CT, control; HKG, housekeeping genes; XAV^{inh}, XAV939-induced inhibition condition.

5. Discussion and conclusions

This study demonstrates unequivocally, by using cutting-edge RNA-sequencing and laser microdissection of the AE, that the WNT/β-catenin pathway is activated in the proximal bronchial epithelium from patients with COPD. It also highlights that this pathway tightly controls epithelial homeostasis in the adult lung, canonical WNT activation recapitulating the salient COPD features in the airways such as epithelial de-differentiation, loss of polarity, barrier dysfunction and EMT, while its inhibition reversed the abnormal phenotype of the AE derived from severe COPD patients.

The WNT pathways are ubiquitously involved in fetal development and homeostasis of several tissues (49). In the lung, the importance of WNT signalling in branching morphogenesis and lung growth is well established and its role in AE homeostasis recently drew scientists' attention (31, 50, 51). Previous studies focusing on canonical WNT signalling in the bronchial epithelium highlighted the role of WNT in epithelial differentiation (31) and its regulation by cigarette smoke, as well as its interaction with epithelial inflammation (29, 33). To our knowledge, however, only two recent studies investigated the WNT/β-catenin signalling pathway in COPD at the bronchial tissue level. Wang and colleagues, performing microarrays on small airway samples, found a down-regulation of the canonical WNT pathway in both smokers and COPD (32), while Guo and colleagues described lower β-catenin levels in the epithelium of smokers and COPD patients (33), albeit not specifying whether small and/or large airways were analysed.

In the present study, we specifically studied the proximal AE of healthy non-smokers, healthy smokers and COPD patients, and demonstrated in a targeted RNA-seq that the WNT/β-catenin pathway is activated at this level in COPD. This

observation in the *in vitro*, differentiating epithelium was confirmed *in situ*, in the steady-state epithelium, with upregulated expression of β-catenin and transcription of central WNT elements in surgical samples and microdissected AE from COPD, respectively. ALI-reconstituted and laser-microdissected epithelium allowed to avoid mesenchymal cell contamination, hence to study WNT canonical pathway at the epithelial level only. Interestingly, the increase in epithelial (unphosphorylated) β-catenin by immunochemistry correlated with the COPD severity witnessed by the FEV1, consistently with the RNA-seq data where the sharpest WNT upregulation was found in severe disease. In contrast with previous *in vitro* studies (29, 33) where cigarette smoke exposure directly regulated the WNT pathway, no striking changes were observed in smokers without COPD, e.g. no increase in β-catenin (or when comparing former versus unphosphorylated smokers, not shown), except for *MMP2/7* expression which could relate to other upstream pathways. This discrepancy could relate to differences in sampling, experimental design and/or readouts for analysis. Thus, these studies either focus on small airway epithelium, where signalling pathways might be differently regulated by cigarette smoke, or used 16HBE cells in submerged cultures. Interestingly, it has been suggested that proximal-to-distal patterning in the airways results in different architecture, cell composition, and signalling (52). In contrast to our findings in the proximal AE, downregulation of the canonical WNT pathway has been documented in COPD at the alveolar level, underlying emphysema (21-23). The dual dysregulation of WNT in proximal versus distal/alveolar epithelium is to some extent reminiscent of findings regarding TGF-β which are underlying contrasting features of matrix deposition in the airways (airway fibrosis) or matrix disruption in alveoli (emphysema) (53).

AE differentiation, homeostasis, and repair are complex processes requiring close interactions between developmental pathways such as WNT (31, 49), Notch (54-57), and SHH (58). It was recently shown that increased β-catenin signalling decreased the number of fully differentiated ciliated cells, while its inhibition increased

specification towards ciliated cells (31, 50). Corroborating these findings, we observed that the COPD-related decrease in ciliated cell numbers and increase in goblet cells correlated with increased levels of total and unphosphorylated β-catenin, which display a multicellular pattern in the airway epithelium. However, the differences in WNT signalling highlighted in the RNA-seq data were observed in the differentiating epithelium (active stage of differentiation at 14 days of ALI culture). Thus, whether increased WNT activity relates to changes in (basal, goblet/ciliated) cell numbers (and inherent differences in WNT activity) or to increased signalling activation *per se* remains uncertain. Taking into account previous studies showing that WNT activity is similar between goblet and ciliated cells (59) and that this study (Figure 32) as well as our previous study (6) showed unchanged $p63^{+}$ basal cell numbers (in COPD ALI epithelium and lung tissue), it is likely that WNT upregulation in the airways from COPD patients takes place in basal cells. This is in line with a recent study showing that WNT activation in the airway epithelium at the steady state seems restricted to basal cells (59).

In our study, the specific activation of the pathway (by CHIR99021) during the redifferentiation of the adult human AE completely suppressed the differentiation towards ciliated cells evidenced by the downregulation of *MCIDAS* and *FOXJ1*. In contrast, we also show that extrinsic WNT activation suppresses goblet cell differentiation, in line with the observation that β-catenin destabilization in normal epithelium prevented goblet cell specification during early differentiation period (31). Conversely, constitutive β-catenin activation in transgenic mice induced goblet cell hyperplasia (60), suggesting either differences due to the model (e.g., murine *vs* human epithelium, constitutive *vs* induced activation) or that WNT could also have dual effects on goblet cell differentiation according to the context. Finally, our data reveal that *FOXM1* is downregulated following WNT activation, presumably affecting differentiation into club cells, and suggesting that in the airways, WNT/β-catenin signalling globally regulates epithelial lineage specification to both ciliary and secretory cell types.

Epithelial barrier dysfunction in the airways may lead to the disruption of apical junctional complexes and the release of unphosphorylated β-catenin from adherens junctions towards the cytosol (61), resulting in WNT/β-catenin activation. It remained however unclear whether, in turn, WNT activation could promote epithelial barrier dysfunction. We show here that epithelial polarity and barrier function were directly affected upon WNT modulation, WNT activation inducing disruption of epithelial polarity, with decreased expression of PIGR/SC and of junctional proteins (*CDH1* and *TJP1*/ZO-1), whereas WNT inhibition improved both polarity and barrier function in COPD-derived ALI-HBEC. This study also shows that WNT/β-catenin activation increases the canonical TGF-β signalling – witnessed by increased TGF-β_1 production and SMAD2 phosphorylation – and induces EMT, whereas its inhibition decreased those signals. As EMT encompasses the loss of junctional proteins (occludin, E-cadherin) and impaired epithelial polarity, those features probably result from activation of an early EMT programming. Alternatively, they could less likely represent separate events of epithelial dysregulation that occur concomitantly. These observations are consistent with previous studies depicting a tight and complex crosstalk between WNT/β-catenin and TGF-β signalling pathways, which is required to promote EMT in cancer and tissue fibrosis (62). Taken together, these data suggest that dedifferentiation and EMT in the COPD proximal AE also relate, at least partly, to canonical WNT activation and cooperation with TGF-β signalling.

Our study has limitations. First, one cannot exclude an effect of treatments, particularly inhaled corticosteroids in severe patients, on the findings. Mometasone furoate restored impaired WNT/β-catenin activity in a murine model of spinal cord injury (63), and dexamethasone increased canonical WNT components expression in 16HBE cells as well as in the (small) airway epithelium in mice (64). However, *in vitro* studies in primary human bronchial and nasal epithelial cells in ALI culture showed dexamethasone-induced (0.1µM) upregulation of E-cadherin and junctional (but not nuclear) β-catenin (65, 66), rather suggestive of WNT/β-catenin inhibition

by corticosteroids. In addition, correlation with exacerbation or chronic bronchitis phenotypes could not be assessed in this cohort of patients. Second, genetic approaches to activate or silence WNT signalling have not been used in this study to validate data obtained by using chemical inhibitors, a limitation mostly due to the difficulty of obtaining stable transfectants from primary bronchial cells (12). Third, in addition to showing activation of the WNT/β-catenin *in situ* and *in vitro*, we explored its role in promoting the COPD epithelial phenotype *in vitro*, in conditions that are unlikely to recapitulate the chronic nature of the disease. Similarly, the potential contribution of squamous metaplasia or epithelial dysplasia was not evaluated. Finally, a conditional (or inducible) and targeted genetic model with gain- or loss-of-function mutations in β-catenin (67) within the adult mouse AE could be valuable to confirm the implications of our findings for *in vivo* lung homeostasis and disease development, whereas such model remains to be established.

In conclusion, this study indicates that the WNT/β-catenin pathway is upregulated in the proximal AE from COPD patients, probably within progenitor basal cells, contributing to the abnormal airway epithelial phenotype in this disease. It also shows that the inhibition of this pathway restores epithelial homeostasis in the cultured epithelium from severe COPD patients, not only for lineage differentiation but also for epithelial polarity, barrier function, and EMT. Finally, it provides further evidence of WNT crosstalk with canonical TGF-β activation, which in turn induces EMT. This evidence could thus represent a proof-of-concept study paving the way to therapeutic targeting of WNT/β-catenin or its downstream effectors in the COPD lung, providing it is selectively focussed on the lower airway (and not alveolar) epithelium. It also advocates for a better understanding of the implication of developmental pathways (and how they cooperate) in the adult lung signalling network.

6. References

1. World Health Organization. Global Health Estimates 2016: Estimated deaths by age, sex, and cause. 2016 [Available from: https://www.who.int/healthinfo/global_burden_disease/estimates/en/.
2. Salvi SS, Barnes PJ. Chronic obstructive pulmonary disease in non-smokers. Lancet. 2009;374(9691):733-43.
3. Vogelmeier CF, Criner GJ, Martinez FJ, Anzueto A, Barnes PJ, Bourbeau J, et al. Global Strategy for the Diagnosis, Management, and Prevention of Chronic Obstructive Lung Disease 2017 Report. GOLD Executive Summary. Am J Respir Crit Care Med. 2017;195(5):557-82.
4. Saetta M. Airway inflammation in chronic obstructive pulmonary disease. Am J Respir Crit Care Med. 1999;160(5 Pt 2):S17-20.
5. Pini L, Pinelli V, Modina D, Bezzi M, Tiberio L, Tantucci C. Central airways remodeling in COPD patients. Int J Chron Obstruct Pulmon Dis. 2014;9:927-32.
6. Gohy S, Carlier FM, Fregimilicka C, Detry B, Lecocq M, Ladjemi MZ, et al. Altered generation of ciliated cells in chronic obstructive pulmonary disease. Sci Rep. 2019;9(1):17963.
7. Carlier F, Detry B, Sibille Y, Pilette C. COPD epithelial phenotype shows partial reversibility in long-term primary epithelial ALI-cultures. Eur Respir J. 2018;52(suppl 62).
8. Aghapour M, Raee P, Moghaddam SJ, Hiemstra PS, Heijink IH. Airway Epithelial Barrier Dysfunction in Chronic Obstructive Pulmonary Disease: Role of Cigarette Smoke Exposure. Am J Respir Cell Mol Biol. 2018;58(2):157-69.
9. Sohal SS. Chronic Obstructive Pulmonary Disease (COPD) and Lung Cancer: Epithelial Mesenchymal Transition (EMT), the Missing Link? EBioMedicine. 2015;2(11):1578-9.
10. Nusse R, Varmus HE. Many tumors induced by the mouse mammary tumor virus contain a provirus integrated in the same region of the host genome. Cell. 1982;31(1):99-109.
11. Gavin BJ, McMahon JA, McMahon AP. Expression of multiple novel Wnt-1/int-1-related genes during fetal and adult mouse development. Genes Dev. 1990;4(12B):2319-32.
12. Baarsma HA, Konigshoff M. 'WNT-er is coming': WNT signalling in chronic lung diseases. Thorax. 2017;72(8):746-59.
13. Konigshoff M, Eickelberg O. WNT signaling in lung disease: a failure or a regeneration signal? Am J Respir Cell Mol Biol. 2010;42(1):21-31.
14. Angers S, Moon RT. Proximal events in Wnt signal transduction. Nat Rev Mol Cell Biol. 2009;10(7):468-77.
15. Nusse R, Clevers H. Wnt/beta-Catenin Signaling, Disease, and Emerging Therapeutic Modalities. Cell. 2017;169(6):985-99.
16. Metcalfe C, Mendoza-Topaz C, Mieszczanek J, Bienz M. Stability elements in the LRP6 cytoplasmic tail confer efficient signalling upon DIX-dependent polymerization. J Cell Sci. 2010;123(Pt 9):1588-99.

17. Eapen MS, Sharma P, Gaikwad AV, Lu W, Myers S, Hansbro PM, et al. Epithelial-mesenchymal transition is driven by transcriptional and post transcriptional modulations in COPD: implications for disease progression and new therapeutics. Int J Chron Obstruct Pulmon Dis. 2019;14:1603-10.
18. Boucherat O, Morissette MC, Provencher S, Bonnet S, Maltais F. Bridging Lung Development with Chronic Obstructive Pulmonary Disease. Relevance of Developmental Pathways in Chronic Obstructive Pulmonary Disease Pathogenesis. Am J Respir Crit Care Med. 2016;193(4):362-75.
19. Baarsma HA, Skronska-Wasek W, Mutze K, Ciolek F, Wagner DE, John-Schuster G, et al. Noncanonical WNT-5A signaling impairs endogenous lung repair in COPD. J Exp Med. 2017;214(1):143-63.
20. Wu X, van Dijk EM, Ng-Blichfeldt JP, Bos IST, Ciminieri C, Konigshoff M, et al. Mesenchymal WNT-5A/5B Signaling Represses Lung Alveolar Epithelial Progenitors. Cells. 2019;8(10).
21. Skronska-Wasek W, Mutze K, Baarsma HA, Bracke KR, Alsafadi HN, Lehmann M, et al. Reduced Frizzled Receptor 4 Expression Prevents WNT/beta-Catenin-driven Alveolar Lung Repair in Chronic Obstructive Pulmonary Disease. Am J Respir Crit Care Med. 2017;196(2):172-85.
22. Kneidinger N, Yildirim AO, Callegari J, Takenaka S, Stein MM, Dumitrascu R, et al. Activation of the WNT/beta-catenin pathway attenuates experimental emphysema. Am J Respir Crit Care Med. 2011;183(6):723-33.
23. Uhl FE, Vierkotten S, Wagner DE, Burgstaller G, Costa R, Koch I, et al. Preclinical validation and imaging of Wnt-induced repair in human 3D lung tissue cultures. Eur Respir J. 2015;46(4):1150-66.
24. Cho MH, McDonald ML, Zhou X, Mattheisen M, Castaldi PJ, Hersh CP, et al. Risk loci for chronic obstructive pulmonary disease: a genome-wide association study and meta-analysis. Lancet Respir Med. 2014;2(3):214-25.
25. Jiang Z, Lao T, Qiu W, Polverino F, Gupta K, Guo F, et al. A Chronic Obstructive Pulmonary Disease Susceptibility Gene, FAM13A, Regulates Protein Stability of beta-Catenin. Am J Respir Crit Care Med. 2016;194(2):185-97.
26. Durham AL, McLaren A, Hayes BP, Caramori G, Clayton CL, Barnes PJ, et al. Regulation of Wnt4 in chronic obstructive pulmonary disease. FASEB J. 2013;27(6):2367-81.
27. Heijink IH, de Bruin HG, van den Berge M, Bennink LJ, Brandenburg SM, Gosens R, et al. Role of aberrant WNT signalling in the airway epithelial response to cigarette smoke in chronic obstructive pulmonary disease. Thorax. 2013;68(8):709-16.
28. Heijink IH, de Bruin HG, Dennebos R, Jonker MR, Noordhoek JA, Brandsma CA, et al. Cigarette smoke-induced epithelial expression of WNT-5B: implications for COPD. Eur Respir J. 2016;48(2):504-15.
29. Zou W, Zou Y, Zhao Z, Li B, Ran P. Nicotine-induced epithelial-mesenchymal transition via Wnt/beta-catenin signaling in human airway epithelial cells. Am J Physiol Lung Cell Mol Physiol. 2013;304(4):L199-209.

30. Spanjer AI, Menzen MH, Dijkstra AE, van den Berge M, Boezen HM, Nickle DC, et al. A pro-inflammatory role for the Frizzled-8 receptor in chronic bronchitis. Thorax. 2016;71(4):312-22.
31. Malleske DT, Hayes D, Jr., Lallier SW, Hill CL, Reynolds SD. Regulation of human airway epithelial tissue stem cell differentiation by beta-catenin, P300, and CBP. Stem Cells. 2018.
32. Wang R, Ahmed J, Wang G, Hassan I, Strulovici-Barel Y, Hackett NR, et al. Down-regulation of the canonical Wnt beta-catenin pathway in the airway epithelium of healthy smokers and smokers with COPD. PLoS One. 2011;6(4):e14793.
33. Guo L, Wang T, Wu Y, Yuan Z, Dong J, Li X, et al. WNT/beta-catenin signaling regulates cigarette smoke-induced airway inflammation via the PPARdelta/p38 pathway. Lab Invest. 2015.
34. Lamouille S, Xu J, Derynck R. Molecular mechanisms of epithelial-mesenchymal transition. Nat Rev Mol Cell Biol. 2014;15(3):178-96.
35. Milara J, Peiro T, Serrano A, Cortijo J. Epithelial to mesenchymal transition is increased in patients with COPD and induced by cigarette smoke. Thorax. 2013;68(5):410-20.
36. Sohal SS, Reid D, Soltani A, Ward C, Weston S, Muller HK, et al. Reticular basement membrane fragmentation and potential epithelial mesenchymal transition is exaggerated in the airways of smokers with chronic obstructive pulmonary disease. Respirology. 2010;15(6):930-8.
37. Sohal SS, Reid D, Soltani A, Ward C, Weston S, Muller HK, et al. Evaluation of epithelial mesenchymal transition in patients with chronic obstructive pulmonary disease. Respir Res. 2011;12:130.
38. Bartis D, Mise N, Mahida RY, Eickelberg O, Thickett DR. Epithelial-mesenchymal transition in lung development and disease: does it exist and is it important? Thorax. 2014;69(8):760-5.
39. Jolly MK, Ward C, Eapen MS, Myers S, Hallgren O, Levine H, et al. Epithelial-mesenchymal transition, a spectrum of states: Role in lung development, homeostasis, and disease. Dev Dyn. 2018;247(3):346-58.
40. Gohy ST, Hupin C, Fregimilicka C, Detry BR, Bouzin C, Gaide Chevronay H, et al. Imprinting of the COPD airway epithelium for dedifferentiation and mesenchymal transition. Eur Respir J. 2015;45(5):1258-72.
41. Baarsma HA, Spanjer AI, Haitsma G, Engelbertink LH, Meurs H, Jonker MR, et al. Activation of WNT/beta-catenin signaling in pulmonary fibroblasts by TGF-beta(1) is increased in chronic obstructive pulmonary disease. PLoS One. 2011;6(9):e25450.
42. Benjamini Y, Hochberg Y. Controlling the false discovery rate: a practical and powerful approach to multiple testing. Journal of the Royal statistical society: series B (Methodological). 1995;57(1):289-300.
43. Bustin SA, Benes V, Garson J, Hellemans J, Huggett J, Kubista M, et al. The need for transparency and good practices in the qPCR literature. Nat Methods. 2013;10(11):1063-7.

44. Pilette C, Ouadrhiri Y, Dimanche F, Vaerman JP, Sibille Y. Secretory component is cleaved by neutrophil serine proteinases but its epithelial production is increased by neutrophils through NF-kappa B- and p38 mitogen-activated protein kinase-dependent mechanisms. Am J Respir Cell Mol Biol. 2003;28(4):485-98.
45. Pilette C, Godding V, Kiss R, Delos M, Verbeken E, Decaestecker C, et al. Reduced epithelial expression of secretory component in small airways correlates with airflow obstruction in chronic obstructive pulmonary disease. Am J Respir Crit Care Med. 2001;163(1):185-94.
46. Simoes A, Chen Z, Zhao Y, Chen L, Macias V, DiPietro LA, et al. Laser Capture Microdissection of Epithelium from a Wound Healing Model for MicroRNA Analysis. Methods Mol Biol. 2018;1733:225-37.
47. Gohy ST, Detry BR, Lecocq M, Bouzin C, Weynand BA, Amatngalim GD, et al. Polymeric immunoglobulin receptor down-regulation in chronic obstructive pulmonary disease. Persistence in the cultured epithelium and role of transforming growth factor-beta. Am J Respir Crit Care Med. 2014;190(5):509-21.
48. Mahmood MQ, Walters EH, Shukla SD, Weston S, Muller HK, Ward C, et al. beta-catenin, Twist and Snail: Transcriptional regulation of EMT in smokers and COPD, and relation to airflow obstruction. Sci Rep. 2017;7(1):10832.
49. Clevers H. Wnt/beta-catenin signaling in development and disease. Cell. 2006;127(3):469-80.
50. Schmid A, Sailland J, Novak L, Baumlin N, Fregien N, Salathe M. Modulation of Wnt signaling is essential for the differentiation of ciliated epithelial cells in human airways. FEBS Lett. 2017;591(21):3493-506.
51. Brechbuhl HM, Ghosh M, Smith MK, Smith RW, Li B, Hicks DA, et al. beta-catenin dosage is a critical determinant of tracheal basal cell fate determination. Am J Pathol. 2011;179(1):367-79.
52. Domyan ET, Sun X. Patterning and plasticity in development of the respiratory lineage. Dev Dyn. 2011;240(3):477-85.
53. Konigshoff M, Kneidinger N, Eickelberg O. TGF-beta signaling in COPD: deciphering genetic and cellular susceptibilities for future therapeutic regimen. Swiss Med Wkly. 2009;139(39-40):554-63.
54. Boucherat O, Chakir J, Jeannotte L. The loss of Hoxa5 function promotes Notch-dependent goblet cell metaplasia in lung airways. Biol Open. 2012;1(7):677-91.
55. Li S, Hu X, Wang Z, Wu M, Zhang J. Different profiles of notch signaling in cigarette smoke-induced pulmonary emphysema and bleomycin-induced pulmonary fibrosis. Inflamm Res. 2015;64(5):363-71.
56. Tilley AE, Harvey BG, Heguy A, Hackett NR, Wang R, O'Connor TP, et al. Down-regulation of the notch pathway in human airway epithelium in association with smoking and chronic obstructive pulmonary disease. Am J Respir Crit Care Med. 2009;179(6):457-66.
57. Whitsett JA, Kalinichenko VV. Notch and basal cells take center stage during airway epithelial regeneration. Cell Stem Cell. 2011;8(6):597-8.

58. Kugler MC, Joyner AL, Loomis CA, Munger JS. Sonic hedgehog signaling in the lung. From development to disease. Am J Respir Cell Mol Biol. 2015;52(1):1-13.
59. Ruiz Garcia S, Deprez M, Lebrigand K, Cavard A, Paquet A, Arguel MJ, et al. Novel dynamics of human mucociliary differentiation revealed by single-cell RNA sequencing of nasal epithelial cultures. Development. 2019;146(20).
60. Mucenski ML, Nation JM, Thitoff AR, Besnard V, Xu Y, Wert SE, et al. Beta-catenin regulates differentiation of respiratory epithelial cells in vivo. Am J Physiol Lung Cell Mol Physiol. 2005;289(6):L971-9.
61. Heijink IH, Postma DS, Noordhoek JA, Broekema M, Kapus A. House dust mite-promoted epithelial-to-mesenchymal transition in human bronchial epithelium. Am J Respir Cell Mol Biol. 2010;42(1):69-79.
62. Vallee A, Lecarpentier Y, Guillevin R, Vallee JN. Interactions between TGF-beta1, canonical WNT/beta-catenin pathway and PPAR gamma in radiation-induced fibrosis. Oncotarget. 2017;8(52):90579-604.
63. Libro R, Giacoppo S, Bramanti P, Mazzon E. Is the Wnt/beta-catenin pathway involved in the anti-inflammatory activity of glucocorticoids in spinal cord injury? Neuroreport. 2016;27(14):1086-94.
64. Yu Z, Jiang Y, Sun C. Glucocorticoids inhibits the repair of airway epithelial cells via the activation of wnt pathway. Respir Physiol Neurobiol. 2020;271:103283.
65. Carayol N, Vachier I, Campbell A, Crampette L, Bousquet J, Godard P, et al. Regulation of E-cadherin expression by dexamethasone and tumour necrosis factor-alpha in nasal epithelium. Eur Respir J. 2002;20(6):1430-6.
66. Carayol N, Campbell A, Vachier I, Mainprice B, Bousquet J, Godard P, et al. Modulation of cadherin and catenins expression by tumor necrosis factor-alpha and dexamethasone in human bronchial epithelial cells. Am J Respir Cell Mol Biol. 2002;26(3):341-7.
67. Harris-Johnson KS, Domyan ET, Vezina CM, Sun X. beta-Catenin promotes respiratory progenitor identity in mouse foregut. Proc Natl Acad Sci U S A. 2009;106(38):16287-92.

SECTION 4.
CONCLUSIONS AND PERSPECTIVES

1. Conclusions

This thesis first aimed at establishing whether the COPD epithelial phenotype is intrinsically imprinted, or if it depends on extra-epithelial factors such as inhaled triggers/toxics, epithelial-mesenchymal or epithelial-immune crosstalk. It next assessed the activation of the canonical, β-catenin-dependant, WNT pathway in the COPD AE and questioned WNT roles in promoting the expression of the COPD phenotype of airway epithelium.

We first demonstrate that the COPD epithelial phenotype persists *in vitro*, in a cell culture model that we have pushed up to unusually long periods (10 weeks in air-liquid interface). Indeed, in this system where only epithelial cells are allowed to grow, we observed that most of the COPD phenotype features that were observed at early time periods, as previously reported (1, 2) persisted up to 10 weeks. Those features include barrier dysfunction, impaired cell differentiation, inflammation (at least IL-8 production) and altered epithelial polarity. Although EMT indices wear off after a month, pro-EMT signalling seemed to be durably imprinted in COPD, as inflammatory challenges reactivated EMT more strongly in COPD than in control cells.

Secondly, we show unequivocally that the canonical, β-catenin-dependent WNT pathway is activated in the AE of COPD patients, both *in situ* in bronchial tissue and *in vitro* in COPD-derived ALI-cultures. Although complex and intricated networks of developmental and signalling pathways regulate the expression of the COPD epithelial phenotype, including WNT, Notch, SHH, EGFR, JAK-STAT and PI3K (3-8), the isolated extrinsic inhibition of the canonical WNT pathway reduced the expression of several COPD features, such as abnormal cell differentiation, EMT

and impaired epithelial polarity, emphasizing the importance of WNT pathway dysregulation in COPD pathogenesis.

The risk to develop COPD is strongly influenced by cigarette smoking, with a COPD prevalence of 20% amongst ever smokers (9-11). Nevertheless, the Rotterdam Study recently estimated the prevalence of COPD in never smokers around 6% (11), enlightening the pathogenic role of other factors, including occupational exposures, air pollution, and genetic predisposition. In 1993, a study assessing familial aggregation of cross-sectional pulmonary function (FEV1) rejected Mendelian transmission and suggested environmental and/or polygenic genetic influences in determining FEV1, based on residual familial correlation (12). Aside from Mendelian syndromes such as α_1-antitrypsin deficiency, many studies have shown COPD familial clusters independently of cigarette smoke exposure, further questioning the inheritable nature of the disease (13). In addition, it should also be noted that different trajectories may lead to clinically-defined COPD: in addition to accelerated lung function decline (probably reflecting loss of bronchioles) that relates to classical "adult COPD", poor lung growth (and probably poor development of bronchioles following impaired branching morphogenesis) may also lead to paediatric roots of COPD in adults (14).

In the last decade, genomic regions influencing COPD susceptibility have been identified in genome-wide association studies (15-20), such as well-known *FAM13A* (16), but also regions adjacent to regions *MMP12* and *TGFB2* (15). More recently yet, a combined genome-wide association study of more than 60.000 samples from the International COPD Genetics Consortium and UK Biobank identified 82 loci associated with COPD (21). Interestingly, increased expression of FAM13A facilitates β-catenin degradation, therefore contributing to emphysema development in two murine models of COPD (22), while *MMP12* and *TGFB2* are related to WNT signalling, as previously described. In addition, single nucleotide polymorphisms on the *FZD8* gene have been associated with chronic mucus hypersecretion in smokers (23).

Beyond COPD genetic susceptibility, epigenetic marks have also been identified in COPD. In 2005, Ito and colleagues showed in a proof-to-concept study that histone deacetylase (HDAC) mRNA and protein levels were decreased in bronchial biopsies from COPD patients, while increased histone acetyltransferase (HAT) activity and *IL8* mRNA levels were observed (24). Since then, numerous studies have explored the epigenome in smokers and COPD patients, identifying modifications driving genes up- and down-regulation involved in COPD, as recently reviewed (25). Importantly, cigarette smoking globally leads to DNA hypomethylation in small airways as represented in Figure 37 (26), while changes in DNA methylation of the promoters of proinflammatory genes in epithelial cells of COPD patients could participate to epithelial inflammation (27). In addition, specific gene hypermethylation (*SERPINA1*, *FOXA2*, *TNFAIP2*) (28-30) or hypomethylation (*SPDEF*) (29) probably participate to the inheritable nature of the disease.

Finally, while no study has been specifically designed to identify epigenetic modifications in airway progenitor cells (basal and club cells), Staudt and colleagues showed that small airway basal cells that are unable to differentiate in ALI cultures exhibit a different methylation profile than functional basal cells (31), and hypothesize that the lung environment contributes in COPD to maintain DNA methylation in basal cells, therefore impairing stemness, a feature that was confirmed to play a role in COPD pathogenesis (32).

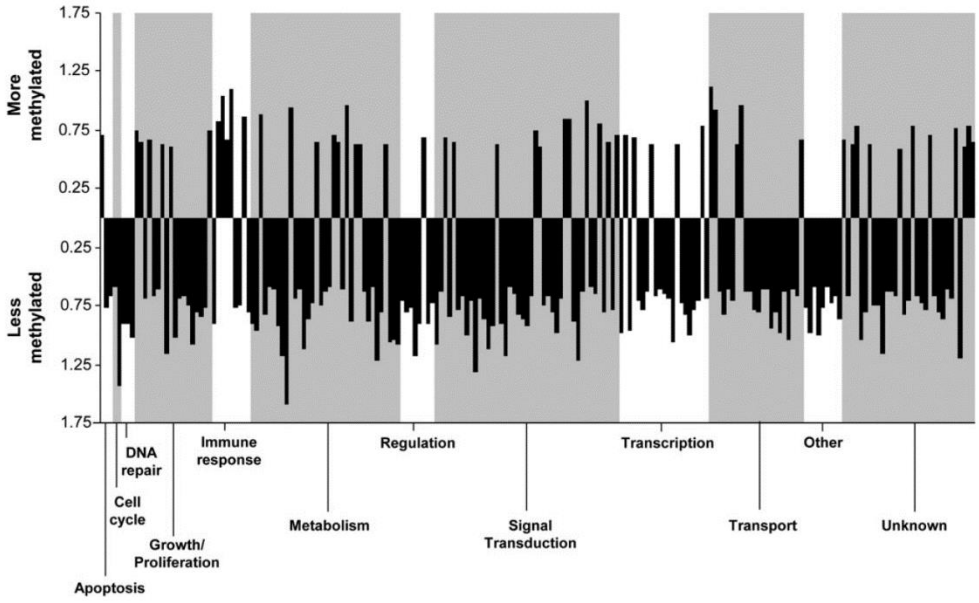

Figure 37 | Altered methylation in smokers
Biological categories of the 204 unique genes that are differentially methylated between smokers and non-smokers (Graph from (26)).

2. Perspectives

2.1. Identifying epigenetic imprinting of airway progenitors in COPD

As abovementioned, no study has yet specifically assessed the COPD epigenetic modifications in airway progenitors. Regarding our study about the memory of epithelial injury in COPD, one could argue that once confluence is reached in ALI-cultures, the reconstituted respiratory epithelium displays few division counts, and that even 10 weeks long cultures do not suffice to apprehend the persistent nature (referred as to “memory”) of the COPD epithelial phenotype. As basal cells first undergo expansion in submerged conditions, it should be assessed whether successive passages of basal cells (multiple expansion steps that include cell divisions) modify the phenotype of the derived ALI-reconstituted epithelium.

In parallel, basal cells isolation from fresh COPD and control samples by FACS-sorting (as routinely performed in our laboratory, as shown in Figure 38) could provide pure epithelial cell populations that can be submitted to epigenetic analyses in a so-called "top-down" approach (Figure 39). These could include whole-genome methylome assessment, histone modifications studies, and/or cutting-edge assay for transposase-accessible chromatin with high throughput sequencing (ATAC-seq). Such analyses may also be applied to club cells, a less well-known progenitor population, but no specific marker has yet been identified to sort club cells.

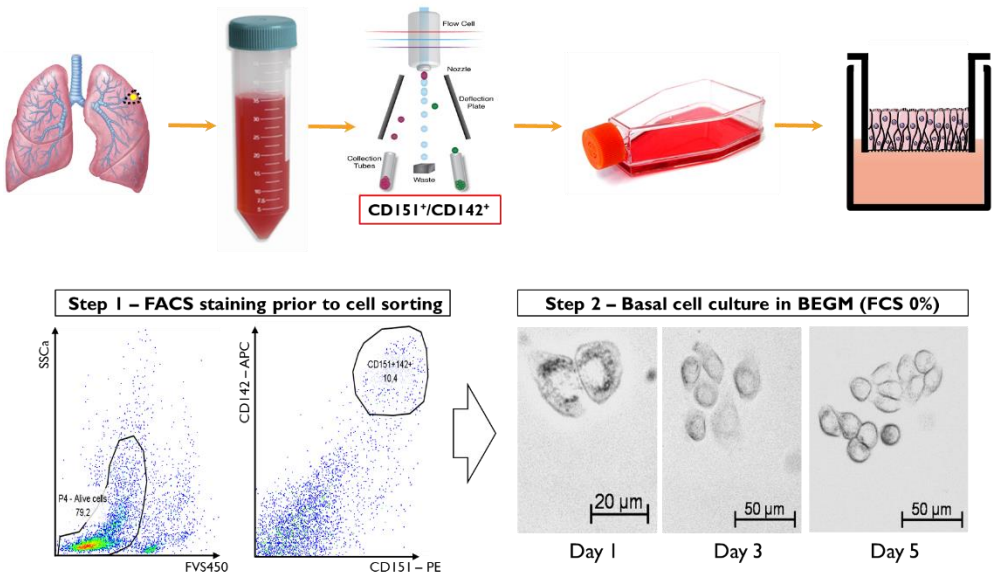

Figure 38 | Basal cells sorting flowchart
After bronchial tissue extraction and digestion in pronase, individualized epithelial cells are stained for CD151 and CD142, and double positive cells are seeded into culture flasks, ultimately leading to the reconstitution of a pseudostratified respiratory epithelium.

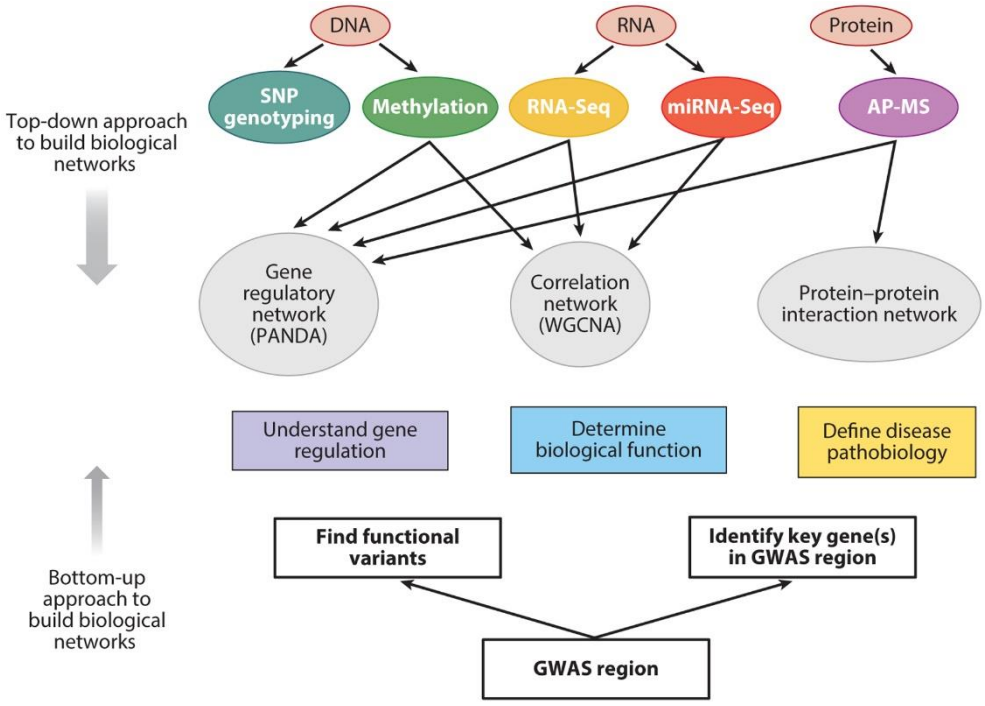

Figure 39 | Comparison of top-down and bottom-up approaches to build biological networks
Image issued from (28).

2.2. Unravelling molecular mechanisms behind EMT in COPD

EMT is an ubiquitous process that is crucial to embryogenesis and tissue repair, as it permits epithelial cells to gain mesenchymal features, including migratory abilities (33). Many pathways may induce EMT, including canonical (SMAD-dependent) and non-canonical TGF-β, WNT, Notch, STAT3, HIF-1α and SHH. In COPD, aberrant EMT is thought to lead to subepithelial fibrosis, therefore contributing to the irreversible narrowing of the small airways. We showed that canonical WNT signalling is activated in the COPD AE and contributes to EMT (34), but other pathways are probably involved.

As STAT3 signalling is triggered by IL-6, previously shown to be increased at the AE level in COPD (Section 2, paragraph 3.6), and as STAT3/JAK was described to regulate EMT in cancer, and to be activated in COPD (8, 35, 36), we led an ancillary experiment to assess the activation of the transcription factor STAT3 in ALI-AE from COPD patients. We observed an increase in STAT3 phosphorylation at tyrosine 705 in COPD-derived ALI cultures at 4 weeks ALI, as depicted in Figure 40. To further explore the role of STAT3 in promoting EMT, STAT3 modulation effects on EMT readouts (fibronectin release, vimentin expression, …) should be assessed in COPD and (non-) smokers-derived ALI-cultures.

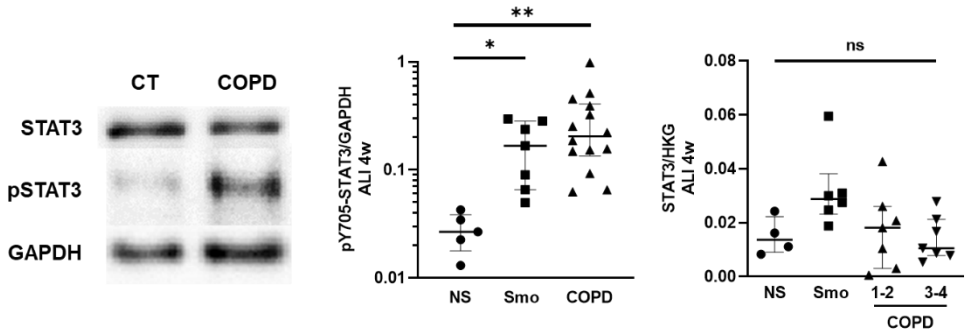

Figure 40 | STAT-3 activation in COPD ALI-HBEC

2.3. Distinguishing epithelial disease from impaired growth in COPD

While COPD has long been considered an exclusively inhaled toxic-induced disease, the emergence of genomics, epigenomics and the study of polymorphisms have identified mutations, single nucleotide polymorphisms and polygenic susceptibility factors that partially explain why only 20% of smokers ultimately develop COPD (see above). Yet this breakthrough still failed to account for the heterogeneity of COPD patients, even within the different clinico-functional COPD subgroups.

In 2015, the paradigm changed following Lange and colleagues' study suggesting that part of the adult population exhibiting irreversible airflow obstruction (and therefore diagnosed with COPD) does not suffer from COPD strictly speaking (14). Indeed, impaired lung development (due to prematurity or recurrent lung infections in childhood, for instance), leads to subnormal lung function parameters in adults, in which COPD will later be evoked whereas no accelerated FEV_1 decline is observed (Figure 41).

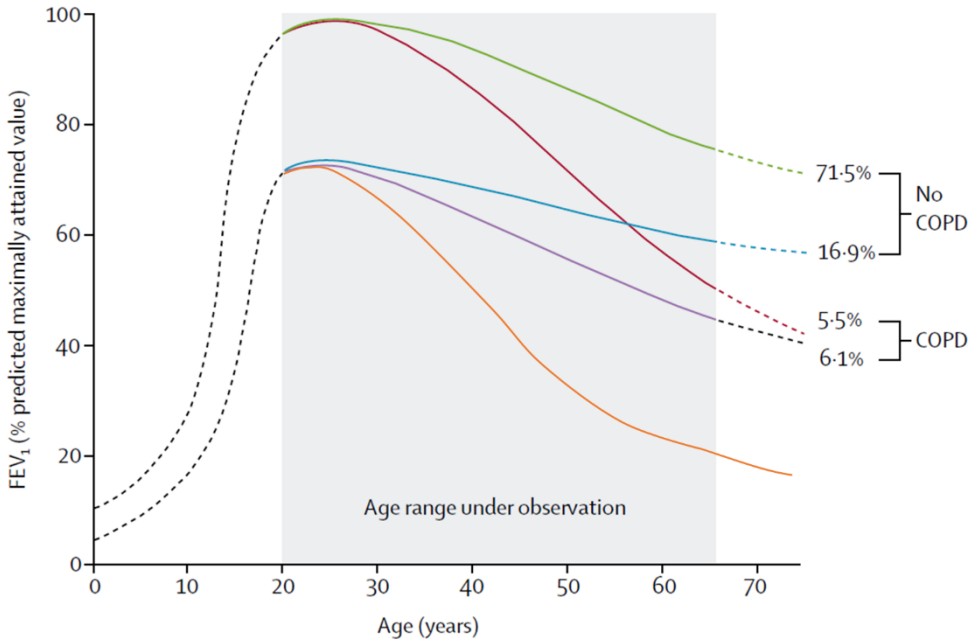

Figure 41 | Lung trajectories leading to COPD
Lung function trajectories from patients' groups with normal or decreased FEV_1. Green line: normal; red line: normal initial FEV_1 with accelerated decline leading to COPD; blue line: small initial lungs but no COPD; purple line: small initial lungs leading to COPD diagnosis; orange line: small lungs and accelerated decline leading to early death (image modified from (37), original data from (14)).

In our studies, patients were allocated to COPD groups according to pulmonary function tests only, as data regarding exacerbations and respiratory symptoms often lack in medical records, while in most cases, virtually no data is available regarding previous pulmonary function tests. In the light of Lange's study, it is therefore likely that the COPD study groups (particularly in Gold I and Gold II groups) are heterogeneously composed from "real COPD patients" and patients with impaired lung growth, potentially diluting the findings described in this manuscript.

Future research in the field should therefore give particular attention to carefully phenotyping COPD patients beyond single lung function results, and consider clinical parameters (exacerbations, dyspnoea), biological findings (serum eosinophils, BAL counts) and lung function trajectories. Obviously, this will require larger patient recruitment and time-consuming data collection (both prospective and retrospective). Alternatively, the screening of enrolled patients for COPD-related polymorphisms or mutations could provide more homogeneous study subgroups, that could lead to better understanding of the disease and development of patient specific therapies.

3. References

1. Gohy ST, Detry BR, Lecocq M, Bouzin C, Weynand BA, Amatngalim GD, et al. Polymeric immunoglobulin receptor down-regulation in chronic obstructive pulmonary disease. Persistence in the cultured epithelium and role of transforming growth factor-beta. Am J Respir Crit Care Med. 2014;190(5):509-21.
2. Gohy ST, Hupin C, Fregimilicka C, Detry BR, Bouzin C, Gaide Chevronay H, et al. Imprinting of the COPD airway epithelium for dedifferentiation and mesenchymal transition. Eur Respir J. 2015;45(5):1258-72.
3. Tilley AE, Harvey BG, Heguy A, Hackett NR, Wang R, O'Connor TP, et al. Down-regulation of the notch pathway in human airway epithelium in association with smoking and chronic obstructive pulmonary disease. Am J Respir Crit Care Med. 2009;179(6):457-66.
4. Belgacemi R, Luczka E, Ancel J, Diabasana Z, Perotin JM, Germain A, et al. Airway epithelial cell differentiation relies on deficient Hedgehog signalling in COPD. EBioMedicine. 2020;51:102572.
5. Pirozzi F, Ren K, Murabito A, Ghigo A. PI3K Signaling in Chronic Obstructive Pulmonary Disease: Mechanisms, Targets, and Therapy. Curr Med Chem. 2019;26(16):2791-800.
6. Vallath S, Hynds RE, Succony L, Janes SM, Giangreco A. Targeting EGFR signalling in chronic lung disease: therapeutic challenges and opportunities. Eur Respir J. 2014;44(2):513-22.
7. Baarsma HA, Konigshoff M. 'WNT-er is coming': WNT signalling in chronic lung diseases. Thorax. 2017;72(8):746-59.
8. Yew-Booth L, Birrell MA, Lau MS, Baker K, Jones V, Kilty I, et al. JAK-STAT pathway activation in COPD. Eur Respir J. 2015;46(3):843-5.
9. Atsou K, Chouaid C, Hejblum G. Variability of the chronic obstructive pulmonary disease key epidemiological data in Europe: systematic review. BMC medicine. 2011;9:7.
10. Rycroft CE, Heyes A, Lanza L, Becker K. Epidemiology of chronic obstructive pulmonary disease: a literature review. Int J Chron Obstruct Pulmon Dis. 2012;7:457-94.
11. Terzikhan N, Verhamme KM, Hofman A, Stricker BH, Brusselle GG, Lahousse L. Prevalence and incidence of COPD in smokers and non-smokers: the Rotterdam Study. European journal of epidemiology. 2016;31(8):785-92.
12. Givelber RJ, Couropmitree NN, Gottlieb DJ, Evans JC, Levy D, Myers RH, et al. Segregation analysis of pulmonary function among families in the Framingham Study. Am J Respir Crit Care Med. 1998;157(5 Pt 1):1445-51.
13. Hersh CP, Hokanson JE, Lynch DA, Washko GR, Make BJ, Crapo JD, et al. Family history is a risk factor for COPD. Chest. 2011;140(2):343-50.
14. Lange P, Celli B, Agusti A, Boje Jensen G, Divo M, Faner R, et al. Lung-Function Trajectories Leading to Chronic Obstructive Pulmonary Disease. N Engl J Med. 2015;373(2):111-22.

15. Cho MH, McDonald ML, Zhou X, Mattheisen M, Castaldi PJ, Hersh CP, et al. Risk loci for chronic obstructive pulmonary disease: a genome-wide association study and meta-analysis. Lancet Respir Med. 2014;2(3):214-25.
16. Cho MH, Boutaoui N, Klanderman BJ, Sylvia JS, Ziniti JP, Hersh CP, et al. Variants in FAM13A are associated with chronic obstructive pulmonary disease. Nat Genet. 2010;42(3):200-2.
17. Hancock DB, Eijgelsheim M, Wilk JB, Gharib SA, Loehr LR, Marciante KD, et al. Meta-analyses of genome-wide association studies identify multiple loci associated with pulmonary function. Nat Genet. 2010;42(1):45-52.
18. Repapi E, Sayers I, Wain LV, Burton PR, Johnson T, Obeidat M, et al. Genome-wide association study identifies five loci associated with lung function. Nat Genet. 2010;42(1):36-44.
19. Wilk JB, Chen TH, Gottlieb DJ, Walter RE, Nagle MW, Brandler BJ, et al. A genome-wide association study of pulmonary function measures in the Framingham Heart Study. PLoS Genet. 2009;5(3):e1000429.
20. Pillai SG, Ge D, Zhu G, Kong X, Shianna KV, Need AC, et al. A genome-wide association study in chronic obstructive pulmonary disease (COPD): identification of two major susceptibility loci. PLoS Genet. 2009;5(3):e1000421.
21. Sakornsakolpat P, Prokopenko D, Lamontagne M, Reeve NF, Guyatt AL, Jackson VE, et al. Genetic landscape of chronic obstructive pulmonary disease identifies heterogeneous cell-type and phenotype associations. Nat Genet. 2019;51(3):494-505.
22. Jiang Z, Lao T, Qiu W, Polverino F, Gupta K, Guo F, et al. A Chronic Obstructive Pulmonary Disease Susceptibility Gene, FAM13A, Regulates Protein Stability of beta-Catenin. Am J Respir Crit Care Med. 2016;194(2):185-97.
23. Spanjer AI, Menzen MH, Dijkstra AE, van den Berge M, Boezen HM, Nickle DC, et al. A pro-inflammatory role for the Frizzled-8 receptor in chronic bronchitis. Thorax. 2016;71(4):312-22.
24. Ito K, Ito M, Elliott WM, Cosio B, Caramori G, Kon OM, et al. Decreased Histone Deacetylase Activity in Chronic Obstructive Pulmonary Disease. New England Journal of Medicine. 2005;352(19):1967-76.
25. Zhang L, Valizadeh H, Alipourfard I, Bidares R, Aghebati-Maleki L, Ahmadi M. Epigenetic Modifications and Therapy in Chronic Obstructive Pulmonary Disease (COPD): An Update Review. COPD: Journal of Chronic Obstructive Pulmonary Disease. 2020;17(3):333-42.
26. Buro-Auriemma LJ, Salit J, Hackett NR, Walters MS, Strulovici-Barel Y, Staudt MR, et al. Cigarette smoking induces small airway epithelial epigenetic changes with corresponding modulation of gene expression. Hum Mol Genet. 2013;22(23):4726-38.
27. Tzortzaki EG, Papi A, Neofytou E, Soulitzis N, Siafakas NM. Immune and genetic mechanisms in COPD: possible targets for therapeutic interventions. Curr Drug Targets. 2013;14(2):141-8.
28. Rotondo JC, Aquila G, Oton-Gonzalez L, Selvatici R, Rizzo P, De Mattei M, et al. Methylation of SERPINA1 gene promoter may predict chronic obstructive

pulmonary disease in patients affected by acute coronary syndrome. Clinical Epigenetics. 2021;13(1):79.
29. Song J, Heijink IH, Kistemaker LEM, Reinders-Luinge M, Kooistra W, Noordhoek JA, et al. Aberrant DNA methylation and expression of SPDEF and FOXA2 in airway epithelium of patients with COPD. Clin Epigenetics. 2017;9:42.
30. Sundar IK, Yin Q, Baier BS, Yan L, Mazur W, Li D, et al. DNA methylation profiling in peripheral lung tissues of smokers and patients with COPD. Clin Epigenetics. 2017;9:38.
31. Staudt MR, Buro-Auriemma LJ, Walters MS, Salit J, Vincent T, Shaykhiev R, et al. Airway Basal stem/progenitor cells have diminished capacity to regenerate airway epithelium in chronic obstructive pulmonary disease. Am J Respir Crit Care Med. 2014;190(8):955-8.
32. Ghosh M, Miller YE, Nakachi I, Kwon JB, Baron AE, Brantley AE, et al. Exhaustion of Airway Basal Progenitor Cells in Early and Established Chronic Obstructive Pulmonary Disease. Am J Respir Crit Care Med. 2018;197(7):885-96.
33. Lamouille S, Xu J, Derynck R. Molecular mechanisms of epithelial-mesenchymal transition. Nat Rev Mol Cell Biol. 2014;15(3):178-96.
34. Carlier FM, Dupasquier S, Ambroise J, Detry B, Lecocq M, Bietry-Claudet C, et al. Canonical WNT pathway is activated in the airway epithelium in chronic obstructive pulmonary disease. EBioMedicine. 2020;61:103034.
35. Huang G, Yan H, Ye S, Tong C, Ying QL. STAT3 phosphorylation at tyrosine 705 and serine 727 differentially regulates mouse ESC fates. Stem Cells. 2014;32(5):1149-60.
36. Li B, Huang C. Regulation of EMT by STAT3 in gastrointestinal cancer (Review). Int J Oncol. 2017;50(3):753-67.
37. Agusti A, Faner R. Lung function trajectories in health and disease. Lancet Respir Med. 2019;7(4):358-64.

SECTION 5.

BIBLIOGRAPHY

1. Publications

1.1. Original publications

Carlier FM, Detry B, Lecocq M, Collin AM, Planté-Bordeneuve T, Verleden SE, Stanciu-Pop CM, Janssens W, Ambroise J, Vanaudenaerde BM, Gohy ST, Pilette C.The memory of airway epithelium damage in smokers and COPD patients. Preprint deposited on BioRxiv. doi: 10.1101/2021.04.21.439437. Submitted to the European Respiratory Journal.

Collin AM, Lecocq M, Detry B, **Carlier FM**, Bouzin C, de Sany P, Hoton D, Verleden S, Froidure A, Pilette C, Gohy S. *Loss of ciliated cells and altered airway epithelial integrity in cystic fibrosis are independent from the CFTR defect.* J Cyst Fibros. 2021 Oct 14;S1569-1993(21)01424-7. doi: 10.1016/j.jcf.2021.09.019. Online ahead of print (IF 2020: 5.482)

Carlier FM, Dupasquier S, Ambroise J, Detry B, Lecocq M, Biétry-Claudet C, Boukala Y, Gala JL, Bouzin C, Verleden SE, Hoton D, Gohy S, Bearzatto B, Pilette C. Canonical WNT pathway is activated in the airway epithelium in chronic obstructive pulmonary disease. EBioMedicine. 2020 Nov;61:103034. doi: 10.1016/j.ebiom.2020.103034. Epub 2020 Oct 10. PMID: 33045470. (IF 2020: 8.143)

Collin AM, Lecocq M, Noel S, Detry B, **Carlier FM**, Aboubakar Nana F, Bouzin C, Leal T, Vermeersch M, De Rose V, Regard L, Martin C, Burgel PR, Hoton D, Verleden S, Froidure A, Pilette C, Gohy S. Lung immunoglobulin A immunity dysregulation in cystic fibrosis. EBioMedicine. 2020 Oct;60:102974. (IF 2020: 8.143)

Gohy S, **Carlier FM**, Fregimilicka C, Detry B, Lecocq M, Ladjemi MZ, Verleden S, Hoton D, Weynand B, Bouzin C, Pilette C. Altered generation of ciliated cells in chronic obstructive pulmonary disease. Sci Rep. 2019 Nov 29;9(1):17963. (IF 2019: 3.998)

Ladjemi MZ, Martin C, Lecocq M, Detry B, Nana FA, Moulin C, Weynand B, Fregimilicka C, Bouzin C, Thurion P, **Carlier F**, Serré J, Gayan-Ramirez G, Delos M, Ocak S, Burgel PR, Pilette C. Increased IgA Expression in Lung Lymphoid Follicles in Severe Chronic Obstructive Pulmonary Disease. Am J Respir Crit Care Med. 2019 Mar 1;199(5):592-602. (IF 2019: 17.452)

1.2. Reviews

Carlier FM, de Fays C, Pilette C. Epithelial barrier dysfunction in chronic respiratory diseases. Front Physiol. 2021 Jun 24;12:691227. (IF 2020: 4.566)

Carlier FM, Sibille Y & Pilette C. The epithelial barrier and immunoglobulin A system in allergy. Clin Exp Allergy 46, 1372-1388 (2016). (IF 2016: 5.638)

2. Posters

Carlier FM, Dupasquier S, Ambroise J, Detry B, Lecocq M, Bearzatto B, Pilette C. Wnt/β-catenin signalling is upregulated in the COPD bronchial epithelium. Poster presentation at the Journées de Recherche Respiratoire de la Société de Pneumologie de Langue française (SPLF) 2019, Brussels (BE)

Carlier FM, Detry BR, Pilette C. STAT3 is activated in COPD airway epithelial cells. Poster presentation at the ERS Lung Science Conference 2019, Estoril (PT)

Carlier FM, Detry BR, Sibille Y, Pilette C. COPD-related epithelial inflammation drives EMT in primary epithelial ALI-cultures. Poster presentation at the European Respiratory Society Congress 2018, Paris (FR)

Carlier FM, Detry BR, Pilette C. Persistence of the COPD broncho-epithelial phenotype in vitro, in long-term primary air/liquid interface culture. Poster

presentation at the Journées de Recherche Respiratoire de la Société de Pneumologie de Langue française (SPLF) 2018, Marseille (FR)

Collin A, Lecocq M, Detry B, **Carlier F**, Noël S, Bouzin C, Leal T, De Rose V, Martin C, Burgel PR, Verleden S, Pilette C, Gohy S. Bronchial immunoglobulins and epithelial pIgR are upregulated in cystic fibrosis. EDT Immunology Day 2018, Liège (BE)

Carlier FM, Detry BR, Pilette C. Rôle de l'inflammation dans la dédifférenciation épithéliale de la BPCO. Poster presentation at the Biennale de l'Espace francophone de pneumologie – Journées de Recherche Respiratoire de la Société de Pneumologie de Langue française (SPLF) 2017, Québec (CA)

3. Oral presentations

Carlier FM, Detry B, Lecocq M, Collin AM, Verleden SE, Stanciu-Pop CM, Rondelet B, Janssens W, Ambroise J, Vanaudenaerde BM, Gohy ST, Pilette C. Airway epithelium memory of injury in chronic obstructive pulmonary disease. IREC Masterclass 2021, Brussels (BE)

Carlier FM, Detry B, Lecocq M, Collin AM, Verleden SE, Stanciu-Pop CM, Rondelet B, Janssens W, Ambroise J, Vanaudenaerde BM, Gohy ST, Pilette C. First RSRQ-J2R-BeRS joined meeting, 2021, virtual meeting (BE, CA, FR)

Carlier FM, Carlier FM, Dupasquier S, Gohy ST, Detry B, Biétry--Claudet C, Boukala Y, Lecocq M, Ambroise J, Bearzatto B, Pilette C. Wnt/β-catenin signalling is increased in COPD epithelium. Oral presentation at the Belgian Respiratory Society Congress 2019, La Hulpe (BE)

Carlier FM, Detry BR, Pilette C. STAT3 is activated in COPD airway epithelial cells. Poster presentation at the European Respiratory Society Congress 2019, Madrid (ES)

Carlier FM, Ambroise J, Dupasquier S, Bearzatto B, Pilette C. Wnt/β-catenin signalling is upregulated in the COPD bronchial epithelium. Poster discussion at the European Respiratory Society Congress 2019, Madrid (ES)

Carlier FM, Carlier FM, Dupasquier S, Gohy ST, Detry B, Biétry--Claudet C, Boukala Y, Lecocq M, Ambroise J, Bearzatto B, Pilette C. Wnt/β-catenin signalling is increased in COPD epithelium. Oral presentation at the Glaxo-Smith-Klein Awards in Pulmonology 2019, Brussels (BE)

Carlier FM, Detry BR, Pilette C. COPD epithelial phenotype shows partial reversibility in long-term primary epithelial ALI-cultures. Oral presentation at the European Respiratory Society Congress 2018, Paris (FR)

Carlier FM, Detry BR, Pilette C. Role of the inflammation in the bronchial epithelium dedifferentiation in COPD. Oral presentation at the IREC PhD Day 2018, Brussels (BE)

Carlier FM, Detry BR, Pilette C. Persistence of the COPD broncho-epithelial phenotype in vitro, in long-term primary air/liquid interface cultures. Oral presentation at the Glaxo-Smith-Klein Awards in Pulmonology 2018, Brussels (BE)

Carlier FM, Dupasquier S, Bearzatto B, Ambroise J, Detry BR, Fregimilicka C, De Beukelaer M, Bouzin C, Pilette C. Les voies de signalisation Wnt et Notch dans la BPCO. Oral presentation at the Biennale de l'Espace francophone de pneumologie – Journées de Recherche Respiratoire de la Société de Pneumologie de Langue française (SPLF) 2017, Québec (CA)

4. Awards

Silver Basic Science Presentation Award at the Glaxo-Smith-Klein Awards in Pulmonology 2019, Brussels (BE)

Best poster Award at the Biennale de l'Espace francophone de pneumologie – Journées de Recherche Respiratoire de la Société de Pneumologie de Langue française (SPLF) 2017, Québec (CA)